

STUDIES OF BIOLOGICALLY RELEVANT IRON-OXYGEN CHEMISTRY

by

Mary Elizabeth Roth

A. B., KENYON COLLEGE  
(1983)

SUBMITTED TO THE DEPARTMENT OF CHEMISTRY  
IN PARTIAL FULFILLMENT OF THE  
REQUIREMENTS FOR THE

DEGREE OF  
DOCTOR OF PHILOSOPHY

AT THE

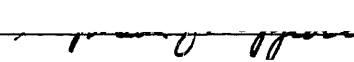
MASSACHUSETTS INSTITUTE OF TECHNOLOGY

SEPTEMBER 1988

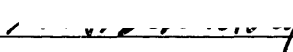
©Massachusetts Institute of Technology, 1988

Signature of Author 

Department of Chemistry  
July 22, 1988

Certified by 

Stephen J. Lippard  
Thesis Supervisor

Accepted by 

Glenn A. Berchtold  
Chairman, Departmental Committee on Graduate Students

MASSACHUSETTS INSTITUTE  
OF TECHNOLOGY

SEP 23 1988 Archives

LIBRARIES

This thesis has been examined by a committee of the Department of Chemistry as follows:

Professor Richard R. Schrock \_\_\_\_\_ Chairman

Professor Stephen J. Lippard \_\_\_\_\_ Thesis Supervisor

Professor W. H. Orme-Johnson \_\_\_\_\_

To  
Dr. Gordon L. Johnson  
Professor of Chemistry  
Kenyon College

and to  
Mom and Dad

and to Andy, of course

No, I am not Prince Hamlet, nor was meant to be;  
Am an attendant lord, one that will do  
To swell a progress, start a scene or two....

T. S. Eliot

# Studies of Biologically Relevant Iron-Oxygen Chemistry

by

Mary Elizabeth Roth

Submitted to the Department of Chemistry on July 22, 1988  
in partial fulfillment of the requirements for the  
Degree of Doctor of Philosophy in Chemistry

## ABSTRACT

Three areas relating to iron-oxygen interactions in biology are presented. The second chapter describes attempts to synthesize a spectroscopic model for the active site of cytochrome oxidase. Towards this end, two new ligands,  $N_2S$ -TTP and  $N_2S$ -xy-TTP, that are capable of binding an iron atom in a porphyrin plane and a copper atom within the distance of a single atom bridge to the iron were synthesized. Iron was added to the ligands but difficulties were encountered in the purification of the metallated products. The addition of copper to  $N_2S$ -TTPFeX, where X =  $Cl^-$ ,  $Br^-$ , or  $SCN^-$ , resulted in species that gave rise to EPR signals characteristic of copper bound to the ligand, but no bimetallic products could be isolated or purified.

Solution characterization of tetranuclear complexes containing a non-planar  $\{Fe_4O_2\}^{8+}$  core is described in the subsequent chapter. The previously synthesized complex  $(Et_4N)[Fe_4O_2(O_2CC_6H_5)_7(H_2Bpz_2)_2]$  and its acetate-bridged analog were studied by  $^1H$  NMR and Raman spectroscopic techniques. A new complex containing the same core unit and 4,4'-dimethylbipyridine as the nitrogen donor ligand,  $[Fe_4O_2(O_2CC_6H_5)_7(Me_2bipy)_2]^+$ , was synthesized and characterized by x-ray crystallography as well as  $^1H$  NMR and Raman spectroscopic methods. The complexes containing  $[(H_2Bpz_2)^-]$  both exhibited a resonance enhanced Raman band at  $\sim 750\text{ cm}^{-1}$ . The intensity of this band increased as the excitation wavelength decreased from 574 to 476 nm. The third complex,  $[Fe_4O_2(O_2CC_6H_5)_7(Me_2bipy)_2]^+$ , exhibited a band at  $\sim 765\text{ cm}^{-1}$  in the Raman spectrum which also appeared to be resonance enhanced. Thus, bands in the  $\sim 750\text{ cm}^{-1}$  region appear to be characteristic of the non-planar  $\{Fe_4O_2\}^{8+}$  cores in these complexes and may arise from a symmetric stretch of the planar  $\{Fe_2O_2\}$  subunit.

The third area of research presented consists of initial investigations of dinuclear iron complexes as catalysts, in the presence of reductants, for the hydroxylation of alkanes by dioxygen. Exploratory reactions with  $[Fe_2O(O_2CCH_3)_2(HBpz_3)_2]$  and  $[Fe_2O(O_2CCH_3)_2(Me_3TACN)_2](PF_6)_2$  are described and discussed. The latter complex demonstrated more catalytic activity than the former, potentially due to its greater stability in the presence of reductants. The simple dinuclear starting material,  $(NEt_4)_2[Fe_2OCl_2]$ , was found to be more active under identical conditions than either of the other complexes. The most successful system established consisted of  $[Fe_2OCl_6]^{2-}$  in the presence of ascorbic acid or its more soluble analog, tetramethylreductic acid, at  $32^\circ C$  under atmospheric dioxygen. For systems containing ascorbic acid,  $\sim 3.8$  mol cyclohexanol per mol  $(NEt_4)_2[Fe_2OCl_6]$  were formed from cyclohexane in 48 hr. Only 0.1 mol cyclohexanone was produced in the same time period. The total yield based on the reductant was  $\sim 20\%$ . Catalytic turnover essentially stopped after 48 hr

probably owing to consumption of the reductant. Addition of more reductant increased the activity of the system to ~70% of its initial activity. The same type of behavior was observed when tetramethylreductic acid replaced ascorbic acid, but the rate of reaction increased. In 4-5 hr, the TMRA system produced around ~3.5 mol of cyclohexanol with only 1/50th that amount of cyclohexanone. Again, the addition of more reductant lead to the formation of more of each product, about 75% of the yield of the first addition. Oxidation of cyclohexene gave 2-cyclohexen-1-ol as the major product, with cyclohexene epoxide as a secondary product and smaller amounts of 2-cyclohexen-1-one also produced. The reactions are characterized by the formation of a purple species prior to the introduction of air. Initial attempts at characterization of the purple species were undertaken but no clear conclusions could be drawn from the results.

Thesis Supervisor: Stephen J. Lippard  
Title: Professor of Chemistry

## TABLE OF CONTENTS

	Page
Dedication.....	3
Quotation.....	4
Abstract.....	5
Table of Contents.....	7
List of Figures.....	9
List of Schemes.....	12
List of Tables.....	12
List of Abbreviations.....	13
Chapter 1 Introduction.....	14
Chapter 2 Toward the Synthesis of a Structural Model for the Active Site of Cytochrome Oxidase.....	19
Experimental.....	35
Results and Discussion.....	46
Ligand Synthesis.....	46
Addition of Iron.....	56
Addition of Copper.....	61
Conclusion.....	67
Chapter 3 Solution Characterization of Tetranuclear Iron-Oxo Compounds Containing a Non-planar $\{\text{Fe}_4\text{O}_2\}^{8+}$ core.....	69
Experimental.....	72
Results.....	78
Synthesis and Structure.....	78
Proton NMR Spectroscopy.....	85
Solution Magnetics.....	90
Raman Spectroscopy.....	90

Discussion .....	100
Chapter 4 Air Oxidation of Cyclohexane to Cyclohexanol Catalyzed by Oxo-Bridged Diiron Complexes: Towards the Development of a Functional Model System for Methane Monooxygenase.....	104
Experimental .....	116
Results and Discussion .....	127
Reactions with $[\text{Fe}_2\text{O}(\text{O}_2\text{CCH}_3)_2(\text{HBpz}_3)_2]$ and $[\text{Fe}_2\text{O}(\text{O}_2\text{CCH}_3)_2-$ $(\text{Me}_3\text{TACN})_2](\text{PF}_6)_2$ .....	127
Reactions comparing the activity of $[\text{Fe}_2\text{O}(\text{O}_2\text{CCH}_3)_2(\text{HBpz}_3)_2]$ , $[\text{Fe}_2\text{O}(\text{O}_2\text{CCH}_3)_2(\text{Me}_3\text{TACN})_2](\text{PF}_6)_2$ , $(\text{Et}_4\text{N})_2[\text{Fe}_2\text{OCl}_6]$ and other iron compounds.....	130
Reactions with $(\text{Et}_4\text{N})_2[\text{Fe}_2\text{OCl}_6]$ and dithiothreitol .....	132
Reactions with $(\text{Et}_4\text{N})_2[\text{Fe}_2\text{OCl}_6]$ and ascorbic acid or tetramethyl reductic acid..	136
Controls .....	140
Factors affecting reactivity of system.....	145
Probing the nature of the oxidant and mechanism .....	152
Preliminary attempts at characterization of the purple species. ....	157
Summary and Conclusions .....	163
Appendix I Vibrational Analysis of $[\text{Fe}_2(\text{O}_2\text{P}(\text{OC}_6\text{H}_5)_2)_2(\text{HBpz}_3)_2]$ .....	167
Experimental .....	169
Results and Discussion .....	171
Appendix II Programs for Collection and Plotting of Sequential Spectra for use with a Perkin-Elmer Series 3600 Data Station and PECUV Software.....	181
Acknowledgements .....	189



## LIST OF FIGURES

	Page
CHAPTER 2	
Figure 1.	$^1\text{H}$ NMR spectrum of $\text{N}_2\text{S-TTP}$ in $\text{CDCl}_3$ ..... 48
Figure 2.	$^1\text{H}$ and $^{13}\text{C}$ NMR spectra of $\text{N}_2\text{S-xy-TTP}$ ..... 52
Figure 3.	Results from HETCOR experiment on $\text{N}_2\text{S-xy-TTP}$ ..... 54
Figure 4.	Aliphatic region of the $^{13}\text{C}$ spectrum of <b>3</b> in $\text{CDCl}_3$ and $^{13}\text{C}$ chemical shifts of 2-pyrrolidone..... 55
Figure 5.	EPR spectra of <b>6a-6c</b> ..... 63
Figure 6.	EPR spectra of <b>7a-7c</b> ..... 63
Figure 7.	EPR spectra of <b>6d</b> and <b>7d</b> ..... 65
CHAPTER 3	
Figure 1.	The UV-visible spectra of $(\text{Et}_4\text{N})[\text{Fe}_4\text{O}_2(\text{O}_2\text{CC}_6\text{H}_5)_7(\text{H}_2\text{Bpz}_2)_2]$ , $[\text{Fe}_4\text{O}_2(\text{O}_2\text{CC}_6\text{H}_5)_7(\text{Me}_2\text{bipy})_2](\text{BPh}_4)$ and <b>4</b> in $\text{CH}_2\text{Cl}_2$ ..... 79
Figure 2.	ORTEP drawing of the anion of $(\text{Et}_4\text{N})[\text{Fe}_4\text{O}_2(\text{O}_2\text{CC}_6\text{H}_5)_7(\text{H}_2\text{Bpz}_2)_2]$ and the cation, $[\text{Fe}_4\text{O}_2(\text{O}_2\text{CC}_6\text{H}_5)_7(\text{Me}_2\text{bipy})_2]^+$ ..... 83
Figure 3.	Diagram of the $\{\text{Fe}_4\text{O}_2\}^{8+}$ core in $(\text{Et}_4\text{N})[\text{Fe}_4\text{O}_2(\text{O}_2\text{CC}_6\text{H}_5)_7(\text{H}_2\text{Bpz}_2)_2]$ and $[\text{Fe}_4\text{O}_2(\text{O}_2\text{CC}_6\text{H}_5)_7(\text{Me}_2\text{bipy})_2](\text{BPh}_4)$ showing bond distances and angles..... 84
Figure 4.	View of tetranuclear core of $[\text{Fe}_4\text{O}_2(\text{O}_2\text{CC}_6\text{H}_5)_7(\text{Me}_2\text{bipy})_2](\text{BPh}_4)$ showing displacement of Fe3 and Fe4 away from the nearly planar, central $\{\text{Fe}_2\text{O}_2\}$ unit..... 84
Figure 5.	$^1\text{H}$ NMR spectra of $(\text{Et}_4\text{N})[\text{Fe}_4\text{O}_2(\text{O}_2\text{CC}_6\text{H}_5)_7(\text{H}_2\text{Bpz}_2)_2]$ and $(\text{Et}_4\text{N})[\text{Fe}_4\text{O}_2(\text{O}_2\text{CCH}_3)_7(\text{H}_2\text{Bpz}_2)_2]$ in $\text{CD}_2\text{Cl}_2$ ..... 86
Figure 6.	$^1\text{H}$ NMR spectra of $[\text{Fe}_4\text{O}_2(\text{O}_2\text{CC}_6\text{H}_5)_7(\text{Me}_2\text{bipy})_2]\text{Cl}$ and $[\text{Fe}_4\text{O}_2(\text{O}_2\text{CC}_6\text{H}_5)_7(\text{Me}_2\text{bipy})_2](\text{BPh}_4)$ in $\text{CD}_2\text{Cl}_2$ ..... 88
Figure 7.	$^1\text{H}$ NMR spectrum of <b>4</b> in $\text{CD}_2\text{Cl}_2$ ..... 90
Figure 8.	Raman spectrum of $(\text{Et}_4\text{N})[\text{Fe}_4\text{O}_2(\text{O}_2\text{CC}_6\text{H}_5)_7(\text{H}_2\text{Bpz}_2)_2]$ in $\text{CH}_3\text{CN}$ with 488 nm excitation..... 91
Figure 9.	Raman spectrum of $(\text{Et}_4\text{N})[\text{Fe}_4\text{O}_2(\text{O}_2\text{CC}_6\text{H}_5)_7(\text{H}_2\text{Bpz}_2)_2]$ in $\text{CH}_3\text{CN}$ collected as various excitation wavelengths. .... 93

Figure 10.	Raman spectrum of $[\text{Fe}_4\text{O}_2(\text{O}_2\text{CC}_6\text{H}_5)_7(\text{Me}_2\text{bipy})_2](\text{BPh}_4)$ in $\text{CH}_2\text{Cl}_2$ with 488 nm excitation.....	94
Figure 11.	First and sixth scan averaged into spectrum shown in Figure 10.....	95
Figure 12.	Raman spectra of $[\text{Fe}_4\text{O}_2(\text{O}_2\text{CC}_6\text{H}_5)_7(\text{Me}_2\text{bipy})_2](\text{BPh}_4)$ from 500 to $1100\text{ cm}^{-1}$ collected at 488 nm and 514 nm excitation .....	98
CHAPTER 4		
Figure 1.	Visible spectra of a 50:1 mixture of dithiothreitol and $(\text{Et}_4\text{N})_2[\text{Fe}_2\text{OCl}_6]$ ..	133
Figure 2.	Rate of formation of cyclohexanol and cyclohexanone for $(\text{Et}_4\text{N})_2[\text{Fe}_2\text{OCl}_6]$ in the presence of AA and TMRA .....	139
Figure 3.	Rate of formation of cyclohexanol for $(\text{Et}_4\text{N})_2[\text{Fe}_2\text{OCl}_6]$ versus $\text{FeCl}_2$ and $(\text{Et}_4\text{N})[\text{FeCl}_4]$ .....	141
Figure 4.	GC traces recorded of samples from cyclohexane oxidation reaction mixtures .....	144
Figure 5.	Effect of solvent on cyclohexanol formation catalyzed by $(\text{Et}_4\text{N})_2[\text{Fe}_2\text{OCl}_6]$ in the presence of AA .....	146
Figure 6.	The effect of base on cyclohexanol formation catalyzed by $(\text{Et}_4\text{N})_2[\text{Fe}_2\text{OCl}_6]$ and $(\text{Et}_4\text{N})[\text{FeCl}_4]$ in the presence of AA .....	150
Figure 7.	Effect of $\text{Et}_3\text{N}$ on cyclohexanol formation catalyzed by $(\text{Et}_4\text{N})_2[\text{Fe}_2\text{OCl}_6]$ and $(\text{Et}_4\text{N})[\text{FeCl}_4]$ in the presence of AA .....	151
Figure 8.	Effect of $\text{Et}_3\text{N}$ on cyclohexanol formation catalyzed by $(\text{Et}_4\text{N})_2[\text{Fe}_2\text{OCl}_6]$ and $(\text{Et}_4\text{N})[\text{FeCl}_4]$ in the presence of TMRA .....	151
Figure 9.	Oxidation of cyclohexene by air catalyzed by $(\text{Et}_4\text{N})_2[\text{Fe}_2\text{OCl}_6]$ in the presence of AA in acetone .....	153
Figure 10.	Autoxidation of cyclohexene catalyzed by $(\text{Et}_4\text{N})_2[\text{Fe}_2\text{OCl}_6]$ in acetone ...	153
Figure 11.	Oxidation of cyclohexene by air catalyzed by $(\text{Et}_4\text{N})[\text{FeCl}_4]$ in the presence of AA in acetone .....	155
Figure 12.	Oxidation of cyclohexene by air catalyzed by $\text{FeCl}_2(\text{anhydrous})$ in the presence of AA in acetone .....	155
Figure 13.	Visible spectra of intensely colored iron-reductive acid complexes .....	160
Figure 14.	Proposed mechanism for the oxidation of alkanes by dioxygen based on a oxo-bridged dinuclear iron catalyst.....	166
APPENDIX I		
Figure 1.	Raman spectra of $[\text{Fe}_2\text{O}(\text{O}_2\text{P}(\text{OC}_6\text{H}_5)_2)_2(\text{HBpz}_3)_2]$ and its $^{18}\text{O}$ substituted derivative in $\text{CH}_2\text{Cl}_2$ with 457.9 nm excitation.....	172

- Figure 2. FTIR spectra of  $[\text{Fe}_2\text{O}(\text{O}_2\text{P}(\text{OC}_6\text{H}_5)_2)_2(\text{HBpz}_3)_2]$  and its  $^{18}\text{O}$  substituted derivative. .... 173
- Figure 3. FTIR difference spectrum generated by subtracting the ( $^{16}\text{O}$ ) spectrum from the ( $^{18}\text{O}$ ) spectrum shown in Figure 2 ..... 174
- Figure 4. Excitation profile of the  $\nu_s$  (Fe-O-Fe) of  $[\text{Fe}_2\text{O}(\text{O}_2\text{P}(\text{OC}_6\text{H}_5)_2)_2(\text{HBpz}_3)_2]$  generated using available wavelengths from an Ar laser..... 179
- Figure 5. UV-visible spectra of  $[\text{Fe}_2\text{O}(\text{O}_2\text{P}(\text{OC}_6\text{H}_5)_2)_2(\text{HBpz}_3)_2]$  and  $[\text{Fe}_2\text{O}(\text{O}_2\text{CCH}_3)_2(\text{HBpz}_3)_2]$  from 250 to 800 nm in  $\text{CH}_2\text{Cl}_2$  ..... 180

## LIST OF SCHEMES

	Page
CHAPTER 2	
Scheme I. Syntheses of N <sub>2</sub> S-TTP and N <sub>2</sub> S-xy-TTP .....	44
Scheme II. Syntheses of complexes based on NH <sub>2</sub> -TPP .....	45

## LIST OF TABLES

	Page
CHAPTER 2	
Table I. <sup>13</sup> C Chemical Shift Assignments .....	49
Table II. EPR g <sub>  </sub> and A <sub>  </sub> Values for Heterobimetallic Products .....	62
CHAPTER 3	
Table I. Summary of Crystal Data, Intensity Collection, and Structure Refinement for [Fe <sub>4</sub> O <sub>2</sub> (O <sub>2</sub> CPh) <sub>7</sub> (Me <sub>2</sub> Bipy) <sub>2</sub> ](BPh <sub>4</sub> ) · CH <sub>3</sub> CN .....	81
Table II. Selected bond lengths and angles for the cation, [Fe <sub>4</sub> O <sub>2</sub> (O <sub>2</sub> CC <sub>6</sub> H <sub>5</sub> ) <sub>7</sub> (Me <sub>2</sub> bipy) <sub>2</sub> ] <sup>+</sup> .....	82
Table III. Assignment of Observed Raman Bands for (Et <sub>4</sub> N)[Fe <sub>4</sub> O <sub>2</sub> (O <sub>2</sub> CC <sub>6</sub> H <sub>5</sub> ) <sub>7</sub> (H <sub>2</sub> Bpz <sub>2</sub> ) <sub>2</sub> ] and (Et <sub>4</sub> N)[Fe <sub>4</sub> O <sub>2</sub> (O <sub>2</sub> CCH <sub>3</sub> ) <sub>7</sub> (H <sub>2</sub> Bpz <sub>2</sub> ) <sub>2</sub> ] .....	92
Table IV. Assignment of Observed Raman Bands for [Fe <sub>4</sub> O <sub>2</sub> (O <sub>2</sub> CPh) <sub>7</sub> (Me <sub>2</sub> Bipy) <sub>2</sub> ](BPh <sub>4</sub> ) .....	97
CHAPTER 4	
Table I. Activity and Product Specificity of Iron Compounds in the Presence of Various Reductants for the Oxidation of Cyclohexane by Air .....	131
Table II. Catalytic Activity of (Et <sub>4</sub> N) <sub>2</sub> [Fe <sub>2</sub> OCl <sub>6</sub> ] and FeCl <sub>3</sub> ·6H <sub>2</sub> O in the Presence of Dithiothreitol for the Oxidation of Cyclohexane by Dioxygen .....	135
Table III. Time Versus Cyclohexanol Produced at Various Catalyst Concentrations .	148
APPENDIX I	
Table I. Assignment of Observed Raman Bands for [Fe <sub>2</sub> O(O <sub>2</sub> P(OC <sub>6</sub> H <sub>5</sub> ) <sub>2</sub> ) <sub>2</sub> (HBpz <sub>3</sub> ) <sub>2</sub> ] .....	175
Table II. Comparison of Vibrational Data for [Fe <sub>2</sub> O(O <sub>2</sub> CCH <sub>3</sub> ) <sub>2</sub> (HBpz <sub>3</sub> ) <sub>2</sub> ], [Fe <sub>2</sub> O(O <sub>2</sub> CCH <sub>3</sub> ) <sub>2</sub> (TACN) <sub>2</sub> ] and [Fe <sub>2</sub> O(O <sub>2</sub> P(OC <sub>6</sub> H <sub>5</sub> ) <sub>2</sub> ) <sub>2</sub> (HBpz <sub>3</sub> ) <sub>2</sub> ] .....	175

LIST OF ABBREVIATIONS

NMR	nuclear magnetic resonance
EPR	electron paramagnetic resonance
MCD	magnetic circular dichroism
EXAFS	extended x-ray absorption fine structure
ENDOR	electron nuclear double resonance
GC	gas chromatography
MS	mass spectrometry
TPP	tetraphenylporphyrin
TTP	tetratolylporphyrin
TPPS	tetra(p-sulfonato)phenylporphyrin
NADH	reduced nicotinamide adenine dinucleotide
MeNAH	reduced N-methyl nicotinamide
OAc	acetate
bipy	bipyridine
Ph	phenyl
Bz	benzyl
br	broad
s	singlet
d	doublet
t	triplet
m	multiplet
hr	hour
min	minute

CHAPTER 1  
Introduction

Iron-oxygen interactions are important in a wide variety of biochemical processes. Iron plays a role in almost all types of reactivity associated with oxygen metabolism. The biochemistry of oxygen consists of its transport and storage as well as its roles in oxygenation chemistry and its reduction to water as a terminal oxidant, supplying energy for oxidative phosphorylation in aerobic organisms. Proteins involved in all these functions contain iron.<sup>1</sup> In hemoglobin and myoglobin, the heme iron center forms the site for reversible binding of dioxygen. For oxygen to bind to iron reversibly, only a weak interaction can occur between the two since the bond between oxygen and iron must be readily broken when the transport protein reaches its destination.<sup>2</sup> Iron, however, is also found in enzymes that catalyze the oxygenation of substrates. Cytochrome P450 and its isozymes are monooxygenases that catalyze the transfer of one atom of dioxygen to the substrate. These enzymes contain a heme center not unlike that in hemoglobin or myoglobin but the iron now plays a critical role in activating the oxygen for cleavage of the O-O bond and formation of a highly oxidizing species.<sup>1,3</sup> Many dioxygenases that activate dioxygen for the transfer of both atoms of oxygen to the substrate also contain heme or non-heme iron centers.<sup>1,4</sup> Iron is featured as well in the

---

<sup>1</sup> (a) Ingraham, L.L.; Meyer, D.L. *Biochemistry of Oxygen*; Plenum: New York, 1985. (b) Nozaki, M.; Yamamoto, S.; Ishimura, Y.; Coon, M.J.; Ernster, L.; Estabrook, R.W., eds. *Oxygenases and Oxygen Metabolism*; Academic, New York, 1982. (c) Wrigglesworth, J.M.; Baum, H. in *Iron in Biochemistry and Medicine, II*; Jacobs, A.; Worwood, M., eds., Academic: New York, 1980, 29-86.

<sup>2</sup> (a) Collman, J.P.; Halbert, T.R.; Suslick, K.S.; in *Metal Ion Activation of Dioxygen*; Spiro, T.G., ed., Wiley: New York, 1980, 2-72. (b) Rifkind, J.M.; *Adv. Inorg. Biochem.* 1988, 7, 155-244.

<sup>3</sup> (a) Coon, M.J.; White, R.E. in *Metal Ion Activation of Dioxygen*; Spiro, T.G., ed., Wiley: New York, 1980, 73-123. (b) Wagner, G.C.; Gunsalus, I.C. in *The Biological Chemistry of Iron*; Dunford, H.B.; Dolphin, D.; Raymond, K.R.; Sieker, L., eds., Reidel, Dordrecht, Holland, 1982, 405-412. (c) Ullrich, V.; Ahr, H.J.; Castle, L.; Kuthan, H.; Nastainczyk, W.; Ruf, H.H. in *The Biological Chemistry of Iron*; Dunford, H.B.; Dolphin, D.; Raymond, K.R.; Sieker, L., eds., Reidel, Dordrecht, Holland, 1982, 413-425. (e) Ortiz de Montellano, P.R., ed. *Cytochrome P450, Structure, Mechanism, and Biochemistry*; Plenum: New York, 1986.

<sup>4</sup> (a) Wood, J.M. in *Metal Ion Activation of Dioxygen*; Spiro, T.G., ed., Wiley: New York, 1980, 163-180. (b) Que, L. *Adv. Inorg. Biochem.* 1983, 5, 167-199.

biochemistry of hydrogen peroxide. Catalase, which catalyzes the decomposition of  $\text{H}_2\text{O}_2$  to water and dioxygen, is an iron metalloenzyme, as are some of the peroxidases, which catalyze the one electron oxidation of substrates by hydrogen peroxide.<sup>1,5</sup> The versatility of iron in its chemistry with oxygen is further demonstrated by its presence at the active site of cytochrome oxidase, where the four electron reduction of dioxygen to water takes place.<sup>6</sup> This site also contains a copper ion, and the resting state of the enzyme is believed to contain an oxo-bridge between the two metals.

The propensity of iron to form oxo- and hydroxo-bridges relates to another important aspect of iron-oxygen interactions, those involved in iron metabolism and storage. The tendency for iron to form insoluble oligomeric ferric-oxo complexes through hydration at physiological pH in aerobic conditions is a very important reaction in iron metabolism.<sup>7</sup> Oxygen species play a role both in the autoxidation of Fe(II) to Fe(III) and in the formation of the oxo- and hydroxo-linkages. This tendency for iron to form Fe-O bonds is a problem for many microorganisms. In order to sequester enough iron from their aqueous environment for proper functioning, these organisms have developed molecules with extremely high affinity for iron to aid in solubilizing and transporting this essential element.<sup>8</sup> This same propensity for iron-oxygen oligomerization is better controlled in higher organisms. For instance, iron is stored as polyiron-oxo units in ferritin. The core of the protein is known to grow through aggregation of iron by formation of oxo- and hydroxo-bridges, the initial steps of which require dioxygen. In the protein, the aggregation of iron-oxo units is controlled and

---

<sup>5</sup> Dunford, H.B.; Araiso, T.; Job, D.; Ricard, J.; Rutter, R.; Hager, L.P.; Wever, R.; Kast, W.M.; Boelens, R.; Ellfolk, N.; Rönberg, M. in *The Biological Chemistry of Iron*; Dunford, H.B.; Dolphin, D.; Raymond, K.R.; Sieker, L., eds., Reidel, Dordrecht, Holland, 1982, 337-355.

<sup>6</sup> Brunori, M.; Antonini, G.; Malatesta, F.; Sarti, P.; Wilson, M.T. *Adv. Inorg. Biochem.* 1988, 7, 93-153, and other references cited in the first footnote in Chapter 1.

<sup>7</sup> (a) May, P.M.; Williams, D.R. in *Iron in Biochemistry and Medicine, II*; Jacobs, A.; Worwood, M., eds., Academic: New York, 1980, 1-28. (b) Aisen, P. in *The Biological Chemistry of Iron*; Dunford, H.B.; Dolphin, D.; Raymond, K.R.; Sieker, L., eds., Reidel, Dordrecht, Holland, 1982, 63-83.

<sup>8</sup> Nielands, J.B. in *Iron in Biochemistry and Medicine, II*; Jacobs, A.; Worwood, M., eds., Academic: New York, 1980, 529-572.



reversible.<sup>9</sup> Also, dinuclear, Fe-O-Fe, structural units have been discovered in a number of proteins.<sup>10</sup> In several of these proteins, as in ferritin, iron-oxo interactions are important to their function and well as their structure. Hemerythrin contains an oxo-bridged dinuclear iron active site and is the oxygen transport enzyme in some marine invertebrates.<sup>11</sup> Similarly, methane monooxygenase is an oxygenase enzyme believed to contain an oxo- or hydroxo-bridged dinuclear iron core.<sup>12</sup>

Interestingly, considering the ubiquitous participation of iron in most aspects of oxygen biochemistry, there is one process from which it is conspicuously absent. The chemistry that is, in essence, the reverse of that catalyzed by cytochrome oxidase, the oxidation of two molecules of water to dioxygen, does not involve iron. The evolution of dioxygen from water, important in photosynthesis, has been shown to be dependent on manganese.<sup>1,13</sup> Spectroscopic studies have suggested that the oxygen evolution site in Photosystem II may contain a di- or tetranuclear oxo-bridged manganese unit.<sup>14</sup> Thus, in this enzyme, manganese is present in a structural unit common to iron involved in chemistry in which one might well expect iron to be involved. The reason that manganese rather than iron has been adapted by nature to catalyze oxygen evolution from water, is only one of many questions about iron-oxygen biochemistry that remain unanswered.

---

<sup>9</sup> (a) Harrison, P.M.; Clegg, G.A.; May, K. in *Iron in Biochemistry and Medicine, II*; Jacobs, A.; Worwood, M., eds., Academic: New York, 1980, 131-171. (b) Crichton, R.R. in *The Biological Chemistry of Iron*; Dunford, H.B.; Dolphin, D.; Raymond, K.R.; Sieker, L., eds., Reidel, Dordrecht, Holland, 1982, 45-83. (c) Theil, E. *Adv. Inorg. Biochem.* 1983, 5, 1-38.

<sup>10</sup> (a) Lippard, S.J. *Angew Chem., Int. Ed. Engl.* 1988, 27, 344-361. (b) Que, L. *ACS Symp. Ser.* 1988, in press.

<sup>11</sup> Wilkins, R.G.; Harrington, P.C. *Adv. Inorg. Biochem.* 1983, 5, 51-85.

<sup>12</sup> (a) Dalton, H.; Leak, D.J. in *Gas Enzymology*, Degn, H.; Cox, R.P.; Toftlund, H., eds., Reidel: Dordrecht, Holland, 1985, 169-186. (b) Woodland, M.P.; Patil, D.S.; Cammack, R.; Dalton, H. *Biochim. Biophys. Acta* 1986, 873, 237-242.

<sup>13</sup> Dismukes, G. C. *Photochem. Photobiol.* 1986, 43, 99-115.

<sup>14</sup> (a) de Paula, J.C.; Beck, W.F.; Brudvig, G.W. *J. Am. Chem. Soc.* 1986, 108, 4002-4009. (b) Brudvig, G. W.; Crabtree, R. H.; *Proc. Natl. Acad. Sci. USA* 1986, 83, 4586-4588.

One way in which to study factors that control the reactivity of iron with dioxygen or reduced oxygen species is through the synthesis and characterization of discrete model compounds. Significant contributions toward understanding the structure and function of such proteins as hemoglobin,<sup>2a,15</sup> cytochrome P450<sup>15,16</sup> and hemerythrin<sup>10</sup> have been achieved by this method. The following chapters describe model studies related to the topics introduced above. In the next chapter, progress toward the synthesis of a structural model for the active site of cytochrome oxidase is presented and discussed. The third chapter and first appendix deal with studies on tetranuclear and dinuclear iron-oxo compounds. In addition to being relevant to iron aggregation, the tetranuclear complexes have manganese analogs synthesized by other researchers who have proposed them as models for the oxygen evolution site in Photosystem II. The final chapter presents initial attempts to develop a model monooxygenase system for alkane oxidation based on a dinuclear iron catalyst. In such a system, intended as a model for methane monooxygenase, iron-oxygen interactions would be important to both the structure and function of the active species.

---

<sup>15</sup> Baldwin, J.E.; Perlmutter, P. *Top. Curr. Chem.* **1984**, *121*, 181-220.

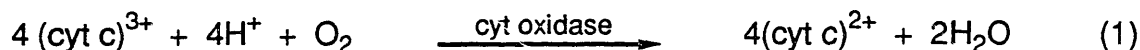
<sup>16</sup> (a) McMurray, T.J.; Groves, J.T. in *Cytochrome P450, Structure, Mechanism, and Biochemistry*; Ortiz de Montellano, P.R., ed. Plenum: New York, 1986, 1-28. (b) Mansuy, D. *Pure and Appl. Chem.* **1987**, *59*, 759-770.

## CHAPTER 2

### Toward the Synthesis of a Structural Model for the Active Site of Cytochrome Oxidase

Cytochrome oxidase plays a critical role in the metabolism of all respiring cells.<sup>1</sup> By catalyzing the four electron reduction of dioxygen to water, it allows cells to utilize O<sub>2</sub> to oxidize their foodstuffs. The enzyme also acts as a proton pump, building an electrochemical proton gradient across the inner mitochondrial membrane. The energy thus conserved is used by the cell for ATP synthesis. The enzyme is found in similar form in all eukaryotes and some prokaryotes. Its minimal functioning unit contains four metal centers which exhibit unique spectral characteristics. Because of its key physiological importance, the enzyme has been of great interest to scientist for nearly a hundred years. Although much progress has been made toward elucidating the function and structure of this complex enzyme, a thorough understanding of all its aspects is still far from being reached.

Cytochrome oxidase carries out an amazingly complex and difficult task. To achieve the reduction of O<sub>2</sub>, it must link a one e<sup>-</sup> donor, cytochrome *c*, to a 4 e<sup>-</sup> process (eq 1).



Furthermore, the enzyme accomplishes the reduction without the production of any intermediates, particularly the very reactive and poisonous 1 e<sup>-</sup> product, superoxide. The overall reaction is exothermic and the protein conserves the energy through a proton pumping mechanism. In addition to consuming 4 H<sup>+</sup> from the matrix side of the membrane in the reduction which uses 4e<sup>-</sup> transferred from the cytosol side, the enzyme is believed to transfer up to four more protons across the membrane. The net result is a build up of energy to be used in oxidative phosphorylation.

---

<sup>1</sup> This discussion is based on the following reviews: (a) Wikström, M.; Krab, K.; Saraste, M. *Cytochrome Oxidase: A Synthesis*; Academic: New York, 1981. (b) Brunori, M.; Wilson, M.T. *Trends Biochem. Sci.* **1982**, *8*, 295-299. (c) Chan, S.I.; Martin, C.T.; Wang, H.; Blair, D.F.; Gelles, J.; Brudvig, G.W.; Steens, T.H. In *Biochemical and Biophysical Studies of Proteins and Nucleic Acids*; Lo, T.-B.; Liu, T.-Y.; Li, C.-H., Eds., Elsevier: New York, 1984, 219-239. (d) Freedman, J.A.; Chan, S.H.P. *Bioenerg. Biomembr.* **1984**, *16*, 75-100. (e) Denis, M. *Biochim.* **1986**, *68*, 459-470. (f) Brunori, M.; Antonini, G.; Malatesta, F.; Sarti, P.; Wilson, M.T. *Adv. Inorg. Biochem.* **1988**, *7*, 93-154.

The mammalian enzyme is believed to contain 13 subunits which are situated across the inner mitochondrial membrane. The bacterial enzymes can be as small as 2 or even 1 subunit. All cytochrome oxidase enzymes, however, contain at least four metal centers, two heme *a* and two copper ions.<sup>2</sup> The heme groups, when extracted from the enzyme, are identical although within the enzyme they exhibit different physical properties. Therefore, they have been designated heme *a* and heme *a*<sub>3</sub>, the latter defined as the heme which bind exogenous ligands. The metal ions can be considered as two groups of one heme and one copper each. The copper ion which is located near to heme *a* is labelled Cu<sub>A</sub> and the other copper, which forms a binuclear center with heme *a*<sub>3</sub>, is labelled Cu<sub>B</sub>. The former two, located near the cytosol side of the membrane where cytochrome *c* is found, act as electron transfer and storage agents and are believed to be involved in the proton pumping mechanism. The heme *a*-Cu<sub>B</sub> center, buried in the hydrophobic membrane, forms the site for O<sub>2</sub> binding and reduction.

The physical and spectral properties of these metal centers have intrigued inorganic and well as biological chemists and motivated much work to elucidate the structures of these centers within the enzyme. The enzyme is isolated in what is known as the "resting oxidized" state, but several other forms of the enzyme have also been studied: they include the "pulsed" or "oxygenated" state, the fully reduced state, and partially reduced states with various ligands (CN<sup>-</sup>, NO, N<sub>3</sub><sup>-</sup>) bound. This discussion will deal mainly with the resting oxidized state. Assignment of the spectral features has been a complicated matter due to the presence of all four metals as well as to inhomogeneity of samples and, as a result, has been fraught with controversy.

The first evidence for the existence of the protein, was the observation of the Soret band in the optical spectrum. This band lies at 421 nm in the oxidized protein and is believed to arise from both heme groups. Other optical features from the hemes include a shoulder at

---

<sup>2</sup> Recently, some evidence has accumulated for the presence of at least one Zn and potentially a third Cu ion in the enzyme. See for example, Bombelka, E.; Richter, F-W.; Stroh, A.; Kadenbach, B. *Biophys. Biochem. Res. Commun.* **1986**, *140*, 1007-1014. There is also evidence for the presence of magnesium. See ref. 1f.

~550 nm and a peak at 598 nm. The spectrum shows a weak band at 655 nm which has been assigned the heme  $a_3$ -Cu<sub>B</sub> center and a band at ~830 nm arising from Cu<sub>A</sub>.

The EPR spectrum of the enzyme is extraordinary in several respects. It consists of a typical low spin heme signal with components at  $g = 3.0, 2.2,$  and  $1.5$  and a signal at  $g \sim 2.0$  assigned to Cu(II). Both these signals, however, account for only half the iron or copper in the protein. One heme and copper ion are EPR silent. The visible copper signal is unusual in that it falls at an abnormally low  $g$  value for copper and, at normal X band excitation, shows no hyperfine features. On partial reduction of the enzyme a signal at  $g \sim 6$  appears briefly, but the fully reduced species is completely EPR silent, as would be expected. The  $g \sim 6$  signal suggested the presence of a high spin heme.

The magnetic susceptibility measurements at various temperatures help to explain the phenomenon seen in the EPR spectrum. The results are best fit by the presence of two isolated  $S = 1/2$  centers, assigned as heme  $a$  and Cu<sub>A</sub>, and one  $S = 2$  center. The latter has been suggested to arise from a strong antiferromagnetic coupling between high spin Fe(III) in heme  $a_3$  and Cu<sub>B</sub>(II). For this center to be EPR silent, the required coupling would need to be on the order of  $|J| \geq 200 \text{ cm}^{-1}$ . For such a strong interaction to exist, a ligand known to promote magnetic coupling must bridge the two metals. An alternative explanation, that the  $S = 2$  center is actually an Fe(IV), ferryl center and Cu<sub>B</sub> remains as Cu(I) throughout the redox cycling, has been proved wrong by the detection of an EPR signal in a redox intermediate assignable to Cu<sub>B</sub>. Although the presence of strong antiferromagnetic coupling is generally accepted, the possibility that the EPR silence results from relaxation by the heme iron, potentially in an intermediate spin state, in close proximity to the Cu is still discussed in the literature.<sup>3</sup>

Investigations to elucidate the coordination site and structure of the metal ions in the enzyme have been pursued by both biophysical and inorganic chemists. Extensive EPR, ENDOR, and EXAFS studies have been carried out toward this end. Efforts have also been

---

<sup>3</sup> See for example, Elliot, C.M.; Akabori, K. *J. Am. Chem. Soc.* **1982**, *104*, 2671-2674.

extended to recreate the binding sites, particularly that of the binuclear center, in discrete inorganic model compounds which could be crystallographically characterized. The work to be presented herein is an example of the latter. When this work was begun in 1983, the heme *a*, Cu<sub>A</sub> sites were relatively well characterized, but definitive evidence about the coordination environment of the binuclear center was just beginning to accumulate. The model compounds which had been published either lacked the magnetic and EPR signatures of the center or were not crystallographically characterized. Since that time, a great deal of progress has been made toward establishing the coordination environment of all the metals, although controversy over the binuclear center in the native resting state persists.

The easiest of the metal centers to characterize has been the heme *a* site. MCD, EPR and Raman measurements established the site as low spin with two axial histidines. Babcock confirmed this assignment in 1981 by demonstrating that the EPR signal found in the enzyme could only be reproduced by bis(imidazole) coordination to heme *a*.<sup>1c</sup> Similarly, EPR and ENDOR studies proved that Cu<sub>A</sub> was coordinated by at least 1 S from cysteine and 1 imidazole from histidine.<sup>1c</sup> Although there is some disagreement about the genesis of the unusual EPR signal for Cu<sub>A</sub> site, the model of two nitrogen donors and two cysteine S donors to this site has held up through numerous EXAFS and ENDOR studies (see below).

The lack of an EPR signal and the presence of the second metal of each kind has made elucidation of the binuclear site much more difficult. An imidazolate bridge was initially suggested for the binuclear site since imidazolate was known to promote magnetic coupling.<sup>4</sup> This model required that the O<sub>2</sub> binding site be on the distal side of the heme rather than between the two metals. Several years later, an oxo bridged model was proposed based on the magnitude of coupling seen for oxo bridged model complexes and the fact that dioxygen was the substrate for the enzyme.<sup>5</sup> Early EXAFS studies by Powers *et al.*, indicated that heme *a*<sub>3</sub>

---

<sup>4</sup> Palmer, G.; Babcock, G.T.; Vickery, L.E. *Proc. Natl. Acad. Sci.* **1976**, *73*, 2206-2210.

<sup>5</sup> Reed, C.A.; Landrum, J.T. *FEBS Lett.* **1979**, *106*, 265-267.

contained a distal N donor, probably histidine, and determined the distance between the two metals to be  $\sim 3.75 \text{ \AA}$ .<sup>6</sup> This distance eliminated the possibility of an imidazolate bridge since such a bridge would require an intermetallic distance of at least  $5 \text{ \AA}$ . Furthermore, the authors suggested that the bridging atom was sulfur.<sup>6</sup>

From studying both the Cu X-ray edge and EXAFS of the enzyme in various oxidation states, Powers *et al.* claimed that the changes in the edge structure brought on by reduction of the Cu<sub>B</sub> site could be modelled by similar changes in the edge structure of stellacyanin upon reduction. Using stellacyanin as a model for the Cu<sub>B</sub> site, they then made assignments of the contribution of each copper to the EXAFS spectrum. Thus, the Cu<sub>B</sub> coordination sphere was found to consist of two nitrogen donors and the bridging sulfur with a short Cu-S distance.<sup>6</sup> In later work, they refined this model, adding a sulfur at a long distance from Cu<sub>B</sub>, making the coordination sphere, 2 N and 2 S with one long and one short Cu-S distance.<sup>7</sup> Upon reduction of the enzyme, the Cu-S distances became normal.<sup>6</sup> Other researchers have presented different EXAFS results but Powers and Chance claim that only enzyme from the preparation used for their studies represents the actual resting state of the enzyme *in vivo*.<sup>7a</sup> Recently, they were able to collect data on membrane bound enzyme and found the data collected to be consistent with their previously published results.<sup>8</sup>

Scott *et al.*, however, have claimed that attributing specific Cu EXAFS data to a given Cu site in the enzyme is a risky business.<sup>9</sup> They have shown that two sets of copper sites can fit the data equally well although the different models would give contradictory interpretations of the ligation around the Cu centers. From their studies of Cu EXAFS of cytochrome oxidase, they found no evidence for a short Cu-S distance and have determined a Cu-Fe

---

<sup>6</sup> Powers, L. Chance, B.; Ching, Y.; Angiolillo, P. *Biophys. J.* **1981**, *34*, 465-498.

<sup>7</sup> (a) Powers, L.; Chance, B. *J. Inorg. Biochem.* **1985**, *23*, 207-217. (b) Chance, B.; Powers, L. *Curr. Top. Bioenerg.* **1985**, *14*, 1-19.

<sup>8</sup> Powers, L.; Chance, B.; Ching, Y.C.; Chuan, P. *J. Biol. Chem.* **1987**, *262*, 3160-3164.

<sup>9</sup> (a) Scott, R.A.; Schwartz, J.R.; Cramer, S.P. *Biochemistry*, **1986**, *25*, 5546-5555. (b) Scott, R.A.; Schwartz, J.R.; Cramer, S.P. In *Biological and Inorganic Copper Chemistry*; Karlin, K.D.; Zubieta, J., Eds., Adenine: New York, 1985, 41-52.



distance of  $\sim 3.00 \text{ \AA}$ . By studying a number of different preparations of the enzyme, they found that the differences in the data after manipulations were less than their margin of error except for the preparation used by Powers *et al.* in which they could find no evidence of Fe backscatter. They report the total copper ligation to be  $6 \pm 1$  N or O donors at  $1.99 \pm 0.03 \text{ \AA}$  and  $2 \pm 1$  S donors at  $2.28 \pm 0.02 \text{ \AA}$ .<sup>9</sup> Very recently, in collaboration with Chan, Scott has reported the Cu EXAFS of a  $\text{Cu}_A$  depleted enzyme.<sup>10</sup> From these results, they assign the  $\text{Cu}_B$  coordination sphere as having 3 N or O donors and 1 S or Cl donor. The Cu-S distance is rather long,  $2.3 \text{ \AA}$ , suggesting methionine as a more likely donor than cysteine, but the possibility of  $\text{Cl}^-$  coordination at this site cannot be ruled out.

The discrepancy between these models are not insignificant. Chan has suggested that since  $\text{O}_2$  is bound and reduced at the active site, an oxo or hydroxo bridge in the resting oxidized state is more reasonable than the sulfur proposed by Powers.<sup>11</sup> In support of their results, Powers *et al.*, in 1981, referred to the similarity in the amino acid sequences of stellacyanin to that of subunit II in cytochrome oxidase.<sup>6</sup> A more recent publication on this topic, however, suggests that homologies to blue copper proteins occur at the binding site of  $\text{Cu}_A$ .<sup>12,1f</sup> This study also suggested that there are similarities between the amino acid sequence at the Cu binding site in SOD, the type 3 site in ceuroplasmin and the  $\text{Cu}_B$  site in cytochrome oxidase.<sup>12</sup> ENDOR studies have also suggested that type 3 Cu sites and the  $\text{Cu}_B$  site may be analogous, all having 3 N donors.<sup>1e,f</sup> Unfortunately, inorganic models of the active site have not been able to clarify the situation.

Despite the efforts of many researchers, no crystallographically characterized model compound for the binuclear site exists that exhibits the correct spectral properties. Palmer's early suggestion of an imidazolate bridge has motivated a number of attempts to prepare model compounds to assess the viability of such a bridge for a strongly magnetically coupled system.

---

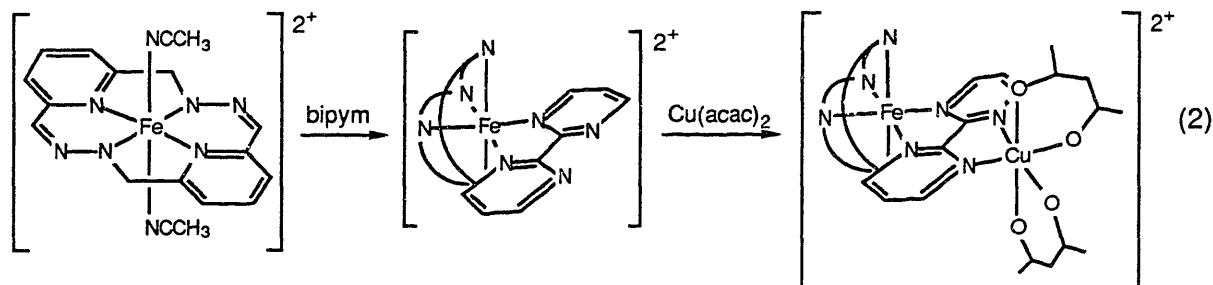
<sup>10</sup> Li, P.M.; Gelles, J.; Chan, S.I.; Sullivan, R.J.; Scott, R.A. *Biochemistry*, **1987**, *26*, 2091-2095

<sup>11</sup> Personal communication from S.I.Chan, 1985.

<sup>12</sup> Malmström, B.G. *Chem. Scr.* **1986**, *26B*, 285-286.

In 1978, Landrum *et al.*<sup>13</sup> examined polymeric and binuclear iron and manganese imidazolate bridged systems. From their studies on the magnetic interactions in these compounds, they concluded that imidazolate was not a good ligand for strong magnetic exchange with these metals and proposed an oxo bridge model.<sup>5</sup> In the following year, Prosperi and Tomlinson published the results of their studies on the reaction of  $\text{Cu}(\text{acac})_2$  with bisimidazole iron porphyrin species.<sup>14</sup> They also concluded that imidazolate did not support any strong interactions between the metals.

L. Wilson and his group have studied imidazolate bridged species for nearly ten years. In their first publications on the subject,<sup>15</sup> they proposed a bipyrimidine (bipym) bridged species for the product of the reaction of  $\text{Cu}(\text{acac})_2$  with a bipym bound Fe(II) macrocyclic complex (eq 2). They found no magnetic exchange between the metals and stated their support



for Reed and Landrum's oxo-bridged model.<sup>15b</sup> More recently, however, Sinn and coworkers have proved that the complex Wilson *et al.* obtained could not have the proposed bipym bridged structure.<sup>16</sup>

Several years later, Wilson *et al.* proposed an imidazolate bridge species synthesized by a method previously introduced by Kovacs and Shepherd. Kovacs and Shepherd started with

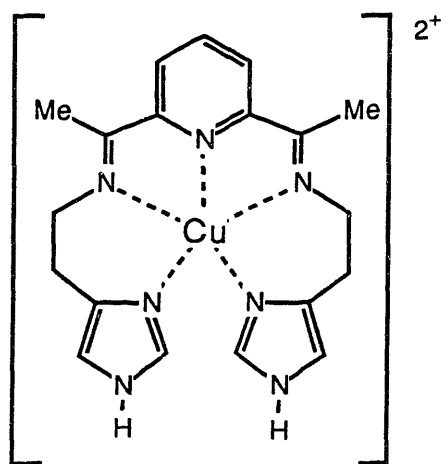
<sup>13</sup> (a) Landrum, J.T.; Reed, C.A.; Hatano, K.; Scheidt, W.R. *J. Am. Chem. Soc.* **1978**, *100*, 3232-3234. (b) Landrum, J.T.; Hatano, K.; Scheidt, W.R.; Reed, C.A. *J. Am. Chem. Soc.* **1980**, *102*, 6729-6735.

<sup>14</sup> Prosperi, T.; Tomlinson, A.G. *J. Chem. Soc., Chem. Commun.* **1979**, 196-197.

<sup>15</sup> (a) Petty, R.H.; Wilson, L.J. *J. Chem. Soc., Chem. Commun.* **1978**, 483-485. (b) Petty, R.H.; Welch, B.R.; Wilson, L.J.; Bottomley, L.A.; Kadish, K.M. *J. Am. Chem. Soc.* **1980**, *102*, 611-620.

<sup>16</sup> Brewer, G.A.; Sinn, E. *Inorg. Chem.* **1984**, *23*, 2532-2537.

a Cu macrocyclic complex where the imidazole moiety was part of the macrocycle.<sup>17</sup> They then allowed this complex to react with a macrocyclic Fe(II) species and showed evidence for the formation of a binuclear compound. Wilson *et al.* chose a 5 coordinate macrocyclic ligand with an available imidazole moiety, [(imidH)<sub>2</sub>DAP], to bind Cu(II). The copper complex was



[Cu(imidH)<sub>2</sub>DAP]<sup>2+</sup>

combined with Fe(TPP)X, where X = Cl<sup>-</sup> or CF<sub>3</sub>OSO<sub>2</sub><sup>-</sup>, in the presence of a strong base.<sup>18</sup> Polycrystalline, analytically pure solids were isolated. When X = Cl<sup>-</sup>, the resulting complex showed characteristics of two isolated S = 1/2 centers. With the CF<sub>3</sub>OSO<sub>2</sub><sup>-</sup> anion, however, the binuclear species was essentially EPR silent and exhibited complex magnetic behavior.

Although a mixture of spin states was apparent, the authors were able to conclude that the species was strongly antiferromagnetically coupled. Unfortunately, the complexes were subject to complicated solution equilibria which precluded solution measurements. In 1985, however, Wilson and coworkers combined the same Cu(II) complex with Mn(TPP) to obtain a complex isoelectronic with a Fe(III)-Cu(II) center which could be isolated and redissolved and which manifested the spectral features of the cytochrome oxidase active site.<sup>19</sup> No crystal structure of the complex has been published.

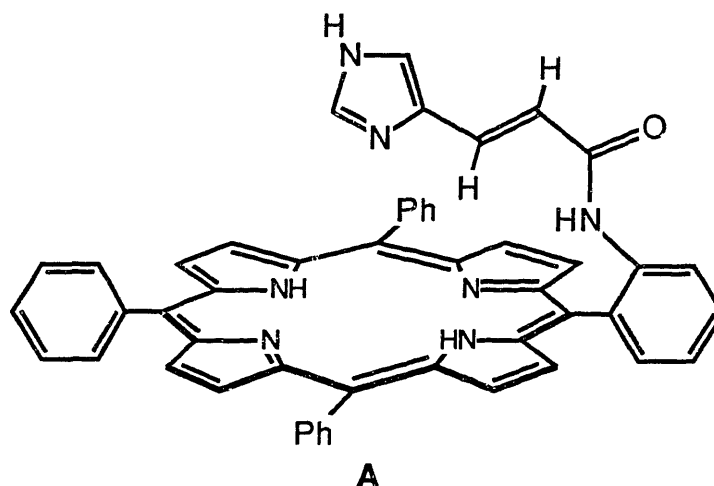
In another study,<sup>20</sup> Wilson and coworkers synthesized a porphyrin with an appended imidazole (A). A binuclear complex was obtained by reaction of the ferric derivative of this porphyrin with Cu(acac)<sub>2</sub>. This imidazolate bridged species, however, showed no magnetic coupling. From their numerous studies, Wilson *et al.* conclude that imidazolate is able, under

<sup>17</sup> Kovacs D.; Shepherd, R.E. *J. Inorg. Biochem.* **1979**, *10*, 67-88.

<sup>18</sup> Dessens, S.E.; Merrill, C.L.; Saxton, R.J.; Ilaria, R.L.; Lindsey, J.W.; Wilson, L.J. *J. Am. Chem. Soc.* **1982**, *104*, 4357-4361.

<sup>19</sup> Chunplang, V.; Wilson, L.J. *J. Chem. Soc., Chem. Commun.* **1985**, 1761-1763.

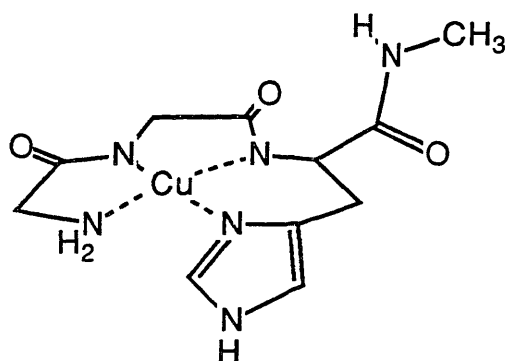
<sup>20</sup> Saxton, R.J.; Wilson, L.J. *J. Chem. Soc., Chem. Commun.* **1984**, 359-361.



certain conditions, promote the type of coupling proposed for the heme  $a_3$ -Cu<sub>3</sub> site.

Unfortunately, they do not discuss the factors which affect the ability of imidazolate to support magnetic exchange in their compounds.

Two other recent publications have also dealt with imidazolate bridged species. Cutler *et al.* synthesized a small polypeptide to use as a Cu binding site.<sup>21</sup> The glycylglycyl-L-



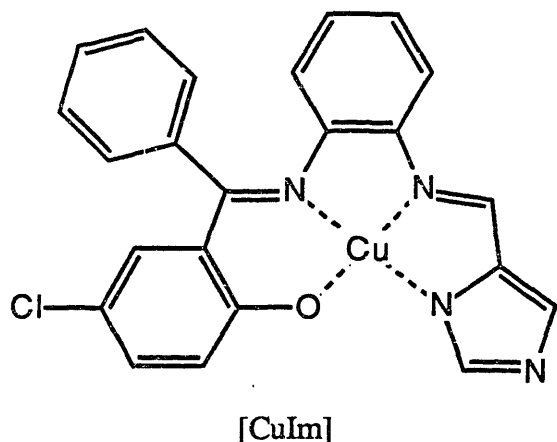
[Cu(glycylglycyl-L-histidine-N-methyl amide)]

histidine-N-methyl amide ligand has four N donors which are proposed to form a squareplanar environment around the copper. The Cu(II) complex was allowed to react with Fe(TPPS)Cl, a water soluble ferric porphyrin. The authors present evidence for the formation of a 1:1 complex which appeared

to be EPR silent, but they cannot isolate the binuclear complex as a solid. Brewer and Brewer have also studied complex formation between a Cu(II) complex with available imidazole binding site, [CuIm], and metalloporphyrins.<sup>22</sup> They found that only the bisligated heme,

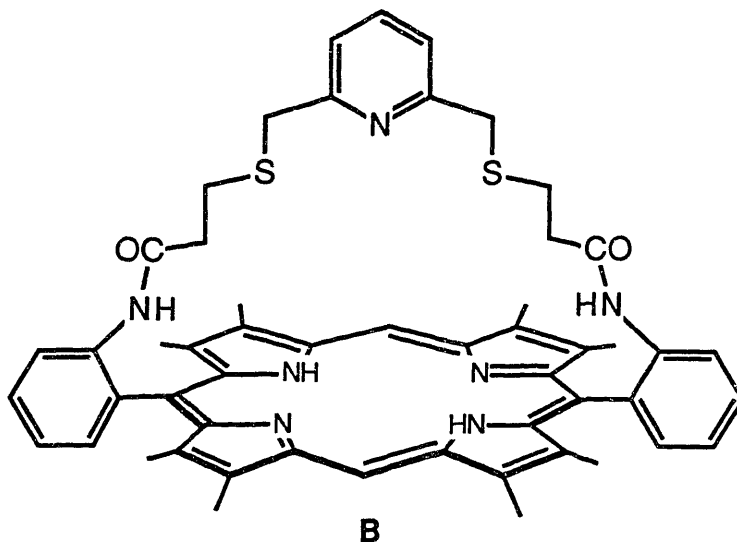
<sup>21</sup> Cutler, A.C.; Brittain, T.; Boyd, P.D.W. *J. Inorg. Biochem.* **1985**, *24*, 199-209.

<sup>22</sup> Brewer, C.T.; Brewer, G.A. *J. Inorg. Biochem.* **1986**, *26*, 247-255.



[[CuIm]<sub>2</sub>Fe(TTP)], could be formed in solution. As with coordination of imidazole to ferric porphyrins, the rate constant for addition of a second [CuIm] is much greater than that for addition of the first. As a result, they observe only a trinuclear species containing a low spin ferric porphyrin.

Several models with oxo or hydroxo bridges have also been reported. Gunter and coworkers synthesized a ligand based on a meso-aryl substituted porphyrin with a strap containing a S-N-S binding site for a copper ion (B).<sup>23</sup> The isolated iron-copper compound which was characterized from chemical analysis as hydroxo bridged, produced an EPR

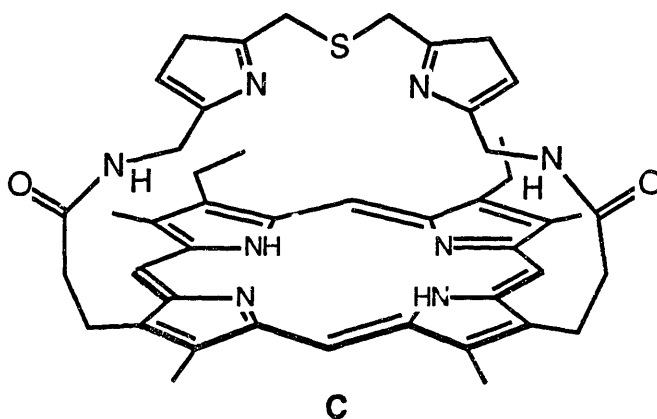


spectrum with both a rhombically distorted, high spin heme iron signal and a broad copper signal with ill-defined hyperfine splitting. Magnetic susceptibility measurements suggested a quantum mechanical mixing or equilibrium of  $S = 3/2$  and  $S = 1/2$  spin states for the heme, but little or no coupling between the metals ions. The authors were able to isolate a small amount

<sup>23</sup> Gunter, J.J.; Mander, L.N.; Murray, K.S.; Clark, P.E. *J. Am. Chem. Soc.* 1981, 103, 6784-6787.

of a second compound containing both copper and iron which gave rise to EPR signals the integration of which accounted for less than 5% of the metal ions present. Single crystals of the compounds could not be obtained, however, to verify the presence or identity of a bridging ligand in these compounds.

Chang *et al.* also developed a strapped porphyrin system.<sup>24</sup> They attached the strap to two  $\beta$  positions on the same side of the porphyrin ring, obtaining an unsymmetrically strapped ligand with a N-S-N site for copper (C). They isolated a heterodinuclear species which they



characterized as oxo bridged. The complex exhibited a band in the IR spectrum at  $880\text{ cm}^{-1}$ , consistent with an M-O-M stretch. The variable temperature magnetic susceptibility measurements for the compound could be fit assuming an  $S = 5/2$  center coupled to an  $S = 1/2$  center with  $-3J = 132 \pm 5\text{ cm}^{-1}$ . The signals in the EPR spectrum integrated to less than 40% of the metal ions present. Coordination around the copper was suggested to be distorted tetrahedral, but again, lack of a crystal structure prohibited definitive identification of the geometry at either metal site.

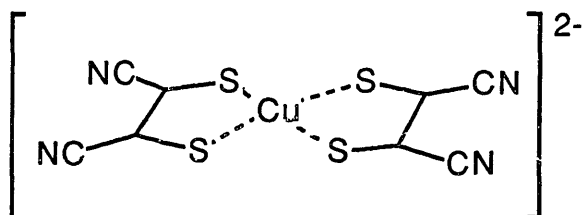
A third oxo bridged model has been presented by Wilson *et al.*<sup>25</sup> They obtained a binuclear complex through the reaction of high valent (TPP)Fe(IV)=O with the Cu(I) complex of [(imidH<sub>2</sub>)DAP]. The presence of a M-O-M stretch in the IR spectrum was confirmed by an

<sup>24</sup> Chang, D.K.; Koo, M.S.; Ward, B. *J. Chem. Soc., Chem. Commun.* **1982**, 716-719.

<sup>25</sup> Saxton, R.J.; Olson, L.W.; Wilson, L.J. *J. Chem. Soc., Chem. Commun.* **1982**, 984-986.

$^{18}\text{O}$  labelling experiment. The complex was EPR silent and showed magnetic behavior which could be fit by strong antiferromagnetic coupling between the centers resulting in an  $S = 1$  ground state, as opposed to the  $S = 2$  ground state proposed for the enzyme.

Two complexes with sulphur bridging between a ferric heme and a Cu(II) ion have been reported by Elliot *et al.*<sup>3,26</sup> A trinuclear species with  $[\text{Cu}(\text{MNT})_2]^{2-}$  sandwiched between



$[\text{Cu}(\text{MNT})_2]^{2-}$

two Fe(TPP) was first synthesized.

EXAFS data on the compound supported the presence of sulfur bridges. No magnetic coupling was observed and the lack of EPR signal

was attributed to relaxation of the Cu(II) by the intermediate spin ferric heme in close proximity. Slight changes in synthetic conditions allowed for the isolation of a complex which was revealed by an x-ray diffraction study to be tetranuclear. The authors proposed that this structure was essentially that of the trinuclear species with a  $[\text{Cu}(\text{MNT})_2]^{2-}$  capping one of the hemes, making the iron 6 coordinate. They claim that the interatomic distances in this complex match well with those reported from EXAFS studies<sup>6,7</sup> of the active site of cytochrome oxidase.

Several research groups have studied the addition of Cu(I) and Cu(II) species to hemes and have proposed interaction through vinyl<sup>27</sup> or carboxylate groups<sup>28</sup> on the porphyrin periphery. In one case, the carboxylate moiety of a tripeptide bound to Cu(II) was proposed to bind to the axial position of the ferric heme.<sup>29</sup> No complex of either type has been isolated as a solid.

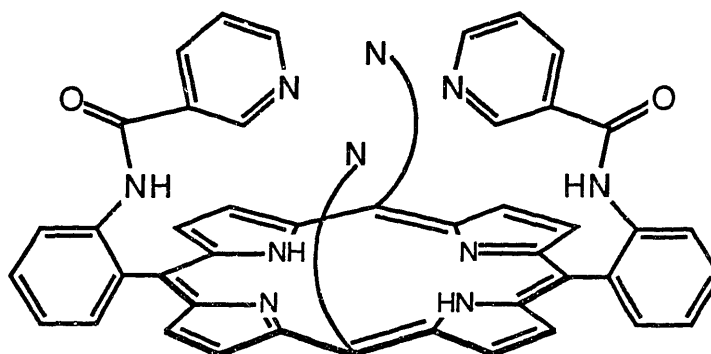
<sup>26</sup> Elliot, C.M.; Akabori, K. *J. Am. Chem. Soc.* **1982**, *104*, 2671-2674.

<sup>27</sup> (a) Sibbett, S.S.; Loehr, T.M.; Hurst, J.K. *Inorg. Chem.* **1986**, *25*, 307-313. (b) Deardoff, E.A.; Carr, P.A.G.; Hurst, J.K. *J. Am. Chem. Soc.* **1981**, *103*, 6611-6616.

<sup>28</sup> Lukas, B.; Miller, J.R.; Silver, J.; Wilson, M.T.; Morrison, I.E.G. *J. Chem. Soc., Dalton Trans.* **1982**, 1035-1040.

<sup>29</sup> Elliot, C.M. Nemi, C.J.; Cranmer, B.K.; Hamburg, A.W. *Inorg. Chem.* **1987**, *26*, 3655-3659.

Only one crystallographically characterized binuclear iron-copper complex with the iron bound in a porphyrin plane has appeared in the literature to date. In 1980, Gunter and coworkers, using a ligand based on the picket-fence design (**D**),<sup>30</sup> were able to bind a Cu(II) to



**D**

four nitrogen donors arranged in a plane parallel to that of the porphyrin base. The crystals obtained of the heterodinuclear chloride bridged complex were poor, but an x-ray diffraction study revealed exceptionally long Fe-Cl and Cu-Cl bonds.<sup>31</sup> The iron appeared to be in a mixed or intermediate spin state. No magnetic interaction between the metals was observed. The lack of coupling was accounted for by the large interatomic distance and a "mismatch" of orbitals between the copper and the bridging chloride.<sup>32</sup> As a result of the square planar geometry around the Cu(II) center, the unpaired  $e^-$  resides in the  $d_{x^2-y^2}$  orbital, oriented perpendicular to the heme axis. This orientation does not allow for  $\sigma$  overlap between the Cu(II) ion and the bridging ligand. Gunter *et al.* concluded that  $\sigma$  overlap is essential to promote strong magnetic interactions between the metal ions. The cyano bridged analog of the crystallographically characterized complex showed more interesting properties owing to the

<sup>30</sup> (a) Buckingham, D.A.; Gunter, M.J.; Mander, L.N. *J. Am. Chem. Soc.* **1978**, *100*, 2899-2901. (b) Elliot, C.M. *J. Chem. Soc., Chem. Commun.* **1978**, 399-400.

<sup>31</sup> Gunter, M.J.; Mander, L.N.; McLaughlin, G.M.; Murray, K.S.; Berry, K.J.; Clark, P.E.; Buckingham, D.A. *J. Am. Chem. Soc.* **1980**, *102*, 1470-1473.

<sup>32</sup> Berry, K.J.; Clark, P.E.; Gunter, M.J.; Murray, K.S. *Nouv. J. Chim.* **1980**, *10*, 581-585.



greater ligand strength and larger size of the cyanide bridge. This complex was presented as a model for the cyano derivative of the active site of the enzyme in a paper published in 1984.<sup>33</sup>

With only a few exceptions, the conclusions presented by Gunter *et al.* have been ignored by other investigators preparing model compounds for the active site of cytochrome oxidase. The hydroxo bridged model prepared by Gunter's group, of course, was designed to promote  $\sigma$  overlap between the bridging ligand and the Cu ion. Strong coupling, however, was not achieved, perhaps because of unfavorable constraints on the binuclear center resulting from the mode of attachment of the copper binding site to the porphyrin base. The model from the Chang group and two recent imidazolate bridged models are the only others that allow appropriate orbital overlap. The use of a pentacoordinate macrocycle by the Wilson group would seem to preclude square planar geometry around the copper and, in the case of the oxo bridged model, would suggest that the copper in the binuclear complex were hexacoordinate. Without crystal structures, it is impossible to speculate about the electronic features of the copper ions in these complexes. Furthermore, the continuing proliferation of imidazolate bridged models seems fruitless in view of the EXAFS data. Except for the fact that Elliot's complexes do show that thiolate bridges between copper and an iron porphyrin are possible, extraordinarily little progress has been made toward the synthesis of a useful model for the active site of cytochrome oxidase beyond that published by Chang in 1982. The most recent EXAFS data from the Cu<sub>A</sub> depleted enzyme suggest that further study of the Chang model, or one similar to it, would be warranted.

Clearly, several factors must be considered when planning the synthesis of a ligand system to be used in a model compound for the binuclear site in cytochrome oxidase. Based on the published models<sup>34</sup> and on the synthetic work carried out previously in this lab,<sup>35</sup> the following synthetic strategy was devised. A meso-tetraaryl substituted porphyrin was chosen

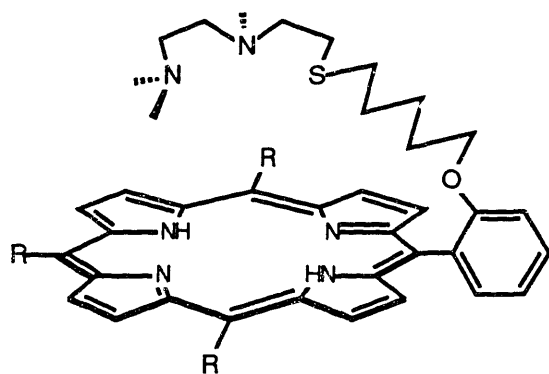
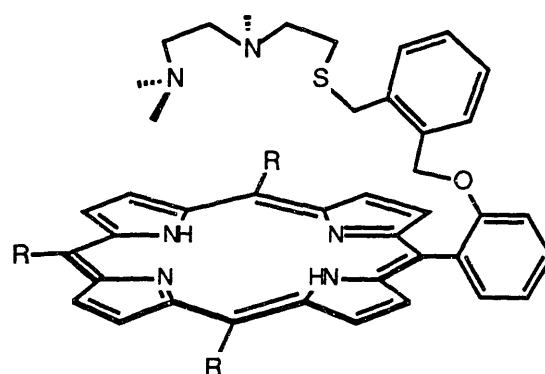
---

<sup>33</sup> Gunter, M.J.; Berry, K.J.; Murray, K.S. *J. Am. Chem. Soc.* **1984**, *106*, 4227-4235.

<sup>34</sup> In addition to the literature cited previously, see also Okamoto, M.; Nishida Y.; Kida, S. *Chem. Lett.* **1982**, 1773-1776.

<sup>35</sup> Spool, A. Ph.D. Thesis, Columbia University, 1984.

for ease of synthesis and to promote crystallinity. A copper coordination site directed over the porphyrin plane but not held at a specific distance from the plane was desired. Flexibility was planned to allow the bridging ligand to bind in the most stable orientation, hopefully one which would provide maximal orbital overlap for magnetic interaction. Potentially, various bridging ligands could be introduced into such a system. A tridentate ligand for copper, N,N,N'-trimethyl-N'-mercaptoethylethylenediamine (N<sub>2</sub>S), was chosen to be attached to the porphyrin through an alkyl linking group to one of the meso aryl groups of the porphyrin. This linkage could be accomplished through an ether functionality involving an ortho hydroxy substituent on a meso phenyl group of the porphyrin and a thioether linkage to the copper binding site. Following these guidelines, the synthesis of N<sub>2</sub>S-TTP was accomplished. To obtain a system with somewhat less conformational freedom an aryl linking group was used in the synthesis of N<sub>2</sub>S-xy-TTP. Iron(III) and copper(II) were added to these ligand systems in hopes of achieving a crystalline model for the active site of cytochrome oxidase.

N<sub>2</sub>S-TTP

R = phenyl

N<sub>2</sub>S-xy-TTP

## Experimental Section

**Materials.** All solvents and organic starting materials were obtained from commercial sources and used without purification unless stated otherwise. Benzene was distilled from CaH<sub>2</sub>, THF and toluene from Na/benzophenone ketyl. Purification of DMF for the synthesis of N<sub>2</sub>S-xy-TTP was achieved by predrying over BaO and distilling the decanted solvent at reduced pressure and room temperature followed by chromatography over activated alumina under N<sub>2</sub> immediately prior to use.

**Physical Measurements.** UV-Visible spectra were recorded on a Perkin-Elmer Lambda 7 spectrophotometer linked to a Perkin-Elmer Series 3600 Data Station. IR spectra were recorded on a Beckman Acculab 10 infrared spectrophotometer and referenced to the 1602 cm<sup>-1</sup> band of polystyrene recorded simultaneously. <sup>1</sup>H and <sup>13</sup>C spectra were obtained from Bruker WM 250 and WM 270 instruments. Multipulse experiments were carried out by using the HETCOR and APT programs for the Varian XL 300 NMR spectrometer. A Varian E-line EPR spectrometer operating between 9.1 and 9.6 GHz was used to obtain EPR data. Spectra were collected at 77 K from frozen solutions and calibrated using the naturally occurring Mn<sup>2+</sup> impurity in SrO.<sup>36</sup> Mass spectrometry measurements were carried out either at the MIT Chemistry Department Spectrometry Laboratory or by Dr. C. Costello and coworkers in the Biemann group, Department of Chemistry, MIT. Elemental Analyses were obtained from Atlantic Microlabs, Atlanta, Georgia.

**5-(2-hydroxyphenyl)-10,15,20-tri(p-tolyl)porphyrin (OH-TTP).** This porphyrin was synthesized according to literature methods<sup>37</sup> as shown in Scheme I. Yield from 43.1 g pyrrole was 5.7 g (~5%) OH-TTP, C<sub>47</sub>H<sub>36</sub>N<sub>4</sub>O. <sup>1</sup>H NMR (CDCl<sub>3</sub>, 250 MHz): δ 8.87, m, 8H (β H); 8.07, d, 6H, 8.00, m, 1H, 7.70, m, 1H, 7.53, d, 6H, 7.35, m, 2H (phenyl H);

<sup>36</sup> Bolton, J.R.; Borg, D.C.; Swartz, H.M. in *Biological Applications of Electron Spin Resonance*; Swartz, H.M.; Bolton, J.R.; Borg, D.C., eds., Wiley: New York, 1972, 100.

<sup>37</sup> Little, R.G.; Anton, J.A.; Ibers, J.A. *J. Heterocyclic Chem.* **1975**, *12*, 343-349.

2.69, s, 9H (tolyl CH<sub>3</sub>); -2.70, s (br), 2H (pyrrole N-H). The hydroxide proton was not located. <sup>13</sup>C NMR (CDCl<sub>3</sub>, 67.3 MHz): δ 155.6; 147 (v br), 139.1, 138.9, 137.4, 134.9, 134.5, 132.0, 131 (br), 130.3, 127.4, 121.1, 120.5, 119.5, 115.4, (111.2), 21.5.

**5-(2-(5-bromo-1-pentoxy)phenyl)-10,15,20-tri(p-tolyl)porphyrin (Br-TTP)** This porphyrin was synthesized by literature methods from OH-TTP.<sup>38</sup> (See Scheme I) It was isolated as an amorphous solid in 85% yield (3.3 g Br-TTP from 3.2 g OH-TTP).

C<sub>52</sub>H<sub>45</sub>N<sub>4</sub>OBr. <sup>1</sup>H NMR (CDCl<sub>3</sub>, 250 MHz): δ 8.91, 8.88, 8.84, 8.82, 8H (β H); 8.14, m, 6H, 7.75, m, 2H, 7.59, m, 6H, 7.36, t, 1H, 7.28, d, 1H (phenyl H); 3.87, t, 2H (-O-CH<sub>2</sub>-); 2.72, s, 9H (tolyl CH<sub>3</sub>); 2.30, t, 2H (-CH<sub>2</sub>-Br); 0.96, m, 4H(methylene); 0.45, m, 2H (methylene); -2.67, s (br), 2H (pyrrole N-H). <sup>13</sup>C NMR (CDCl<sub>3</sub>, 67.3 MHz): δ 155.8, 146.5 (v br), 139.4, 139.3, 137.2, 135.6, 134.4, 131.4, 130.9, 129.7, 127.4, 120.2, 119.8, 116.0, 112.0, 68.0, 32.8, 31.5, 27.6, 24.0, 21.4.

**N,N,N'-trimethyl-N'-mercaptoethylethylenediamine (N<sub>2</sub>S).** This synthesis was based on literature methods.<sup>39</sup> In a flask connected to a Schlenk line, 25 ml (0.20 mole) of N,N,N'-trimethylethylenediamine were dissolved in 200 ml of distilled benzene. The solution was stirred, warmed gently (T < 60 °C) and flushed with N<sub>2</sub>. 12 ml (0.20 mole) of ethylene sulphide were diluted with 50 ml of distilled benzene and added dropwise into the stirring diamine solution over a period of ~20 min. The reaction mixture was warmed and stirred overnight (~20 hrs). During this time a white precipitate formed. The solution was decanted from the precipitate and the benzene removed under vacuum. The product was purified by fractional distillation (bp = ~55 °C at 8 mm Hg) to give 50 - 60% yield of a clear liquid (d = 1.1 g/ml). C<sub>7</sub>H<sub>18</sub>N<sub>2</sub>S. <sup>1</sup>H NMR (CDCl<sub>3</sub>, 250 MHz): δ 2.58, s, 4H; 2.43, m, 4H; 2.22, s, 3H; 2.23, s, 6H. The thiol proton was not located. <sup>13</sup>C NMR (CDCl<sub>3</sub>, 67.3 MHz) δ 60.7, 57.2,

<sup>38</sup> Little, R.G. *J. Heterocyclic Chem.* **1978**, *15*, 203-208.

<sup>39</sup> (a) Lippard, S.J.; Hu, W.J.; Barton, D. *J. Am. Chem. Soc.* **1973**, *95*, 1170-1173. (b) Lippard, S.J.; Karlin, K.D.; *J. Am. Chem. Soc.* **1976**, *98*, 6951-6957.

55.2, 45.6, 42.0, 22.2. On standing in air, the product turned pale yellow, probably from air oxidation to the disulphide.

**5-(2-(9,12-dimethyl-9,12-diaza-6-thia-tridecoxy)phenyl)-10,15,20-tri(p-tolyl)-porphyrin (N<sub>2</sub>S-TTP), (1).** (See Scheme I) Using Schlenk techniques, 3.3 g ( $4.0 \times 10^{-3}$ ) of Br-TTP were dissolved under N<sub>2</sub> in 75 ml of purified DMF containing 10 g of K<sub>2</sub>CO<sub>3</sub>. To this stirred solution, were added 5.0 ml ( $3.4 \times 10^{-2}$  mole) of N<sub>2</sub>S. The mixture was allowed to react for ~20 hr. A solution of 30% H<sub>2</sub>O in MeOH which had been purged with N<sub>2</sub> was added to the DMF mixture to precipitate the porphyrin. The mixture was suction filtered. The solid was vacuum dried and transferred to an inert atmosphere box. Column chromatography on silica gel with an eluant of 5% NH<sub>3</sub>-MeOH in toluene separated the desired product as a slow moving band. The solvent was removed by rotary evaporation. Ether and MeOH were added to the resulting oil. Removal of these solvents under vacuum yielded 2.7 g (74%) of a dull purple solid. C<sub>59</sub>H<sub>62</sub>N<sub>6</sub>OS. <sup>1</sup>H NMR (CDCl<sub>3</sub>, 250 MHz): δ 8.86, 8.82, 8.80, 8.79, 8H (β H); 8.07, m, 6H, 7.24, t, 2H, 7.56, d, 6H, 7.32, m, 2H (phenyl H), 3.88, t, 2H (-O-CH<sub>2</sub>-); 2.71, s, 9H (tolyl CH<sub>3</sub>); 2.19, m, 2.09, s, 2.0, m, 1.96, s 17H (N<sub>2</sub>S); 1.52, t, (-CH<sub>2</sub>-S-); 1.00, m, (methylene); 0.80, m, 2H (methylene); 0.49, m, 2H (methylene); -2.72, s (br), 2H (pyrrole N-H). <sup>13</sup>C NMR (CDCl<sub>3</sub>, 67.3 MHz): δ 158.9, 146.5, 139.3, 137.2, 135.7, 134.4, 131.4, 130.8, 129.7, 127.4, 120.2, 119.8, 119.4, 116.1, 112.1, 68.2, 57.6, 57.2, 55.2, 45.7, 42.0, 31.4, 29.0, 28.2, 24.5, 21.4. FAB-MS (*m/e*): 903 (M<sup>+</sup>), (other major peaks in decreasing order of magnitude) 774, 844, 672, 801, 741, 858.

**5-(2-(2-hydroxymethylbenzyloxy)phenyl)-10,15,20-tri(p-tolyl)-porphyrin (OH-xy-TTP).** Synthesis of this porphyrin was accomplished in a manner analogous to that reported for Br-TTP (Scheme I). The bromoxylyl analog of Br-TTP was the desired product, but only the hydrolyzed product could be isolated. To a solution of 50 ml DMF containing ~1 g K<sub>2</sub>CO<sub>3</sub>, 2.0 g ( $7.6 \times 10^{-3}$  mol) of α,α'-dibromoxylene were added and the mixture stirred until the dibromoxylene had dissolved. 0.40 g ( $6.0 \times 10^{-4}$ ) of OH-TTP were dissolved in a

small amount of DMF and added to the reaction solution. A mixture of MeOH and H<sub>2</sub>O was used to precipitate the porphyrin. The product was isolated as the second band to separate on a silica gel column eluted with 5% CH<sub>3</sub>CN/toluene. Yield: 0.19 g, 40% of (OH-xy-TTP).

C<sub>55</sub>H<sub>43</sub>N<sub>4</sub>O. <sup>1</sup>H NMR (CDCl<sub>3</sub>, 250 MHz): δ 8.86, s, 8.83, d, 8.76, d, 8H (β H); 7.74, t, 1H, 7.55, d, 6H, 7.41, m, 2H (phenyl H); 6.76, m, 1H, 6.58, m, 3H (xylyl H); 4.88, s, 2H (-O-CH<sub>2</sub>-); 3.41, s, 2H (-CH<sub>2</sub>-OH); 2.70, s, 9H (tolyl CH<sub>3</sub>); -2.77, s, 2H (pyrrole N-H). <sup>13</sup>C NMR (CDCl<sub>3</sub>, 67.3 MHz): δ 158.5, 146.5 (v br), 139.2, 138.5, 137.3, 135.7, 134.6, 133.7, 132.2, 131.1, 129.9, 128.3, 127.7, 127.4, 126.9, 120.4, 120.2, 120.0, 115.6, 113.3, 69.4, 61.6. FAB-MS (*m/e*): 794 (M<sup>+</sup>), 673.

**5-(2-(2-(4,7-dimethyl-4,7-diaza-1-thia)-1-benzyloxy)phenyl)-10,15,20-tri(p-tolyl)porphyrin (N<sub>2</sub>S-xy-TTP) (2).** (See Scheme I) In an inert atmosphere box, 0.465 g (6.92 X 10<sup>-4</sup> mol) of OH-TTP was dissolved in 30 ml purified DMF stirred over 1.9 g anhydrous K<sub>2</sub>CO<sub>3</sub> in Schlenk flask. To the stirred solution, 2.14 g of (8.11 X 10<sup>-3</sup> mol) α,α-dibromo-xylene were added. The reaction was followed by TLC on silica gel plates developed in toluene. When the majority of the OH-TTP had reacted to give the faster moving intermediate product (~2-4 hr), 2.5 ml (1.70 X 10<sup>-2</sup> mol) N<sub>2</sub>S were added. The reaction was left to stir for 21 hr. The product was worked up and purified as described for N<sub>2</sub>S-TTP. Yield: 0.270 g, 42% of 2. C<sub>62</sub>H<sub>60</sub>N<sub>6</sub>OS. <sup>1</sup>H NMR (CDCl<sub>3</sub>, 250 MHz): δ 8.94, m, 8H (β H); 8.17, m, 7H, 7.79, t, 1H, 7.60, t, 6H (phenyl H); 6.81, m, 1H, 6.74, 1H, 6.57, m, 2H (xylyl H); 5.20, s, 2H (-O-CH<sub>2</sub>-); 3.02, s, 2H (-CH<sub>2</sub>-S-); 2.74, s, 9H (tolyl CH<sub>3</sub>); 2.16, 2.13, 2.06 (br), 14H, 1.90, s, 3H (N<sub>2</sub>S); -2.62, s (br), 2H (pyrrole N-H). <sup>13</sup>C NMR (CDCl<sub>3</sub>, 67.3 MHz): δ 158.4, 139.4, 137.2, 135.6, 135.0, 134.8, 134.5, 131.7 (br), 131.0, 129.7, 129.5, 128.1, 127.4, 126.7, 120.2, 119.9, 119.7, 115.8, 112.8, 68.0, 57.0, 54.9, 45.6, 33.2, 28.6, 21.4.

**5-(2-aminophenyl)-10,15,20-triphenylporphyrin (NH<sub>2</sub>-TPP).** This porphyrin was prepared by literature methods<sup>40</sup> as shown in Scheme II. C<sub>44</sub>H<sub>31</sub>N<sub>5</sub>. <sup>1</sup>H NMR (CDCl<sub>3</sub>, 250 MHz){literature values in brackets} :δ 8.88, m, 8H (β H){8.6-9.1}; 8.25, m, 6H, 7.91, d, 1H, 7.78, m, 9H, 7.60, t, 1H, 7.18, t, 1H, 7.08, d, 1H (phenyl H){6.8-8.3}; 3.53, s (br), 2H (NH<sub>2</sub>){3.36}; -2.70, s (br), 2H (pyrrole N-H){-2.66}. <sup>13</sup>C NMR (CDCl<sub>3</sub>, 67.3 MHz): δ 146.9, 142.2, 142.0, 134.8, 134.5, 131.1(br), 129.6, 127.7, 126.7, 120.5, 120.1, 117.5, 115.2.

**Reaction of (NH<sub>2</sub>-TPP) with Cl(C=O)(CH<sub>2</sub>)<sub>3</sub>Br.** (See Scheme II) In a manner similar to that described for **2**, 0.595 g (3.2 X 10<sup>-3</sup> mol) Cl(C=O)(CH<sub>2</sub>)<sub>3</sub>Br, diluted in a small amount of purified DMF, was added dropwise to 0.220 g (3.50 X 10<sup>-4</sup> mol) NH<sub>2</sub>-TPP in 50 ml purified DMF with 1.9 g K<sub>2</sub>CO<sub>3</sub> present. On addition of the acid halide, the solution turned blue-green but after several hours, became maroon again. The DMF was removed under vacuum. Column chromatography separated two products. Major product, **3**: 5-(2-(2-pyrroli-donyl)phenyl)-10,15,20-triphenylporphyrin. C<sub>48</sub>H<sub>35</sub>N<sub>5</sub>O. <sup>1</sup>H NMR (CDCl<sub>3</sub>, 250 MHz):δ 8.92, m, 8H (β H); 8.27, m, 7H, 7.79, m, 12H (phenyl H); 2.30, t, 2H (methylene); 1.72, t, 2H(methylene); 0.79, m, 2H (methylene); -2.78, s (br), 2H (pyrrole N-H).<sup>13</sup>C NMR (CDCl<sub>3</sub>, 67.3 MHz): δ 175.2, 142.1, 142.0, 140.4, 138.4, 136.4, 134.6, 131.2 (br), 129.4, 127.8, 126.7, 125.8, 120.5, 120.3, 49.9, 30.6, 18.3. FAB-MS (*m/e*): 698 (MH<sup>+</sup>). FD-MS(*m/e*): 697 (M<sup>+</sup>). Minor Product, **4**: 5-(2-(5-carboxypentylamido)phenyl)-10,15,20-triphenylporphyrin. C<sub>48</sub>H<sub>36</sub>N<sub>5</sub>O<sub>2</sub>. <sup>1</sup>H NMR (CDCl<sub>3</sub>, 250 MHz):δ 8.88, s, 6H, 8.79, d, 2H (β H); 8.63, d, 1H, 8.21, s (br), 6H, 8.10, d, 1H, 7.78, m, 10H, 7.52, t, 1H (phenyl H); 2.45, t, 2H (methylene); 1.43, t, 2H(methylene); 0.98, m, 2H (methylene); -2.79, s (br), 2H (pyrrole N-H). Acidic proton not observed. <sup>13</sup>C NMR (CDCl<sub>3</sub>, 67.3 MHz): δ 171.5, 141.9,

---

<sup>40</sup> Collman, J.P., Brauman, J.I.; Doxsee, K.M.; Halbert, T.R.; Bunnenberg, E.; Linder, R.E.; La Mar, G.N.; Del Gaudio, J.; Lang, G.; Spartalian, K. *J. Am. Chem. Soc.* **1980**, *102*, 4182-4190.

141.6, 139.0, 134.5, 134.1, 131.5 (br), 129.6, 127.9, 126.8, 122.8, 121.2, 120.6, 113.2, 60.2, 33.8, 26.6. EI-MS (*m/e*): 715 ( $M^+$ ), 698, 630.

**Reaction of (NH<sub>2</sub>-TPP) with  $\alpha,\alpha'$ -dibromoxylene and N<sub>2</sub>S.** (See Scheme II) This reaction was carried out in an attempt to prepare an amine linked porphyrin analogous to N<sub>2</sub>S-xy-TTP. The same synthetic method was used except that the porphyrin solution was warmed before addition of N<sub>2</sub>S. TLC revealed the formation of an intermediate product, but reaction with N<sub>2</sub>S appeared incomplete. Purification by column chromatography led to the separation of large amount of green, decomposed material. The major porphyrin product isolated from the reaction contained no N<sub>2</sub>S. This product was identified as 5-(2-(N-(dihydro-3,4-benzopyrrolyl)phenyl)-10,15,20-triphenyl-porphyrin, **5**. C<sub>52</sub>H<sub>37</sub>N<sub>5</sub>. <sup>1</sup>H NMR (CDCl<sub>3</sub>, 250 MHz):  $\delta$  9.00, d, 2H, 8.86, s, 4H, 8.81, d, 2H ( $\beta$  H); 8.22, m, 6H, 7.76, m, 11H, 7.26, d, 1H, 7.03, t, 1H (phenyl H); 6.73, m, 2H, 6.45, m, 2H (xylyl H); 3.95, s, 4H (benzyl H); -2.62, s (br), 2H (pyrrole N-H). <sup>13</sup>C NMR (CDCl<sub>3</sub>, 67.3 MHz):  $\delta$  148.5, 142.2, 142.1, 138.5, 137.3, 134.5, 131.2 (br), 129.3, 127.7, 127.1, 126.3, 121.7, 120.4, 120.2, 115.2, 113.7, 56.7. FAB-MS (*m/e*): 732 ( $M^+$ ), 630.

**Addition of iron to porphyrins.** The ferrous porphyrins were prepared as described in the literature<sup>40</sup> and air oxidized to the ferric species. Filtration of the solutions removed excess ferrous salts and washing with aqueous acid and water was required to remove the lutidine used in the synthesis. Purification of the ferric porphyrins could be achieved with difficulty by column chromatography on silica gel by using CH<sub>2</sub>Cl<sub>2</sub> or toluene with NH<sub>3</sub>-MeOH as the eluant. The porphyrins were collected from the column as a mixture of hydroxo- and  $\mu$ -oxo derivatives. The modified porphyrins exhibited UV-Vis spectra which were identical to that reported for (FeTPP)<sub>2</sub>O.<sup>41</sup> and displayed the characteristic Fe-( $\mu$ -oxo) stretch at  $\sim 850$  cm<sup>-1</sup> in

---

<sup>41</sup> Buchler, J.W. in *The Porphyrins*, Dolphin, D., ed., Academic: New York, 1978, Vol I, 415.



the IR spectrum.<sup>42</sup> The NMR spectra of these complexes, however, frequently showed the presence of high spin ferric species with the  $\beta$ -H resonances at  $\sim 80$  ppm downfield.<sup>43</sup> Unfortunately, decomposition also occurred during column chromatography resulting in considerable loss of compound. The ferric porphyrins were obtained in only  $\sim 50$  % yield compared to nearly quantitative yields reported in the literature.<sup>40</sup>

**Synthesis of  $N_2S$ -TTPFeX complexes.** The ferric porphyrin was isolated from the reaction mixture as the  $\mu$ -oxo derivative as determined by UV-Vis spectroscopy. The Br<sup>-</sup> and SCN<sup>-</sup> derivatives were synthesized by treatment of the unpurified  $\mu$ -oxo porphyrin with saturated, acidified, aqueous solutions of the sodium salt of the desired anion as described in the literature.<sup>44</sup>

**$N_2S$ -TTPFeBr (6).** To 0.298 g of unpurified  $(N_2S-TTPFe)_2O$  in  $\sim 50$  ml of  $CH_2Cl_2$  were added 10 ml of a saturated, acidified, aqueous solution of NaBr. The two solutions formed an emulsion. The mixture was stirred for 24 hr. No separation of the aqueous and organic layers occurred. All solvent was removed to give a mixture of brown and white solids. The brown solid was dissolved in  $CH_2Cl_2$ . Hexane was added to the solution and the solvents were removed by rotary evaporation to give 0.373 g (94%) of 6·2 HBr. IR (KBr pellet): no bands in the Fe-( $\mu$ -oxo) stretching frequency region. UV-Vis (tol, nm) 395 (sh), 425, 513, 580, 598, 670 (sh), 702. <sup>1</sup>H NMR ( $CDCl_3$ , 270 MHz):  $\delta$  81(sh), 80 (br) ( $\beta$  H); 14.6, 13.2 (meta H); remaining spectrum broad and complex. EPR ( $CH_2Cl_2$ /tol glass) g 5.798, 2.028.

**$N_2S$ -TTPFeSCN (7)** The same procedure was used as described for 6. Yield: 98% of 7·2HSCN IR (KBr pellet): no bands in the Fe-( $\mu$ -oxo) stretching frequency region, C-N stretch,  $2010\text{ cm}^{-1}$ . UV-Vis (tol, nm) 340 (sh), 420, 512, 570 (sh), 600 (sh), 670 (sh), 702.

---

<sup>42</sup> Cowen, I. A. *J. Am. Chem. Soc.* **1969**, *91*, 1980-1983.

<sup>43</sup> (a) La Mar, G.N.; Eaton, G.R.; Holm, R.H.; Walker, F.A. *J. Am. Chem. Soc.* **1973**, *95*, 63-75. (b) Goff, H.M. in *Iron Porphyrins*; Lever, A.P.B.; Gray, H.B.; eds., Addison Wesley: Reading, MA, 1983, Vol I, 237-281.

<sup>44</sup> Torrens, M.A.; Straub, D.K.; Epstein, L.M. *J. Am. Chem. Soc.* **1972**, *94*, 4162-4167.

$^1\text{H}$  NMR ( $\text{CDCl}_3$ , 270 MHz):  $\delta$  75 (br) ( $\beta$  H); 13.0 (sh), 12.7 (meta H); remaining spectrum broad and complex. EPR ( $\text{CH}_2\text{Cl}_2/\text{tol}$  glass) g 5.996, 2.048.

**$\text{N}_2\text{S-TTPFeCl}$  (8)** A different procedure was used to obtain this compound. The crude ferric porphyrin mixture was purified by column chromatography on silica gel. The column was developed with a gradient elution of  $\text{NH}_3\cdot\text{MeOH}$  in toluene. A mixture of hydroxo and  $\mu$ -oxo derivatives of the porphyrin was collected from the column. The solvents were removed, the product dissolved in  $\text{CH}_2\text{Cl}_2$  and washed with 0.1N HCl followed by washings with water until neutral. The solution was dried over  $\text{Na}_2\text{SO}_4$ . Ethanol was added and the solvent removed by rotary evaporation. The addition of hexane to the product in  $\text{CH}_2\text{Cl}_2$  followed by rotary evaporation gave a dull black solid. The product was identified by its UV-Vis spectrum which was identical to that of  $\text{TPPFeCl}$ .<sup>41</sup>

**$\text{N}_2\text{S-xy-TTPFeCl}$  (9).** This complex was prepared as described for **8**.

**$\text{N}_2\text{S-xy-TTPFe}(\text{CN})_2$ .**  $(\text{Et}_4\text{N})\text{CN}$  was synthesized by literature methods<sup>45</sup> and used after one recrystallization. 0.045 g ( $2.9 \times 10^{-4}$  mol) of this salt was dissolved in methanol. To the stirred solution, 0.049 g ( $4.8 \times 10^{-5}$  mol) of **9** was added. The solution turned deep emerald green. The methanol was removed by rotary evaporation. The remaining solid was dissolved as much as possible in THF and filtered to remove excess salts. The solvent was removed from the filtrate by rotary evaporation followed by drying under vacuum.  $^1\text{H}$  NMR ( $\text{CDCl}_3$ , 250 MHz):  $\delta$  4.04 (br),  $[\text{N}(\text{CH}_2\text{CH}_3)_4]^+$ , 1.45 (br),  $[\text{N}(\text{CH}_2\text{CH}_3)_4]^+$  (all other peaks 0-15 ppm unidentifiable), -14.3, s, -14.4, d ( $\beta$  H).  $^{13}\text{C}$  NMR ( $\text{CDCl}_3$ , 67.3 MHz) aliphatic region:  $\delta$  67.6, 57.6, 57.1, 55.2, 53.5  $[\text{N}(\text{CH}_2\text{CH}_3)_4]^+$ , 45.5, 42.4, 41.8 and 41.0 (br) (*meso* C), 34.6, 29.5, 19.2, 8.13  $[\text{N}(\text{CH}_2\text{CH}_3)_4]^+$ . Impurities were apparent in the spectra but all attempts at purification by precipitation from hexane/ $\text{CCl}_4$  gave products which exhibited  $^1\text{H}$  NMR spectra with broader resonances and additional peaks in the region of the  $\beta$  protons.

---

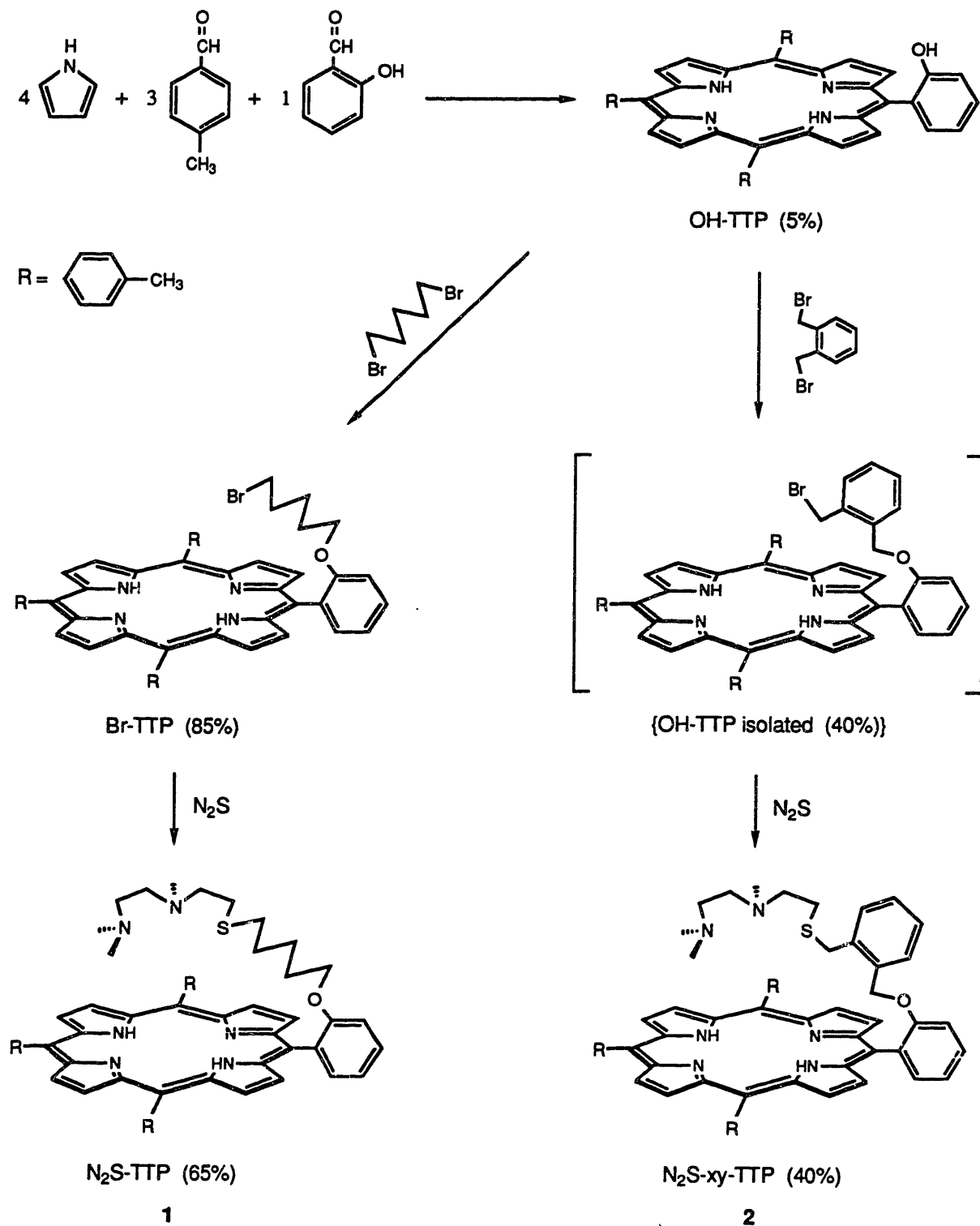
<sup>45</sup> Webster, O.W.; Mahler, W.; Benson, R.E. *J. Am. Chem. Soc.* **1962**, *84*, 3678-3784.

**N<sub>2</sub>S-TTPFe(CN)<sub>2</sub>.** This complex was synthesized as described above using ~0.04 g (2.5 X 10<sup>-4</sup> mol) of (Et<sub>4</sub>N)CN and 0.034 g (3.4 X 10<sup>-5</sup> mol) of **6**. <sup>1</sup>H NMR (CDCl<sub>3</sub>, 250 MHz): δ 3.68 (br), [N(CH<sub>2</sub>CH<sub>3</sub>)<sub>4</sub>]<sup>+</sup>, 1.38 (br), [N(CH<sub>2</sub>CH<sub>3</sub>)<sub>4</sub>]<sup>+</sup> (all other peaks 0-15 ppm unidentifiable), -12.0, -12.4, -12.7, -13.0 (β H). A white precipitate formed with time in solutions of this complex.

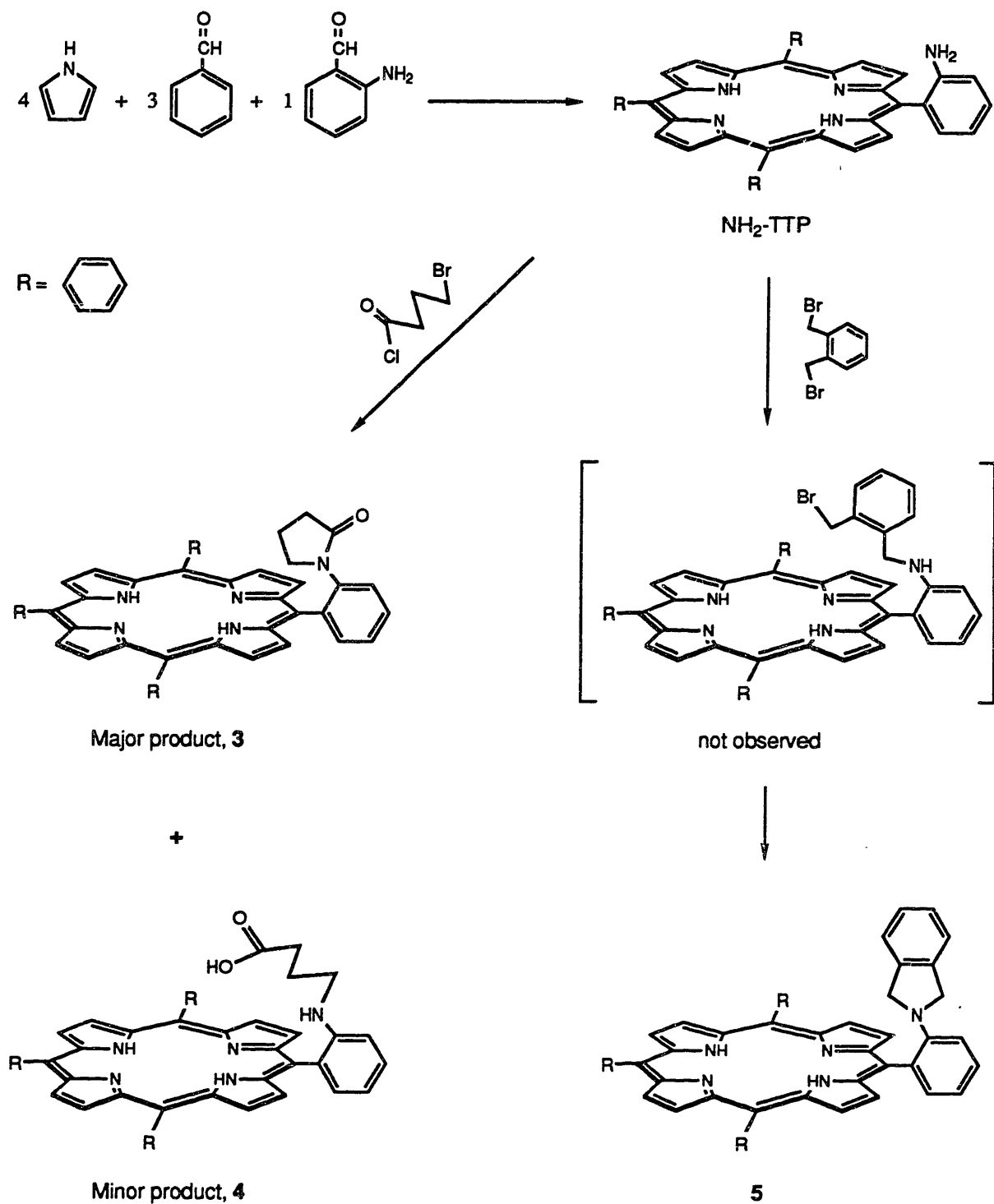
**N<sub>2</sub>S-TTPFeBF<sub>4</sub> · 2HBF<sub>4</sub>.** An analytically pure sample of N<sub>2</sub>S-TTPFeBF<sub>4</sub> · 2HBF<sub>4</sub> was obtained by repurifying 0.225 g of **8** by silica gel chromatography under N<sub>2</sub> in 10% THF/toluene with a gradient elution of NH<sub>3</sub>·MeOH. After the solvents were removed from the major fraction, the resulting oil was dissolved in MeOH with solid NaCl present and the solution made acidic with HBF<sub>4</sub> etherate. Addition of ether and removal of the solvents under vacuum gave 0.145 g (~55%) of N<sub>2</sub>S-TTPFeBF<sub>4</sub> · 2HBF<sub>4</sub> · MeOH. Calc. for C<sub>59</sub>H<sub>62</sub>N<sub>6</sub>OS-FeB<sub>3</sub>F<sub>12</sub> · MeOH: C, 57.58; H, 5.32; S, 2.56. Found: C, 57.27; H, 5.48, S, 2.65.

**Addition of Cu(II) to ligand. Method I.** Solutions of Cu(II) salts [Cu(NO<sub>3</sub>)<sub>2</sub>, Cu(BF<sub>4</sub>)<sub>2</sub>, CuSO<sub>4</sub>, or CuCl<sub>2</sub>] were allowed to stir in contact with solutions of **6** and **7** in CH<sub>2</sub>Cl<sub>2</sub>. The organic layer was extracted from the mixture, dried over Na<sub>2</sub>SO<sub>4</sub> and the solvents removed by rotary evaporation. EPR spectra of the resulting solids exhibited signals characteristic of high spin heme and Cu(II) ions. **Method II.** Stoichiometric amounts of freshly recrystallized Cu(OAc)<sub>2</sub>·H<sub>2</sub>O were allowed to react with **9** in MeOH for various lengths of time. The solvent was removed under vacuum. EPR spectroscopy confirmed the presence of Cu(II) in the resulting complex, but the appearance of two g<sub>||</sub> signals suggested that the product was inhomogeneous. All attempts at purification failed. Washing the product with 0.1N HCl or a saturated aqueous solution of NaCl at pH = 3 caused nearly complete removal of the Cu(II) from the ligand as determined by EPR spectroscopy.

## Scheme 1



## Scheme II



## Results and Discussion

**Ligand Synthesis.** The syntheses of ligands **1** and **2** were designed to allow coordination of a Cu(II) ion within bridging distance of an Fe(III) ion bound to a porphyrin. Both ligands were obtained in a straightforward manner in relatively good yield (Scheme I). The overall synthesis of **1** required four steps. The first two steps were accomplished by literature methods without difficulty. The synthesis of N<sub>2</sub>S proceeded smoothly provided that the reaction was carried out at sufficient dilution. Polymerization to an intractable white solid resulted when the ethylene sulfide was added too quickly to the diamine or the reaction solution was too concentrated. Toluene was substituted for benzene on several occasions but yields were only half those achieved in benzene. The <sup>1</sup>H NMR spectrum of N<sub>2</sub>S at 250 MHz in CDCl<sub>3</sub> was unexpectedly complex. (See inset, Figure 1) The methyl resonances were readily assigned as the two barely resolved singlets at 2.22 and 2.23 ppm. The methylene resonances, however appeared as a complicated multiplet with twofold symmetry centered at ~2.43 ppm and a singlet at 2.58 ppm, each of which account for 4 protons. The complexity of the spectrum suggests that a conformational preference, potentially supported by hydrogen bonding between the thiol proton and the amine nitrogens, exists in solution. By comparison, the <sup>13</sup>C NMR spectrum of this compound was relatively simple, exhibiting 6 resonances for the 7 carbons present. The two terminal amino methyl carbons resonances are coincident. Assignment of the <sup>13</sup>C spectrum is given in Table I.

The only difficulty encountered in the synthesis of **1** was the air sensitivity of the final product. When the reaction between N<sub>2</sub>S and Br-TTP was not carried out under an inert atm, only unidentifiable decomposition products were isolated. The sensitivity of this compound to O<sub>2</sub> is not unusual. All porphyrins with pedant thiols and some with pendant amines show this sensitivity, which probably results from the ability of the porphyrin to promote the formation

of singlet oxygen.<sup>46</sup> In the <sup>1</sup>H NMR spectrum in CDCl<sub>3</sub>, the resonances of the N<sub>2</sub>S "tail" occur between 1.9 and 2.4 ppm (Figure 1). These resonances overlap each other, but the singlets from the methyl groups are again distinguishable at 2.09 and 1.96 ppm. The internal methyl group resonance has shifted upfield of that for the terminal methyl groups indicating that the N<sub>2</sub>S is bound to the porphyrin. The slight upfield shift of all the resonances in the "tail" results from the porphyrin ring current and suggests that the tail is, to some extent, directed over the porphyrin plane. Unfortunately, the extreme flexibility of the alkane linkage could allow for the "tail" to hang outside of cylinder containing the porphyrin plane as well. The <sup>13</sup>C spectrum of **1** confirms the identity of the ligand. In order to assign this spectrum, the <sup>13</sup>C spectra of OH-TTP and Br-TTP were recorded. With the aid of off-resonance decoupled spectra, reference values for the <sup>13</sup>C chemical shifts of TPP<sup>47</sup> and tables of substituent effects, the spectra of all three porphyrins could be assigned (Table I).<sup>48</sup>

The synthesis of **2**, using a xylene rather than alkane linkage, was designed to yield a ligand with more steric restraint than **1**. Models suggested that an ortho substituted xylene linkage would direct the "tail" over the porphyrin and restrict its ability to wag away from the plane. Initially, the synthesis was attempted in a manner completely analogous to **1** (Scheme I). The product isolated from the reaction of OH-TTP with  $\alpha$ ,  $\alpha'$ -dibromoxylene, however, would not react with N<sub>2</sub>S. The identity of the product was determined by FAB Mass Spec which found the parent ion at m/e = 794, 64 mass units less than expected for the intermediate.

---

<sup>46</sup> Baldwin, J.E.; Perlmutter, P. *Top. Curr. Chem.* **1984**, *121*, 181-220.

<sup>47</sup> Janson, T.R.; Katz J.J. in *The Porphyrins*, Dolphin, D., ed., Academic: New York, 1978, Vol IV, 1-59.

<sup>48</sup> One peak in the aromatic region of all the spectra is not accounted for in the assignments. This resonance occurs at 111.2 ppm in OH-TTP and at ~116 ppm in the spectra of the other two compounds. It also appears in the spectra of OH-xy-TTP and **2** and has been assigned as a quarternary carbon by an Attached Proton Test performed on ligand **2** (to be discussed later). The shift of the resonance when the porphyrin is modified suggests that it is a part of the ligand. Only local effects of substituent change were considered in making the assignments presented in Table I. The extreme asymmetry of the ligand was essentially ignored. Therefore, this resonance is most likely a *meso* carbon the shift of which cannot be predicted by the rudimentary methods used for the assignment of these spectra. Also, a small peak appears about 0.2 ppm downfield of the C<sub>1</sub> resonance in all the spectra and has been assigned as a splitting of the C<sub>1</sub> resonance due to the asymmetry of the porphyrin.

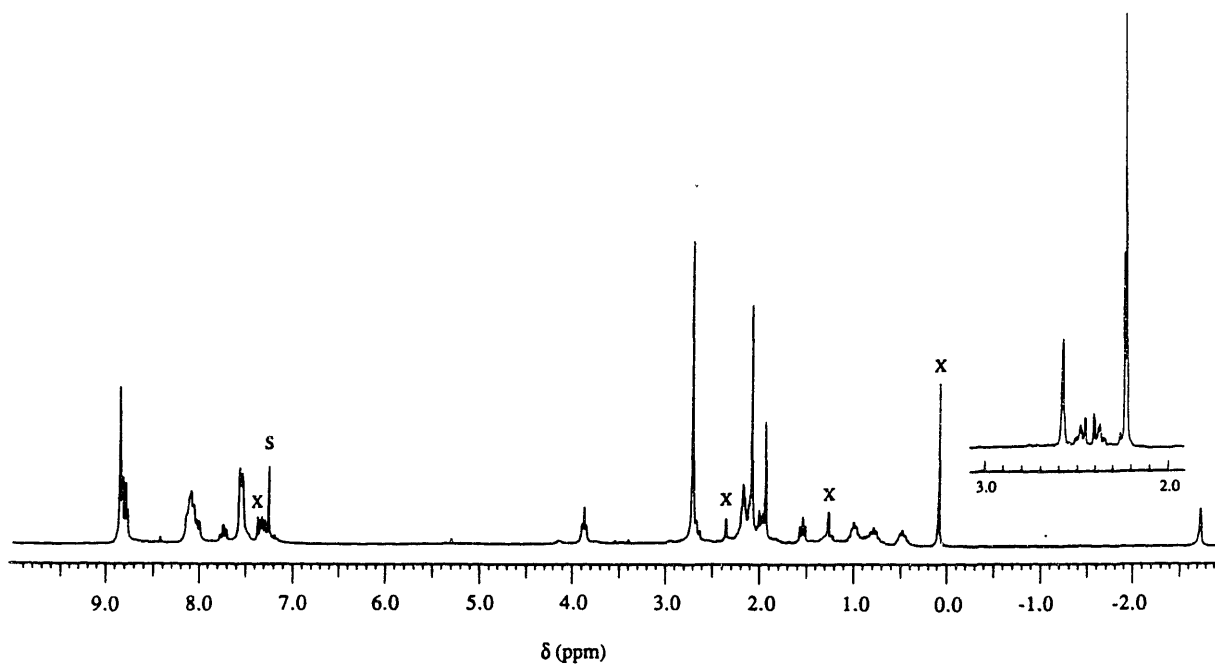
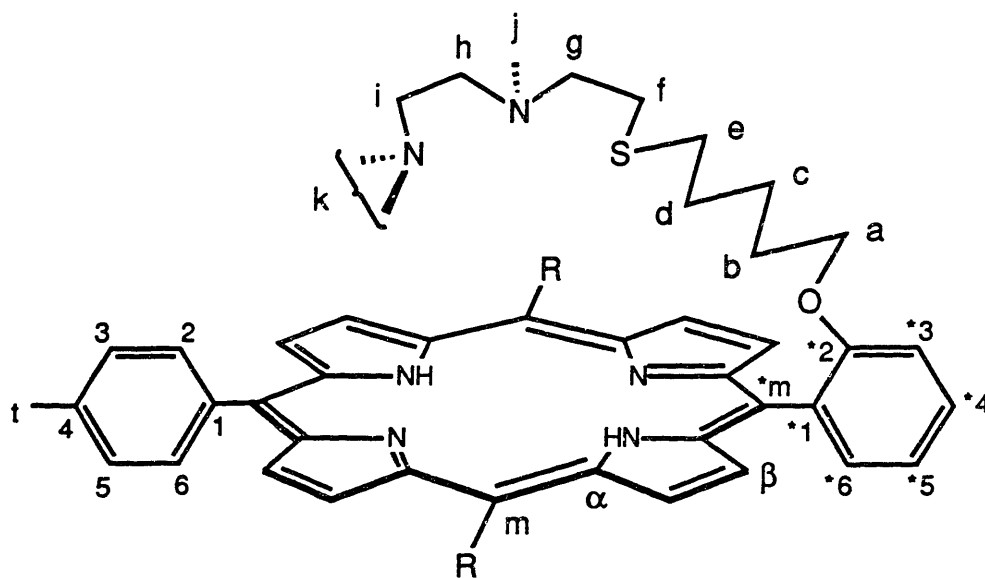


Figure 1.  $^1\text{H}$  NMR spectrum of **1** in  $\text{CDCl}_3$ . The peaks marked with S are from the solvent; those marked with X are from impurities. The inset shows the  $^1\text{H}$  NMR spectrum of  $\text{N}_2\text{S}$  in  $\text{CDCl}_3$ .



Labelling scheme for Table I



Table I

 $^{13}\text{C}$  CHEMICAL SHIFT ASSIGNMENTS

$\text{C}^a$	TPP <sup>47</sup>	OH-TTP	Br-TTP	$\text{N}_2\text{S}$	$\text{N}_2\text{S-TTP}$
$\text{C}_\alpha$	145.8	147	147		147
$\text{C}_\beta$	130.6	131.3	130.9		130.8
$\text{C}_m$	119.6	120.5	119.8		119.8
$\text{C}_1$	141.7	138.9	139.3		139.3
$\text{C}_2$	134.0	134.5	134.4		134.4
$\text{C}_3$	126.1	127.4	127.4		127.4
$\text{C}_4$	127.5	137.4	137.2		137.2
$\text{C}_5$	126.1	127.4	127.4		127.4
$\text{C}_6$	134.0	134.5	134.4		134.4
* $\text{C}_m$		121.1	120.2		120.2
* $\text{C}_1$		132.0	131.4		131.4
* $\text{C}_2$		155.0	158.8		158.9
* $\text{C}_3$		115.4	112.0		112.1
* $\text{C}_4$		130.3	129.7		129.7
* $\text{C}_5$		119.5	119.4		119.4
* $\text{C}_6$		134.9	135.6		135.7
$\text{C}_a$			68.0		68.2
$\text{C}_b$			27.6		29.0
$\text{C}_c$			24.0		24.5
$\text{C}_d$			32.8		28.2
$\text{C}_e$			31.5		31.4
$\text{C}_f$				21.9	29.0
$\text{C}_g$				60.5	57.6
$\text{C}_h$				56.9	57.2
$\text{C}_i$				55.0	55.2
$\text{C}_j$				41.7	42.0
$\text{C}_k$				45.4	45.7
$\text{C}_{\text{tol}}$		21.5	21.4		21.4

<sup>a</sup> See labelling scheme on previous page.

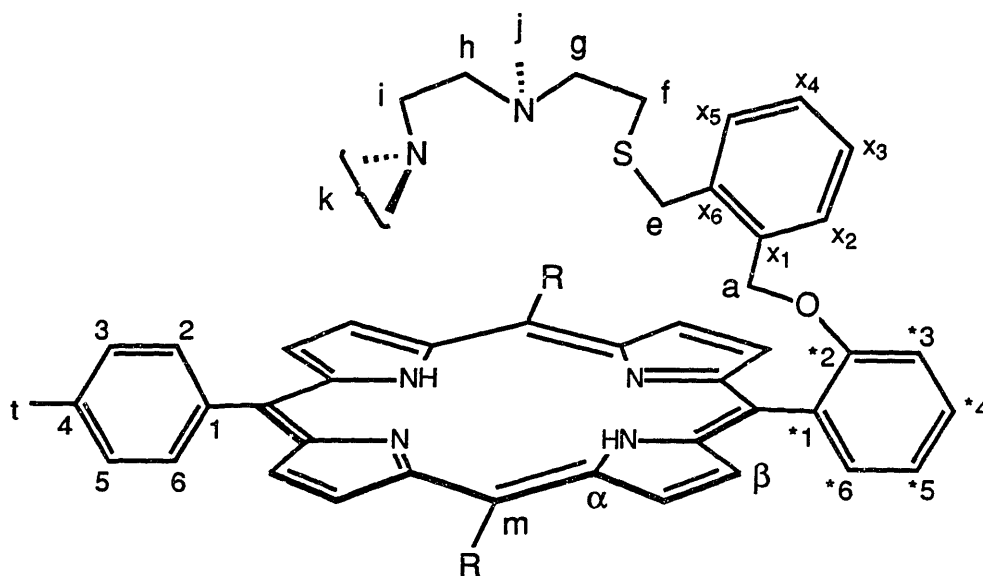
Furthermore, the parent ion in the mass spectrum displayed an isotopic array which precluded the presence of bromine. Clearly, the reactive benzyl bromide had been hydrolyzed during the aqueous work-up of the porphyrin. Once this difficulty had been identified, a one pot synthesis carefully excluding water was devised. This synthesis is not as proceed in as high yield or with as few byproducts as the synthesis of **1**, probably due to the extreme reactivity of the benzyl bromide compared to that of the alkyl bromide used in the synthesis of **1**.

The NMR spectra of **2** have been thoroughly analyzed using 2D as well as 1D methods. The resonances from the "tail" in the  $^1\text{H}$  NMR spectrum of **2** in  $\text{CDCl}_3$  do not bear much resemblance to those of the free  $\text{N}_2\text{S}$  or the pattern seen in **1**. However, **2**, like all porphyrins, shows very solvent dependent  $^1\text{H}$  NMR spectra. When the spectrum of the ligand in benzene is recorded, the "tail" resonances appear as two singlets and three clearly defined, complex multiplets, one pair of which show the symmetry observed in the spectrum of free  $\text{N}_2\text{S}$ . (See inset, Figure 2a) The aromatic proton resonances from the xylyl linker are found upfield of the porphyrin phenyl resonances. The pattern of multiplets seen for these protons is again very solvent dependent. In deuterated THF they appear as three multiplets in a 2:1:1 ratio. (Figure 2a) Many of the resonances in the  $^{13}\text{C}$  NMR spectrum of **2** could be assigned by analogy to **1**. Assigning the six additional phenyl carbons from the xylyl linker, though, was not possible by this method. In order to assign the resonances, two multipulse NMR experiments were performed.

Deuterated THF was the solvent chosen for these experiments because **2** had been observed to decompose in chlorinated hydrocarbon solvents even under  $\text{N}_2$ . In THF, several solvent dependent changes in the  $^{13}\text{C}$  spectrum were observed. The  $\text{C}_g$  and  $\text{C}_h$  resonances from the "tail", which had been coincident in  $\text{CDCl}_3$ , were now resolved (Figure 2b). The peak at 135.2 which corresponds to the  $\text{C}_2, \text{C}_6$  resonance was broadened. The broadening is a manifestation of the asymmetry of the porphyrin which makes the three tolyl groups inequivalent. This inequivalence causes the  $\text{C}_2, \text{C}_6$  shifts of at least one of the tolyl groups on the porphyrin to be slightly different than the others, resulting in a broader peak for this

resonance. Similarly, in the  $^1\text{H}$  spectrum, the tolyl methyl resonance has begun to split into more than one signal.

The Attached Proton Test allows for differentiation of methyl and methyne resonances from methylene and quaternary resonances. The quaternary carbons from the xylyl group were located in this experiment (136.6, 136.1 ppm), which also affirmed many of the assignments made for **1**, particularly the assignment of the "tail" methyl resonances at 42.3 and 46.0 ppm for **2** in THF (42.0 and 45.7 for **1** in  $\text{CDCl}_3$ ). A HETCOR experiment matching the 6.4 to 8.2 ppm region of the  $^1\text{H}$  spectrum to the 110 to 140 ppm region in the  $^{13}\text{C}$  experiment was used for identification of the xylyl methyne resonances. In addition, since the  $^{13}\text{C}$  phenyl resonances of the tolyl groups had been assigned by analogy to **1**, the 2D data allowed for assignment of individual phenyl resonances in the  $^1\text{H}$  spectrum. The data from the HETCOR experiment are shown in Figure 3. The assignments of the spectra in Figure 2 have been made using all available information.



Labelling Scheme for Figures 2 and 3

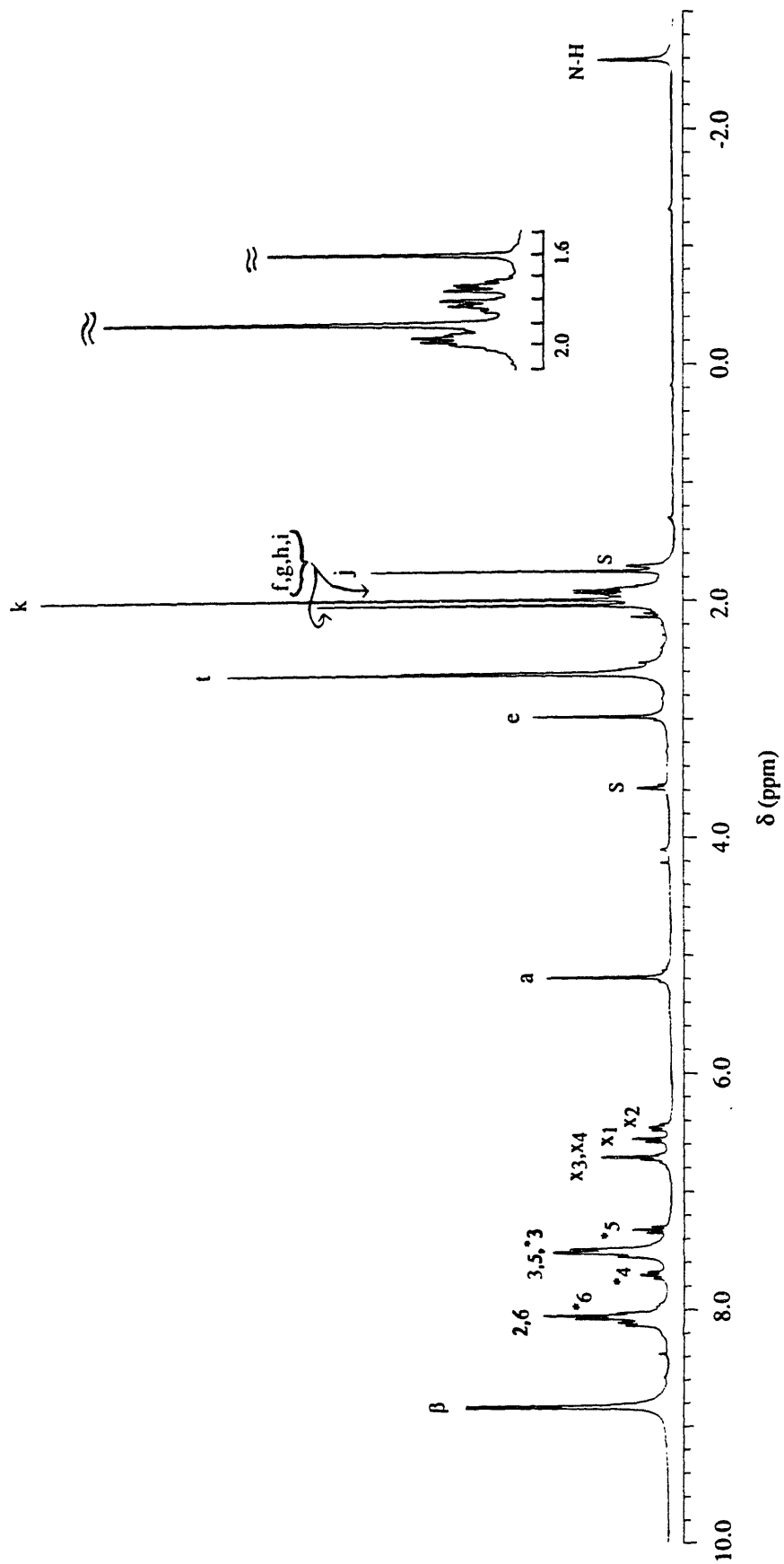


Figure 2a.  $^1\text{H}$  NMR spectrum of 2 in deuterated THF. Inset: 1.5-2.1 ppm region of the  $^1\text{H}$  NMR spectrum of 2 in  $\text{C}_6\text{D}_6$  showing the symmetric multiplet pattern for methylene resonances in the "tail".

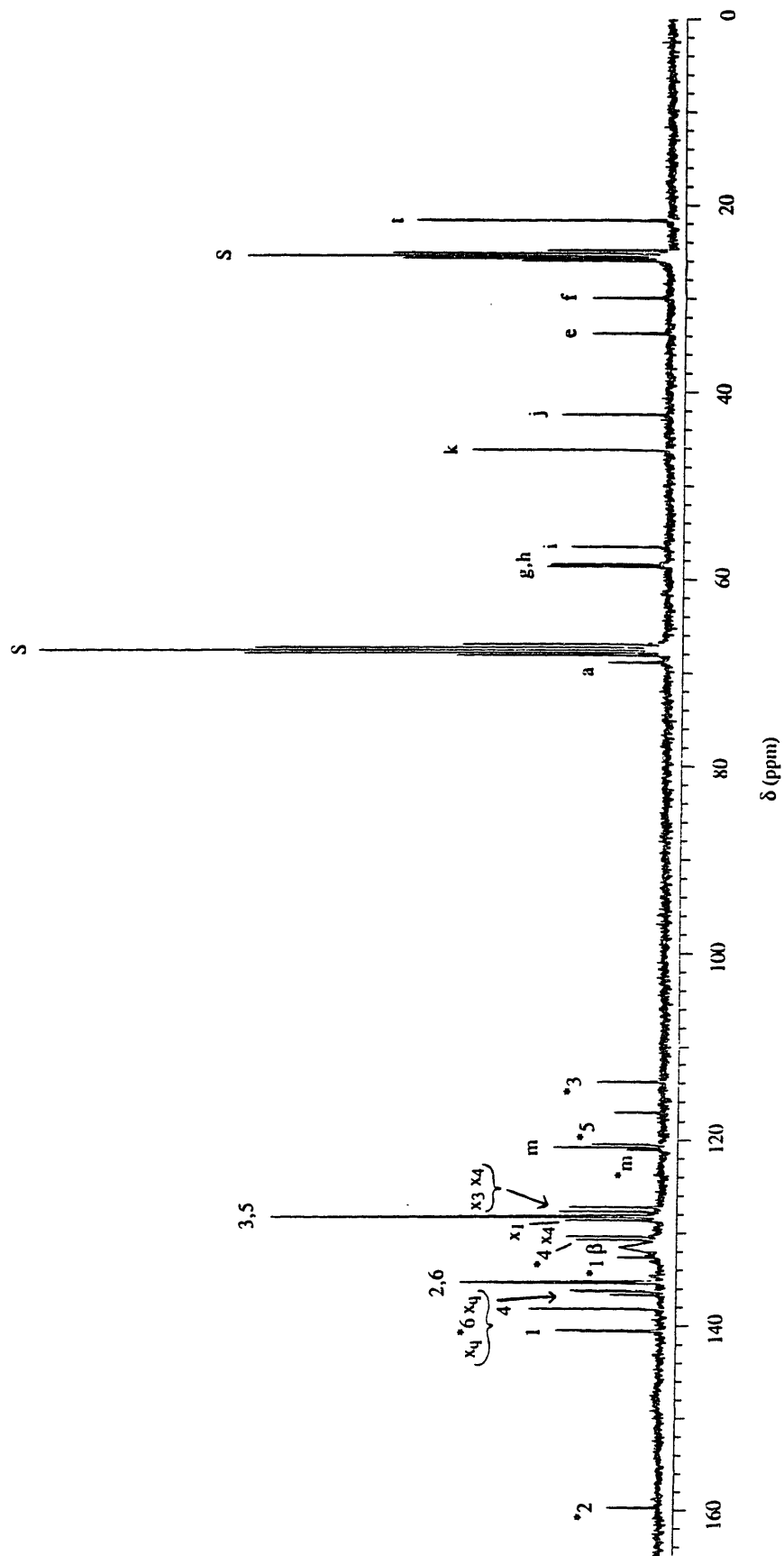


Figure 2b.  $^{13}\text{C}$  NMR spectrum of 3 in deuterated THF.

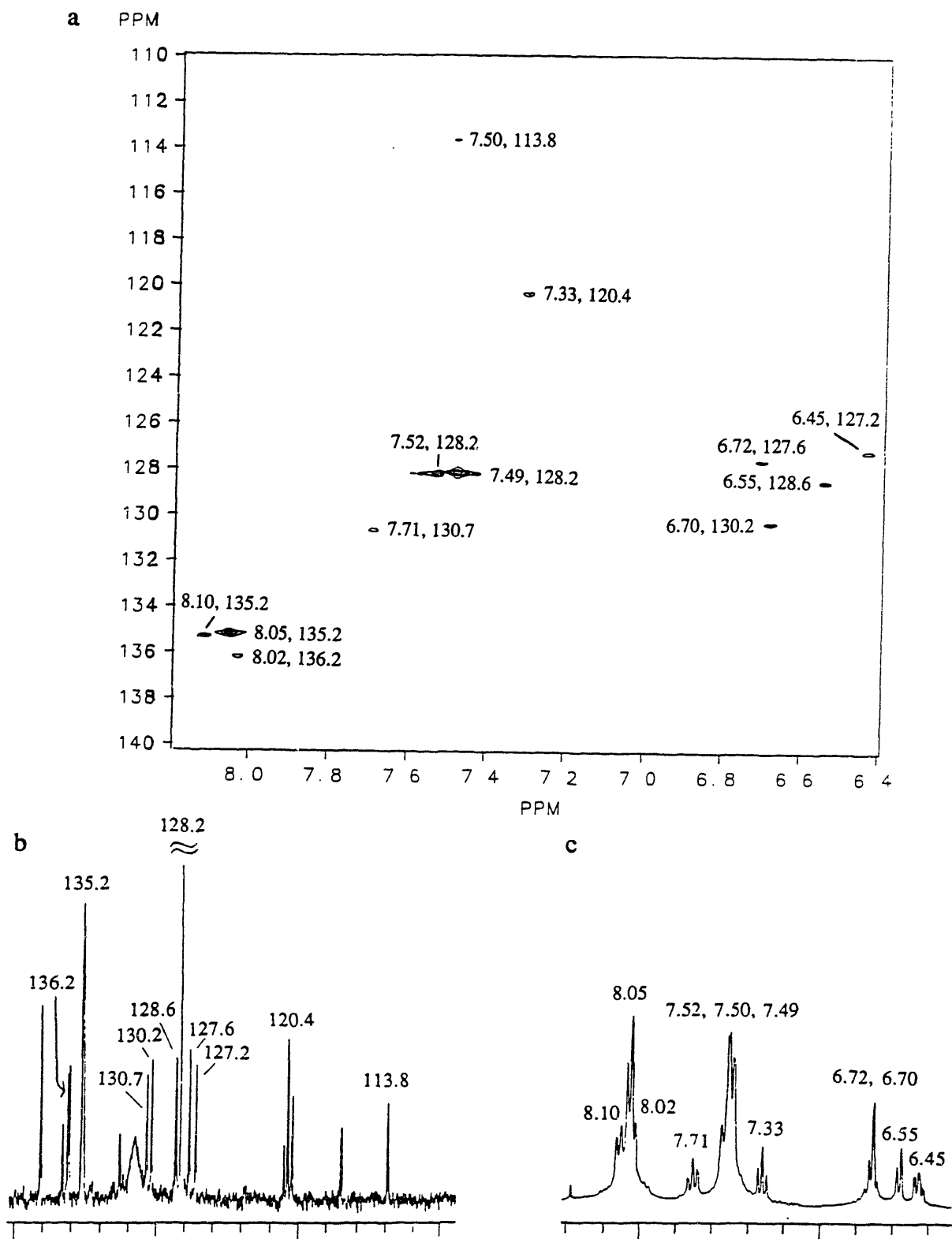


Figure 3. Results from HETCOR experiment on 2. a) 2D data. Cross peaks are labelled with proton and carbon resonances. b) 140-110 ppm region of carbon spectrum of 2. Peaks are labelled by chemical shift. Unlabelled peaks are from quaternary carbons. c) 8.4-6.2 ppm region of proton spectrum of 2 with peaks labelled by chemical shift.

Based on the successful of the syntheses of **1** and **2**, similar ligands were designed using  $\text{NH}_2\text{-TPP}$  as the starting porphyrin (Scheme II). For one of these ligands, an amide link to the porphyrin base was planned. By using the  $\omega$  substituted acyl halide,  $\text{Cl}(\text{C}=\text{O})(\text{CH}_2)_3\text{Br}$ , the synthesis of a "tailed" porphyrin with a dangling bromide, analogous to  $\text{Br-TTP}$ , was attempted. Unfortunately, the most stable product under the reaction conditions appeared to be the cyclic amide, **3**, resulting from displacement of the terminal bromide by the amide nitrogen. When this porphyrin was first isolated, it was thought to be the desired product. The  $^1\text{H}$  NMR showed three methylene resonances at reasonable chemical shifts for the desired compound. In the  $^{13}\text{C}$  NMR spectrum, however, the aliphatic resonances and the carbonyl resonance appeared at chemical shifts that were inconsistent with the proposed structure. Furthermore, the product would not react with  $\text{N}_2\text{S}$ . Again, mass spectral data led to the correct identification of the compound. The parent ion peaks occurred at  $m/e = 697$  which corresponds to the molecular weight of the desired product minus 81, the mass of the bromide and proton lost in the cyclization reaction. The aliphatic  $^{13}\text{C}$  resonances also matched well with those of the cyclic amide, pyrrolidone, as shown in Figure 4. A minor product was isolated from the reaction as well. All spectral data suggest that it was the expected product, **4**.

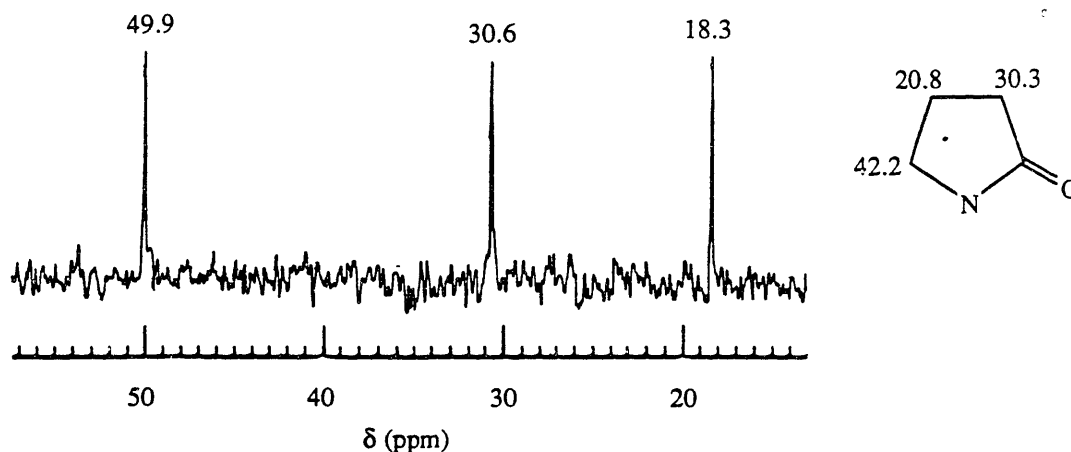


Figure 4. Aliphatic region of the  $^{13}\text{C}$  spectrum of **3** in  $\text{CDCl}_3$  and  $^{13}\text{C}$  chemical shifts of 2-pyrrolidone.

Since  $\alpha,\alpha'$ -dibromoxylene was known to react with amines, a ligand completely analogous to **2** based on  $\text{NH}_2$ -TPP was attempted. Once again, the cyclized compound, **5**, was the major product isolated from the reaction. In this case, the high symmetry of the xylene resonances in the  $^1\text{H}$  and  $^{13}\text{C}$  NMR spectra was at first perplexing. When the identity of **3** was established, however, the nature of the major product from this reaction also became clear. The addition of  $\alpha,\alpha'$ -dibromoxylene to  $\text{NH}_2$ -TPP was followed by TLC and the first product observed to form was the cyclized product, **5**. Upon addition of  $\text{N}_2\text{S}$ , a second spot appeared on the TLC plate. This spot was later found to correspond to  $\text{NH}_2$ -TPP, the starting material. Thus, **5** formed readily under the reaction conditions and decomposed in the presence of  $\text{N}_2\text{S}$ . The results from these experiments demonstrate the reactivity of the amino protons in  $\text{NH}_2$ -TPP and the propensity of the nitrogen to form five membered rings. Had the reactants chosen contained extra carbons for the linking moiety, these syntheses might have been more successful.

**Addition of Iron.** The addition of iron to  $\text{N}_2\text{S}$ -TTP and  $\text{N}_2\text{S}$ -xy-TTP was accomplished by using a relatively mild method. Ferrous salts were allowed to react with the porphyrin in refluxing THF/toluene solution in the presence of a non-coordinating base, 2,6-lutidine. Air oxidation of the reaction mixture yielded the  $\mu$ -oxo diiron(III) species which form readily and are stable in the basic reaction solution. Excess ferrous salts were removed by filtration but further purification proved to be difficult. Very polar eluants were necessary to move the ferric porphyrin on a silica gel column and the product smeared over the column giving no apparent separation. Alumina gel chromatography did not give any better results. Initial attempts appeared so futile that the product, isolated from the reaction mixture by rotary evaporation, was washed with water to remove excess lutidine and used without further purification. The porphyrin into which the iron had been inserted had been purified and it was assumed that little decomposition occurred during the insertion. Also, since copper ions should only bind to



porphyrins containing an intact "tail", it was believed that the final product could be purified by fractional crystallization.

In order to synthesize various five coordinate ferric porphyrins to use for reactions with Cu(II) salts, a method published by Torrens *et al.*<sup>44</sup> was chosen. In this method, an aqueous, saturated, acidic salt solution is added to the ferric porphyrin in benzene yielding a biphasic mixture which is stirred for 6 or more hours. Since, (N<sub>2</sub>S-TTPFe)<sub>2</sub>O is not very soluble in benzene, CH<sub>2</sub>Cl<sub>2</sub> was employed. When the aqueous solution was added to the porphyrin solution, however, an emulsion resulted. Interactions between the acid and the basic amino groups in the "tail" were thought to be the cause of the emulsion. After 15-20 hr of stirring, the solvents were removed from the emulsion under vacuum and the porphyrin product extracted from the resulting solids in CH<sub>2</sub>Cl<sub>2</sub>. Both **6** and **7** were obtained in this manner. An attempt was made to synthesize the OAc<sup>-</sup> derivative by the method, but isolated solids always exhibited bands in the optical spectrum indicative of the μ-oxo diiron(III) porphyrin as well as those of the OAc<sup>-</sup> product.

The products, **6** and **7**, were characterized by various spectral methods. Their optical spectra were very similar to that of FeTPPCL. The band occurring at slightly higher energy than the Soret band, however, was dependent on the axial ligand. For the Cl<sup>-</sup> complex, the maximum occurs at 375 nm, for Br<sup>-</sup>, at 398 nm, and for SCN<sup>-</sup>, at 340 nm. Also, a band was observed for **6** and **7** at ~600 nm that is not apparent in FeTPPCL. While the IR spectra of **6** and **7** showed no Fe-(μ-oxo) stretch, the spectrum of **7** showed a band at 2010 cm<sup>-1</sup>, in the range expected for axially bound SCN<sup>-</sup>.<sup>49</sup> The <sup>1</sup>H NMR spectra of these two compounds also suggested that the desired products had been obtained. The β pyrrole and meta phenyl proton resonances in the spectrum of **6** in CDCl<sub>3</sub> appeared at chemical shifts similar to those for FeTPPCL. The β-H resonance at ~80 ppm, however, was split. The tolyl-CH<sub>3</sub> resonance was apparent at 7.41 ppm but the remainder of the peaks were broad and unidentifiable. Similarly,

---

<sup>49</sup> Scheidt, W.R.; Young, J.L.; Geiger, D.K.; Taylor, K.; Hatano, K. *J. Am. Chem. Soc.* **1982**, *104*, 3367-3374.

the  $\beta$ -H resonance for **7** was found at  $\sim 75$  ppm, the same value reported for TPPFeSCN.<sup>49</sup> The meta phenyl protons in the spectrum of **7** are unsymmetrical and overlapping at 13.0 and 12.7 ppm. The literature spectrum of TPPFeSCN<sup>49</sup> also shows unsymmetrical resonances at 13.1 and 12.0 for these protons. In this spectrum, however, the downfield resonance is the sharper of the two, whereas the opposite is true in the spectrum of **7**. Again the tolyl resonance at 6.54 ppm was the only identifiable feature in the 0-12 ppm region of the spectrum. The EPR spectra of the two compounds were typical for high spin ferric porphyrins.

While these spectral data revealed the likely presence of the desired axial ligand in **6** and **7**, they give no information on the purity of the complexes or the integrity of the ligand. The resonances in the upfield region of the  $^1\text{H}$  NMR spectra were so broad as to yield no valuable information. Several sharp peaks occurred in this region, but were later determined to be solvent peaks. The porphyrins appeared to have a strong affinity for the small alkanes used to precipitate them, and obtaining solvent free solids, as determined by  $^1\text{H}$  NMR, was a difficult task. Nonetheless, despite the uncertainty about the purity of **6** and **7**, they were used for exploratory reactions with Cu(II) salts.

When crystallization of the binuclear metalloporphyrin products achieved from reactions with **6** and **7** with Cu(II) proved to be extremely difficult, further attempts were made to purify the ferric porphyrins. Column chromatography under  $\text{N}_2$  of the ferrous derivative of OH-xy-TTP was achieved without difficulty. The same method was tried for  $\text{N}_2\text{S}$ -xy-TTP with no success. The product was distributed over the entire column without any apparent separation. Fractions from the column were oxidized and examined by UV-Vis spectroscopy. The intensity of the band at  $\sim 600$  nm was seen to vary. Some experimentation proved that this band disappeared if the complex was washed with water made slightly acidic (pH 5) with HCl. This result suggested that the band at  $\sim 600$  nm might arise from iron weakly bound to the  $\text{N}_2\text{S}$  site. The presence of weakly bound iron might also explain the smearing on the column which did not occur with the OH-xy-TTPFe(II). Such a weakly bound iron species would adhere

well to the oxygen rich silica gel and the iron could be in equilibrium between the complex and the gel.

To avoid this problem,  $(N_2S-TTPFe)_2O$  isolated from the THF/toluene reaction mixture was washed repeatedly with weak acid before purification was attempted. Column chromatography on silica gel in air with a gradient elution of  $NH_3 \cdot MeOH$  in  $CH_2Cl_2$  allowed for separation of the product as a slow moving band in 3%  $NH_3 \cdot MeOH$ . Several impurities could be washed down the column with low polarity eluant, but the product band was very closely followed by another band. The product was collected and solvents removed by rotary evaporation. The  $^1H$  NMR spectrum of the product displayed peaks for the beta phenyl, meta phenyl and tolyl methyl protons at chemical shifts characteristic of both  $\mu$ -oxo and five coordinate hydroxo complexes. The  $\mu$ -oxo form appeared to be the predominant one. Although extremely broad and ill defined, other resonances in the spectrum appeared reasonable for the desired complex. The same results were achieved for  $(N_2S-xy-TTPFe)_2O$  except that a slightly more polar eluant was necessary to develop the product on the column and several more impurities were separated. The purified products were washed with weak aqueous solutions of HCl to obtain the five coordinate chloride derivatives, **8** and **9**. Unfortunately, the yields for these two complexes were only ~50%, suggesting that considerable decomposition occurred during the addition of iron or on the column.

Even more disturbing than the low yield was the observation that, although the band collected off the columns initially moved as one spot on a TLC plate, 24 hr later, after removal of the eluant and redilution, the same compound developed as two or more spots. Originally, this observation was attributed to decomposition on silica which became apparent in more concentrated solutions. However, other data suggested that the products might decompose in air in chlorinated solvents. A TLC taken of samples of **8** and **9** which had been left for several months to crystallize from  $CHCl_3$  layered with hexane showed no spot corresponding to the pure complexes. Chlorinated solvents were used widely in work with the porphyrin complexes and the tendency of these complexes to decompose may have been a source of some

of the difficulties encountered. Purifying these compounds without chlorinated solvents required the use of a ternary eluant system. A silica gel column run under  $N_2$  developed in a gradient of  $NH_3 \cdot MeOH$  in 10% THF/tol gave clean separation of a sample of **8** which had been previously purified but developed as multiple spots on a TLC plate. The isolated product was treated with  $HBF_4$  etherate in the presence of solid  $NaCl$ . After repeated filtration and removal of solvents under vacuum, a fine dark powder was obtained. The product was not the chloride derivative, as expected, but analyzed as the  $BF_4^-$  derivative,  $N_2S-TTPFeBF_4 \cdot 2HBF_4$ .

The bis(cyano) derivatives of **8** and **9** were synthesized by treatment of these complexes with excess  $(Et_4N)CN$ . The low spin cyano complexes should have displayed  $^1H$  NMR spectra with sharper resonances and these complexes were desired as starting materials for reaction with  $Cu(II)$ . The  $^1H$  NMR spectra of the resulting complexes, however, were extremely complex due to the asymmetry of the porphyrins. This asymmetry was clearly reflected in the  $\beta$  pyrrole proton resonances which are found upfield of TMS for low spin ferric porphyrins.<sup>50</sup> In the spectrum of  $N_2S-TTPFe(CN)_2$ , the four  $\beta$  protons appear as clearly resolved singlets between -12.0 and -13.0 ppm. In  $N_2S-xy-TTPFe(CN)_2$ , they appear as a broad singlet and a doublet nearly coincident at -14.3 and -14.4 ppm. The  $^{13}C$  spectrum of the latter complex was also collected. While the aromatic region was too complex to assign, the aliphatic region showed peaks for all the carbons in the "tail." This spectrum provided the first good evidence that the ligand remained intact during insertion of the iron and purification of the ferric complexes. The bis(cyano) species, however, proved to be stable only in the presence of excess  $(Et_4N)CN$ . Precipitation of the complexes in hexane/  $CCl_4$  and other attempts at purification always gave products that exhibited  $^1H$  NMR spectra with broader resonances and additional peaks upfield of TMS. The presence of new low spin impurities in the samples was perplexing, but was probably a manifestation of the inherent instability of these ferric

---

<sup>50</sup> In ref. 43b, Goff discusses the effects on the  $\beta$  H resonances of increasing asymmetry in the porphyrin.

porphyrins in chlorinated solvents in air. Also, the lability of the cyanide ligand made the cyano complexes unsuitable as precursors to CN<sup>-</sup> bridged bimetallic complexes.

**Addition of Copper.** Studies of the addition of Cu(II) to the ferric porphyrin species were complicated by lack of characteristic spectral changes. The optical spectra of the bimetallic complexes tended to be indistinguishable from those of the ferric porphyrin starting material. The <sup>1</sup>H NMR spectra of the Cu(II) containing complexes showed broader or, in some cases, shifted resonances, but, as for the high spin ferric porphyrins, revealed no detailed information. For complexes based on **7**, changes in the C-N stretching frequency could be monitored by IR spectroscopy, but, in general, only EPR spectroscopy provided insight into the coordination of the Cu(II) by the ligand. Unfortunately, even this technique could not be used to its fullest. Integration of the spectra to determine the stoichiometry of the metals ions present was not possible when these studies were carried out.

Initially, attempts to synthesize bimetallic complexes were carried out with **6** and **7**. An attempt to add a stoichiometric amount of Cu(OAc)<sub>2</sub>·H<sub>2</sub>O to **6** in EtOH yielded a product with an EPR spectrum showing two Cu g<sub>||</sub> signals. Repeated precipitation of the product from pentane reduced the magnitude of one of the signals but did not completely eliminate it. The g<sub>||</sub> and A<sub>||</sub> values of the major signal were indicative of nitrogen atom coordination.<sup>51</sup> A general method was then developed whereby aqueous solutions containing excess copper(II) salts were allowed to stir in contact with CH<sub>2</sub>Cl<sub>2</sub> solutions of **6** and **7**. The organic layer was extracted and the product precipitated from pentane or hexane. This method was based on the assumption that, since the copper salts were insoluble in CH<sub>2</sub>Cl<sub>2</sub>, only Cu(II) bound to the ligand would remain in the organic layer. This procedure was carried out using Cu(NO<sub>3</sub>)<sub>2</sub>, Cu(BF<sub>4</sub>)<sub>2</sub>, CuSO<sub>4</sub>, and CuCl<sub>2</sub>. Syntheses of bimetallic complexes using the first three salts, which contain anions that do not bind strongly to the axial position of ferric porphyrins, gave Cu g<sub>||</sub> and A<sub>||</sub> values dependent on the axial ligand on the ferric porphyrin reactant (Table II).

---

<sup>51</sup> Peisach, J.; Blumberg, W.G. *Arch. Biochem. Biophys.* **1974**, *165*, 691.

Table II

COPPER EPR  $g_{||}$  AND  $A_{||}$  VALUES FOR HETEROBIMETALLIC PRODUCTS

Cu(II) Reagent	N <sub>2</sub> S-TTPFeBr (6)		N <sub>2</sub> S-TTPFeSCN (7)	
	$g_{  }$	$A_{  }$ (mK)	$g_{  }$	$A_{  }$ (mK)
Cu(NO <sub>3</sub> ) <sub>2</sub>	2.184	17.8	2.239	17.2
Cu(BF <sub>4</sub> ) <sub>2</sub>	2.181	17.8	2.193	17.9
Cu(SO <sub>4</sub> )	2.184	17.3	2.237	16.7
CuCl <sub>2</sub>	2.207	15.5	2.211	15.4

The IR spectra of the three products obtained from reactions with **6** were relatively uninformative. In the product of **6** and Cu(NO<sub>3</sub>)<sub>2</sub>, **6a**, the presence of band from free NO<sub>3</sub><sup>-</sup> could be detected. The EPR spectrum (Figure 5) shows both a high spin ferric porphyrin signal at  $g = 5.383$  and a Cu(II) signal with  $g_{\perp} = 2.056$  and  $g_{||} = 2.184$  ( $A_{||} = 17.8$  mK). The  $g_{||}$  and  $A_{||}$  values are reasonable for the Cu(II) bound to the N<sub>2</sub>S site and the Cu  $g_{\perp}$  signal shows clear superhyperfine splitting. Careful examination of the Cu  $g_{||}$  region reveals the presence of a very minor amount of a second Cu(II) signal. Interestingly, while the EPR spectrum of the product of **6** and Cu(BF<sub>4</sub>)<sub>2</sub>, **6b**, (Figure 5) exhibits only a relatively small Cu(II) signal, this signal has remarkably similar values to those of **6a** ( $g_{\perp} = 2.063$ ,  $g_{||} = 2.181$ ,  $A_{||} = 17.8$  mK) and its also shows distinct superhyperfine splitting. The product of **6** and CuSO<sub>4</sub>, **6c**, displays a large Cu signal in its EPR spectrum (Figure 5) but the signal clearly contains contributions from two different  $g_{||}$  values. The predominant signal, however, has values similar to **6a** and **6b**:  $g_{\perp} = 2.055$  and  $g_{||} = 2.184$  ( $A_{||} = 17.3$  mK).

IR spectroscopy was more useful in characterizing the products of **7** and the Cu(II) salts. When Cu(NO<sub>3</sub>)<sub>2</sub> and CuSO<sub>4</sub> were the source of Cu(II), the products, **7a** and **7c** respectively, showed two strong C-N stretching bands in their IR spectra, one at  $\sim 2010$  cm<sup>-1</sup> and the other at  $\sim 2080$  cm<sup>-1</sup>. The first band is indicative of axially bound thiocyanate. The

other probably arises from free thiocyanate present as the counterion. In the IR spectrum of the product from  $\text{Cu}(\text{BF}_4)_2$ , **7b**, only very weak C-N stretching bands are apparent and the larger band occurs at  $2090\text{ cm}^{-1}$ . The majority of axially bound thiocyanate must have been displaced. These data are consistent with the EPR spectral data.(Figure 6) The spectrum of **7a** contains a clean Cu(II) signal which is larger than the porphyrin signal and has the following parameters:  $g_{\perp} = 2.026$ ,  $g_{\parallel} = 2.239$  ( $A_{\parallel} = 17.2\text{ mK}$ ). The spectrum of **7c** appears strikingly similar to **7a** (Figure 6) and has Cu(II) values of  $g_{\perp} = 2.052$ ,  $g_{\parallel} = 2.237$  ( $A_{\parallel} = 16.7\text{ mK}$ ). By contrast, **7b** displays a weaker Cu(II) signal which contains more than one component. The values measured for the stronger signal are closer to those of **6a-6c** than to **7a** or **7c**:  $g_{\perp} = 2.049$ ,  $g_{\parallel} = 2.193$  ( $A_{\parallel} = 17.9\text{ mK}$ ). These results strongly suggest that the axial ligand on the ferric porphyrin influences the Cu(II) EPR signal.

The influence of the axial ligand is further supported by the results from the reaction of **6** and **7** with  $\text{CuCl}_2$ . The  $\text{Cl}^-$  anion is a good axial ligand for ferric porphyrins and in these reactions it appears to displace the axial ligand in **6** and **7**. The UV-Vis spectra of the complexes from  $\text{CuCl}_2$  with **6**, **6d**, and **7**, **7d**, are more similar to that of  $\text{FeTPPCl}$  than those of **6** or **7**. The IR spectrum of **7d**, shows only a free thiocyanate C-N stretch at  $2090\text{ cm}^{-1}$ . The EPR spectra of these two complexes (Figure 7) are essentially identical with  $g_{\perp} = 2.055$  and  $g_{\parallel} = 2.207$  ( $A_{\parallel} = 15.5\text{ mK}$ ) and  $g_{\perp} = 2.062$  and  $g_{\parallel} = 2.211$  ( $A_{\parallel} = 15.4\text{ mK}$ ).

The  $g_{\parallel}$  and  $A_{\parallel}$  values of the Cu signals in the EPR spectra of the bimetallic complexes and the apparent dependence of the Cu signal on the ferric porphyrin axial ligand were considered to be encouraging results. The Cu(II) did not appear to be loosely associated with the porphyrin but actually bound to the  $\text{N}_2\text{S}$  coordination site. The dependence of the Cu(II) signal on the axial ligand suggested that this ligand might be bridging the two metal centers. There was no evidence supporting intra- versus intermolecular bridging, but all the data supported incorporation of the Cu(II) into the ligand. The type of complex desired seemed to be at hand. Unfortunately, all attempts at crystallization or purification of the bimetallic complexes failed. The complexes appeared to decompose on silica or alumina TLC plates and

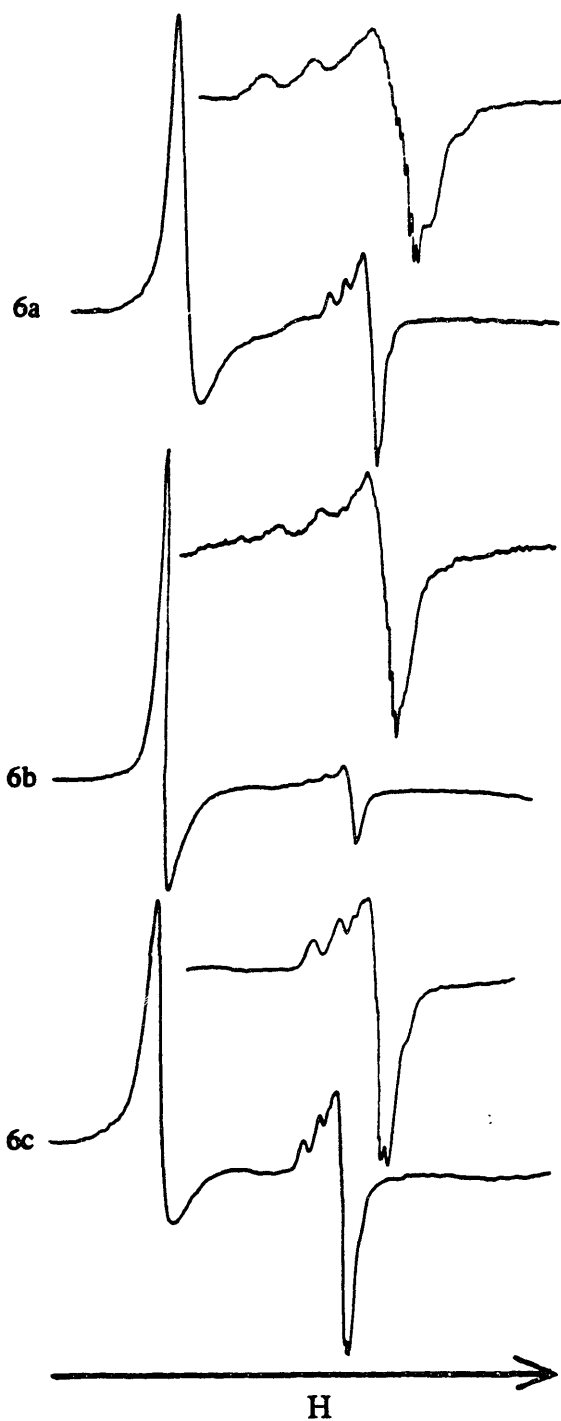


Figure 5. EPR spectra of 6a-6c. Insets are offset and expanded to show superhyperfine coupling.

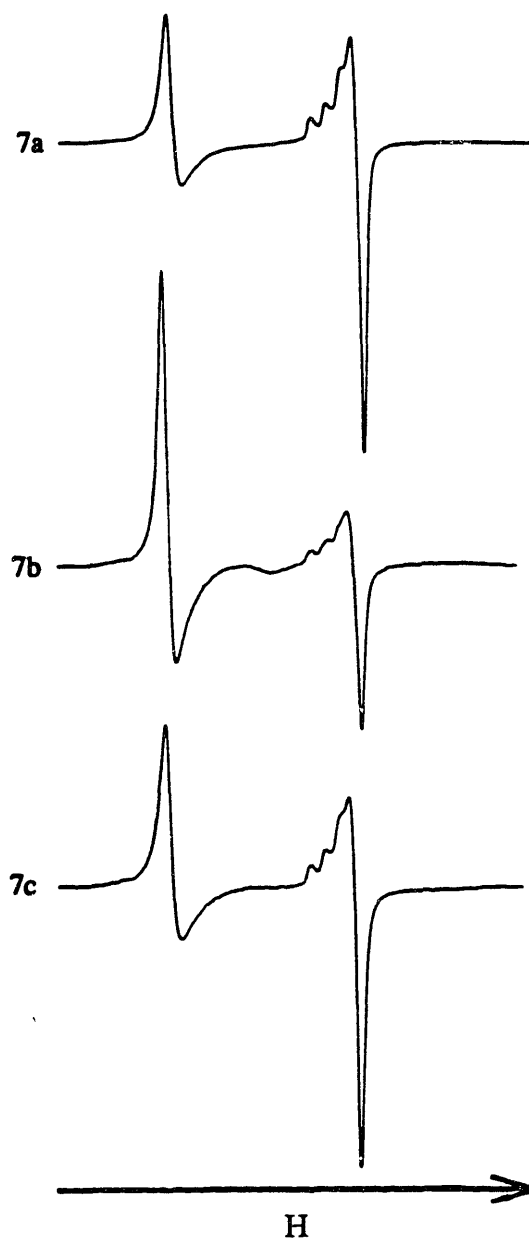


Figure 6. EPR spectra of 7a-7c.



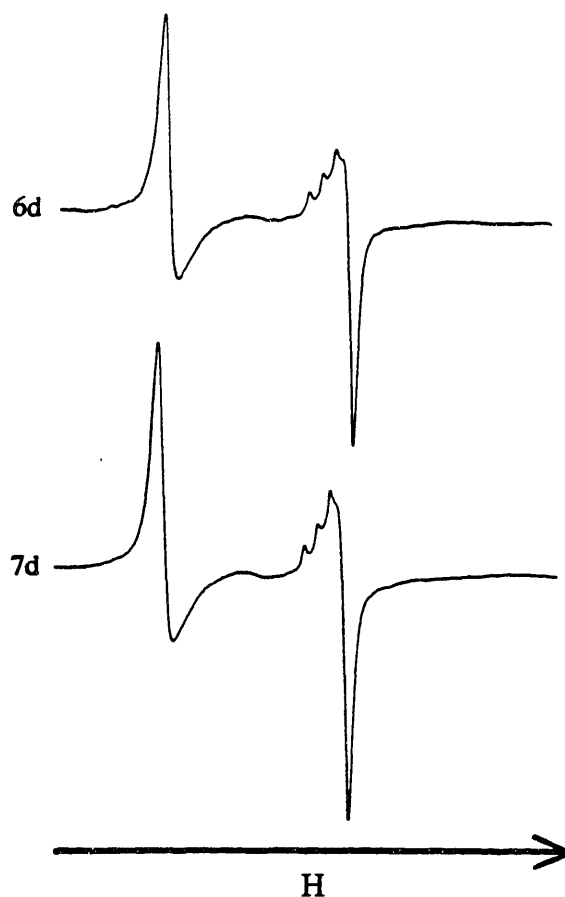


Figure 7. EPR spectra of 6d and 7d.

no reasonable separation could be achieved. Several samples were sent for elemental analysis and none analyzed for the desired complex. The complexes always formed amorphous solids during any crystallization attempt. The conformational lability of the porphyrin, the presence of polymeric species and the structural similarity between impurities and the desired complexes may all have played a role in rendering purification by crystallization or precipitation impossible. Because of these difficulties, focus turned to obtaining purified ferric porphyrin complexes before attempting addition of copper ion.

When purified **9** was obtained, a stoichiometric addition of  $\text{Cu}(\text{OAc})_2 \cdot \text{H}_2\text{O}$  to the ferric porphyrin was carried out.  $\text{Cu}(\text{OAc})_2$  was chosen as a reagent because it forms a non-hygroscopic crystalline salt. Freshly recrystallized material, presumed to contain 1  $\text{H}_2\text{O}$  per  $\text{Cu}(\text{OAc})_2$ , was weighed out and allowed to react with **9** in MeOH. The same procedure was carried out three times. In each case the results were essentially the same. The UV-Vis

spectrum of the resulting complex showed bands characteristic of five coordinate high spin and  $\mu$ -oxo diiron(III) porphyrins. The EPR spectra showed small high spin ferric porphyrin signals and Cu(II) signals comprised of two components. One component exhibited a  $g_{\parallel}$  value of  $\sim 2.25$  and the other  $\sim 2.20$ . While one signal or the other could be reduced by trituration of the solid with weak, aqueous HCl (pH 3) or precipitation from hexane or ether, neither signal could be completely eliminated. Washing with a strongly acid aqueous solution (pH 1-2) eliminated the optical bands associated with the  $\mu$ -oxo species but also removed the majority of the copper from the ligand as determined by the reduction of the Cu(II) signal in the EPR spectrum. A second acid wash failed to remove the remaining Cu(II) and both  $g_{\parallel}$  signals were still present. The Cu(II) could be restored by allowing a  $\text{CH}_2\text{Cl}_2$  solution of it to stir with an aqueous solution of  $\text{CuCl}_2$ . The spectrum of the resulting complex was essentially identical to that of **6d** and **7d** with only a small amount of a signal with larger  $g_{\parallel}$  apparent. On the third attempt, the bimetallic porphyrin was stirred with a saturated solution of NaCl adjusted to pH 3 with HCl. The intent was to remove any residual  $\text{OAc}^-$  which might remain loosely bound to the copper forming one of the copper species observed by EPR. The result was that, again, nearly all the Cu(II) ion was washed out of the ligand. Clearly, the  $\text{N}_2\text{S}$  site does not bind Cu(II) tightly.

These results suggested a potential design flaw in the  $\text{N}_2\text{S}$ -TTP and  $\text{N}_2\text{S}$ -xy-TTP ligand systems. The two aliphatic nitrogens and the thio ether form a site which does not particularly favor the binding of Cu(II) ions. While Cu(II) does appear to be taken up by the ligand, the metal ion can be washed away with as mild an agent as saturated aqueous NaCl. The use of  $\text{Cu}(\text{OAc})_2 \cdot \text{H}_2\text{O}$  as a Cu(II) source was probably not adventitious. All attempts to synthesize bimetallic species either from **6** or **9** using this reagent have led to products containing more than one type of copper. The  $\text{OAc}^-$  anions may interfere with the axial ligation on the porphyrin. Acetate, however, does not bind strongly enough to ferric porphyrin to allow for ready isolation of the five coordinate ferric porphyrin species and may lead instead to formation of intermolecular  $\mu$ -oxo or  $\mu$ -acetato bridges in the bimetallic systems. Nonetheless,

regardless of the Cu(II) reagent employed, the extreme lability of the Cu(II) in the N<sub>2</sub>S site would add to the difficulty of purifying a binuclear porphyrin complex. The N<sub>2</sub>S coordination site, however, should bind Cu(I) favorably which suggests that in future studies, a strategy using the addition of Cu(I) ions to the ligand systems may yield more interesting results.

## Conclusion

The task of constructing a synthetic model for the active site of cytochrome oxidase is clearly a difficult one. This fact is borne out not only by the problems encountered in the work presented here but also in the failure of any group of researchers to prepare and crystallize such a model over the past ten years, despite many attempts. The successful model will probably require a ligand system with sufficient structural rigidity to direct the copper ion over the porphyrin ring but not to constrain it so much as to interfere with optimal interactions between the two metals. The models published have been based on either meso aryl or  $\beta$  substituted porphyrins. The aryl substituted porphyrins have been used because they can be synthesized in relatively high yield and are usually crystalline complexes. The  $\beta$  substituted porphyrins better resemble naturally occurring porphyrins, which could be important in promoting the desired interaction between the metals, but until recently<sup>46</sup> have been significantly more difficult to synthesize. In addition, they lack the aryl rings known to promote crystallinity.

A wide variety of methods have been used to provide a bound copper in the published models. Some researchers have allowed a copper ion, complete with its own ligand set, to react with an iron porphyrin, relying solely on the "self assembly" method to produce the desired bridged compound. In other cases, the copper binding site has been strapped across the porphyrin plane to ensure that the copper will be bound in close proximity to the iron. While more success has been achieved with the latter method, the "straps" introduce potential for considerable steric restrictions on the copper binding site which could affect the interactions between the copper and iron. There is a possibility that the copper in the enzyme is constrained

to a specific configuration required for its function. If such is the case, it will be extremely difficult for inorganic chemists to synthesize a model without more knowledge about the coordination environment.

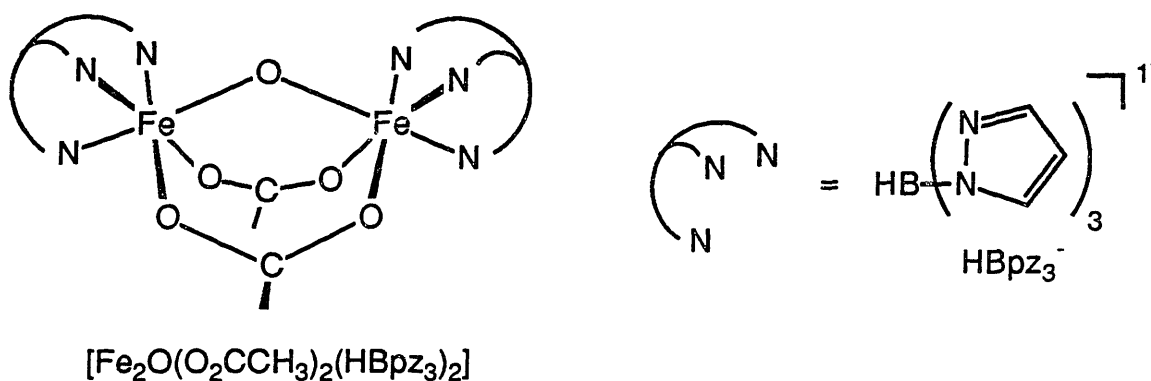
Clearly, the sensitivity of the iron porphyrins to chlorinated hydrocarbon solvents and air limited the studies reported herein. As a result, the potential of the ligand systems for use in structural models of cytochrome oxidase has not been fully investigated. Since the N<sub>2</sub>S site would most likely bind Cu(I) more tightly than Cu(II), the synthesis of Fe(II)-Cu(I) or Fe(III)-Cu(I) species and a study of their reactivity with an O donor oxidant or with air could yield interesting results. On oxo bridged species synthesized in this manner would be especially interesting since the bridge in the resting state of the enzyme is believed to originate from the substrate dioxygen. The flexibility of the "tail," however, might still impair crystallization of binuclear species. Even in dilute solutions, intermolecular interactions might occur leading to the formation of polymeric species. A ligand system similar to **1** or **2** but containing a second arm to block the distal side of the heme and prevent intermolecular bridges might yield an ideal system. The second arm could either provide steric bulk to block axial coordination to the iron or an appended base to bind at this site. This strategy has been employed for hemoglobin and cytochrome P450 models but has not yet been seen in the literature for cytochrome oxidase models.<sup>46</sup>

The likelihood of achieving an x-ray diffraction structure of the active site of cytochrome oxidase has been greatly increased by the isolation of the small, one or two subunit, bacterial oxidases. Techniques for collecting EXAFS from these enzymes while membrane bound have been established. Knowledge of the actual structure of the site is thus more likely to be elucidated by these methods than by an inorganic model. The unique properties and activity of the site, however, will undoubtedly continue to motivate inorganic chemists to attempt to recreate the structure and its chemistry in synthetic systems.

### CHAPTER 3

## Solution Characterization of Tetranuclear Iron-Oxo Compounds Containing a Non-planar $\{\text{Fe}_4\text{O}_2\}^{8+}$ core

The first good structural model for the protein hemerythrin was synthesized by W. H. Armstrong in our laboratory in 1983.<sup>1</sup> Hemerythrin, an oxygen transport protein, is one of an emerging class of non-heme iron proteins containing an oxo-bridged diiron core.<sup>2</sup> The structure of this complex which utilizes the facially capping hydrotris(1-pyrazolyl)borate [(HBpz<sub>3</sub>)<sup>-</sup>] ligand is shown below. The optical, resonance Raman, Mossbauer and magnetic



properties of  $[\text{Fe}_2\text{O}(\text{O}_2\text{CCH}_3)_2(\text{HBpz}_3)_2]$ , closely mimic those of the protein. Several other model compounds containing the same  $\mu$ -oxo bis( $\mu$ -acetato) diiron core have been synthesized since 1983.<sup>3</sup> All of these compounds, however, like  $[\text{Fe}_2\text{O}(\text{O}_2\text{CCH}_3)_2(\text{HBpz}_3)_2]$ , contain

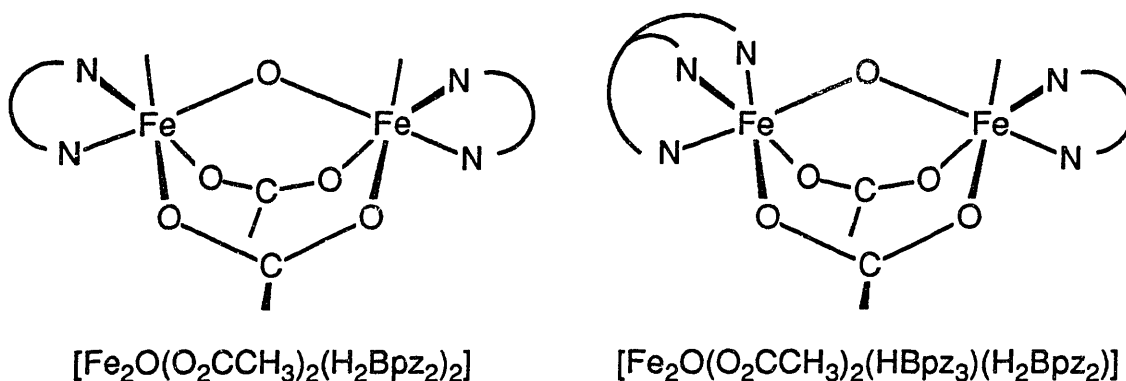
<sup>1</sup> (a) Armstrong, W.H.; Lippard, S.J. *J. Am. Chem. Soc.* **1983**, *105*, 4837-4838. (b) Armstrong, W.H.; Spool, A.; Papaefthymiou, G.C.; Frankel, R.B.; Lippard, S.J. *J. Am. Chem. Soc.* **1984**, *106*, 3653-3667.

<sup>2</sup> For recent reviews see (a) Lippard, S.J. *Angew. Chem., Int. Ed. Engl.* **1988**, *27*, 344-361. (b) Que, L. *ACS Symp. Ser.* **1988**, in press.

<sup>3</sup> (a) Wieghardt, K.; Pohl, K.; Gebert, W. *Angew. Chem., Int. Ed. Engl.* **1983**, *22*, 727. (b) Chaudhuri, P.; Wieghardt, K.; Nuber, B.; Weiss, J. *Angew. Chem., Int. Ed. Engl.* **1985**, *24*, 778-779. (c) Wieghardt, K.; Pohl, K.; Ventur, D. *Angew. Chem., Int. Ed. Engl.* **1985**, *24*, 392-393. (d) Borovik, A.S.; Murch, B.P.; Que, L.; Papaefthymiou, V.; Munck, E. *J. Am. Chem. Soc.* **1987**, *109*, 7190-7191. (e) Murch, B.P.; Bradley, F.C.; Que, L. *J. Am. Chem. Soc.* **1986**, *108*, 5027-5028. (f) Toftlund, H.; Murray, K.S.; Zwack, P.R.; Taylor, L.F.; Anderson, O.P. *J. Chem. Soc., Chem. Commun.* **1986**, 191-193. (g) Borovik, A.S.; Que, L.; Papaefthymiou, V.; Munck, E.; Taylor, L.F.; Anderson, O.P. *J. Am. Chem. Soc.* **1988**, *110*, 1986-1988. (h) Borovik, A.S.; Que, L. *J. Am. Chem. Soc.* **1988**, *110*, 2345-2347. (i) Gomez-Romero, P.; Nieves, C.-P.; Ben-Hussein, A.; Jameson, G.B. *J. Am. Chem. Soc.* **1988**, *110*, 1988-1990.

coordinatively saturated iron atoms and, therefore, cannot model the function of hemerythrin which contains an open site for oxygen coordination.

In attempts to synthesize a compound with open coordination sites, a mixture of  $(\text{HBpz}_3)^-$  and dihydrobis(1-pyrazolyl)borate,  $(\text{H}_2\text{Bpz}_2)^-$ , were used in the synthesis of the Armstrong model compound from the dinuclear starting material,  $(\text{Et}_4\text{N})_2[\text{Fe}_2\text{OCl}_6]$ . The target compounds were  $[\text{Fe}_2\text{O}(\text{O}_2\text{CCH}_3)_2(\text{H}_2\text{Bpz}_2)_2]$ , with two open coordination sites, or  $[\text{Fe}_2\text{O}(\text{O}_2\text{CCH}_3)_2(\text{HBpz}_3)(\text{H}_2\text{Bpz}_2)]$ , with one site available, as in the biological system.



A product was isolated from the reaction mixture that exhibited optical and vibrational spectra similar to those of  $[\text{Fe}_2\text{O}(\text{O}_2\text{CCH}_3)_2(\text{HBpz}_3)_2]$ . An x-ray diffraction study of a single crystal of the product isolated when benzoate was used, however, revealed that neither of the desired compounds had formed. Instead, the complex  $(\text{Et}_4\text{N})[\text{Fe}_4\text{O}_2(\text{O}_2\text{CC}_6\text{H}_5)_7(\text{H}_2\text{Bpz}_2)_2]$ , **1**, containing a tetranuclear iron core with two  $\mu_3$ -oxygen atoms had been isolated.<sup>4</sup> Once its structure was known, **1** could be synthesized in nearly quantitative yield by using stoichiometric amounts of reactants.<sup>4</sup> Solution structural studies have established the integrity of the complex in organic solvents and allowed for the confirmation of the structure of the analogous complex with bridging acetates,  $(\text{Et}_4\text{N})[\text{Fe}_4\text{O}_2(\text{O}_2\text{CCH}_3)_7(\text{H}_2\text{Bpz}_2)_2]$ , **2**. The same core structure was also obtained when 4,4'-dimethyl-2,2'-bipyridine ( $\text{Me}_2\text{bipy}$ ) was the nitrogen donor ligand, yielding  $[\text{Fe}_4\text{O}_2(\text{O}_2\text{CC}_6\text{H}_5)_7(\text{Me}_2\text{-bipy})_2]^+$ , **3**. Another research group

<sup>4</sup> Armstrong, W.H.; Roth, M.E.; Lippard, S.J. *J. Am. Chem. Soc.* **1987**, *109*, 6318-6326.

has synthesized manganese compounds with the same core structure, suggesting that the general formula  $[M_4O_2(O_2CR)_7(L)_2]^n$  where L is a bidentate nitrogen donor may be common for a number of transition metals.

Despite the accidental nature of the synthesis of the first of these complexes, the  $[M_4O_2]^{n+}$  species are important for several reasons. As small iron aggregates, the  $[Fe_4O_2]^{8+}$  complexes are of interest in relation to the aggregation of iron for storage in the body. Also, the manganese analogs have been proposed as models for the oxygen evolving site in Photosystem II.<sup>5</sup> A full understanding of the similarities and differences in the properties and chemistry of the analogous manganese and iron complexes may begin to explain the presence of manganese rather than iron in the protein which oxidizes water to dioxygen. <sup>1</sup>H NMR and Raman spectroscopic studies of **1**, **2**, and **3**, as well as the crystal structure of **3**, will be presented herein. The synthesis of **3** proved that the pyrazolylborate ligand played no essential role in the stabilization of the tetranuclear core. The synthesis of another analog, however, with N,N,N',N'- tetramethylethylenediamine (Me<sub>4</sub>-en) as the nitrogen donor ligand was not as successful, suggesting that not all bidentate nitrogen donor ligands will promote the formation of the  $[Fe_4O_2]^{8+}$  core. The results of these studies will be discussed in relation to iron aggregation and the present models for the oxygen evolving center in PSII.

## Experimental Section

**Materials.** Potassium dihydrobis(1-pyrazolyl)borate (KH<sub>2</sub>Bpz<sub>2</sub>) was purchased from Strem Chemical Inc., Newburyport, MA. All other reagents and solvents were obtained from commercial sources and used without purification. Elemental analyses were performed by Atlantic Microlab, Inc., Atlanta, GA.

---

<sup>5</sup> Vincent, J.B.; Christmas, C.; Huffman, J.C.; Christou, G.; Chang, H.-R.; Hendrickson, D.N. *J. Chem. Soc., Chem. Commun.* **1987**, 236-238.



**Physical Measurements.** Uv-vis-near-IR spectral measurements were made using Perkin-Elmer Lamda 7 and Lamda 9 spectrophotometers. The  $^1\text{H}$  NMR spectra were recorded with Bruker WM 250 instrument from samples containing  $\text{CH}_2\text{Cl}_2$  as an internal reference ( $\delta$  5.32). Positive shifts are referred to and reported as downfield from tetramethylsilane. FTIR spectra were collected on an IBM System 9000 interfaced to an IBM IR/32 spectrometer. Pellets for the IR spectra were prepared from 0.2 to 1.0 mg complex in 100 mg of KBr. Solution magnetic susceptibilities were measured in  $\text{CD}_2\text{Cl}_2$  or  $\text{CD}_3\text{Cl}$  by using the Evans NMR method.<sup>6</sup> Diamagnetic corrections of  $-781 \times 10^{-6}$  cgs mol $^{-1}$  for **1**,  $-522 \times 10^{-6}$  cgs mol $^{-1}$  for **2** and  $-994 \times 10^{-6}$  cgs mol $^{-1}$  for **3** were calculated from Pascal's constants.<sup>7</sup> A constitutive correction of  $+8.0 \times 10^{-6}$  cgs mol $^{-1}$  was applied for each pyrazole ring and the following values were used for other groups: benzoate,  $-67 \times 10^{-6}$  cgs mol $^{-1}$ ; acetate,  $-30 \times 10^{-6}$  cgs mol $^{-1}$ ;  $\text{O}^{2-}$ ,  $-7 \times 10^{-6}$  cgs mol $^{-1}$ .<sup>8</sup> The mass susceptibility of  $\text{CD}_2\text{Cl}_2$  and  $\text{CD}_3\text{Cl}$  were taken to be  $-0.549 \times 10^{-6}$  cgs g $^{-1}$  and  $-0.497 \times 10^{-6}$  cgs g $^{-1}$ , respectively.<sup>9</sup> A Spex 1401 double monochromator equipped with a cooled RCA 31034 photomultiplier tube with photon-counting electronics was used to acquire the Raman data. The spectrometer was interfaced with a North Star or, later, a Digital Equipment Corporation, Inc. computer for ease of collection, manipulation, storage, and plotting of data. The spectra were plotted on a 4662 Tetrax Interactive Digital Plotter. A tunable argon laser (Coherent Radiation Innova 70 or Spectra Physics Model 164) was used for all excitation wavelengths. A backscattering geometry was employed and the samples spun in sealed 5 mm NMR tubes. Incident powers of 50 to 125

---

<sup>6</sup> (a) Evans, D.F.; *J. Chem. Soc.* **1958**, 2003-2005. (b) Live, D.H.; Chan, S.I. *Anal. Chem.* **1970**, *42*, 791-792.

<sup>7</sup> (a) Mulay, L.N. In *Physical Methods of Chemistry. Part IV. Determination of Mass Transport, and Electrical-magnetic Properties*; Weissberger, A., Rossiter, B.W., Eds.; Wiley: New York, 1972; Chapter VIII. (b) Carlin, R.L. *Magnetochemistry*; Springer-Verlag: New York, 1986, p 3.

<sup>8</sup> Earnshaw, A. *Introduction to Magnetochemistry*; Academic: London, 1968.

<sup>9</sup> Weast, R.C., Ed. *Handbook of Chemistry and Physics*; CRC: Boca Raton, FL, 1983, p E-115.

mW were used with slit settings of 300/400/300 to 400/500/400. Up to 5 scans were collected and averaged to improve signal to noise for some spectra.

**Tetraethylammonium ( $\mu$ -Oxo)bis[trichlorodiferrate(III)],  $(\text{Et}_4\text{N})_2[\text{Fe}_2\text{OCl}_6]$**  To 14.1 g (52.2 mmol)  $\text{FeCl}_3 \cdot 6\text{H}_2\text{O}$  in 300 ml pure EtOH, 3.82 g (52.2 mmol) n-butylamine in 200 ml EtOH were added dropwise over 5 hr. The solution darkens from orange to deep red during the addition. 9.60 g (52.2 mmol)  $\text{Et}_4\text{NCl}$  (90%) dissolved in 150 ml EtOH were then added dropwise over 1 hr, during which time a white solid formed. The mixture was cooled overnight at 5 °C. The solvents were removed by rotary evaporation. The addition of  $\text{CH}_3\text{CN}$  to the resulting solids yielded an orange solution with a yellow solid. The solid was removed by suction filtration and  $\text{CHCl}_3$  was added to the filtrate. A deeply colored oil separated from the  $\text{CH}_3\text{CN}$  solution and was collected using a separatory funnel. The  $\text{CHCl}_3$  was removed by rotary evaporation, the resulting amorphous solid dissolved in  $\text{CH}_3\text{CN}$  and precipitated with THF. After drying under vacuum, the yield was 8.99 g (57%) of  $(\text{Et}_4\text{N})_2[\text{Fe}_2\text{OCl}_6]$ .

Crystallization was achieved from a  $\text{CH}_3\text{CN}/\text{THF}$  solution at -20 °C. Anal. Calcd for  $\text{C}_{16}\text{H}_{40}\text{Cl}_6\text{Fe}_2\text{N}_2\text{O}$ : C, 32.02, H, 6.72; N, 4.67; Cl, 35.44. Found: C, 32.07, H, 6.71; N, 4.65; Cl, 35.20.

**Tetraethylammonium Bis( $\mu_3$ -oxo)heptakis( $\mu$ -benzoato)bis[dihydrobis(1-pyrazolyl)borato]tetra ferrate(III),  $(\text{Et}_4\text{N})[\text{Fe}_4\text{O}_2(\text{O}_2\text{C}\text{C}_6\text{H}_5)_7(\text{H}_2\text{Bpz}_2)_2]$ , (1).**

This complex was prepared as described in reference 4.

**Tetraethylammonium Bis( $\mu_3$ -oxo)heptakis( $\mu$ -acetato)bis[dihydrobis(1-pyrazolyl)borato]tetra ferrate(III),  $(\text{Et}_4\text{N})[\text{Fe}_4\text{O}_2(\text{O}_2\text{C}\text{CH}_3)_7(\text{H}_2\text{Bpz}_2)_2]$ , (2).**

This compound was synthesized following the now published method.<sup>4</sup> To a stirred solution of  $\text{CH}_3\text{CN}$ , was added 0.380 g (0.632 mmol) of  $(\text{Et}_4\text{N})_2[\text{Fe}_2\text{OCl}_6]$ . After the compound dissolved, 0.182 g (2.22 mmol) of  $\text{NaO}_2\text{CCH}_3$  was added and vigorous stirring was continued for 2 hrs. Slowly, the orange-brown solution changed to a dark red-brown color.

0.120 g (0.645 mmol) of  $\text{KH}_2\text{Bpz}_2$  was dissolved in 15 ml of  $\text{CH}_3\text{CN}$  and added dropwise to the reaction mixture over several minutes. During the addition, the color of the solution changed to green-brown. The solution was stirred for another 45 min then stored at  $5^\circ\text{C}$  for 24 hrs at which time white solids were filtered out. The filtrate was reduced to an oil, redissolved in  $\text{CHCl}_3$  and stored again at  $5^\circ\text{C}$ . The compound did not crystallize or precipitate very readily. Eventually, repeating the above procedure and removing as much  $\text{CH}_3\text{CN}$  as possible yielded a mixture of green solids and white crystals. The latter could be washed away with only minor loss of product by using small amounts of  $\text{CHCl}_3$ . Washing with  $\text{H}_2\text{O}$ , as suggested by Armstrong,<sup>4</sup> caused the compound to change color but removed the white solid much more efficiently. The solid could be recrystallized as very dark green microcrystalline needles. After powdering and vacuum drying the yield was 0.200 g (60%) of **2**. Anal. Calcd for  $\text{C}_{34}\text{H}_{57}\text{B}_2\text{Fe}_4\text{N}_9\text{O}_{16}$ : C, 37.36; H, 5.26; N, 11.53. Found: C, 36.58; H, 5.22; N, 11.32.  $^1\text{H}$  NMR ( $\text{CD}_2\text{Cl}_2$ , 250 MHz):  $\delta$  17.3, 16.9 (sh), 14.1 (sh), 13.4, 12.5, 10.9 (v br), 8.0 (v br), 3.09, 1.27. FTIR (KBr,  $\text{cm}^{-1}$ ): 2407, 2287, 1737, 1590 (s), 1562, 1420 (s), 1343, 1299, 1209, 1199, 1186, 1155, 1058, 1024, 1000, 984, 885, 763, 684, 661, 648, 617, 558, 497. UV-vis-near IR ( $\text{CH}_2\text{Cl}_2$ ):  $\lambda$  nm ( $\epsilon_{\text{Fe}} \text{cm}^{-1} \text{M}^{-1}$ ) 255 (sh), 317 (2400), 350 (2700), 466 (440), 570 (60), 1020 (~5).

**Bis( $\mu_3$ -oxo)heptakis( $\mu$ -benzoato)bis[4,4'-dimethyl-2,2'-bipyridyl]tetra-**  
**ferrate(III) Chloride,  $[\text{Fe}_4\text{O}_2(\text{O}_2\text{CC}_6\text{H}_5)_7(\text{Me}_2\text{bipy})_2](\text{Cl})$  (**3a**).** This compound was synthesized in the same manner as **2** by using 1.07 g (1.78 mmol) of  $(\text{Et}_4\text{N})_2[\text{Fe}_2\text{OCl}_6]$  and 0.852 g (5.91 mmol) of  $\text{NaO}_2\text{CC}_6\text{H}_5$ . Since  $\text{Me}_2\text{bipy}$  does not dissolve in  $\text{CH}_3\text{CN}$ , 0.315 g (1.71 mmol) was added to the reaction mixture as a suspension in 20 ml of  $\text{CH}_3\text{CN}$ . The solution underwent a slight color change, but it was not as intense as in the reaction with  $\text{KH}_2\text{Bpz}_2$ . Another 0.96 g of  $\text{Me}_2\text{bipy}$  was then added as a solid. After stirring for 2 hrs, the reaction mixture was suction filtered. The solids removed by filtration were dull green. The filtrate was stored at  $5^\circ\text{C}$  and solids began to form overnight. An attempt was made to collect

this solid, but it was very soluble in  $\text{CHCl}_3$  and redissolved upon washing with this solvent. The solution was concentrated, dissolved in  $\text{CH}_3\text{CN}$  and after a few minutes a precipitate began to form. In an attempt to form the  $(\text{PF}_6)^-$  salt, 0.301 g (1.85 mmol) of  $\text{NH}_4\text{PF}_6$  was added and the solution stirred for 1 hr. A white precipitate which formed during this time was removed by filtration. As the  $\text{CH}_3\text{CN}$  evaporated from the filtrate, precipitate began to form. The brown precipitate formed a green-brown solution in  $\text{CH}_2\text{Cl}_2$ . When small amounts of  $\text{CH}_3\text{CN}$  were added to a concentrated  $\text{CHCl}_3$  solution, crystalline material formed on the bottom of the flask. The red-brown microcrystalline material which was collected turned dull brown on loss of solvent. Despite the addition of  $\text{NH}_4\text{PF}_6$ , a chemical analysis of the product after drying under vacuum revealed the complex to be the chloride salt. The yield was 0.833 g (62%) of **3a**. Anal. Calcd for  $\text{C}_{73}\text{H}_{59}\text{ClFe}_4\text{N}_4\text{O}_{16}$ : C, 58.17; H, 3.94; N, 3.72. Found: C, 57.43; H, 4.01; N, 3.79.  $^1\text{H}$  NMR ( $\text{CD}_2\text{Cl}_2$ , 250 MHz): 23.3, 19.5 (br), 16.3, 9.2, 7.5, 6.5, 6.0, 4.0, 3.6, 3.0 (sh). FTIR (KBr,  $\text{cm}^{-1}$ ): 1617, 1598, 1546, 1491, 1447, 1402, 1175, 1070, 1025, 832, 719, 689, 675, 649, 522, 471. UV-vis-near IR ( $\text{CH}_2\text{Cl}_2$ ):  $\lambda$  (nm,  $\epsilon_{\text{Fe}} \text{ cm}^{-1} \text{ M}^{-1}$ ) 279 (11,900), 340 (sh), 300 (sh), 400 (sh), 465 (450), 560 (sh, 80).

**Bis( $\mu_3$ -oxo)heptakis( $\mu$ -benzoato)bis[4,4'-dimethyl-2,2'-bipyridyl]tetra-**  
**ferrate(III) Tetrphenylborate,  $[\text{Fe}_4\text{O}_2(\text{O}_2\text{CC}_6\text{H}_5)_7(\text{Me}_2\text{bipy})_2](\text{B}(\text{C}_6\text{H}_5)_4)$  (**3b**).**

Method A. When excess  $\text{NaB}(\text{C}_6\text{H}_5)_4$  was added to **3a** in a  $\text{CH}_2\text{Cl}_2/\text{CH}_3\text{CN}$  mixture and the solution filtered and reduced in volume by rotary evaporation, a green-brown oil formed. Addition of  $\text{CH}_3\text{CN}$  caused the oil to redissolve and then crystallize out of solution. Suction filtration separated the dark green-brown microcrystals from the red filtrate. Method B. As described above, 0.505 g (0.841 mmol) of  $(\text{Et}_4\text{N})_2[\text{Fe}_2\text{OCl}_6]$  were allowed to react with 0.425 g (2.95 mmol) of  $\text{NaO}_2\text{CC}_6\text{H}_5$  in  $\text{CH}_3\text{CN}$  for 0.5 hr. 0.156 g (0.847 mmol) of 4,4'-dimethyl-2,2'-bipyridine in 10 ml of  $\text{CH}_2\text{Cl}_2$  was then added dropwise to the solution and the solution stirred for another 1.5 hr. A pale green solid was separated from the green-brown solution by suction filtration. The solvents were removed by rotary evaporation to yield an

amorphous brown solid which, upon the addition of CH<sub>3</sub>CN, dissolved but began to precipitate immediately. After 1 hr of cooling at 5 °C, the brown precipitate was collected. The red-brown filtrate was saved. The brown solid was dissolved in a 50/50 mixture of CH<sub>2</sub>Cl<sub>2</sub>/CH<sub>3</sub>CN and 0.15 g (0.43 mmol) NaB(C<sub>6</sub>H<sub>5</sub>)<sub>4</sub> was added to the mixture. The solvents were removed by rotary evaporation and the amorphous solid dissolved in CH<sub>3</sub>CN and left at room temperature overnight. The complex forms green-brown microcrystals, leaving a red supernatant. Yield: 0.37 g (49%) of **3b**. Recrystallization by slow evaporation from solutions of CH<sub>2</sub>Cl<sub>2</sub> or CHCl<sub>3</sub> diluted with CH<sub>3</sub>CN yielded deep red-brown, x-ray quality crystals. Anal. Calcd for C<sub>97</sub>H<sub>79</sub>BF<sub>4</sub>N<sub>4</sub>O<sub>16</sub>: C, 65.05; H, 4.45; N, 3.13. Found: C, 64.61; H, 4.35; N, 3.00. <sup>1</sup>H NMR (CD<sub>2</sub>Cl<sub>2</sub>, 250 MHz): δ, 22.7, 19.5 (sh), 18.7, 16.1, 9.2, 7.37, 7.04, 6.88, 6.5, 6.0, 3.9, 3.5. FTIR (KBr, cm<sup>-1</sup>): 1621, 1598, 1556, 1534, 1491, 1446, 1399, 1176, 1069, 1026, 830, 722, 706, 674, 606, 523, 473. UV-vis-near IR (CH<sub>2</sub>Cl<sub>2</sub>): λ, nm (ε<sub>Fe</sub> cm<sup>-1</sup> M<sup>-1</sup>) 273 (12,150), 288 (sh), 300 (sh), 340 (sh), 408 (sh), 466 (450), 565 (sh, ~85). Upon evaporation at room temperature, the filtrate deposited small brown crystalline needles. The UV-vis and <sup>1</sup>H NMR spectra of this product are identical to those of **3a** and a chemical analysis confirmed the identity of the minor product. Anal. Calcd for C<sub>73</sub>H<sub>59</sub>ClFe<sub>4</sub>N<sub>4</sub>O<sub>16</sub>: C, 58.17; H, 3.94; N, 3.72. Found: C, 58.02; H, 4.03; N, 3.54.

**Attempted synthesis of Bis(μ<sub>3</sub>-oxo)heptakis(μ-benzoato)bis[N,N,N',N'-tetramethylethylenediamine]tetraferate(III) Hexafluorophosphate, [Fe<sub>4</sub>O<sub>2</sub>(O<sub>2</sub>CC<sub>6</sub>H<sub>5</sub>)<sub>7</sub>(Me<sub>4</sub>-en)<sub>2</sub>](PF<sub>6</sub>).** In the same manner as described for **2**, 1.04 g (1.73 mmol) of (Et<sub>4</sub>N)<sub>2</sub>[Fe<sub>2</sub>OCl<sub>6</sub>] were allowed to react with 0.845 g (5.86 mmol) of NaO<sub>2</sub>CC<sub>6</sub>H<sub>5</sub> for 2 hr. Dropwise addition of 0.196 g (1.69 mmol) of Me<sub>4</sub>-en dissolved in 50 ml CH<sub>3</sub>CN caused a slight color change. Several drops of neat Me<sub>4</sub>-en were then added to assure complete reaction. After another 2 hrs of stirring, the reaction was filtered to remove a white solid. The filtrate was concentrated to 50 ml and 0.299 (1.83 mmol) NH<sub>4</sub>PF<sub>6</sub>, dissolved in 20 ml of CH<sub>3</sub>CN, was added. A white precipitate began to form in the solution during the

addition. The reaction mixture was stirred for 1 hr and the white solid removed by filtration. The deep red-brown filtrate was concentrated to an oil, redissolved in 20 ml  $\text{CHCl}_3$  and stored at 5 °C. The solution became a slurry of white needles, most of which were removed by filtration. Some of the white compound redissolved on washing with  $\text{CHCl}_3$ . THF was added to the solution which caused the precipitation of more salt. The white salts were again filtered out and a concentrated solution in  $\text{CHCl}_3$  with some THF added was stored at 5 °C. Within 48 hrs, red-brown crystals as well as a reddish-yellow precipitate were apparent on the bottom of the flask. After several more days, the amount of solids had not appeared to increase. The crystals were collected and liquid-liquid diffusion of  $\text{CH}_2\text{Cl}_2$  into hexanes was used to grow single crystals. The crystals were brittle and appeared to lose solvent. An x-ray diffraction data set collected on one weakly diffracting crystal was complete enough to allow for a rough structural determination. The crystal was an isomorph of  $[\text{Fe}_{11}\text{O}_6(\text{OH})_6(\text{O}_2\text{CC}_6\text{H}_5)_{15}]$ . Addition of THF to solutions from the original filtrate allowed for separation of more of this complex. The THF soluble fraction was then reduced in volume, dissolved in  $\text{CH}_2\text{Cl}_2$  and precipitated with ether. When solutions of this product were reduced in volume by rotary evaporation with toluene present, a precipitate forms of the sides of the flask. After drying under vacuum, the deep brown solid was scraped from the flask to give 0.370 g of **4**. UV-vis-near IR ( $\text{CH}_2\text{Cl}_2$ ):  $\lambda$ , nm ( $\epsilon_{\text{Fe}} \text{ cm}^{-1} \text{ M}^{-1}$ ) 270 (sh), 300 (sh), 345 (sh), 408 (sh), 460 (sh, ~330), 540 (sh, ~85).

## Results

**Synthesis and Structure.** Formation of the tetranuclear  $\{\text{Fe}_4\text{O}_2\}^{8+}$  core first observed in the structure of **1** occurs both with a different bridging carboxylate group and with a different nitrogen donor ligand. The synthesis and structure of **1** has been fully described in reference 4. The syntheses of the analogous compounds **2** and **3** were carried out in a similar manner.

The only difference in the synthesis of **2** compared to **1** is that the acetate bridged complex is much less crystalline and, therefore, more difficult to isolate as a pure solid.

The cationic species, **3**, forms under the same conditions as **1**. When the nitrogen donor ligand was added to the red-brown iron-benzoate mixture, however, only a slight color change occurred. Unlike the synthesis of **1** and **2**, during which the solution develops a distinctly green hue, the solution just became more brown in color upon addition of Me<sub>2</sub>bipy. Nonetheless, the color change was distinguishable and appeared complete within about 20 min. The solid suspended in the solution appeared to be white, as in the case of **1**, but upon suction filtration was revealed to be pale green. Since the solid was not soluble in any common organic solid it was determined to be mostly NaCl, as expected. Both the brown and green crystals of **3** which can be isolated depending on the anion present form red-brown solutions in CH<sub>3</sub>CN and green-brown solutions in CH<sub>2</sub>Cl<sub>2</sub>. The UV-vis spectrum of **3** is very similar to that of **1** as can be seen in Figure 1. The solubility of **3** differs considerably from that of **1**. It is essentially insoluble in CH<sub>3</sub>CN and only moderately soluble in chlorinated solvents. The presence of the [B(C<sub>6</sub>H<sub>5</sub>)<sub>4</sub>]<sup>-</sup> counterion improves the solubility of the compound in chlorinated

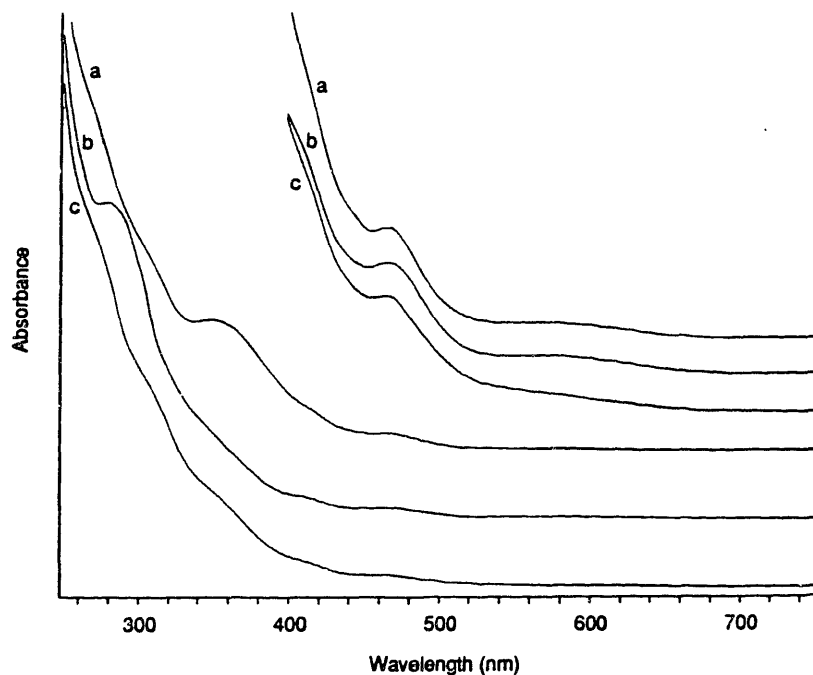


Figure 1. The UV-visible spectra of (a) **1**, (b) **3b**, (c) **4** in CH<sub>2</sub>Cl<sub>2</sub>.

solvents. Crystallization of **3b** could only be achieved by slow evaporation of ~95/5 CH<sub>3</sub>CN/CH<sub>2</sub>Cl<sub>2</sub> solutions. Only oils or amorphous solids could be obtained with hexanes or ethers.

In addition to **3**, a red complex is formed during the synthesis. The complex is very soluble in CH<sub>3</sub>CN as well as CH<sub>2</sub>Cl<sub>2</sub>. It appears very similar to [Fe(Me<sub>2</sub>bipy)<sub>3</sub>]Cl<sub>2</sub> but has a slightly different visible spectrum (Red: 340(sh), 490, 525 nm versus [Fe(Me<sub>2</sub>bipy)<sub>3</sub>]Cl<sub>2</sub>: 328, 397(sh), 503(sh), 527 nm) and different solubility properties. The red complex is probably a mononuclear species, judging from the lack of visible bands below 525 nm.

Attempts to synthesize a tetranuclear complex using Me<sub>4</sub>-en as the nitrogen donor ligand were less successful than those employing Me<sub>2</sub>bipy. Even less of a color change was apparent on the addition of this ligand to the iron-benzoate mixture. Initially only tetraethylammonium salts could be isolated from chilled CHCl<sub>3</sub> solutions of the product. On addition of THF, a red, crystalline solid formed. An x-ray diffraction study of this complex, however, revealed it to be [Fe<sub>11</sub>O<sub>6</sub>(OH)<sub>6</sub>(O<sub>2</sub>CC<sub>6</sub>H<sub>5</sub>)<sub>15</sub>].<sup>10</sup> More of the undecanuclear complex could be precipitated from the solution by addition of THF. The UV-visible spectrum of the remaining solution was similar to that of **1** and **3** (Figure 1), although the band at ~560 nm is much less distinct. This complex was very soluble in CH<sub>3</sub>CN and chlorinated solvents. All attempts to crystallize the product, **4**, gave oils or amorphous solids. A solid could be precipitated with ether and toluene. Addition of [B(C<sub>6</sub>H<sub>5</sub>)<sub>4</sub>]<sup>-</sup> to solutions of the complex did not yield a more crystalline solid as was the case for **3**. Possibly, **4**, is a mixture of compounds. Clearly, the tetranuclear core did not form as readily in with Me<sub>4</sub>-en as the nitrogen donor as with Me<sub>2</sub>bipy or (H<sub>2</sub>Bpz<sub>2</sub>)<sup>-</sup>.

An x-ray diffraction study of **3b**<sup>11</sup> (Table I) revealed the structure of the cation to be analogous to that of the anion in **1** (Figure 2). The cation has approximate C<sub>2</sub> symmetry and consists of four iron atoms with two μ<sub>3</sub>-oxo bridges, seven bridging carboxylates and two

---

<sup>10</sup> Gorun, S.M.; Papaefthymiou, G.C.; Frankel, R.B.; Lippard, S.J. *J. Am. Chem. Soc.* **1987**, *109*, 3337-3348.

<sup>11</sup> Collection and refinement of data were carried out by Dr. Simon Bott. Final refinement is still in progress. A full description of the solution and structure will appear in *Inorg. Chem.*



Me<sub>2</sub>bipy ligands. Two pairs of iron atoms, Fe1Fe4 and Fe2Fe3, are doubly bridged by benzoates. The pairs are held together by single benzoate bridges between Fe1Fe3 and Fe2Fe4, around the perimeter of the structure, and between Fe1Fe2, across the core of the structure. The Fe-O bond distances for the doubly bridged pairs are shorter than the third Fe-O distance for each  $\mu_3$ -oxo atom. (Figure 3, Table II) Thus, the doubly bridged iron atoms exhibit a shorter Fe...Fe distance than those singly bridged around the periphery. To accommodate this structure, Fe3 and Fe4 are displaced by nearly 0.9 Å from the mean plane of the central, nearly planar, {Fe<sub>2</sub>O<sub>2</sub>} unit (Figure 4). The nitrogen donor ligands fill out the coordination sphere of these two iron atoms such that all the iron atoms are in a distorted octahedral environment.

Table I  
Summary of Crystal Data, Intensity Collection, and Structure Refinement for  
[Fe<sub>4</sub>O<sub>2</sub>(O<sub>2</sub>CPh)<sub>7</sub>(Me<sub>2</sub>Bipy)<sub>2</sub>](BPh<sub>4</sub>) · CH<sub>3</sub>CN

Formula	C <sub>99</sub> H <sub>82</sub> BF <sub>4</sub> N <sub>5</sub> O <sub>16</sub>
Formula Weight	1832.0
Space Group	P1
a, Å	13.805(3)
b, Å	18.730(6)
c, Å	20.469(4)
$\alpha$ , °	108.47(2)
$\beta$ , °	104.87(2)
$\gamma$ , °	97.57(4)
V, Å <sup>3</sup>	4719
Z	2
D <sub>calcd</sub> , g cm <sup>-3</sup>	1.29
D <sub>obsd</sub> , g cm <sup>-3</sup>	1.30 (1)
radiation	Mo K $\alpha$
abs coeff, cm <sup>-1</sup>	6.64
data collected	3° ≤ 2 $\theta$ ≤ 42°; +h, ±k, ±l
total no. of data collected	11174
average, R <sub>av</sub>	0.064
total number of unique data	10107
no. of unique data with I > 3 $\sigma$ (I)	5442
number of variable parameters	590
R	0.0872
R <sub>w</sub>	0.1167

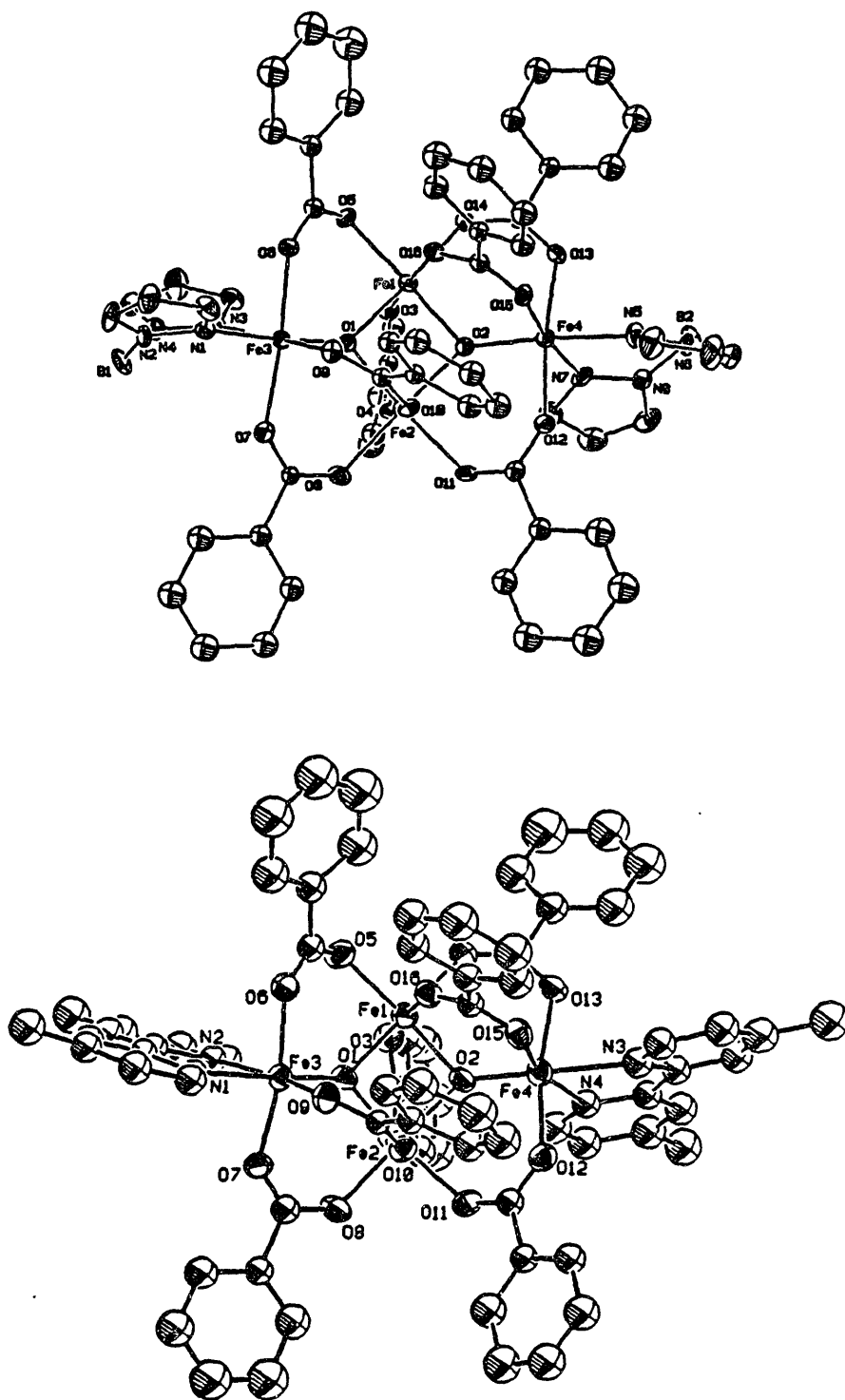


Figure 2. ORTEP drawing of the anion of **1** (top) and the cation, **3** (bottom), showing 50% probability thermal ellipsoids. The labels for the carbon atoms have been excluded for clarity.

Table II

## Selected bond lengths (Å) and angles (°) for the cation, 3.

Fe1.....Fe2	2.868(4)	Fe1 ---- O1	1.97(1)
Fe1.....Fe3	3.451(5)	Fe1 ---- O2	1.92(1)
Fe1.....Fe4	3.305(4)	Fe1 ---- O3	2.05(1)
Fe2.....Fe3	3.307(4)	Fe1 ---- O5	2.01(1)
Fe2.....Fe4	3.470(5)	Fe1 ---- O14	2.02(1)
Fe3.....Fe4	5.765(5)	Fe1 ---- O16	2.08(1)
Fe2 ---- O1	1.91(1)	Fe3 ---- N1	2.16(2)
Fe2 ---- O2	1.97(1)	Fe3 ---- N2	2.10(2)
Fe2 ---- O4	2.05(1)	Fe3 ---- O1	1.82(1)
Fe2 ---- O8	2.01(1)	Fe3 ---- O6	2.05(1)
Fe2 ---- O10	2.09(1)	Fe3 ---- O7	2.03(1)
Fe2 ---- O11	2.01(1)	Fe3 ---- O9	2.00(1)
Fe4 ---- N3	2.18(2)	Fe4 ---- N4	2.15(1)
Fe4 ---- O2	1.81(1)	Fe4 ---- O12	2.05(1)
Fe4 ---- O13	2.08(1)	Fe4 ---- O15	2.01(1)
Fe2 -- O1 -- Fe1	95.4(6)	Fe3 -- O1 -- Fe1	131.1(5)
Fe3 -- O1 -- Fe2	124.9(6)	Fe1 -- O2 -- Fe2	94.9(6)
Fe4 -- O2 -- Fe1	124.3(5)	Fe4 -- O2 -- Fe2	133.2(7)
Fe2.....Fe1.....Fe3	62.33(9)	Fe1.....Fe2.....Fe3	67.52(9)
Fe2.....Fe1.....Fe4	68.0(1)	Fe1.....Fe2.....Fe4	62.0(1)
Fe4.....Fe1.....Fe3	117.1(1)	Fe3.....Fe2.....Fe4	116.52(9)
Fe2.....Fe3.....Fe1	50.16(8)	Fe1.....Fe4.....Fe2	50.01(8)
Fe1.....Fe3.....Fe4	30.68(7)	Fe1.....Fe4.....Fe3	32.19(7)
Fe2.....Fe3.....Fe4	32.59(6)	Fe2.....Fe4.....Fe3	30.89(5)
O2 -- Fe1 -- O1	83.9(5)	O2 -- Fe1 -- O5	168.9(6)
O2 -- Fe1 -- O14	96.6(6)	O2 -- Fe1 -- O3	88.5(5)
O2 -- Fe1 -- O16	88.0(5)	O1 -- Fe1 -- O5	89.3(5)
O1 -- Fe1 -- O14	171.9(5)	O1 -- Fe1 -- O3	87.1(5)
O1 -- Fe1 -- O16	96.8(5)	O5 -- Fe1 -- O14	91.3(6)
O5 -- Fe1 -- O3	99.9(5)	O5 -- Fe1 -- O16	84.1(5)
O14 -- Fe1 -- O3	84.9(5)	O14 -- Fe1 -- O16	91.3(5)
O3 -- Fe1 -- O16	174.5(6)		
O1 -- Fe2 -- O2	84.3(5)	O1 -- Fe2 -- O8	97.0(5)
O1 -- Fe2 -- O11	169.0(5)	O1 -- Fe2 -- O4	91.4(5)
O1 -- Fe2 -- O10	88.2(5)	O2 -- Fe2 -- O8	175.6(5)
O2 -- Fe2 -- O11	88.2(5)	O2 -- Fe2 -- O4	85.1(5)
O2 -- Fe2 -- O10	95.8(5)	O8 -- Fe2 -- O11	91.1(5)
O8 -- Fe2 -- O4	90.7(5)	O8 -- Fe2 -- O10	88.5(5)
O11 -- Fe2 -- O4	95.9(5)	O11 -- Fe2 -- O10	84.6(5)
O4 -- Fe2 -- O10	179.0(6)		
O1 -- Fe3 -- O9	96.2(6)	O1 -- Fe3 -- O7	95.1(5)
O1 -- Fe3 -- O6	95.2(5)	O1 -- Fe3 -- N2	96.3(6)
O1 -- Fe3 -- N1	172.0(6)	O9 -- Fe3 -- O7	89.5(5)
O9 -- Fe3 -- O6	92.8(5)	O9 -- Fe3 -- N2	167.3(6)
O9 -- Fe3 -- N1	91.9(6)	O7 -- Fe3 -- O6	169.1(6)
O7 -- Fe3 -- N2	87.1(6)	O7 -- Fe3 -- N1	85.6(5)
O6 -- Fe3 -- N2	88.4(5)	O6 -- Fe3 -- N1	83.6(5)
N2 -- Fe3 -- N1	75.7(6)		
O2 -- Fe4 -- O15	97.3(5)	O2 -- Fe4 -- O12	94.5(6)
O2 -- Fe4 -- O13	94.1(6)	O2 -- Fe4 -- N4	97.3(6)
O2 -- Fe4 -- N3	171.7(6)	O15 -- Fe4 -- O12	95.1(5)
O15 -- Fe4 -- O13	90.0(5)	O15 -- Fe4 -- N4	164.7(7)
O15 -- Fe4 -- N3	89.9(6)	O12 -- Fe4 -- O13	169.4(6)
O12 -- Fe4 -- N4	88.4(5)	O12 -- Fe4 -- N3	88.8(6)
O13 -- Fe4 -- N4	84.3(5)	O13 -- Fe4 -- N3	81.8(6)
N4 -- Fe4 -- N3	75.2(6)		

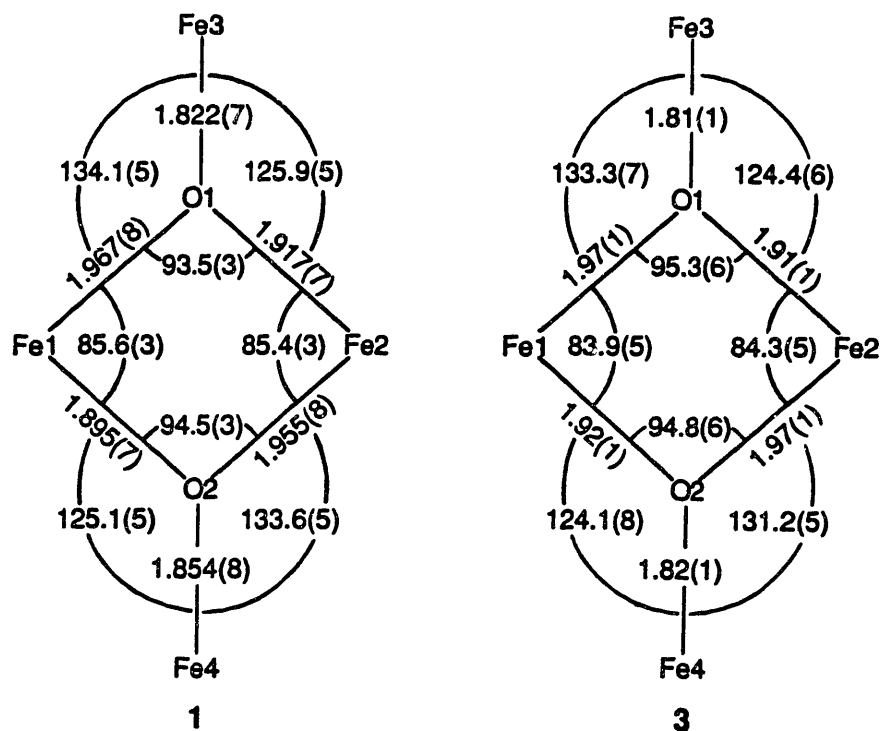


Figure 3. Diagram of the  $\{Fe_4O_2\}^{8+}$  core in 1 and 3 showing bond distances (Å) and angles (°).

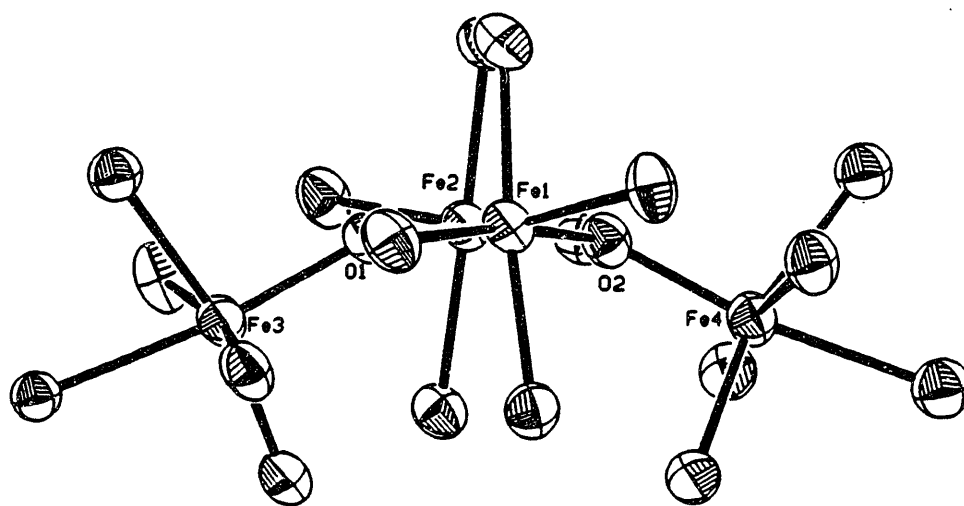


Figure 4. View of tetranuclear core of 3 showing displacement of Fe3 and Fe4 away from the nearly planar, central  $\{Fe_2O_2\}$  unit. Only the iron and oxygen atoms are shown for clarity.

**Proton NMR Spectroscopy.** Despite the relatively simple appearance of the  $^1\text{H}$  NMR spectrum of **1** in  $\text{CD}_2\text{Cl}_2$ , no assignments could be made on the basis of the chemical shifts and integration alone. Comparison of the spectra of **1** and **2**, with reference to the appropriate dinuclear compounds,  $[\text{Fe}_2\text{O}(\text{O}_2\text{CCH}_3)_2(\text{HBpz}_3)_2]$  and  $[\text{Fe}_2\text{O}(\text{O}_2\text{CC}_6\text{H}_5)_2(\text{HBpz}_3)_2]$ ,<sup>1</sup> allowed for tentative assignments of the spectra. In general, the proton NMR spectra of **1** and **2** (Figure 5) demonstrate that their basic tetranuclear structure is retained in solution. The spectra are concentration dependent with some line widths increasing with increasing concentrations, probably due to ion pairing. As would be expected in this case, a more polar solvent,  $\text{CD}_3\text{CN}$ , changes the appearance of the spectra.

The resonances which appear farthest downfield in the spectrum of **1** dissolved in  $\text{CD}_2\text{Cl}_2$  can be assigned to eight of the twelve pyrazolyl ring protons. The integration of these signals supports this assignment with the peak at 17.1 ppm and the pair of peaks at 13.5 and 12.5 ppm corresponding to 4 protons each. Although it is impossible to assign definitively these resonances without further experiments, these peaks probably arise from the H-4 and H-5 protons since the H-3 proton resonance appears broader and farther upfield in the spectrum of the dinuclear acetate bridged compound.<sup>1</sup> Although there are two symmetrically inequivalent sets of pyrazoles in **1**, the resonances for either the H-4 or the H-5 protons must be coincident, forming the peak at 17.1 ppm, while the other set of protons gives rise to the pair of peaks at 13.5 and 12.5 ppm. Similarly, in the spectrum of **2**, signals are observed at 17.3, 13.5 and 12.4 ppm. These signals, however, are overlapped by two broader signals at 16.8 and 14.2 ppm. In addition, the spectrum of **2** in  $\text{CD}_2\text{Cl}_2$  shows two more broad resonances at 10.9 and 8.1 ppm. Either of these bands could arise from the H-3 proton. The other three resonances can be assigned to the methyl groups of the bridging acetates. In  $\text{CD}_3\text{CN}$ , the pyrazolyl resonances appear sharper though still overlapped by the methyl resonances. Also, the broad band at 8.1 ppm appears much sharper and occurs at 7.7 ppm and an additional small resonance is apparent at 6.6 ppm.

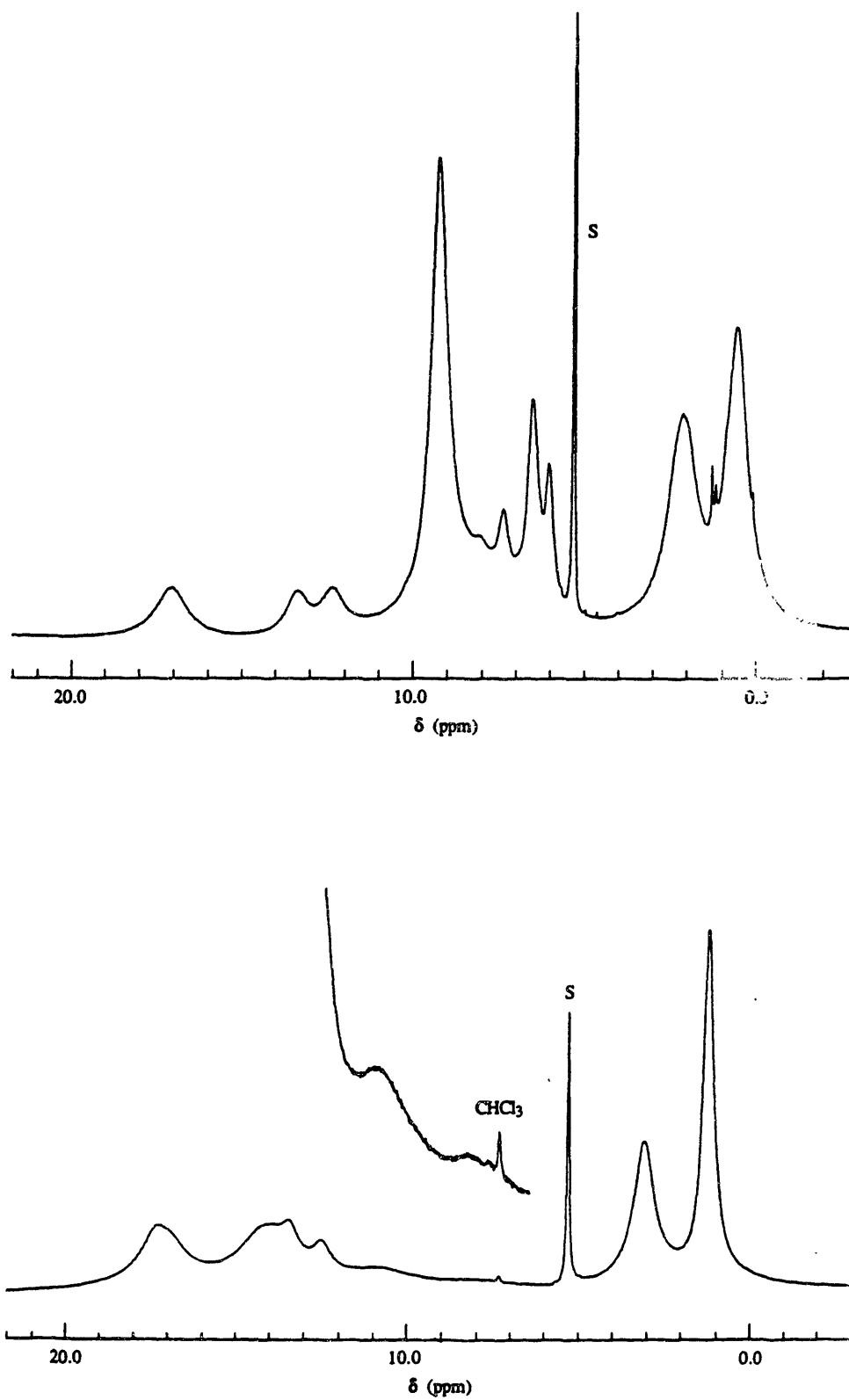


Figure 5.  $^1\text{H}$  NMR spectra of 1 (top) and 2 (bottom) in  $\text{CD}_2\text{Cl}_2$ . The peak marked with S is the solvent peak.

The H-3 pyrazolyl resonances cannot be observed in the spectrum of **1** due to the numerous broad bands between 5 and 11 ppm. These signals undoubtedly arise from the phenyl protons on the bridging benzoates. The three relatively sharp peaks at 7.3, 6.5 and 6.0 ppm probably arise from the para protons which are farthest from the paramagnetic iron atoms. Since only three peaks are observed, the para protons of two symmetrically distinct benzoates must be accidentally coincident at 6.5 ppm. The relative intensity of these peaks supports this assignment. Also, when the spectrum is recorded in CD<sub>3</sub>CN, a shoulder is visible on the peak at 6.5 ppm.

The very broad signals found at 2.1 and 0.6 ppm in the spectrum of **1** in CD<sub>2</sub>Cl<sub>2</sub> are those most dramatically affected by a change in solvent. In CD<sub>3</sub>CN, these peaks appear with line widths only one quarter those seen in CD<sub>2</sub>Cl<sub>2</sub> and are shifted to 2.9 and 1.0 ppm. These resonances are assigned to the methylene and methyl protons, respectively, of the Et<sub>4</sub>N<sup>+</sup> cation. The H-B resonance expected at approximately 2.0 ppm appears to be coincident with the methylene resonance and is only detectable by integration. The effect on the analogous peaks at 3.1 and 1.2 ppm in the spectrum of **2** is similar but not as dramatic. These two peaks become sharper but no significant change in chemical shift is observed.

The <sup>1</sup>H NMR spectra of **3a** and **3b** (Figure 6) suggest that the benzoate resonances assigned for **1** are characteristic of the tetranuclear core structure. The spectrum of **3a** in CD<sub>2</sub>Cl<sub>2</sub> exhibits a set of resonances at 9.2, 7.5, 6.5 and 6.0 ppm analogous to those seen in the spectrum of **1**. The same resonances are also observed for **3b** in CD<sub>2</sub>Cl<sub>2</sub> although the peak at 7.5 is masked by the resonances from the phenyl rings of the [B(C<sub>6</sub>H<sub>5</sub>)<sub>4</sub>]<sup>-</sup> anion (7.37, 7.04 and 6.87 ppm). The downfield regions of the spectra of **3a** and **3b** show resonances which, like those in **1** and **2**, can be assigned to the protons closest to the iron core, for these compounds, the pyridyl protons. These resonances at 22.7, 19.5, 18.7 and 16.1 in the spectrum of **3b** are shifted further downfield than the pyrazolyl proton resonances in **1** and **2**, potentially as a result of the greater ring current of the pyridine ring. Integration of the

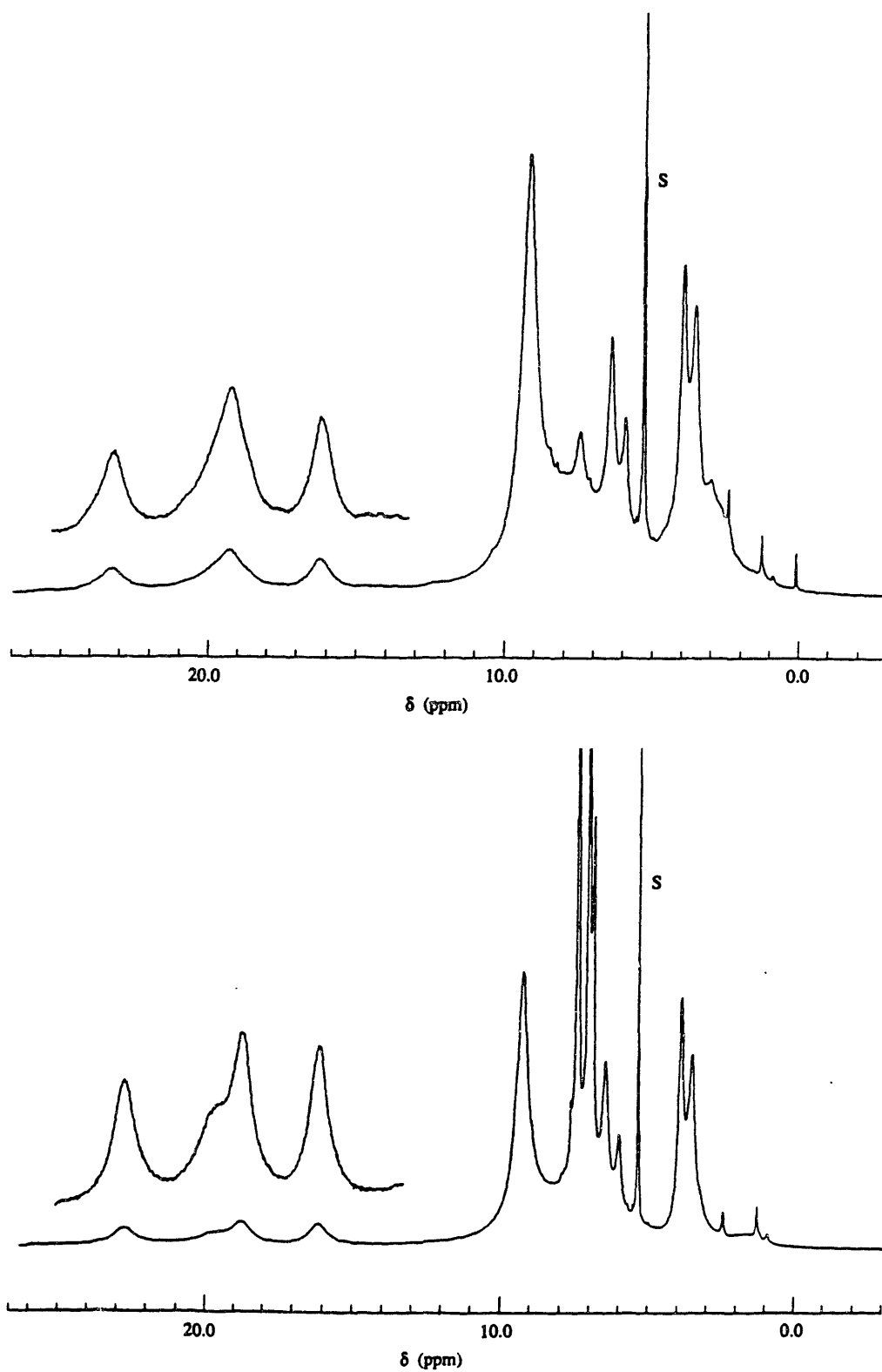


Figure 6.  $^1\text{H}$  NMR spectra of **3a** (top) and **3b** (bottom) in  $\text{CD}_2\text{Cl}_2$ . The peak marked with S is the solvent peak.



spectrum suggests that the four resonances can be assigned to eight of the twelve pyridyl protons. The remaining four protons are most likely coincident with the benzoate resonances between 5 and 11 ppm, as occurs for the H-3 pyrazolyl protons in the spectrum of **1**. Unlike the spectrum of **1**, however, each of the downfield resonances in the spectrum of **3b** appears to be of equal intensity, corresponding to two protons. There is no accidental coincidence of the symmetrically inequivalent pyridyl protons. The asymmetry of the two rings on each bipyridine is also born out by the appearance of two resonances for the methyl groups at 3.9 and 3.5 ppm.

The spectrum of **3a** varies only slightly from that of **3b**. In the spectrum of **3a**, there are only three resonances in the downfield region assigned to eight pyridyl protons. Two proton resonances, which are better resolved in the spectrum of **3b**, are nearly coincident, forming the broad resonance at 19.4 ppm. The methyl proton resonances occur at 4.0 and 3.6 ppm and overlap another broad resonance centered at ~3.0 ppm. From integration, this latter peak would not appear to be part of the integral structure of **3a** and, therefore, may arise from water hydrogen bound to the complex. The same feature was apparent in spectra of **3a** obtained from two different reaction mixtures (See Experimental). The similarity of the spectra of **3a** and **3b** to that of **1** suggested the formulation of the cation **3** as the bipyridyl analog of **1** before an x-ray diffraction study of **3b** confirmed its structure.

Unfortunately, the  $^1\text{H}$  NMR spectrum of **4** in  $\text{CD}_2\text{Cl}_2$  (Figure 7) has not been as helpful in characterizing this product. Although the UV-visible spectrum of **4** is similar to that of **1** and **3** (Figure 1), its  $^1\text{H}$  NMR spectrum in  $\text{CD}_2\text{Cl}_2$  does not display the characteristic set of benzoate resonances. An intense resonance occurs at 9.3 ppm similar to the 9.2 ppm bands in the other compounds, but no other analogies between the spectra can be drawn. One reason for the disparity between the the spectrum of **4** and those of **1** and **3** may be the presence of aliphatic as opposed aromatic protons on the nitrogen donor ligand. Nonetheless, a less complicated spectrum would be expected if the complex contained the same core as **1** and **3**. The product, **4**, would thus appear to be a different type of complex or a mixture of complexes.

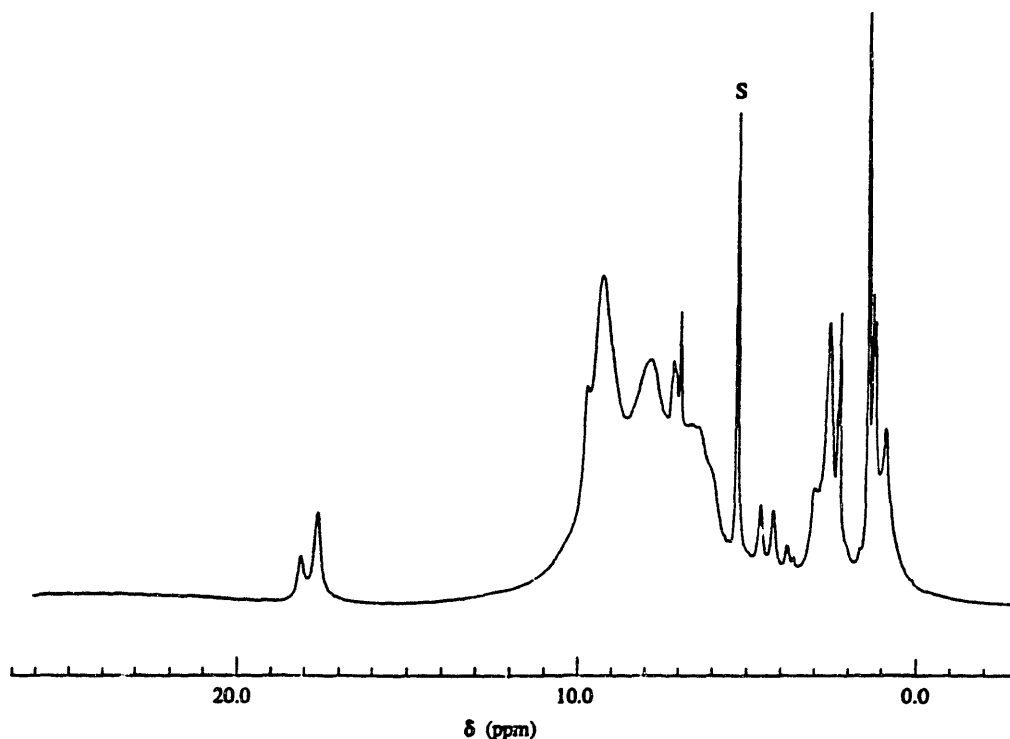


Figure 7.  $^1\text{H}$  NMR spectrum of **4** in  $\text{CD}_2\text{Cl}_2$ . The solvent peak is marked with an S.

**Solution Magnetics.** The room temperature magnetic susceptibilities of **1**, **2**, and **3b** in solution were measured by the Evans method as further confirmation of their integrity in solution. The value of  $\mu_{\text{Fe}} = 2.34 \mu_{\text{B}}$  at 295 K calculated for **1** by this method is in close agreement with the solid state value of  $2.33 \mu_{\text{B}}$  at 300 K.<sup>4</sup> A value of  $2.41 \mu_{\text{B}}$  was calculated for **2** and  $2.27 \mu_{\text{B}}$  for **3b**. These values are reasonable for the proposed tetranuclear structure and helped to identify these complexes as analogues of **1**. The larger room temperature magnetic moment of the tetranuclear  $[\text{Fe}_4\text{O}_2]^{8+}$  compounds compared to the dinuclear  $[\text{Fe}_2\text{O}]^{4+}$  compounds is reflected in the magnitude of the isotropic shifts observed for pyrazolyl protons. The most shifted resonance is found at 17.1 ppm in **1** versus 12.2 ppm in  $[\text{Fe}_2\text{O}(\text{O}_2\text{CC}_6\text{H}_5)_2(\text{HBpz}_3)_2]$ .<sup>1</sup>

**Raman Spectroscopy.** The Raman spectra of **1** and **2** exhibit one strong band that can be attributed to a vibration of the  $\{\text{Fe}_4\text{O}_2\}^{8+}$  core. The spectrum of **1** in  $\text{CH}_3\text{CN}$  at 488 nm excitation from 250 to  $1550 \text{ cm}^{-1}$  is shown in Figure 8. The band assigned as a core vibration

occurs at  $746\text{ cm}^{-1}$ . An assignment of the bands in the spectrum of **1** is given in Table III. The spectrum of **2** is essentially the same as that of **1** except for the absence of the benzoate ring vibrations (Table III). Without  $^{18}\text{O}$  labelling experiments, the band at  $476\text{ cm}^{-1}$  cannot be unequivocally identified as a vibration of the iron-oxo core. The band, however, shows considerable resonance enhancement, as can be seen in Figure 9. Owing to instrumental limitations and difficulties associated with the opacity of the sample solution, collection of a complete enhancement profile was not possible. The band increases in intensity as the excitation energy increases from 514 to 476 nm. The optical spectra of **1**, **2** and **3** all exhibit a shoulder or band at 460-470 nm (Figure 1). Potentially, this optical band may be responsible for the enhancement. The dinuclear complexes, however, show maximum enhancement in the ultraviolet region, which may also be the case for the tetranuclear complexes.<sup>12</sup>

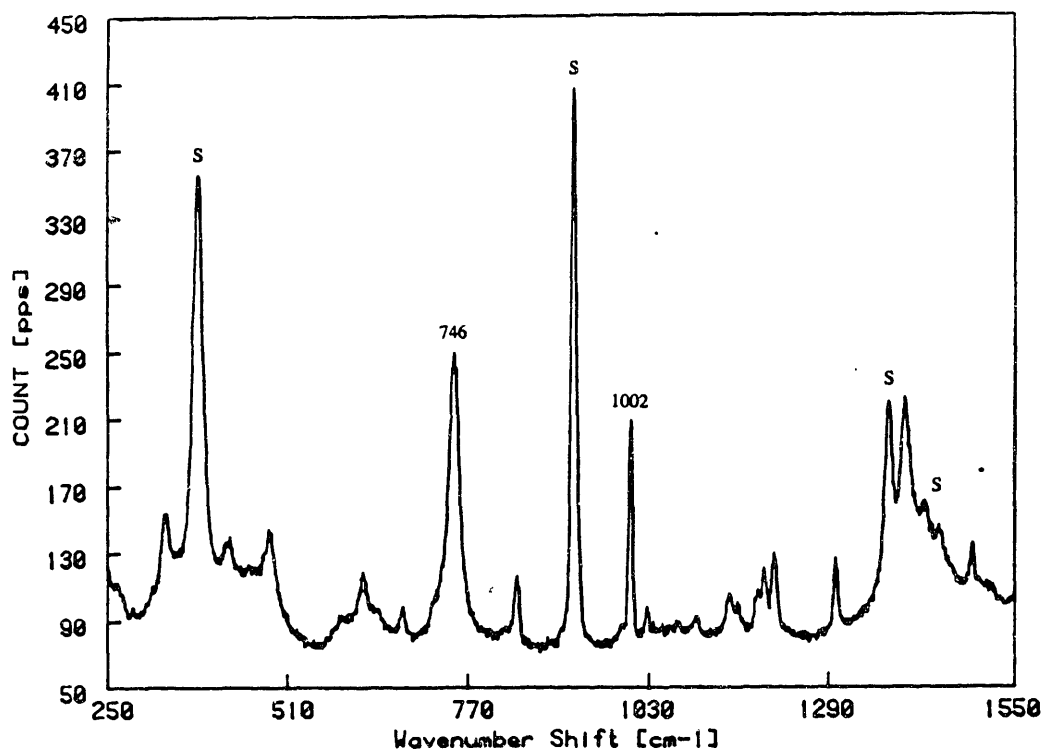


Figure 8. Raman spectrum of a 65 mM solution of **1** in  $\text{CH}_3\text{CN}$  with 488 nm excitation.

<sup>12</sup> Sander-Loehr, *J. ACS Symp. Ser.* 1988, in press. See also reference in Footnote a, Table III.

Table III

## ASSIGNMENT OF OBSERVED RAMAN BANDS FOR 1 AND 2

Band (cm <sup>-1</sup> )		Probable Source
1	2	
243	--	Fe-N(ligand), Fe-O(carboxylate) <sup>a</sup>
331	345	Fe-N(ligand), Fe-O(carboxylate)
379 <sup>b</sup>	395	Fe-N(ligand), Fe-O(carboxylate)
423		Et <sub>4</sub> N <sup>+</sup>
480	450	Fe-N(ligand), Fe-O(carboxylate)
616		benzoate
673	650	Et <sub>4</sub> N <sup>+</sup>
746 <sup>c</sup>	746	{Fe <sub>4</sub> O <sub>2</sub> } core
839		benzoate
927 <sup>b</sup>	925	(H <sub>2</sub> Bpz <sub>2</sub> ) <sup>-d</sup>
980 (sh)	980	(H <sub>2</sub> Bpz <sub>2</sub> ) <sup>-</sup>
1002		benzoate
1027		benzoate
1099	1100	(H <sub>2</sub> Bpz <sub>2</sub> ) <sup>-</sup>
1147		benzoate
1156		benzoate
1186	1180	benzoate
1196	1198	(H <sub>2</sub> Bpz <sub>2</sub> ) <sup>-</sup>
1210	1210	(H <sub>2</sub> Bpz <sub>2</sub> ) <sup>-</sup>
1298	1298	(H <sub>2</sub> Bpz <sub>2</sub> ) <sup>-</sup> , Et <sub>4</sub> N <sup>+</sup>
1397	1395 (less intense)	benzoate, (H <sub>2</sub> Bpz <sub>2</sub> ) <sup>-</sup>
1492		benzoate, Et <sub>4</sub> N <sup>+</sup>

<sup>a</sup> These low frequency bands have been assigned by analogy to bands in the same region of the spectrum of the binuclear compound. See Czernuszewicz, R.S.; Sheats, J.E.; Spiro, T.G. *Inorg. Chem.* **1987**, *26*, 2063-2067.

<sup>b</sup> These bands are hidden under the solvent bands in Figure 8.

<sup>c</sup> The frequency of this band was determined from the spectrum of the compound in THF.

<sup>d</sup> Ligand bands were assigned based on the spectrum of [Fe(HBpz<sub>3</sub>)<sub>2</sub>]ClO<sub>4</sub> described in reference 1b.

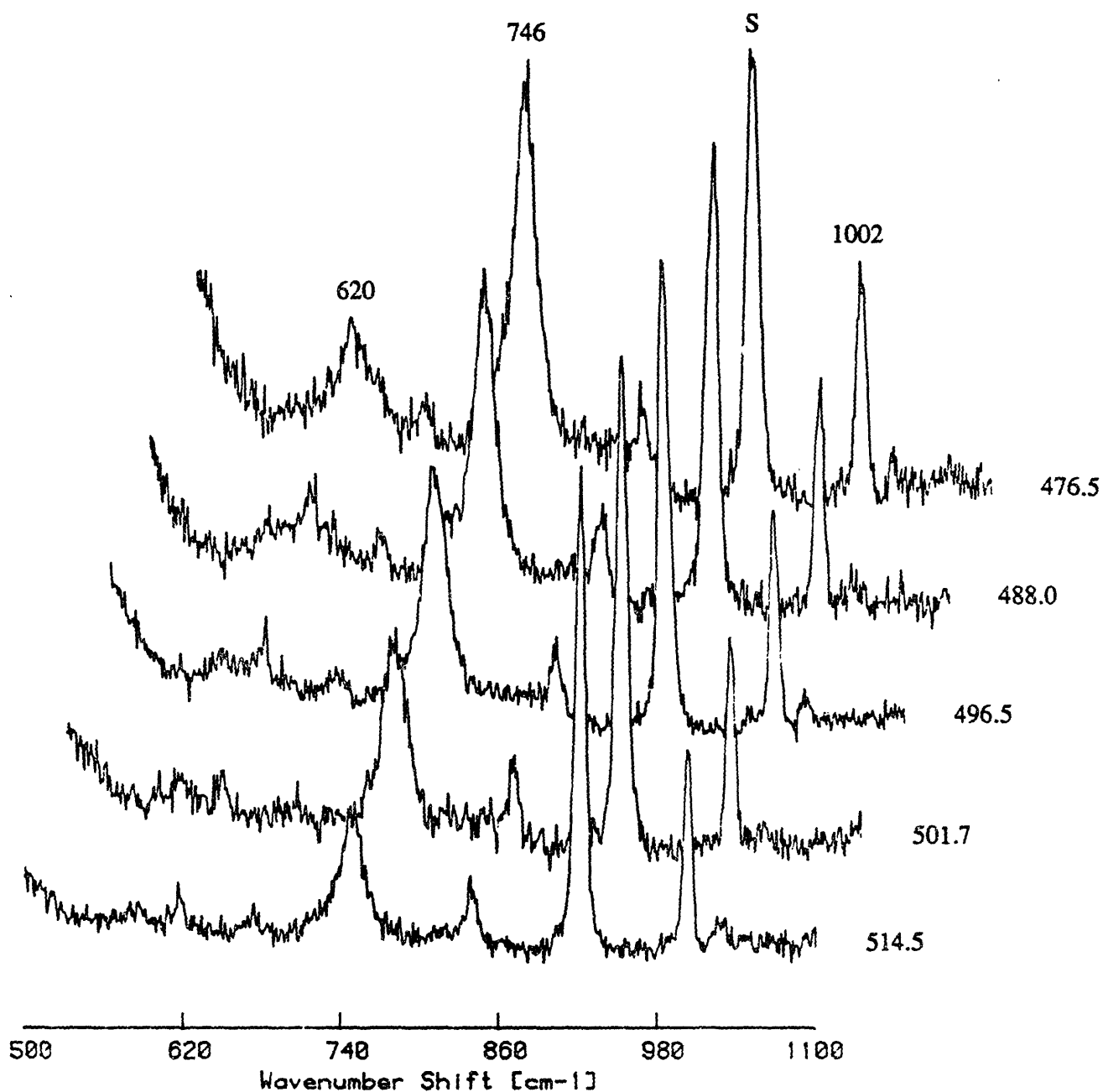


Figure 9. Raman spectrum of 1 in  $\text{CH}_3\text{CN}$  collected as various excitation wavelengths. The data was collected from a 85 mM solution. Several scans were averaged for all spectra at excitation wavelengths below 501.7 nm. Excitation wavelengths are given in nm.

The Raman spectrum of **3b** in  $\text{CH}_2\text{Cl}_2$  shown in Figure 10 was difficult to obtain. The complex is only moderately soluble in  $\text{CH}_2\text{Cl}_2$  and nearly insoluble in  $\text{CH}_3\text{CN}$ . Fluorescence was also a problem, resulting in the upward slope of the baseline above  $1000\text{ cm}^{-1}$ . Furthermore, the relative intensity of the bands appeared to change with time, suggesting that the complex was either decomposing or that the intensities of some of the bands were very sensitive to slight changes in temperature. Figure 11 displays the first and last scan collected and averaged into the spectrum shown in Figure 10. The bands at  $1484$ ,  $1554$  and  $1616\text{ cm}^{-1}$  have increased in intensity during data collection. These bands are strong bands in the spectrum of  $[\text{Fe}(\text{Me}_2\text{bipy})_3]\text{Cl}_2$ , suggesting that decomposition to this complex may have occurred.

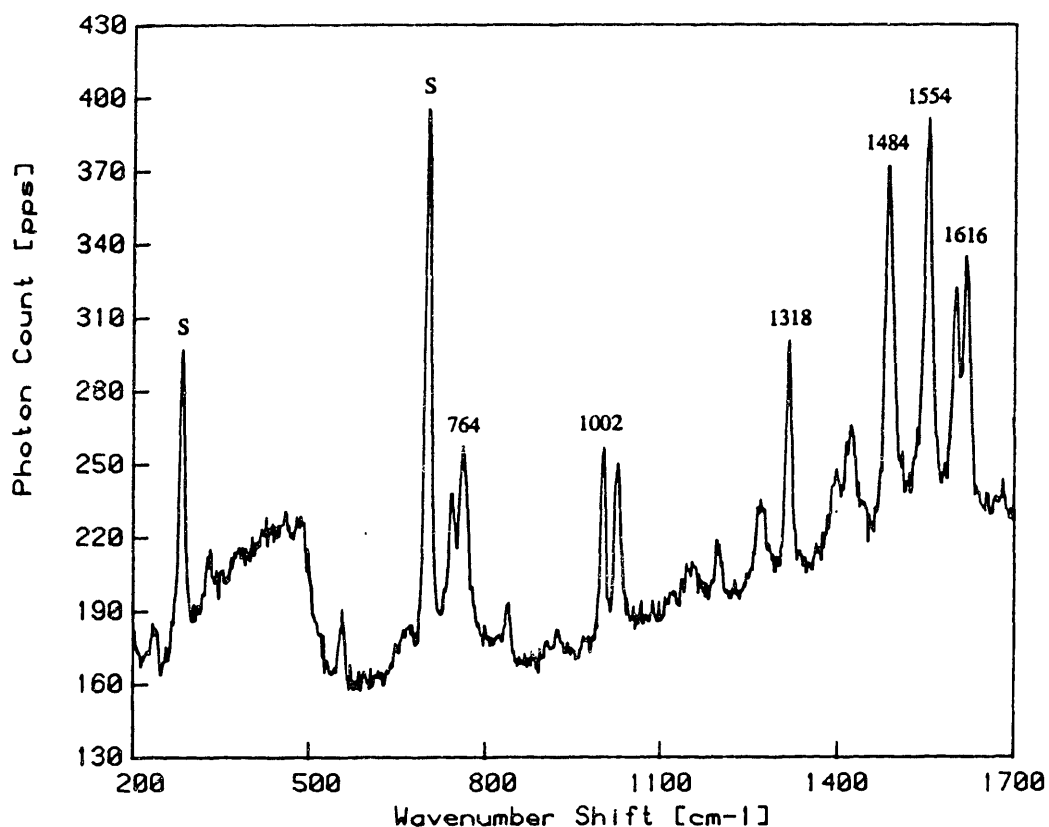


Figure 10. Raman spectrum of a 90 mM solution of **3b** in  $\text{CH}_2\text{Cl}_2$  with 488 nm excitation. Six scans were averaged into the spectrum shown with the initial spectrum given twice as much weight as the other five.

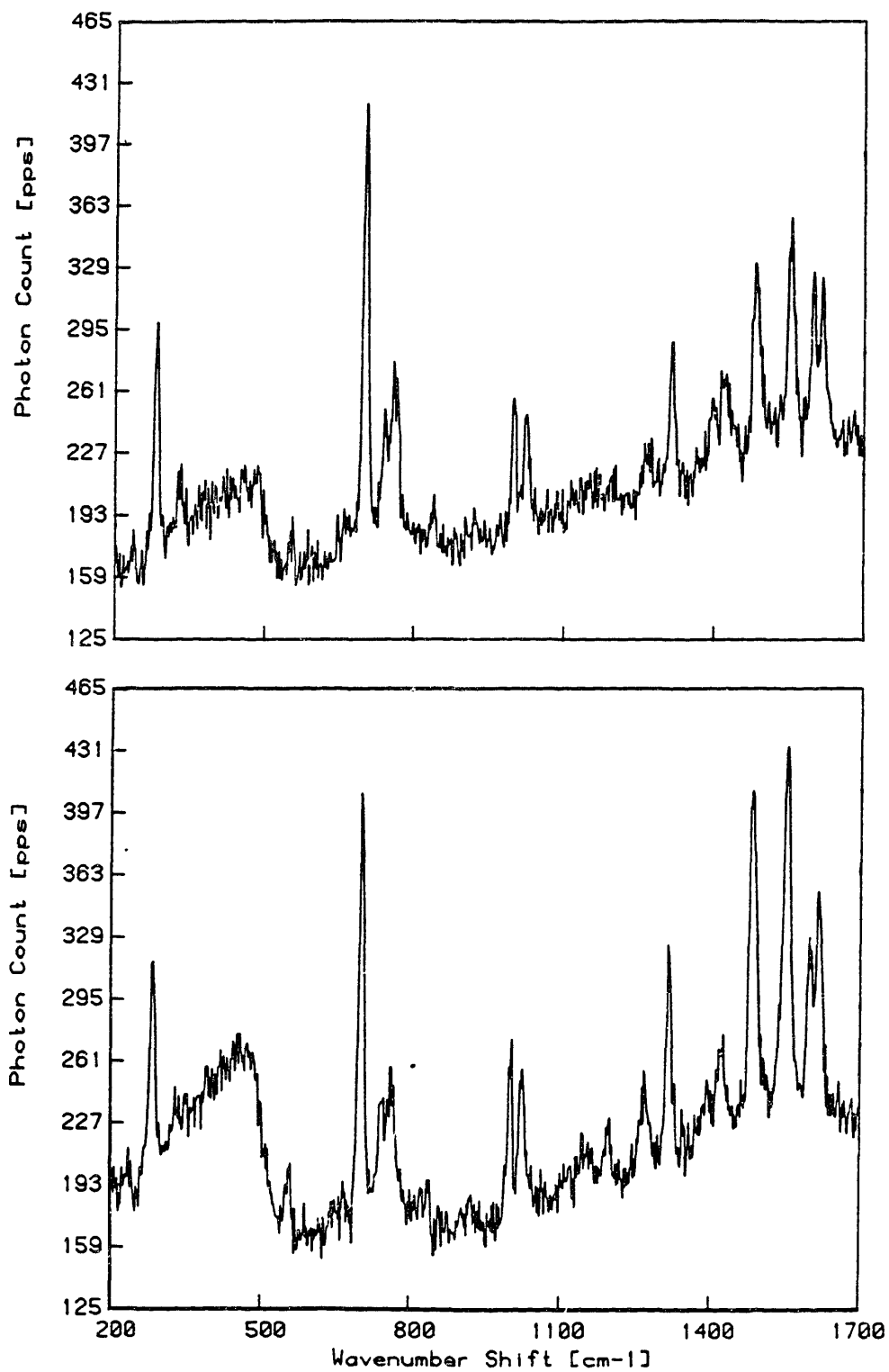


Figure 11. First (top) and sixth (bottom) scan averaged into spectrum shown in Figure 10. Note change in intensity of bands in 1400-1700 cm<sup>-1</sup> region.

The spectrum of **3b** shows only four bands of significant intensity at energies greater than  $600\text{ cm}^{-1}$  which do not occur in the spectrum of  $[\text{Fe}(\text{Me}_2\text{bipy})_3]\text{Cl}_2$  (Table IV). Of these bands, three at  $840\text{ cm}^{-1}$ ,  $1002\text{ cm}^{-1}$ , and  $1600\text{ cm}^{-1}$  are attributable to benzoate vibrations. The fourth, occurring at  $764\text{ cm}^{-1}$ , is presumed to be analogous to the  $746\text{ cm}^{-1}$  band in **1** and **2**. It should be noted that the solvent,  $\text{CH}_2\text{Cl}_2$ , also exhibits a band at  $742\text{ cm}^{-1}$ . This band, however, is broad and of only one-tenth the intensity of the solvent band at  $704\text{ cm}^{-1}$ ,<sup>13</sup> such that it can only account for part of the intensity in the  $750\text{ cm}^{-1}$  region in the spectrum of **3b**. Also, spectra of **3a**, collected between  $200$  and  $1700\text{ cm}^{-1}$  showed essentially the same features as those in **3b**. The band at  $\sim 765\text{ cm}^{-1}$  was clearly apparent in those spectra as well.

In Figure 12, the spectra of **3b** at  $514\text{ nm}$  and  $488\text{ nm}$  excitation are shown. Comparing the intensity of the peak at  $764\text{ cm}^{-1}$  to that of the peak at  $1002\text{ cm}^{-1}$  in the two spectra shows that the  $764\text{ cm}^{-1}$  band exhibits similar enhancement to the  $746\text{ cm}^{-1}$  peak in **1**. (The  $1002\text{ cm}^{-1}$  peak should exhibit little or no resonance enhancement.) The  $764\text{ cm}^{-1}$  band is considerably more intense at the higher energy of excitation. By contrast, the peaks at  $744\text{ cm}^{-1}$  and  $1026\text{ cm}^{-1}$ , which arise mainly from the coordinated  $\text{Me}_2\text{bipy}$  ligand, are more intense at the lower excitation energy. The other ligand bands at higher frequency exhibit even greater changes in intensity with the  $1484\text{ cm}^{-1}$  and  $1554\text{ cm}^{-1}$  lines becoming more intense than the solvent band at  $704\text{ cm}^{-1}$ . The increase in intensity of these bands from  $488$  to  $514\text{ nm}$  suggests that there may be some metal-ligand( $\text{Me}_2\text{bipy}$ ) charge transfer character in the absorption band at  $\sim 560\text{ nm}$  in the visible spectrum of **3b**.

The presence of the band at  $\sim 750\text{ cm}^{-1}$  in the Raman spectra of **1**, **2** and **3** and the clear resonance enhancement of this band in the visible region support the assignment of the band as a  $\{\text{Fe}_4\text{O}_2\}^{8+}$  core vibration. Unfortunately, the Raman spectra of other tetranuclear  $\mu_3$ -oxo complexes have not been published. This band occurs at considerably higher energy than the

---

<sup>13</sup> (a) Schrader, B.; Meier, W., eds, *Raman/IR Atlas of Organic Compounds*; Verlag-Chemie: Weinham, Germany, 1975. (b) *The Sadtler Standard Spectra* (Raman); Sadtler Research Laboratories, Inc.: Philadelphia, 1974.



Table IV

## ASSIGNMENT OF OBSERVED RAMAN BANDS FOR 3B

Band (cm <sup>-1</sup> )		
3b <sup>a</sup>	[Fe(Me <sub>2</sub> bipy) <sub>3</sub> ]Cl <sub>2</sub> <sup>b</sup>	Probable Source
234		B(C <sub>6</sub> H <sub>5</sub> ) <sub>4</sub> <sup>-c</sup> , Me <sub>2</sub> bipy
334		Fe-N(ligand), Fe-O(carboxylate) <sup>d</sup>
486		Fe-N(ligand), Fe-O(carboxylate)
558	560	Me <sub>2</sub> bipy
618		benzoate
668 (br)		
744	746	Me <sub>2</sub> bipy
764		{Fe <sub>4</sub> O <sub>2</sub> }
840		benzoate
924		
1002		benzoate, B(C <sub>6</sub> H <sub>5</sub> ) <sub>4</sub> <sup>-</sup>
1026	1026	Me <sub>2</sub> bipy, benzoate, B(C <sub>6</sub> H <sub>5</sub> ) <sub>4</sub> <sup>-</sup>
1154		benzoate, solvent
1200	1202	Me <sub>2</sub> bipy
1270	1272	Me <sub>2</sub> bipy
1318	1322	Me <sub>2</sub> bipy
1396	1376	Me <sub>2</sub> bipy
1484	1488	Me <sub>2</sub> bipy
1554	1556	Me <sub>2</sub> bipy
1600		benzoate, B(C <sub>6</sub> H <sub>5</sub> ) <sub>4</sub> <sup>-</sup>
1616	1624	Me <sub>2</sub> bipy

<sup>a</sup> Values were obtained from spectra of the sample in CH<sub>2</sub>Cl<sub>2</sub> with data collected at every 2 cm<sup>-1</sup>.

<sup>b</sup> Values were obtained from a spectrum of the compound in CH<sub>3</sub>CN collected between 500 and 1700 cm<sup>-1</sup>.

<sup>c</sup> Contributions from the phenyl rings of the anion were determined by comparison of literature spectra of P(C<sub>6</sub>H<sub>5</sub>)<sub>4</sub>Cl, Si(C<sub>6</sub>H<sub>5</sub>)<sub>4</sub>, Ge(C<sub>6</sub>H<sub>5</sub>)<sub>4</sub>, Sn(C<sub>6</sub>H<sub>5</sub>)<sub>4</sub>, and Pb(C<sub>6</sub>H<sub>5</sub>)<sub>4</sub> (Reference 13)

<sup>d</sup> See Table III.

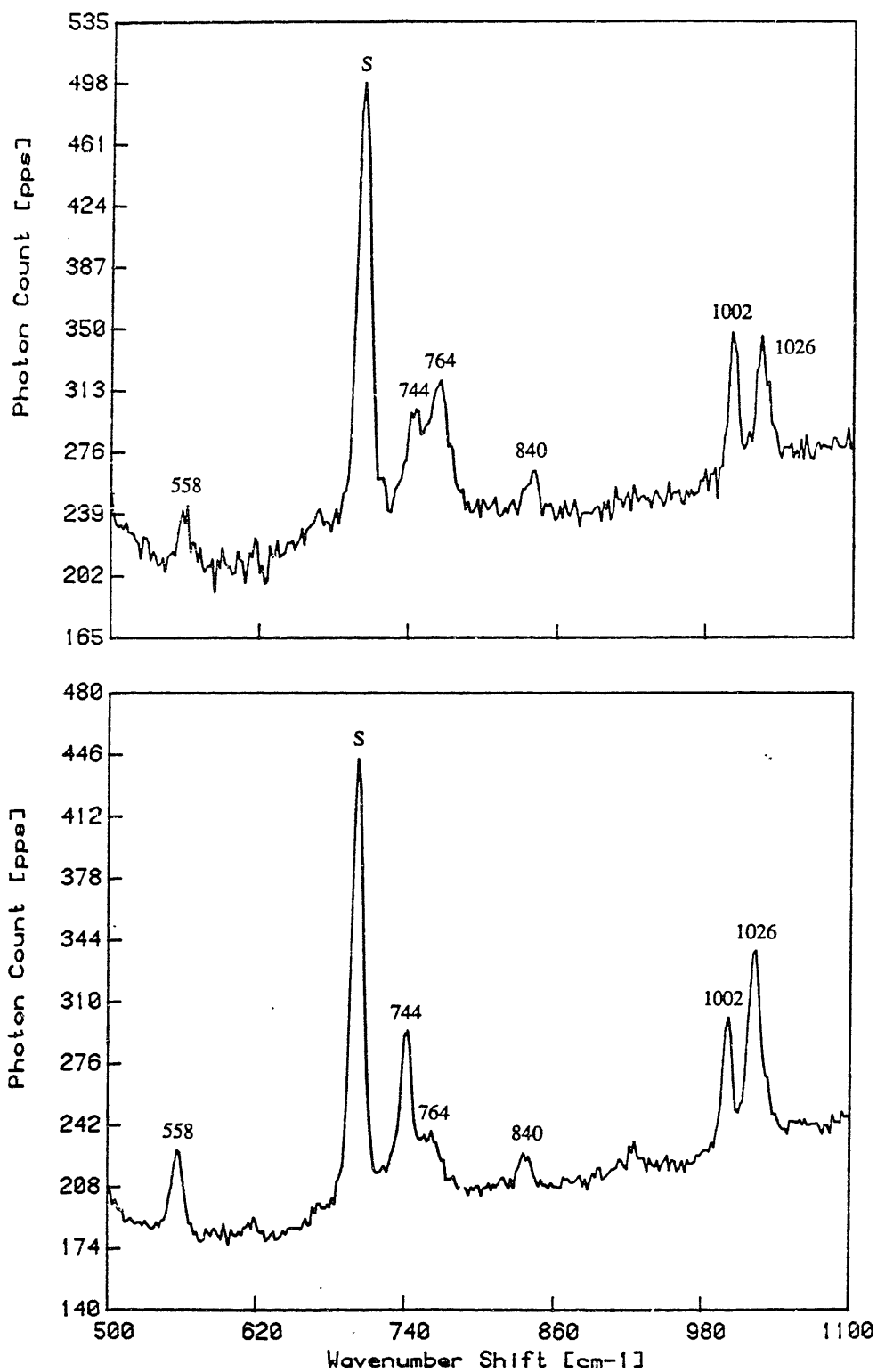


Figure 12. Raman spectra of 3b in  $\text{CH}_2\text{Cl}_2$  collected at 488 nm (top) and 514 nm (bottom) excitation.

symmetric iron-oxo stretch in any of the dinuclear complexes.<sup>1b,12,14</sup> The symmetric stretch for the trinuclear basic iron acetates also lies at much lower energy.<sup>15</sup> The  $\sim 750\text{ cm}^{-1}$  band, however, falls in the range expected for  $\{\text{M}_2\text{O}_2\}$  systems. For example, an IR band at  $688\text{ cm}^{-1}$  in the spectrum of  $[\text{Mn}_2\text{O}_2(\text{bipy})_4]^{3+}$  has been attributed to an  $\{\text{Mn}_2\text{O}_2\}$  stretching frequency.<sup>16</sup> Bis( $\mu$ -oxo)dimolybdenum complexes also show several bands in this region assigned to metal-oxo stretching frequencies.<sup>17</sup> According to Wing and Callahan, a  $\{\text{M}_2\text{O}_2\}$  species with local  $\text{D}_{2h}$  symmetry should give rise to four vibrations, two which are Raman active and two which are IR active, in the  $600$  to  $800\text{ cm}^{-1}$  range. Careful examination of the spectra in Figure 9 reveals that there is a second resonance enhanced feature in the spectrum of **1** at  $\sim 620\text{ cm}^{-1}$ . Also, **1**, **2** and **3** all show bands in this region in the IR spectrum. Unfortunately, a number of ligand bands also occur in this region making it difficult to detect the bands attributable to iron-oxo vibrations. The  $\{\text{Fe}_4\text{O}_2\}$  core of **1**, **2** and **3** contains an  $\{\text{M}_2\text{O}_2\}$  subunit which is nearly planar, but does not approximate  $\text{D}_{2h}$  symmetry as a result of inequivalent Fe-O bond lengths. Nonetheless, it may be the source of the observed Raman band. The intensity of the band  $\sim 750\text{ cm}^{-1}$  suggests that it arises from an allowed transition and, since the energy of the band is similar to those of bis( $\mu$ -oxo) systems, it is very tentatively assigned to a symmetric stretch of the  $\{\text{Fe}_2\text{O}_2\}$  subunit. This strong band is clearly characteristic of the tetranuclear core in **1**, **2**, and **3**. As spectra of other tetranuclear compounds become available, it will be interesting to see if analogous bands will be found in those spectra or if the lack of planarity in the core of **1**, **2** and **3** is crucial to the vibration which gives rise to the band at  $\sim 750\text{ cm}^{-1}$ .

---

<sup>14</sup> Spool, A.; Williams, I.D.; Lippard, S.J. *Inorg. Chem.* **1985**, *24*, 2156-2162.

<sup>15</sup> Cannon, R.D.; White, R.P. *Prog. Inorg. Chem.* **1988**, in press, and references therein.

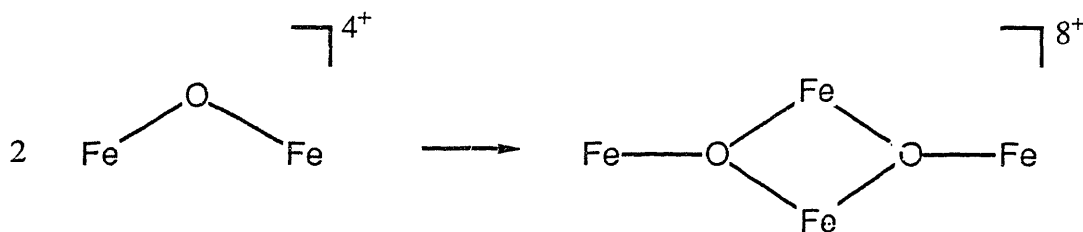
<sup>16</sup> Cooper, S.R.; Calvin, M. *J. Am. Chem. Soc.* **1977**, *99*, 6623-6630.

<sup>17</sup> Wing, R.M.; Callahan, K.P. *Inorg. Chem.* **1969**, *8*, 871-874.

## Discussion

When the structure of **1**, was first published,<sup>18</sup> very few oxo bridged tetranuclear complexes were known. Only two other complexes with triply bridging oxo atoms have appeared in the literature. The first,  $[\text{Fe}_4\text{O}_2(\text{O}_2\text{CCF}_3)_6(\text{H}_2\text{O})_6]$  was synthesized from the corresponding mixed valence, trinuclear "basic iron acetate."<sup>19</sup> The second,  $[\text{Fe}_4\text{O}_2(\text{O}_2\text{CC}_6\text{H}_5)_4(\text{BICOH})_2(\text{BICO})_2]\text{Cl}_2$ , was synthesized in this laboratory in a separate attempt to synthesize a dinuclear species with an open coordination site.<sup>18,20</sup> The  $\{\text{Fe}_4\text{O}_2\}^{8+}$  unit, however, also appears within the structure of an octanuclear aggregate,  $[\text{Fe}_8\text{O}_2(\text{OH})_{12}(\text{TACN})_6]\text{Br}_8 \cdot 9\text{H}_2\text{O}$ ,<sup>21</sup> and in the structures of two minerals, amaranthite, and leucophosphate,<sup>20</sup> suggesting that it may be preferred unit in larger aggregates. Of the tetranuclear units, however, only that in **1**, **2** and **3** varies distinctly from planarity.

The core of **1** and  $[\text{Fe}_4\text{O}_2(\text{O}_2\text{CC}_6\text{H}_5)_4(\text{BICOH})_2(\text{BICO})_2]\text{Cl}_2$  may be viewed formally as the condensation of two  $\mu$ -oxo diiron units as shown below. The structures of



the compounds support this formulation in that **1** can be described as two triply bridged dinuclear iron units held together by the  $\mu_3$ -oxo bonds and the three single benzoate bridges. Similarly, the structure of  $[\text{Fe}_4\text{O}_2(\text{O}_2\text{CC}_6\text{H}_5)_4(\text{BICOH})_2(\text{BICO})_2]\text{Cl}_2$  can be viewed as two discrete  $[\text{Fe}_2\text{O}(\text{O}_2\text{CC}_6\text{H}_5)_2(\text{BICOH})(\text{BICO})]^-$  units held together solely by the  $\mu_3$ -oxo bonds.

<sup>18</sup> Lippard, S.J. *Chem. Brit.* **1968**, 222-229.

<sup>19</sup> Ponomerev, V.I.; Atovmyan, L.O.; Bobkova, S.A.; Turté, K.I.; *Dokl. Acad. Nauk. SSSR.* **1984**, 274, 368-372.

<sup>20</sup> Gorun, S.M.; Lippard, S.J. *Inorg. Chem.*, in press.

<sup>21</sup> Wieghardt, K.; Kohl, K.; Jibril, I.; Huttner, G. *Angew. Chem., Intl. Ed. Engl.* **1984**, 23, 77-78.

It is significant that in the synthesis of both of these types of compounds the residual coordinating ability of the  $\mu$ -oxo ligand is strong enough to bind another iron in competition with chloride and residual water in solution. This interaction reflects the affinity of ferric ions for oxygen even when the oxygen atom is formally coordinatively saturated, an affinity clearly capitalized upon in biology.

In ferritin, an iron storage protein found in mammals, plants and some bacteria, iron atoms are stored as large polyiron-oxo aggregates wrapped in a hydrophobic coating.<sup>22</sup> In mammalian species, these aggregates are usually polycrystalline in nature with a structure similar to  $\text{Fe}_2\text{O}_3 \cdot 9\text{H}_2\text{O}$ , ferrihydrate. The oxygen atoms are a hexagonally close packed with the iron atoms situated between the layers in a semi-regular manner. All the iron are in an octahedral environment. The initial step in the aggregation of iron in the ferritin core has been proposed to be the formation of,  $\mu$ -oxo diiron species.<sup>10,22a,c</sup> Other low nuclearity species have been detected in partially filled cores.<sup>22a,c</sup> The syntheses of the  $[\text{Fe}_4\text{O}_2(\text{O}_2\text{CR})_7(\text{L})_2]^n$  complexes and  $[\text{Fe}_4\text{O}_2(\text{O}_2\text{CC}_6\text{H}_5)_4(\text{BICOH})_2(\text{BICO})_2]\text{Cl}_2$  from dinuclear units demonstrate the ease with which the aggregation can occur and suggest possible structural types for the low nuclearity intermediates. While other tetranuclear species have been synthesized from, or can be envisioned as a condensation of, dinuclear units,<sup>23</sup> none of these compounds contains  $\mu_3$ -oxo bridges proposed for the ferritin core and necessary for efficient packing of the iron atoms.

The largest discrete iron-oxo unit structurally characterized is  $[\text{Fe}_{11}\text{O}_6(\text{OH})_6(\text{O}_2\text{CC}_6\text{H}_5)_{15}]$  which contains an iron core structure of  $\mu_3$ -oxo and  $\mu$ -hydroxo bridges surrounded by bridging benzoates. It was originally synthesized in a manner similar to 1-3 but

---

<sup>22</sup> (a) Harrison, P.M.; Clegg, G.A.; May, K. in *Iron in Biochemistry and Medicine, II*; Jacobs, A.; Worwood, M., eds., Academic: New York, 1980, 131-171. (b) Crichton, R.R. in *The Biological Chemistry of Iron*; Dunford, H.B.; Dolphin, D.; Raymond, K.R.; Sieker, L., eds., Reidel, Dordrecht, Holland, 1982, 45-83. (c) Theil, E.C. *Adv. Inorg Biochem.* **1983**, *5*, 1-38. (d) Smith, J.M.; Helliwell, J.R.; Papiz, M.Z. *Inorg. Chim. Acta* **1985**, *106*, 193-196. (e) Mann, S.; Bannister, J.V.; Williams, R.J.P. *J. Mol. Biol.* **1986**, *188*, 225-232.

<sup>23</sup> (a) Jameson, D.L.; Xie, C.L.; Hendrickson, D.N.; Potenza, J.A.; Schugar, H.J.; *J. Am. Chem. Soc.* **1987**, *109*, 740-746. (b) Murch, B.P.; Boyle, P.D.; Que, L. *J. Am. Chem. Soc.* **1985**, *107*, 6228-6229.

without the addition of nitrogen donors.<sup>10</sup> This complex has now been crystallized in at least five different morphologies<sup>24</sup> and was the only crystalline material isolated out of the synthesis of **4**. The fact that the undecanuclear complex formed even in the presence of Me<sub>4</sub>-en suggests that the equilibrium between different species of varying nuclearity can be readily perturbed. Addition of base to the synthesis of [Fe<sub>11</sub>O<sub>6</sub>(OH)<sub>6</sub>(O<sub>2</sub>CC<sub>6</sub>H<sub>5</sub>)<sub>15</sub>] has been shown to promote the formation of the aggregate.<sup>25</sup> In the attempted synthesis of [Fe<sub>4</sub>O<sub>2</sub>(O<sub>2</sub>CC<sub>6</sub>H<sub>5</sub>)<sub>7</sub>(Me<sub>4</sub>-en)<sub>2</sub>] the basicity of Me<sub>4</sub>-en must have had more influence on the reaction than its iron binding capacity.

The core structure of **1-3** has also been associated with another metal center in biology, that of Photosystem II. The oxygen evolving center in PS II is known to require four manganese ions for optimal functioning.<sup>26</sup> Recently, the center has been formulated as a pair of dinuclear oxo-bridged manganese units or tetranuclear manganese-oxo unit.<sup>27</sup> The first tetranuclear species to be proposed as a model for this site is a manganese analog of **1-3**, [Mn<sub>4</sub>O<sub>2</sub>(O<sub>2</sub>CCH<sub>3</sub>)<sub>7</sub>(bipy)<sub>2</sub>], **5**. Christou *et al.* synthesized the manganese compound from a trinuclear "basic manganese acetate" starting material.<sup>5</sup> They claim that it is a reasonable model because of the two sets of metal ion types within the core. They also claim that the Mn...Mn distances in the molecule match well with those reported from EXAFS data for the reaction center.<sup>5</sup>

The developing comparison of the chemistry and properties of the two analogous systems will be very interesting. Thus far, the chemistry of the manganese system would appear to be richer. The tetranuclear species, **5**, has been isolated in two oxidation states, the monocation and the neutral species, where one manganese has been reduced to the (+2) state.<sup>5</sup> A related tetranuclear complex with two metals in the (+2) only and six bridging acetates was

---

<sup>24</sup> Rardin, R.L.; Roth, M.E.; Michlitz, W.; Lippard, S.J. unpublished results.

<sup>25</sup> Rardin, R.L.; Lippard, S.J. unpublished results.

<sup>26</sup> Dismukes, G. C. *Photochem. Photobiol.* **1986**, *43*, 99-115.

<sup>27</sup> (a) de Paula, J.C.; Beck, W.F.; Brudvig, G.W. *J. Am. Chem. Soc.* **1986**, *108*, 4002-4009. (b) Brudvig, G. W.; Crabtree, R. H.; *Proc. Natl. Acad. Sci. USA* **1986**, *83*, 4586-4588.

synthesized from a mixed-valence trinuclear starting material.<sup>28</sup> Yet another tetranuclear complex has been isolated where the core forms a distorted cubane structure with one corner occupied by a chloride ion.<sup>29</sup> This structural diversity has not yet been found for the iron complexes and may not exist. While the undecanuclear complex appears to be the stable byproduct frequently isolated from syntheses of iron-oxo species, a hexanuclear manganese complex is formed in many of the manganese syntheses.<sup>29</sup> These differences may be basic to the nature of the metal ions and may help to explain the role of manganese in iron evolution chemistry.

The identification of the Raman band characteristic of the tetranuclear iron core is of significance to both topics discussed above. The manganese complexes analogous to **1-3** should exhibit a band in the same region of the spectrum though shifted in energy to account for the change in mass as seen for  $[\text{Mn}_2\text{O}(\text{O}_2\text{CCH}_3)_2(\text{HBpz}_3)_2]$  compared to  $[\text{Fe}_2\text{O}(\text{O}_2\text{CCH}_3)_2(\text{HBpz}_3)_2]$ <sup>30</sup>. The other manganese species might also exhibit bands characteristic of the changes in the core structure. If iron- and manganese-oxo species of these types can be identified by their Raman bands then it may be possible to detect them in new complexes or, using resonance Raman techniques, in biological systems. Such a tool would be of great use in probing the chemistry of iron storage as well as other biologically important metal centers.

---

<sup>28</sup> Christmas, C.; Vincent, J.B.; Huffman, J.C.; Christou, G.; Chang, H.-R.; Hendrickson, D.N. *J. Chem. Soc., Chem. Commun.* **1987**, 1303-1305.

<sup>29</sup> Personal communication from G. Christou, 1988.

<sup>30</sup> Sheats, J.E.; Czernuszewicz, R.S.; Dismukes, G. C.; Rheingold, A. L.; Vasili, P.; Stubbe, J.; Armstrong, W.H.; Beer, R.H.; Lippard, S.J. *J. Am. Chem. Soc.* **1987**, *109*, 1435-1444.

## CHAPTER 4

Air Oxidation of Cyclohexane to Cyclohexanol Catalyzed by Oxo-Bridged Diiron Complexes:  
Towards the Development of a Functional Model System for Methane Monooxygenase



The most abundant iron containing prosthetic group found in biological systems is unquestionably the heme. Heme iron plays a critical role in the functioning of a wide variety of proteins. It is involved in chemistry as diverse as the reversible binding and transport of dioxygen in hemoglobin and the activation of dioxygen for the oxidation of hydrocarbons in cytochrome P450. The prevalence of another iron containing unit, the ( $\mu$ -oxo)diiron center, in proteins which carry out a similarly diverse variety of functions has begun to emerge.<sup>1</sup> The first such diiron center to be detected was in hemerythrin (Hr), an oxygen transport protein found in marine invertebrates. Perhaps not surprisingly, this type of site has very recently been identified in methane monooxygenase (MMO), an enzyme that uses dioxygen to oxidize methane to methanol.<sup>2</sup>

The monooxygenase component in methanotrophs was first identified in the early 1970's but it was several years before the protein which carries out the first step in the metabolism of methane by these microbes was isolated and purified.<sup>2,3</sup> Once isolated, the enzyme was found to oxidize a number of alkane and alkene substrates to monooxygenated products. The most thoroughly studied of the methane monooxygenases, that isolated from *Methylococcus capsulatus* (Bath), contains three components. The active site of the enzyme occurs in component A which was found to contain non-heme iron and zinc but no acid labile sulfur. Spectral studies originally led to the speculations that this component might contain a 2Fe-2S site or an Fe(SR)<sub>4</sub> site like that in rubredoxin. The lack of acid labile sulfur contradicted the first possibility and the presence of 2Fe per mole protein argued against a mononuclear site. EPR spectroscopic studies of the enzyme suggested that it might contain

---

<sup>1</sup> For recent reviews see (a) Lippard, S.J. *Angew Chem. Int. Ed. Engl.* **1988**, *27*, 344-361. (b) Que, L. *ACS Symp. Ser.* **1988**, in press.

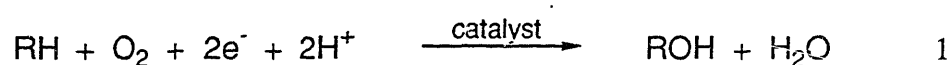
<sup>2</sup> (a) Dalton, H.; Leak, D.J. in *Gas Enzymology*, Degn, H.; Cox, R.P.; Toftlund, H., eds., Reidel: Dordrecht, Holland, 1985, 169-186. (b) Woodland, M.P.; Patil, D.S.; Cammack, R.; Dalton, H. *Biochim. Biophys. Acta* **1986**, *873*, 237-242.

<sup>3</sup> Dalton, H. *Adv. Appl. Microbiol.*, **1980**, *26*, 71-88

two antiferromagnetically coupled irons, and the spectra of the partially reduced enzyme bore a striking similarity to those of semimethemerythrin. The visible spectra reenforced the similarity between the site in MMO and that in Hr and ribonucleotide reductase (RR), another well studied, diiron oxo protein. Two recent EXAFS studies on methane monooxygenase have been able to confirm the presence of a diiron center in this enzyme.<sup>4</sup>

As addressed in the introduction to the previous chapter, significant success has been achieved in synthesizing structural models of the oxo bridged diiron centers. The  $\mu$ -oxo bis-( $\mu$ -carboxylato)diiron core structure found in Hr and believed to occur in RR has been reproduced in a number of compounds. Only recently, however, has interest turned to developing functional models of the diiron proteins. To achieve the reversible binding of dioxygen characteristic of hemerythrin, the synthesis of a ligand with specific steric requirements will probably be required, as was the case for hemoglobin. Many of the first model systems for cytochrome P450, however, were based on simple tetraarylmethylporphyrins. Similarly, a functional model for methane monooxygenase based on the known diiron model complexes appeared as an appealing possibility.

The activity of methane monooxygenase bears some resemblance to that of cytochrome P450 in that they are both monooxygenases, transferring only one atom of O<sub>2</sub> to the substrate, the other becoming water (eq 1). Both enzymes are capable of oxidizing a wide



variety of substrates but there is little evidence yet as to whether or not they proceed through a similar mechanism. Considerable work on cytochrome P450 systems has involved iron porphyrin model compounds and activated oxygen donors.<sup>5</sup> These studies have been useful in

---

<sup>4</sup> (a) Ericson, A.; Hedman, B.; Hodgson, K.O.; Green, J.; Dalton, H.; Bentsen, J.; Beer, R. H.; Lippard, S.J. *J. Am. Chem. Soc.* **1988**, *110*, 2330-2332. (b) Prince, R.C.; George, G.N.; Savas, J.C.; Cramer, S.P.; Patel, R.N. *Biochim. Biophys. Acta* **1988**, *952*, 220-229.

<sup>5</sup> For recent reviews see (a) McMurray, T.J.; Groves, J.T. in *Cytochrome P450, Structure, Mechanism, and Biochemistry*; Ortiz de Montellano, P.R., ed. Plenum: New York, 1986, 1-28. (b) Mansuy, D. *Pure and Appl. Chem.* **1987**, *59*, 759-770.

elucidating aspects of the mechanism of cytochrome P450. While the results from these studies may provide useful guidelines for studying the diiron systems, the use of activated oxygen donors may be less suited to the latter case. Simple mononuclear manganese, iron, cobalt and copper complexes have been shown to be sufficient catalysts for oxidation chemistry with activated oxygen donors.<sup>6</sup> Therefore, dioxygen was chosen as the oxidant for use in initial studies to explore the potentially unique properties of the diiron centers for the oxidation of hydrocarbons, particularly alkanes.

There are several difficulties, however, inherent in model monooxygenase chemistry using dioxygen as the oxidant. During the reaction the O-O bond must be broken and the oxygen must be reduced from an oxidation state of (0) in dioxygen to (2-) in the oxidized product or water. Therefore, this process has been referred to as "reductive dioxygen activation."<sup>7</sup> Usually, the role of the catalyst is to bind O<sub>2</sub> and donate some of its electrons to initiate the activation process. Thus, frequently, at the end of the oxidation reaction, the catalyst is in an oxidized form and an additional reductant must be used to complete the catalytic cycle. In nature, of course, the electrons required for the reduction may be transferred specifically when needed. In bench top chemistry, the reductant must be present in the reaction mixture such that model oxygenase systems, which are specifically designed to generate a highly oxidizing species from dioxygen, must also contain a reductant. Clearly, the reductant may react directly with dioxygen and may compete with the substrate for the highly oxidizing intermediate. As a result, reactions which may be catalytic in the metal species present often show low yields based on the reductant.

Despite these obstacles, the task was undertaken to develop a functional model for methane monooxygenase based specifically on a dinuclear oxo-bridged iron catalyst. Initially,

---

<sup>6</sup> (a) Franklin, C.C.; Van Atta, R.B.; Fan Tai, A.; Valentine, J.S. *J. Am. Chem. Soc.* **1984**, *106*, 814-816. (b) Van Atta, R.B.; Franklin, C.C.; Valentine, J.S. *Inorg. Chem.* **1984**, *23*, 4123-4125.

<sup>7</sup> Tabushi, I.; Yazaki, A. *J. Am. Chem. Soc.* **1981**, *103*, 7371-7373.

the known hemerythrin model compounds,  $[\text{Fe}_2\text{O}(\text{O}_2\text{CCH}_3)_2(\text{HBpz}_3)_2]$ ,<sup>8</sup> **1**, and  $[\text{Fe}_2\text{O}(\text{O}_2\text{CCH}_3)_2(\text{Me}_3\text{TACN})_2](\text{PF}_6)_2$ ,<sup>9</sup> **2**, were tested for activity toward the oxidation of cyclohexane in the presence of various reductants under an atmosphere of pure  $\text{O}_2$  or in air. While some activity was observed, much more interesting chemistry was discovered based on the simple dinuclear starting material,  $(\text{Et}_4\text{N})_2[\text{Fe}_2\text{OCl}_6]$ , **3**. This complex was found to oxidize cyclohexane to cyclohexanol and cyclohexanone catalytically in the presence of dithiothreitol. However, the simple mononuclear compound,  $(\text{Et}_4\text{N})[\text{FeCl}_4]$ , showed as much activity. When allowed to react with ascorbic acid or tetramethyl reductic acid, though, **3** formed a complex characterized by a purple color which was capable of oxidizing cyclohexane to cyclohexanol, selectively, producing only a minor amount of cyclohexanone. This activity proved specific to **3** and did not appear to involve free radicals. The results of the experiments with the hemerythrin model compounds and those of studies on the  $[\text{Fe}_2\text{OCl}_6]^{2-}$  based systems will be presented and discussed in this chapter. As a background to this chemistry, a brief review of iron and manganese based model monooxygenase systems utilizing dioxygen as an oxidant is presented below.

Because of the integral role of iron in oxygenase chemistry in biology, researchers have been studying systems based on iron or manganese catalysts which utilize dioxygen for the oxidation of alkanes and alkenes for over 30 years. Among the first of these was that which has become known as the Udenfriend system. Udenfriend, in the early '50s, discovered that a mixture of ascorbic acid and ferrous or ferric ion in the presence of dioxygen and a hydrocarbon substrate led to the production of oxidized hydrocarbon products.<sup>10</sup> The system was

---

<sup>8</sup> (a) Armstrong, W.H.; Lippard, S.J. *J. Am. Chem. Soc.* **1983**, *105*, 4837-4838. (b) Armstrong, W.H.; Spool, A.; Papaefthymiou, G.C.; Frankel, R.B.; Lippard, S.J. *J. Am. Chem. Soc.* **1984**, *106*, 3653-3667.

<sup>9</sup> Chaudhuri, P.; Wieghardt, K.; Nuber, B.; Weiss, J. *Angew. Chem., Int. Ed. Engl.* **1985**, *24*, 778-779.

<sup>10</sup> (a) Shilov, A.E. *Activation of Saturated Hydrocarbons by Transition Metal Complexes*; Reidel: Dordrecht, Holland, 1984, 106-113. (b) Groves, J.T. in *Metal Ion Activation of Dioxygen*; Spiro, T.G., ed., Wiley: New York, 1980, 125-162. (c) Hamilton G.A.; in *Molecular Mechanism of Oxygen Activation*; Hayaishi, O. ed., Academic: New York, 1974. (d) Hamilton, G.A.; Workman, R.J.; Woo, L. *J. Am. Chem. Soc.* **1964**, *86*, 3390-3391.

able to hydroxylate aromatics and alkanes and epoxidize alkenes, but only in low yields. Initially, this chemistry was thought to be the same as that resulting from aqueous mixtures of ferrous iron and peroxide (Fenton chemistry). Some years later, Hamilton reexamined the system and proposed that it proceeded through an "oxenoid," or oxygen atom transfer, mechanism as opposed to the free radical mechanism previously proposed.<sup>8,11</sup> He extended the system using chelated iron and a number of other reducing agents. Ullrich also developed a hydroxylating system using ferrous ion in aqueous acetone in the presence of base and mercaptobenzoic acid with O<sub>2</sub> as the oxidant.<sup>12</sup> This system was also able to oxidize cyclohexane to a mixture of cyclohexanol and cyclohexanone, aromatic substrates to mono- and di-alcohols and to demethylate anisole. Like Hamilton, Ullrich proposed an oxenoid mechanism for the reaction. More recent research on these systems, however, have suggested that the chemistry in these systems is free radical with a metal-oxygen species acting as a radical oxidant rather than an oxo transfer agent.<sup>6a</sup>

Mimoun and Sere de Roch published another system using ferrous ion and a reductant, diphenylhydrazine, but their system gave different product distributions than seen in the Ullrich or Hamilton systems.<sup>13</sup> Using ferrous or ferric ion in the presence of organic acid and the reductant in acetone, they were able to produce four turnovers of cyclohexanol from cyclohexane along with minor amounts of cyclohexanone. The yield based on the reductant was ~20%. Using isopentane as a substrate, the researchers were able to calculate a 1°/2°/3° reactivity ratio of ~1/5/25. The same system, however, gave no epoxide product from the oxidation of cyclohexene. For the alkene, the major product was the allylic alcohol. Essentially the same reactivity resulted when ortho-diaminobenzene was the reductant used. Since the reactivity was not inhibited by the presence of a radical trap, the authors proposed a non-radical, iron-peroxo intermediate for the oxidation reactions. Interestingly, though, the

---

<sup>11</sup> Hamilton, G.A. *J. Am. Chem. Soc.* **1964**, *86*, 3391-3392.

<sup>12</sup> Ullrich, V. *Z. Naturforsch. B* **1969**, *24b*, 699-704

<sup>13</sup> Mimoun, H.; Sere de Roch, I. *Tetrahedron* **1975**, *31*, 777-784.

oxidation of cyclohexane did not appear to be metal ion specific. Similar yields and product distributions were achieved using ferrous, ferric, manganous, or vanadyl ions as catalysts. About half the reactivity was observed for cupric ion and a quarter the reactivity with nickelous ion, with only slightly less specificity. These results seem to contradict the integral role of iron in the proposed active species.<sup>10a</sup>

Because of the presence of a heme group in cytochrome P450, several researchers turned their efforts to developing porphyrin based monooxygenase model systems. One researcher who was particularly interested in the role of the metal in dioxygen activation was Tabushi. He and his coworkers published a series of papers on systems utilizing dioxygen for the oxidations of hydrocarbons consisting of a metalloporphyrin catalyst in the presence of reductants. In the first of these, Mn(TTP)Cl was the catalyst and NaBH<sub>4</sub> was used as the reductant.<sup>14</sup> Studying the oxidation of cyclohexene, Tabushi *et al.* discovered that the major product was cyclohexanol which they determined was a secondary reduction product from the initial epoxide formed.<sup>15</sup> Since the simple reductant appeared to be unsuitable for this type of system, these researchers adapted a colloidal Pt/H<sub>2</sub> reductant which could be used in the presence of pure O<sub>2</sub>.<sup>7</sup> Again with manganese porphyrins as catalyst but now with an imidazole cocatalyst, high yields of epoxides from alkenes were achieved. Oxidation of adamantane gave mostly tertiary alcohol with much lower turnovers than observed for alkenes. This system was improved by using a water soluble porphyrin and aqueous solvents.<sup>16</sup> Under these conditions, 162 mols product could be produced per mol catalyst consumed. Also, monoepoxidation of polyolefins with high regio- and stereospecificity was discovered to be characteristic of the system.<sup>16</sup> Based on the relative reactivity of alkenes and the high yields of epoxides, the authors suggested that the same intermediate formed by the addition of iodozylbenzene (PhIO) to manganese porphyrins was formed as the active oxidant in these systems.<sup>7</sup> This group has

---

<sup>14</sup> Tabushi, I; Koga, N. *J. Am. Chem. Soc.* **1979**, *101*, 6456-6458.

<sup>15</sup> A similar study with (B<sub>14</sub>N)BH<sub>4</sub> was also published: Perrée-Fauvet, M.; Gaudemer, A. *J. Chem. Soc., Chem. Commun.* **1981**, 874-875.

<sup>16</sup> Tabushi, I; Morimitsu, K. *J. Am. Chem. Soc.* **1984**, *106*, 6871-6872.

also carried out a complete kinetic study of the oxidation of cyclohexene by dioxygen catalyzed by an iron picket-fence porphyrin in the presence of colloidal Pt/H<sub>2</sub> and 1-methylimidazole (1-MeIm).<sup>17</sup> From this study they determined that successful dioxygen activation required the presence of a proton donor and that acyl groups increased the catalytic activity of the system, probably by assisting in the O-O bond cleavage as had been previously suggested.<sup>18</sup>

In an attempt to study a reaction more closely related to that in cytochrome P450, this group also developed a catalytic system using MeNAH, a NADH analog, as the reductant with FMN (flavin mononucleotide) as an electron transfer catalyst.<sup>19</sup> Both of these components have biological analogs. The remainder of the system consists of the manganese porphyrin, 1-MeIm, and benzoic acid in an aqueous ethanol solution. Each component has a parallel in the biological system. Good recycling numbers with high percentages of epoxides and regio-selective epoxidation of nerol were reported. A turnover rate of 9 mol/min for nerol oxidation was achieved. The yield on MeNAH is reported to be 33%. The high yield on reductant is due in part to a high ratio of productive decomposition versus non-productive decomposition of the active oxidizing species. The greater productivity may be a result of the presence of the electron transfer reagent and may reflect the role of the NADH-flavin couple in the native cytochrome P450 system. When iron porphyrin was substituted for manganese, however, the activity of the system was reduced significantly.

Mansuy and coworkers have also been interested in developing model cytochrome P450 systems using dioxygen. In 1984, they published a biphasic system with MnTTPCl as the catalyst and sodium ascorbate as the reductant.<sup>20</sup> The porphyrin was dissolved in benzene and the ascorbate in water. A phase transfer catalyst, trioctylmethyl amine (TOMA) was also

---

<sup>17</sup> Tabushi, I.; Kodera, M.; Yodoyama, M. *J. Am. Chem. Soc.* **1985**, *107*, 4466-4473.

<sup>18</sup> (a) Groves, J.T.; Watanabe, Y.; McMurray, T.J. *J. Am. Chem. Soc.* **1983**, *105*, 4489-4490, and references therein. (b) Khenkin, A.M.; Shteinman, A.A.; *J. Chem. Soc., Chem. Commun.* **1984**, 1219-1220.

<sup>19</sup> Tabushi, I.; Kodera, M. *J. Am. Chem. Soc.* **1986**, *108*, 1101-1103.

<sup>20</sup> Fontecave, M.; Mansuy, D. *Tetrahedron* **1984**, *40*, 4297-4311.

required for activity in the system. A variety of alkenes were transformed to their corresponding epoxides with production of little or no side products at rates up to 0.6 mol/ mol catalyst/ hr. Alkanes were also oxidized, mainly to ketones and aldehyde, at rates comparable to those observed for alkenes. No oxidation of primary C-H bonds were detected and the relative rate of 3° to 2° sites was determined to be ~2.3 from the oxidation of methylcyclohexane. The oxidation of alcohols to ketones or aldehydes was also efficiently accomplished by the reaction mixture. Unfortunately, after two hours of reaction time the reactivity stopped owing to consumption of the reductant by competing reactions and direct oxidation by O<sub>2</sub>. Reducing the pH of the aqueous layer or the partial pressure of O<sub>2</sub> introduced into the system slowed the decomposition of the ascorbate but also lowered the rate of productive oxidation of substrate. Yields on the reductant were never more than 1 or 2%. No decomposition of the metalloporphyrin, however, was ever detected and the system could be reactivated by adding more reductant. From their studies, the authors believed that the active species in this reaction was not the same as that produced by the addition of PhIO to MnTPPCL.

More recently, the same research group has presented a new system based on MnTPPCL which shows much higher turnover and much greater yields based on reductant.<sup>21</sup> In this new system, 1-methylimidazole and acetic acid are required and zinc powder is used as the reductant. The zinc powder is added slowly over 0.5 hr to yield up to 75 turnovers of epoxide from cyclooctene (2.5 mol/ mol catalyst/ min) with 50% yield on the reductant. Alkanes are not as good substrates, with only 6 turnovers of alcohol and 8 of ketone formed from cyclooctane (15% yield on reductant). While these values represent some of the best achieved for this type of system, even more impressive is the ability of the system to convert totally 2 mmol of substrate to epoxide within 1 hr, although with lower yield based on reductant.

---

<sup>21</sup> Battioni, P.; Bartoli, J.F.; Leduc, P.; Fontecave, M.; Mansuy, D. *J. Chem. Soc., Chem. Commun.* 1987, 791-792.



An iron porphyrin based system has also recently appeared in the literature.<sup>22</sup> Shilov *et al.* have communicated the hydroxylation of cyclic alkanes and the demethylation of anisole catalyzed by an iron porphyrin in the presence of zinc amalgam and methylviologen. Acetic anhydride was used as a cocatalyst. Up to 67 mols of product per mol catalyst are produced from a cycloalkane with rates up to 1.1 cycles per minute, which compare favorably with rates of ~10 cycles per minute reported for cytochrome P450 and are the best reported for alkane oxidation in the literature. When <sup>18</sup>O labelled dioxygen was used, the labelled oxygen was found in both the product and in acetate formed from the anhydride, confirming the role of the acyl group in O-O bond cleavage.

Electrochemistry has also been used successfully to supply reducing equivalents in several porphyrin based systems. Among the first of these was reported by Khenkin and Shteinman who used Fe(TPP)Cl in the presence of acetic anhydride and O<sub>2</sub> to affect the oxidation of cyclohexane to cyclohexanol.<sup>21</sup> This system was a precursor to that presented immediately above. Only 7% electrochemical yield was observed. Murray *et al.* used Mn(TPP)Cl with 1-MeIm and benzoic anhydride for the epoxidation of alkenes and achieved electrochemical yields over 50%.<sup>23</sup> Their rates of reaction, however, were quite slow, only ~2 mol/ mol catalyst/ hr. When Mansuy *et al.* adapted their Mn(TTP)/ 1-MeIm/ acetic acid/ zinc system for electrochemical reduction, they achieved slightly lower yields on electrons consumed but observed turnover rates up to 1.7 mol/ mol catalyst/ min for epoxidation and 0.1 mol/ mol catalyst/ min for alkane oxidation.<sup>24</sup>

For the past five years, D.H.R. Barton and his group have studied a system they call the "Gif" system. Initially, they used iron powder, acetic acid and hydrogen or sodium sulfide

---

<sup>22</sup> Karasevich, E.I.; Khenkin, A.M.; Shilov, A.E. *J. Chem. Soc., Chem. Commun.* **1987**, 731-732.

<sup>23</sup> Creager, S.E.; Raybuck, S.A.; Murray, R.W. *J. Am. Chem. Soc.* **1986**, *108*, 4225-4227.

<sup>24</sup> Leduc, P.; Battioni, P.; Bartoli, J.F.; Mansuy, D. *Tetrahedron Lett.* **1987**, *29*, 205-208.

in pyridine to oxidize adamantane.<sup>25</sup> The role of the sulfide was soon determined to be that of an initiator, activating the surface of the iron. Heating the reaction was found to be as effective as the presence of sulfide and this component was eliminated from the system. Speculating that the iron powder was acting as a source of catalyst as well as a reductant, they isolated a brown iron-carboxylate containing mixture which analyzed as  $[\text{Fe}_3\text{O}(\text{O}_2\text{CCH}_3)_6(\text{py})_3] \cdot 0.5 \text{ py}$ . They then demonstrated that reactions with the pure mixed-valent, trinuclear complex and zinc as a reductant gave as good yields with higher selectivity than the previous system. The oxidation of alkanes by the system was characterized by formation of ketones and an unusual, high preference for secondary over tertiary sites. Alkenes were not oxidized by the system<sup>25e</sup> and the presence of alcohols, even in great excess, had no effect on the production of adamantone from adamantane.<sup>25f</sup> Recently, these researchers have demonstrated selective oxidation of steroids and related complexes by the Gif system.<sup>26</sup> The selectivity can be controlled by ring substituents and methylene oxidation occurs preferentially even in the presence of double bonds.

As they probed the mechanism of activity in the Gif system,<sup>25e,f</sup> Barton *et al.* discovered that the acid could be varied but that the pyridine was essential to the reactivity of the system. Diluting the solvent or using substituted pyridines dramatically affected the yields and product distribution. The importance of pyridine and high selectivity for secondary carbon oxidation were explained in part by the discovery of coupled pyridines and coupled pyridine-

---

<sup>25</sup> (a) Barton, D.H.R.; Gastiger, M.; Motherwell, W.B.; *J. Chem. Soc., Chem. Commun.* **1983**, 41-43. (b) Barton, D.H.R.; Hay-Motherwell, R.S.; Motherwell, W.B. *Tetrahedron Lett.* **1983**, *24*, 1979-1982. (c) Barton, D.H.R.; Boivin, J.; Ozbalik, N.; Schwartzentruber, K.M. *Tetrahedron Lett.* **1984**, *25*, 4219-4222. (d) Barton, D.H.R.; Boivin, J.; Ozbalik, N.; Schwartzentruber, K.M.; Jankowski, K. *Tetrahedron Lett.* **1985**, *26*, 447-450. (e) Barton, D.H.R.; Boivin, J.; Gastiger, M.; Morzycki, J.; Hay-Motherwell, R.S.; Motherwell, W.B.; Ozbalik, N.; Schwartzentruber, K.M. *J. Chem. Soc., Perkin Trans. I* **1986**, 947-955. (f) Barton, D.H.R.; Boivin, J.; Motherwell, W.B.; Ozbalik, N.; Schwartzentruber, K.M.; Jankowski, K. *Nouv. J. Chim.* **1986**, *10*, 387-398.

<sup>26</sup> (a) Barton, D.H.R.; Boivin, J.; Hill, C.H. *J. Chem. Soc., Perkin Trans. I* **1986**, 1797-1804. (b) Barton, D.H.R.; Boivin, J.; Crich, D.; Hill, C.H. *J. Chem. Soc., Perkin Trans. I* **1986**, 1805-1808. (c) Barton, D.H.R.; Beloeil, J.-C.; Billion, J.B.; Boivin, J.; Lallemand, P.L.; Mergui, S.; Morellet, N.; Jankowski, K. *Nouv. J. Chim.* **1986**, *10*, 439-446.

substrate products in the product mixture.<sup>25d,f</sup> The specificity of the reaction had been found to be dependent on the rate at which O<sub>2</sub> was introduced into the system. In reactions with high 2° specificity, large amounts of tertiary pyridine coupled products were isolated. Pyridine radicals formed by zinc reduction in the presence of iron were competing with oxygen for the tertiary radicals in a radical side reaction. The low amount of secondary coupled products found was taken as evidence that the major oxidation mechanism was not dependent on a radical intermediate.

The preference for oxidation at 2° carbons was suggested to result from an iron carbene type intermediate.<sup>25d-f</sup> Zinc and acetic acid were believed to reduce dioxygen to an activated form. Studies with reduced oxygen species, however, all showed little or no activity without zinc present. Therefore, the authors suggest that zinc fulfils a dual role, reducing O<sub>2</sub> and reducing the iron catalyst.<sup>27</sup> The only reduced oxygen species which demonstrated high activity in the system was superoxide. Hydrogen peroxide was decomposed by the iron and zinc without oxidizing substrate. Thus, superoxide has been proposed as the active oxidant in the system.<sup>23f</sup>

The nature of the iron catalyst remains, however, very ambiguous. An iron bipyridine complex was also isolated from a reaction mixture after an oxidation run and [Fe(2,2'-bipy)<sub>3</sub>]Cl<sub>2</sub> or [Fe(2,2'-bipy)<sub>3</sub>](OAc)<sub>2</sub> were demonstrated to be as efficient catalysts as the trinuclear compound.<sup>25d</sup> In fact, when a series of iron and iron-mixed metal complexes were tested in the system, many of them were quite active.<sup>25e</sup> Another curious result was the lack of dependence of the reactivity of the system on the amount of catalyst present. Varying the concentration over three orders of magnitude resulted in essentially the same yield and product distribution. In this series, the turnover number varied from 0.65 to 3370.<sup>25e</sup> Shilov and Shul-

---

<sup>27</sup> In the same system, electrochemical reduction can replace zinc: Balavoine, G.; Barton, D.H.R.; Boivin, J.; Gref, A.; Ozbalik, N.; Riviere, H. *Tetrahedron Lett.* **1986**, *27*, 2849-2852.

pin claim that the catalyst need not be iron, that copper, tin, and cobalt give similar results. These researchers suggest that the active oxygen transfer agent is a pyridine-oxo cation.<sup>28</sup>

Interestingly, a trinuclear iron acetate has been proposed as a catalyst for the oxidation of complicated olefins to epoxides.<sup>29</sup> When the olefins were treated with  $[\text{Fe}_3\text{O}(\text{O}_2\text{CC}(\text{CH}_3)_3)_6(\text{CH}_3\text{OH})_3]\text{Cl}$  without solvent under  $\text{O}_2$  good yields of epoxides were formed. The epoxidation of a number of olefinic acetates including geranyl acetate was accomplished in this manner. One mole of  $\text{O}_2$  was consumed per mole epoxide formed. The reaction was inhibited by 2,6-di-*tert*butyl-*p*-cresol suggesting the presence of a radical intermediate in the mechanism.

With the exception of the Gif system, which may or may not require an iron catalyst, the majority of work on dioxygen activating systems for the oxidation of hydrocarbons has been based on porphyrin species. Development of such systems based on non-heme iron catalysts is still a field open to much advancement. The following reports our progress in this area.

## Experimental Section

**Materials.** All solvents were obtained from commercial sources. When specified,  $\text{CH}_3\text{CN}$  was dried by distillation from  $\text{CaH}_2$ . Acetone was dried by 2 or 3 distillations from  $\text{K}_2\text{CO}_3$  immediately after addition of the drying agent. If the acetone is left in contact with  $\text{K}_2\text{CO}_3$  too long, decomposition of the solvent results. Small amounts of isopropanol detectable by GC remained in the solvent even after distillation. For some reactions, cyclohexane was purified by washing with  $\text{H}_2\text{SO}_4$ , neutralizing with aqueous  $\text{NaCO}_3$  and distilled from benzophenone ketyl. Purity of purchased cyclohexene (Aldrich, 99+) was checked by GC and purified when necessary by chromatography over a short, activated alumina column. The oxidation products of these substrates were purchased from commercial sources. Dithionite, dithiothreitol, mer-

---

<sup>28</sup> Shilov, A.E.; Shul'pin, G.B. *Russian Chemical Reviews*, **1987**, *56*, 442-464.

<sup>29</sup> Ito, S.; Inoue, K.; Mastumoto, M. *J. Am. Chem. Soc.* **1982**, *104*, 6450-6452.

captoethanol, and zinc were obtained from commercial sources and used without purification. Ascorbic acid was obtained from Gibco Laboratories, Inc. and used without purification or after being powdered and dried under vacuum. Tetramethyl reductic acid was supplied by Dr. Lloyd Taylor of Polaroid Corp., Cambridge, MA. This reductant was twice recrystallized from  $\text{CHCl}_3$  and dried under vacuum before use. The polynuclear iron compounds were synthesized according to the literature.<sup>8,9,30</sup>  $[\text{Fe}_2\text{O}(\text{bipy})_2(\text{Cl})_2]\text{Cl}_2$  was received from Dr. J.R. Hartman of this laboratory.  $(\text{Et}_4\text{N})_2[\text{Fe}_2\text{OCl}_6]$  was prepared as specified in the previous chapter. All simple metal chlorides were used as received from commercial sources. Oxygen, compressed air and nitrogen were all obtained from Colort, Inc., Hingham, MA.

**Physical Measurements.** All  $^1\text{H}$  and  $^{13}\text{C}$  NMR spectra were recorded on Bruker WM250, WM 270 or Varian XL 300 instruments. UV-Visible spectra were recorded on a Perkin-Elmer Lambda 7 Spectrophotometer interfaced to a Series 3600 data station. Samples were analyzed for oxidation products by using a Hewlett-Packard 5890A gas chromatograph interfaced with a Model 3393A integrator and fitted with a FFAP (Hewlett-Packard) column ( $530 \mu \times 10 \text{ m}$ ). Early reactions were analyzed on a Carbowax film column ( $530 \mu \times 10 \text{ m}$ ) but the bonded phase column proved much more durable.

To allow for quantitation of the products versus a standard by comparing the integrals produced by the GC, the "response ratio" of the products versus the standard, methylbenzoate, had to be determined. Several solutions of known concentrations of the products and standard with ratios from ~1:1 to ~10:1 were prepared. Each of these solutions was analyzed by GC several times. From the integrals obtained, the response ratios were calculated using:

$$\frac{[\text{x}]}{[\text{std}]} = \frac{\text{C} \cdot (\text{x integral})}{(\text{std integral})}$$

The constants for cyclohexanol and cyclohexanone were checked several times during a year and no change was noted. While some dependence on concentration was observed, the values

---

<sup>30</sup> Gorun, S.M.; Papaefthymiou, G.C.; Frankel, R.B.; Lippard, S.J. *J. Am. Chem. Soc.* **1987**, *109*, 3337-3348.

were always within error of each other so that an average value has been used. The values obtained for cyclohexanol and cyclohexanone were also within error of each other so a single value was used for both products. Ratios for cyclohexene oxidation products were determined on two occasions. Although a slight difference in response between the different products was apparent, the variance was less than 5% and an average value was again used. Oxidation products were identified by retention times as compared to authentic samples. Cyclohexanol and dehydrotetramethyl reductic acid were identified in GC-MS traces kindly recorded by Ms. Xudong Feng of this lab.

**Protocol 1.** Initial experiments with **1** and **2** were carried out in acetonitrile under an atmosphere of pure O<sub>2</sub> or exposed to air. Since cyclohexane is not miscible with CH<sub>3</sub>CN, the reactions were biphasic. Varying amounts of ascorbic acid (AA), dithionite (dt), or zinc were added to 0.5-3.0 X 10<sup>-5</sup> moles of the metal complexes in 10-20 ml of solution and the mixtures stirred vigorously. None of the reductants was soluble. On some occasions the reactions were heated or base was added to the solutions before the addition of reductant. Aliquots of the reaction mixtures were analyzed by GC at various times after the addition of reductant. Only the cyclohexane layer was analyzed because no convenient method could be found for removing the dissolved catalyst from the CH<sub>3</sub>CN layer. In subsequent reactions, the cyclohexane layer was removed at the end of the reaction and washed with water followed by drying with a saturated solution of NaCl and over Na<sub>2</sub>SO<sub>4</sub>. Water was added to the CH<sub>3</sub>CN layer and the products extracted from the mixture with ether. This ether extract was washed once with a small amount of water, or several times if the ether was highly colored, until the majority of color was removed. Next the ether was washed one or two times with 10% HCl or saturated aqueous NH<sub>4</sub>Cl followed by drying as described for the cyclohexane layer. The volume of the final ether solution was reduced by rotary evaporation when necessary. The cyclohexane and ether solutions were analyzed by GC. A known amount of standard was added to the solutions to allow for quantitation of the products. Yields for the experiments

were calculated as twice the yield of cyclohexanone plus the yield of cyclohexanol divided by the total number of moles of catalyst used for the reaction and multiplied by 100. This value has been referred to as "oxidative yield". For mononuclear complexes, yields were based on 2 iron required for an oxidative cycle. Controls were run without any metal complex present and with  $[\text{Fe}(\text{HBpz}_3)_2]$ , all of which gave no oxidation products. Reactions with  $\text{FeCl}_3$  and **3** as catalyst were also tested, originally as controls.

When ascorbic acid was added to solutions of **1**, the green-brown color began to fade almost immediately. Within several hours the solution became quite pale and orange in color. Eventually, the  $\text{CH}_3\text{CN}$  solution appeared orange and the cyclohexane layer pink. Dithionite had a different effect on the color of solutions of **1**. This reductant caused only a slow loss of color and gradual development of an orange hue. The presence of zinc, either powder or granular, had essentially no effect on the color of solutions of **1**. Neither ascorbic acid nor dithionite had a very dramatic effect on solutions of **2**. AA caused the solutions to fade slowly so that in ~6 days the solutions lost the majority of their color. The loss of color occurred much more quickly at higher temperatures ( $t = \sim 4$  hr). The ascorbic acid solids in these solution became grey or lavender during the course of the reaction. The color of  $[\text{Fe}(\text{HBpz}_3)_2]$  was also bleached by AA. Solutions with  $\text{FeCl}_3$  faded when AA was added but solutions of **3** darkened and deposited a flocculent lavender precipitate. The precipitate turned grey during the course of the reaction. The solution above the precipitate was pale yellow. The solids collected at the end of the reaction could be dissolved in MeOH to form a deep purple solution which rapidly lost color on standing in air.

**Protocol 2.** In a small round bottom flask,  $2.5 \times 10^{-5}$  mol of **3** or  $5 \times 10^{-5}$  mol of a mononuclear complex was added to 10 ml acetonitrile or acetone and stirred. Next, 5 ml cyclohexane were transferred into the solution. Unlike acetonitrile, acetone is completely miscible with cyclohexane. Either  $2.5 \times 10^{-4}$ ,  $5.0 \times 10^{-4}$  or  $2.5 \times 10^{-3}$  mol of reductant was then added as a solid. The flask was fit with a vacuum adapter with open stopcock or a drying

tube packed with anhydrous  $\text{CaSO}_4$ . When the reductant was insoluble, it was removed at the end of the reaction by vacuum filtration and washed with ether. The filtrate was reduced in volume by rotary evaporation. On some occasions, when the reductant was soluble, the reaction mixture was filtered and the filtrate extracted with ether as described for the  $\text{CH}_3\text{CN}$  layer in Protocol 1. After a qualitative analysis of the final solution by GC, an appropriate amount of standard was added to the solution and further GC traces recorded to quantitate the yield of oxidation products. The yields are reported as "oxidative yield" (see above).

By using this procedure, a series of iron containing complexes was analyzed for activity in the presence of twenty equivalents of the following reductants in acetone: ascorbic acid (AA), tetramethyl reductic acid (TMRA), sodium ascorbate (NaA), dithiothreitol (dt), mercaptoethanol (me), and dithionite (dt). Reactions with dtt and me were carried out under  $\text{O}_2$  as described in Protocol 3. The TMRA used was only recrystallized once and was not analyzed for purity. Control reactions for each reductant with no iron catalyst present were run.

1/ AA: **1** was not very soluble in acetone but usually completely dissolved after the addition of cyclohexane forming a green-brown solution. When AA was added to the mixture, the green color became more grey and then turned to pink. / TMRA: The addition of this reductant caused the solution to become darker and more grey which then developed into a deep blue-purple color. After 4 hr the color had faded appreciably and after ~20 hr the solution was orange-red. A visible spectrum of this solution revealed the presence of  $[\text{Fe}(\text{HBpz}_3)_2]^+$  as the source of the color. / NaA: The presence of this reductant had no appreciable effect on the color of the reaction mixture. / dtt: When dtt was added to the solution, precipitate started to form immediately so that the mixture soon appeared dull brown. Once the precipitate had been filtered out, however, the solution did not appear to have changed in color. / dt: The addition of this reductant did not appear to have an immediate affect on the color of the solution, but after ~20 hr the solution was orange, possibly due to the presence of  $[\text{Fe}(\text{HBpz}_3)_2]^+$ .

2/ AA: This complex dissolved readily to acetone and cyclohexane to form a deep orange solution. The addition of AA appeared to have no effect on the color of the solution for



up to 40 hr. The solids filtered out of the reaction were slightly orange in color. / TMRA: Upon addition of TMRA, the solution immediately darkened to deep brown color. The color began to fade very soon after it reached its darkest hue. After ~20 hr the solution was again orange although a visible spectrum disclosed slight changes in the position of the maxima characteristic of **2**. / NaA: No apparent change resulted from the addition of this reductant. / dtt: The solution of **2** was also not effected by the addition of dtt. No color change occurred although after a few minutes a fine, brown, particulate precipitate began to form. Unlike the solutions with **1**, only a small amount of precipitate accumulated. / dt: No apparent change resulted from the addition of this reductant.

**3/ AA:** **3** formed a deep yellow-orange solution in acetone. Addition of AA caused the solution to darken to almost black and a fine purple precipitate to form. The solution over the precipitate was pale yellow. / TMRA: The solution turned deep maroon as the TMRA dissolved and faded very slowly, becoming greenish-tan after ~20 hr. / NaA: Addition of this reductant has little immediate effect of the color of the solution. Eventually, the mixture appeared tan. The solution was pale yellow and the solid grey-brown. The solid turned brick red after being filtered out of the solution. / dtt: The addition of this reductant caused the solution to darken immediately to very deep blue. Within several minutes a sticky brown solid began to form on the sides of the flask. After 2 hr, the blue had completely faded and the solution appeared yellow. / me: While the solution darkened to blue as with dtt, it faded much more quickly, returning to yellow within 10 min. An orange solid was deposited on the sides of the flask. / dt: The reductant did not appear to cause the reaction mixture to fade. It appeared slightly more orange with time. When the reductant was filtered out, it appeared to have taken on an orange color while the filtrate appeared yellow.

(Et<sub>4</sub>N)[FeCl<sub>4</sub>]/ AA: The complex dissolved in the solvent substrate mixture to form a pale yellow solution. Addition of AA caused the solution to lighten slightly then darken to a deeper shade of yellow. / TMRA: Addition of the reductant caused the solution to become pale grey-green as it dissolved. Within 30 min, the solution appeared yellow again. / NaA: No

change occurred on addition of the reductant to the solution. When the NaA was filtered out of the reaction mixture, it turned brick red. / dtt: When the dtt was added, the solution turned translucent blue-green. The color faded slowly and a white solid was deposited on the bottom of the flask. / me: Reaction proceeded as with dtt but no solid formed. / dt: The reductant caused no change in the color of the solution.

$\text{FeSO}_4 \cdot 7\text{H}_2\text{O}$  / AA: This compound was not very soluble in the reaction mixture and was essentially colorless. Addition of AA caused no apparent change in the color of the solution. / TMRA: Same as with AA. / NaA: No real color change was apparent during the reaction, but when the reductant was filtered out of the reaction it turned deep purple on the frit. / dtt: Addition of dtt did not cause a color to develop. The solution appeared murky white. / me: Same as with dtt. Solids became slightly yellow in color by the end of the reaction. / dt: No change in color was apparent throughout the reaction.

$[\text{Fe}(\text{HBpz}_3)_2]\text{Cl}$  / AA: This complex formed a deep red-orange solution in acetone but began to precipitate on addition of cyclohexane. The addition of AA caused the precipitate to redissolve and the solution to fade rapidly to pink. / TMRA: Addition of TMRA had the same effect as AA. / NaA: Addition of this reductant did not cause the complex to dissolve but did lead to rapid loss of color to pink. / dtt: Interestingly, dtt did not cause a rapid loss of color when added to solutions of  $[\text{Fe}(\text{HBpz}_3)_2]\text{Cl}$ . With time, the solution faded but remained pale orange throughout. / me: As with dtt, the solution did not fade on addition of reductant. Upon sitting overnight, however, the solution became pink. / dt: Within 10 min of addition of the reductant the solution was pink.

$[\text{Fe}_2\text{O}(\text{bipy})_2\text{Cl}_2]\text{Cl}_2$  was not very soluble in acetone forming a green-brown solution with green-brown solids. The addition of cyclohexane caused more compound to precipitate out of solution. All the reductants had essentially the same effect on the color of the solution. The final color of the solution and any solids was deep red to red-orange. AA and dtt caused the color to change almost immediately. TMRA brought the complex completely into solution,

but a fine precipitate was deposited after several min. Both NaA and dt caused a slow change of color to red.

[Fe<sub>11</sub>O(OH)<sub>6</sub>(O<sub>2</sub>CC<sub>6</sub>H<sub>5</sub>)<sub>15</sub>]/ AA: This complex was sufficiently soluble in acetone and cyclohexane to dissolve completely for these reactions, forming a yellow-orange solution. The addition of AA caused the solution to darken through a greenish grey color to nearly black. A dark purple precipitate was then formed. The filtrate which resulted after removal of the solid was completely colorless. / TMRA: When TMRA was added to the solution, it immediately began to darken passing through grey to dark purple. This color had not faded even after ~20 hr. / NaA: While initially it did not appear as though this reductant had any effect on the color of the solution, the filtrate after removal of the solid was more green in color than is characteristic of this compound. / dtt: Addition of the reductant caused the solution to darken towards brown and a brown precipitate to form. / dt: This reductant had very little effect on the color of the solution. The final filtrate may have been slightly less orange than the initial solution.

**Protocol 3.** (Reactions with dithiothreitol) Typically, 15.0 mg ( $2.5 \times 10^{-5}$ ) of **3** (or  $5 \times 10^{-5}$  mol of mononuclear catalysts) were dissolved in a mixture of 10 ml acetonitrile or acetone and 5 ml cyclohexane which had been purged with O<sub>2</sub> for 5-10 min. After allowing several minutes for the catalyst to dissolve, the purging with O<sub>2</sub> was stopped and the reaction left under an atmosphere of pure O<sub>2</sub>. The dtt was then added as a solid. It dissolved almost instantaneously and the solution very quickly developed a very dark blue color. Within one or two minutes the solution began to fade and a dark brown precipitate began to form. The length of time necessary for the reaction to fade depended on the amount of dtt present. With  $2.5 \times 10^{-3}$  moles dtt present, the reactions were usually very pale blue within 3 to 4 hr with most of the color loss occurring within the first 30 min. When reactions were run with FeCl<sub>3</sub>, the yellow color from FeCl<sub>3</sub> faded on addition of the reductant but no other change occurred throughout the reaction. No precipitate formed in these reactions. In one experiment, freshly distilled lutidine was added in a stoichiometric amount (1 mol/ 1 Fe) to solutions of dtt in

acetone which were then added to reaction mixtures containing **3** and FeCl<sub>3</sub>. On this occasion the mixture containing FeCl<sub>3</sub> behaved in an identical manner to that containing **3**. All reaction mixtures were analyzed without work up. Quantitation was achieved by adding a known amount of methyl benzoate standard directly to the reaction mixture before analysis. Results are reported as oxidative yield (see above).

**Protocol 4.** In an inert atmosphere box,  $2.5 \times 10^{-5}$  mol of **3** or  $5 \times 10^{-5}$  mol of a mononuclear compound was added to 10 ml of dried solvent. Approximately,  $5 \times 10^{-5}$  mol of reductant was added to the solution followed by 5.0 ml ( $4.6 \times 10^{-2}$  mol) of cyclohexane or 2.0 ml ( $2.0 \times 10^{-2}$  mol) of cyclohexene. Substrates were freeze/pump/thawed 3 times prior to use. Methyl benzoate ( $1.6 \times 10^{-5}$  mol) was added as an internal standard present throughout the reaction. The systems were tested for products while under N<sub>2</sub> then brought out of the box, immersed in a heater/shaker bath and opened to a Schlenk line supplied with dry, compressed air. The solutions were monitored for oxidation at various times from 15 min to 96 hr. When ascorbic acid was the reductant, a second addition of  $5 \times 10^{-5}$  mol of reductant was made after 48 hr. For reactions with TMRA, the second addition was made after 5 hr. Control reactions for both substrates were run with no catalyst present or no reductant present.

In experiments in which the concentration of catalyst was varied, a solution of  $2.5 \times 10^{-5}$  mol of **3** in 10 ml acetone was prepared. A 5.0 ml aliquot and a 1.0 ml aliquot were transferred to flasks in place of the addition of the catalyst as a solid. More acetone was added to the solutions to bring the total volume to 10 ml and the concentrations to one-half and one-tenth those of the normal system. The amount of reductant added was also decreased to keep the ratio of reductant to catalyst at 20 to 1. The full 5.0 ml of substrate was added to each reaction and a system at full concentration was always run simultaneously for comparison.

To test the effect of base on the reactivity of the catalysts, stoichiometric amounts of distilled lutidine or 99% pure Et<sub>3</sub>N (Aldrich) were added to the solutions before the addition of reductant. For the first experiment, 1 ml of a solution made by diluting 54.4 mg of lutidine to

10 ml in acetone ( $5.08 \times 10^{-5}$  mol/ ml) was added to the reaction mixtures. On the second occasion, the lutidine was dried by passage over a small column of activated alumina before 54.0 mg of it was diluted to 10 ml in acetone ( $5.04 \times 10^{-5}$  mol/ ml). For the experiments with  $\text{Et}_3\text{N}$ , 28.0 mg were dissolved in 10 ml of acetone giving a  $2.27 \times 10^{-5}$  mol/ ml solution. Again, 1 ml aliquots were added to the reactions such that, for these experiments, the stoichiometry was 1 mole of base per 2 mole of iron or other metal ion.

The effect of the presence of a radical trap in the reaction mixtures was examined by adding 2,6-di(*tert*-butyl)-4-methylphenol (BHT) to the systems. Crystalline BHT was weighed out and added to the iron solutions before the addition of reductant and exposure to oxygen. Unfortunately, the BHT was very hygroscopic and, despite being stored under vacuum overnight, was clearly still wet when transferred into the inert atmosphere box.

The determination of  $k_{\text{H}}/k_{\text{D}}$  was carried by direct competition of  $\text{C}_6\text{H}_{12}$  and  $\text{C}_6\text{D}_{12}$ . For these experiments, 2.0 ml of cyclohexane and 2.0 ml of perdeuteriocyclohexane were added to the system instead of 5 ml of cyclohexane. The cyclohexanols derived from the two substrates could be separated nearly completely on the FFAP column. Integrals generated from the GC traces were used to approximate the amount of each product which had formed in a given period of time.

For systems containing **3**, a purple precipitate formed within several minutes of the addition of AA under  $\text{N}_2$ . When  $(\text{Et}_4\text{N})[\text{FeCl}_4]$  was the catalyst, no darkening was apparent in the solution until after it was exposed to air, at which time a small amount of the purple precipitate could be observed to form. Ferrous chloride was essentially insoluble in the acetone/cyclohexane mixture, but on exposure to air, a purple suspension formed and faded to a pale green color within 2 hr. The addition of AA to solutions of  $\text{FeCl}_3$ , appeared to reduce the iron, causing the solution to become more pale. On the addition of air, however, there was no change in the color of the solution. If **2** was left in the presence of AA under  $\text{N}_2$  for several hours the solution became essentially indistinguishable from one containing **3**. When exposed to air, however, an orange color was regenerated in the solution.

When TMRA, which is soluble in acetone, was added to **3** under  $N_2$ , a purple solution formed. When this reductant was added to solutions of  $(Et_4N)[FeCl_4]$ , they turned a deeper shade of yellow but no darkening was apparent when air was introduced into the system. Interestingly, TMRA caused  $FeCl_2$  to dissolve in acetone, forming a yellow solution which turned deep blue on exposure to air. With  $FeCl_3$  and **2**, TMRA had essentially the same effect as AA. Solutions of **2**, again, faded back to orange with time in air or under  $N_2$ .

When the reactions were run in the presence of base, some differences in were observed. Reaction mixtures containing **3** and either AA or TMRA were affected slightly, if at all, by the presence of base. In both cases, more of the purple species may have formed but the difference in color was not very distinct. When base was added to solutions of  $(Et_4N)[FeCl_4]$ , however, they darkened perceptively and the addition of reductant led to formation of a purple solid or purple solution. In these reactions, there appeared to be less purple species formed, such that less purple solid accumulated on the addition of AA and the purple solution resulting from the addition of TMRA was less intense in color than when **3** was the catalyst present.

Controls with a number of simple metal chlorides were run using this protocol. Nickelous chloride was completely insoluble in the acetone/ cyclohexane solution. No reaction between the compound and AA or TMRA was ever apparent. Stannous chloride was not soluble in the reaction mixture, although it did appear to become a fine suspension. No color developed at any point during the reactions. The pale pink manganous chloride was also insoluble and showed little change over the course of reaction with either reductant. Cobaltous chloride was very soluble in acetone forming a bright blue solution. Once again, no reaction with the reductants was apparent. Cupric chloride, by contrast, appeared to be efficiently reduced by AA or TMRA. The green-yellow solutions became colorless or very pale yellow on addition of the reductants and did not develop any color on exposure to air. In the case of AA, the reductant slowly dissolved into the solution during the course of the reaction. When TMRA was the reductant, the addition of cyclohexane caused a small amount

of pale yellow solid to settle out of the solution before the mixture was exposed to air.

Manganous and cupric chloride were also tested in the presence of stoichiometric amounts of base ( $\text{NEt}_3$ , see above) and TMRA. With base and TMRA in the solution, the manganous chloride appeared to dissolve slightly forming a pale yellow solution. During the course of the reaction, the pink solid was transformed into a pale yellow solid. Addition of base to the solution containing cupric chloride caused it to turn deep red-orange in color. When TMRA was added, the solution paled, turning blue briefly, then colorless. A small amount of fine yellow solid had formed before the mixture was exposed to air and continued to accumulate throughout the course of the reaction.

## Results and Discussion

**Reactions with 1 and 2.** The first dinuclear compound examined for potential catalytic activity for cyclohexane oxidation under dioxygen was the known hemerythrin compound, **1**. In a mixture of  $\text{CH}_3\text{CN}$  and cyclohexane under either a static atmosphere of  $\text{O}_2$  or a flow of  $\text{O}_2$ , this complex showed no catalytic activity. When reductants were added to the system, however, small amounts of cyclohexanol and cyclohexanone were formed. Ascorbic acid (AA) and dithionite (dt) were the first reductants employed. Both granular and powdered zinc were also tried, but, at best, only trace amounts of oxidation products were detected.<sup>31</sup> Even in the presence of the other reductants, more than ~100% oxidative yield was never achieved. Both cyclohexanol and cyclohexanone were produced in all the experiments, but the relative yield of the products was dependent on the reductant used. When ascorbic acid was the

---

<sup>31</sup> Very recently, the use of **1** in the presence of zinc and acetic acid as a catalyst for the oxidation of cyclohexane and adamantane by  $\text{O}_2$  has been communicated. Kitajima, N.; Fukui, H.; Yoshihiko, M. *J. Chem. Soc., Chem. Commun.* **1988**, 485-486. These reactions are run in dichloromethane. Whether the lack of reactivity for this compound reported herein is a result of solvent effect or the lack of acetic acid in the system has not been determined.

reductant, nearly twice as much alcohol as ketone was formed. When dithionite was used, the opposite distribution was observed.

One reason the oxidative yields were low might be the instability of the catalyst toward reduction by either of the reducing agents. Electrochemical reduction of **1** is irreversible.<sup>8b</sup> Also, the color of the solutions changed during the reactions, suggesting that decomposition was occurring. For this reason, the complex **2** was next examined for activity. The methylated triazacyclononane ligand appears to lend more structural stability to the  $\{\text{Fe}_2\text{O}(\text{O}_2\text{CCH}_3)_2\}^{2+}$  core such that a semi-stable one electron reduction product of **2** could be isolated.<sup>32</sup> It was thought that the greater stability of this compound toward reduction might make it catalytically more active.

This may, in fact, be true. Reactions with **2** and ascorbic acid always produced more oxidation products than those with **1**. When a solution of **2** with 20 equivalents of AA in a 2/1 cyclohexane/ $\text{CH}_3\text{CN}$  solution was refluxed under an atmosphere of  $\text{O}_2$  for ~18 hr, an oxidative yield of 235% was achieved with a 7/1 ratio of cyclohexanol to cyclohexanone. The reaction mixture, however, had lost the orange color characteristic of **2** within the first 4 hr and had developed a lavender hue (see below). The effects of changing the solvent to  $\text{CH}_2\text{Cl}_2$  and of adding water,  $\text{Et}_3\text{N}$ , pyridine, or imidazole to the solution were examined. No activity was detected when  $\text{CH}_2\text{Cl}_2$  was the solvent, perhaps because of the low solubility of **2** in this solvent and the complete insolubility of AA. When the solvent was 20% water in  $\text{CH}_3\text{CN}$ , the addition of AA caused the solution to fade almost immediately and led to a very low oxidative yield. The presence of base affected the ratio of products, increasing the amount of ketone formed, more than the oxidative yield. When an analogous system of just **2** and AA was allowed to react under atmospheric oxygen at room temperature for 5 days, similar yields to those achieved with reflux under  $\text{O}_2$  were observed and the solution retained an orange color.

---

<sup>32</sup> Hartman, J.R.; Rardin, R.L.; Chaudhuri, P.; Pohl, K.; Wieghardt, K.; Nuber, B.; Weiss, J.; Papaefthymiou, G.C.; Frankel, R.B.; Lippard, S.J. *J. Am. Chem. Soc.* **1987**, *109*, 7387-7396.



The AA, however, appeared grey by the end of the reaction. The best yield achieved for **2** and AA was 428% with a 7/1 ratio of alcohol to ketone. For this reaction, the catalyst was dissolved in 5 ml of CH<sub>3</sub>CN with an equivalent volume of substrate and a 100 fold excess of AA was added. The reaction was allowed to proceed for 126 hr under air at room temperature until nearly all the orange color had faded from the solution.

During various investigations on systems containing **2**, the AA was observed after a certain amount of reaction time to develop a lavender color. This color was particularly noticeable if the reactants were mixed under N<sub>2</sub>. On one occasion, the lavender solid was isolated from the reaction and added to a mixture of CH<sub>3</sub>CN and cyclohexane. After ~20 hr the mixture was tested for oxidation and a significant amount of products had formed. This result led to the conjecture that the reactivity in systems with **2** arises, at least in part, from the same catalytic species formed directly from **3** and AA, as discussed in a later section.

At a later date, as a result of the series of experiments to be described just below, attention was returned to this complex. The complex appeared to show significant activity with TMRA as well as AA. Also, when second and third additions of TMRA were made to systems containing **2** further oxidation occurred. The appearance of a brown color seemed to be indicative of an active solution. After several hours the brown would fade back to orange, although changes in the visible spectrum of the solution suggested that decomposition was occurring as well. A difference spectrum of the brown solution minus the original orange solution revealed a single maximum ~520 nm, similar to those seen in solutions of **3** and TMRA (see below). When **2** was tested in the presence of AA, under the conditions described in Protocol 4, the mixture containing this catalyst became lavender if left under N<sub>2</sub> for a sufficient length of time. Upon exposure to air, oxidation of cyclohexane occurred and the solution slowly faded back to orange. The majority of products had formed within ~10 hr. After ~24 hr, the oxidative yield was 194% with 5/1 ratio of alcohol to ketone. At this time, the reductant was filtered out and a new portion of reductant added. After another 24 hr the yield was 325% with the same ratio of products. A peak not corresponding to either of the

cyclohexane oxidation products appeared in the GC trace even before the solution was exposed to air. This peak had not been observed in initial reactions with this catalyst because the compound from which it arose had been lost in the work up, probably into the aqueous phase during the extraction. The peak has a similar retention time to acetic acid and may result from loss of acetate on reaction with AA.<sup>33</sup> A similar reaction with a 10 fold excess of TMRA produced an oxidative yield of 114% in the first hour but showed very little reactivity after that period and did not begin to fade until well after the first hour. Again the third peak was present in the GC trace and a second addition of reductant produced more products. The ratio of products was ~4/1. These results were considered to be encouraging since the system appeared to be cycling through an active species.

Efforts were made to study the purple black solution which resulted from the addition of 10 fold excess TMRA to **2** under N<sub>2</sub> by NMR spectroscopy but the spectra collected could not be interpreted. The <sup>1</sup>H NMR spectrum appeared to contain both **2** and another paramagnetic species while none of the resonances in the <sup>13</sup>C spectrum except those of TMRA could be assigned. Since the system based on **3** and these reductants appeared to be cleaner and more catalytic (see below), no further experimentation was carried out with this catalyst.

**Reactions comparing the activity of 1, 2, 3 and other iron compounds.** In an attempt to determine if dinuclear oxo-bridged species were better catalysts than mononuclear species, a series of reactions with a number of iron compound was carried out. Great care was taken to treat each reaction in an identical manner and acetone was chosen as the solvent. Each of eight different compounds including **1**, **2**, and **3** was tested for activity toward the oxidation of cyclohexane by O<sub>2</sub> in the presence of six different reductants. The results of this series are presented in Table I. From this table it is clear that the question of reactivity is more than just one of nuclearity or of the presence of an oxo bridge. For dtt and me, (Et<sub>4</sub>N)[FeCl<sub>4</sub>] and **3**

---

<sup>33</sup> This peak also appeared in traces of the products from reactions catalyzed by **1**, as noted in Table I. Since **1** also contains bridging acetates, this fact supports the proposal that the peak may arise from acetic acid.

Table I

ACTIVITY AND PRODUCT SPECIFICITY OF IRON COMPOUNDS IN THE PRESENCE OF VARIOUS REDUCTANTS  
FOR THE OXIDATION OF CYCLOHEXANONE BY AIR  
Values given are % oxidative yield and specificity as the ratio of cyclohexanol/ cyclohexanone

Catalyst	Reductants						
	AA	RA	NaA	dt <sup>t</sup> *	me*	dt	
1	15 2.2/1 <sup>a</sup>	57 2.1/1 <sup>a</sup>	<10 --a	47 1.9/1 <sup>a</sup>	nd	<10 <sup>a</sup>	
2	173 3.6/1 <sup>a</sup>	127 4.2/1 <sup>a</sup>	<10 --a	35 14.7/1 <sup>a</sup>	nd	<10 <sup>a</sup>	
3	265 30/1	309 20/1	82 14/1	374 5.8/1	216 3.7/1	<10	
(Et <sub>4</sub> N)[FeCl <sub>4</sub> ]	43 36/1	48 35/1	80 8.5/1	372 10/1	303 7/1	<10	
FeSO <sub>4</sub> ·7H <sub>2</sub> O	<10 --	73 1.8/1	<10 --	21 8/1 <sup>a</sup>	<10 2/1	<10	
[Fe(HBpz <sub>3</sub> )]Cl	20 -- <sup>b</sup>	22 -- <sup>b</sup>	<10 --	236 3.6/1 <sup>a</sup>	34 4/1	<10	
[Fe <sub>2</sub> O(bipy) <sub>2</sub> Cl <sub>2</sub> ]Cl <sub>2</sub>	26 11/1	44 9/1	<10 --	<10 --	nd	<10	
Fe <sub>11</sub> <sup>c</sup>	<10 --	231 2.1/1	<2 --	52 3.1/1 <sup>b</sup>	nd	<10	
Reaction time, hrs	~40	~20	~40	2(O <sub>2</sub> )	1.5(O <sub>2</sub> )	~45	

All reactions were run as described under Protocol 2 in the Experimental Section except in the columns marked with an asterick which were run according to Protocol 3.

nd = no data

<sup>a</sup> GC trace showed significant or major peak other than cyclohexanol or cyclohexanone.

<sup>b</sup> The total [Fe] in these solutions was only half that in the other reactions.

<sup>c</sup> [Fe<sub>11</sub>O(OH)<sub>6</sub>(O<sub>2</sub>CC<sub>6</sub>H<sub>5</sub>)<sub>15</sub>] The concentrations of these solutions were 5 X 10<sup>-5</sup> in Fe and yields are reported per 2 Fe.

appear to be equally good catalysts. For AA and TMRA, however, only **2** and **3** appear to be significantly active. Neither the other dinuclear oxo-bridged species or the mononuclear species show much reactivity. It is interesting that the undecanuclear complex appeared somewhat active in the presence of TMRA but not at all with AA. In both cases, addition of reductant caused the formation of purple species. Unfortunately, however, the TMRA used was not as pure as samples used later. Also, each experiment was only carried out once, so it is possible that either of the results may be inaccurate. The reaction mixture containing **1** also turned blue when TMRA was added but showed no activity. Dithionite was apparently unreactive under the conditions of the experiments. In general, these results caused a return of attention to **2** as described above and encouraged further investigation of systems based on **3** and AA or TMRA.

**Reactions with **3** and dtt.** When **3** was discovered to be an active catalyst in the presence of AA (see below), its reactivity with other reductants was also investigated. The addition of dtt to reaction mixtures containing **3** in CH<sub>3</sub>CN or acetone led to the production of a deep blue color which faded rapidly. Since dtt, unlike AA or dt, was soluble in the solvents used, no solids were present in the mixture at the beginning of the reaction. As the solution faded, however, a brown precipitate formed. At the end of the reaction, the solution was yellow or pale green with a considerable quantity of brown solid having accumulated. The progression of colors is very similar to that reported for the Ullrich system. This similarity is not surprising since in that system, several equivalents of base were added to the ferrous ion before it was allowed to react with mercaptobenzoic acid and O<sub>2</sub>. A visible spectrum of the blue color, generated by addition of 50 equivalents of dtt to a CH<sub>3</sub>CN solution of **3**, is shown in Figure 1. The color faded rapidly, but the intensity could be regenerated by bubbling O<sub>2</sub> through the solution. For the solution described, full intensity could be restored only once and the spectrum of the regenerated color was slightly different from that of the original (Figure 1).

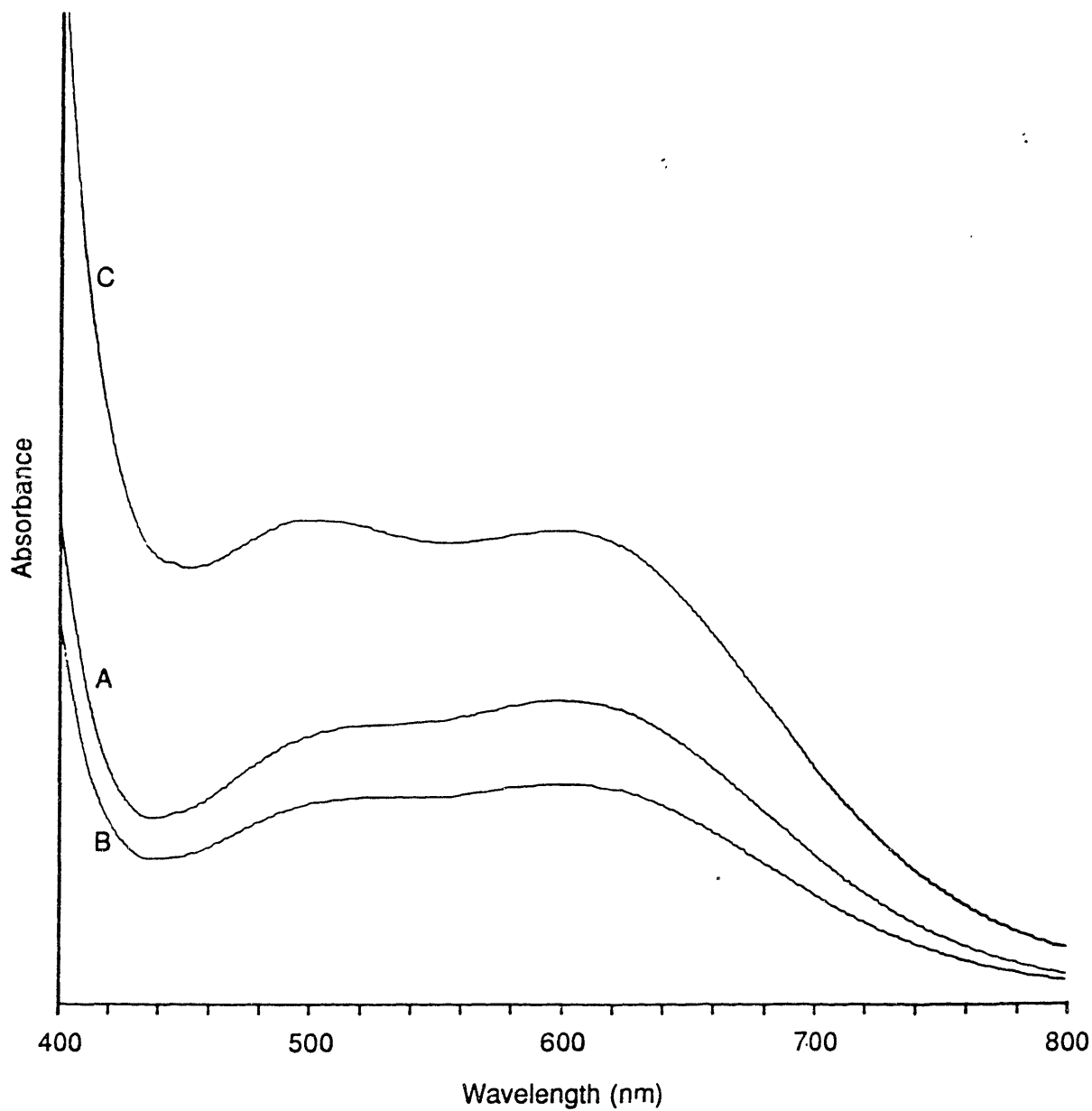


Figure 1. Visible spectra of a 50:1 mixture of dithiothreitol and 3 in CH<sub>3</sub>CN. A) Initial spectrum. B) Spectrum recorded after 10 min. C) Spectrum recorded after bubbling O<sub>2</sub> through the solution.

The addition of dtt to solutions of  $\text{FeCl}_3 \cdot 6\text{H}_2\text{O}$  led to a slight darkening of the solution but no sustained blue color was observed.

Systems with **3** and varying amounts of dtt were capable of oxidizing cyclohexane to cyclohexanol and cyclohexanone. As was not surprising considering the experiment described above, initial oxidation runs clearly showed that more products were formed under pure  $\text{O}_2$  than under air. Under  $\text{N}_2$ , the blue color formed and faded but no substrate oxidation occurred. After this dependence was established, all reactions were run as described in Protocol 3. Greater yields were also achieved in acetone as compared to acetonitrile. The results from reactions of **3** with dtt were reasonably reproducible, always gave higher yields than the mononuclear control,  $\text{FeCl}_3 \cdot 6\text{H}_2\text{O}$ , and the system responded to changes in the catalyst to reductant ratio in a systematic manner (Table II).

In an attempt to see if the  $\{\text{Fe}_2\text{O}\}^{4+}$  moiety was important in the reaction or if its role were equivalent to that of ferric ion and an endogenous base, stoichiometric amounts of freshly distilled lutidine were added to solutions of dtt before they were added to systems containing  $\text{FeCl}_3 \cdot 6\text{H}_2\text{O}$  or **3**. The addition of the base to the  $\text{FeCl}_3 \cdot 6\text{H}_2\text{O}$  system led to the production of almost the same catalytic yield as a system containing **3** and no base. Due to the amount of  $\text{H}_2\text{O}$  in the solvent, though, no conclusions could be drawn from this result. The base may simply have formed  $\text{OH}^-$  which subsequently reacted with the iron to give  $\{\text{Fe}_2\text{O}\}$  species. The addition of base to a system containing **1** raised the yield by a factor of 1.5 to ~1200% (Table II).

The ability of these systems to oxidize cyclohexanol to cyclohexanone was tested and found to be negligible for either **1** or  $\text{FeCl}_3 \cdot 6\text{H}_2\text{O}$ . In both cases, an unidentified product appeared in the GC trace during the reaction, but very little ketone formed. Octane was also tried as a substrate for this system and a wide variety of primary, secondary and tertiary products, both alcohols and ketones, were formed but in very low yield.

The results of the series of experiments presented in Table I turned the focus away from systems using dtt or mercaptoethanol since  $(\text{Et}_4\text{N})[\text{FeCl}_4]$  appeared to be as good a catalyst as

Table II

CATALYTIC ACTIVITY OF (Et<sub>4</sub>N)<sub>2</sub>[Fe<sub>2</sub>OCl<sub>6</sub>] AND FeCl<sub>3</sub>·6H<sub>2</sub>O IN THE PRESENCE OF DITHIOETHITOL FOR THE OXIDATION OF CYCLOHEXANE BY DIOXYGEN

Catalyst	(Et <sub>4</sub> N) <sub>2</sub> [Fe <sub>2</sub> OCl <sub>6</sub> ]						FeCl <sub>3</sub> ·6H <sub>2</sub> O			
# of runs	2	1	1	1	5	1	1	1	1	1
Ratio cat/red	1/11	1/20	1/25	1/50	1/100	1/100	2/100	2/100	2/100	2/100
Other	none	none	none	none	none	base	none	none	base	base
-one/-ol	1/5.2	1/5.8	1/7.4	1/8.5	~1/11	1/7.7	1/3.3	1/5.8	1/11.5	1/11.5
% yield	252	374	529	778	862†	1200	60*	132*	700*	700*

Reaction conditions described in Experimental Section under Protocol 3.

\* Yield based on 2 Fe per oxidative cycle

† Range of yields 812 to 908 % for this procedure

**3** in these systems. This result was checked in separate experiments. Unlike  $\text{FeCl}_3 \cdot 6\text{H}_2\text{O}$ ,  $(\text{Et}_4\text{N})[\text{FeCl}_4]$  solutions develop a pale blue color on the addition of dtt. The color is much less intense than in solutions containing **1**, but does not seem to fade as quickly and no brown precipitate forms in these solutions. It is possible that the same catalytic species is formed in both systems only to a much smaller extent in the mononuclear case, and that the more dilute catalytic species is less likely to react to give the brown precipitate. This hypothesis has not been tested.

**Reactions with 3 and AA or TMRA.** Initially, reactions with  $\text{FeCl}_3 \cdot 6\text{H}_2\text{O}$  and **3** were run in acetonitrile as controls against reactions catalyzed by **1** and **2**. While  $\text{FeCl}_3 \cdot 6\text{H}_2\text{O}$  showed some activity in the presence of AA (this is essentially the Udenfriend system), **3** gave oxidation yields of the same order of magnitude as **2** and with greater selectivity for production of alcohol. Reactions with **2** typically gave cyclohexanol/ cyclohexanone ratios of  $\sim 5/1$ , whereas for **3** in acetonitrile, ratios  $\sim 25/1$  were achieved. Unlike solutions containing  $\text{FeCl}_3 \cdot 6\text{H}_2\text{O}$ , solutions with **3** did not fade on addition of AA but darkened to a brown color which changed to lavender. Careful observation of the addition of a 10 fold excess of AA to a solution of **2** in  $\text{CH}_3\text{CN}$  purged with  $\text{N}_2$ , revealed that the solution appears momentarily to be lavender but then a flocculent, deep purple precipitate forms leaving the solution very pale yellow-green. At the same time, the bulk of the solid AA develops a lavender hue, assumed to result from a coating of the purple compound on the white solid. When the solids were filtered out of the solution, they could be dissolved in MeOH to give a purple solution with a  $\lambda_{\text{max}}$  of  $\sim 520$  nm which faded extremely quickly in air. A purple solution, however, could not be generated by adding excess AA to **3** in MeOH. The solution simply became colorless. If the flocculent solid were collected and dried and left open to air, it gradually became grey-brown and no longer dissolved to give a purple solution.

A number of experiments were carried out with acetonitrile as the solvent and ambient air as the oxidant. Unfortunately, these experiments were plagued by a lack of consistent



reproducibility. Among these experiments were ones which attempted to explore the effect of base on systems containing either  $\text{FeCl}_3 \cdot 6\text{H}_2\text{O}$  or **3**. When stoichiometric amounts of butylamine were added to solutions of  $\text{FeCl}_3 \cdot 6\text{H}_2\text{O}$  before the addition of AA, the resulting reaction mixture gave yields not unlike those of **3** with no base present. The lavender color, however, was not observed in these reactions. Instead, addition of AA to the mixture caused the formation of a reddish brown solid. When this base was added to solutions of **3** either in great excess or in stoichiometric amounts the red-brown solid also formed on reaction with AA. The addition of small quantities of base had little effect on the oxidative yield of these systems, but excess base led to the production of much greater amounts of ketone.

Similarly, the effect of using ascorbate instead of ascorbic acid in these systems was examined. Interestingly, a grey or lavender solid was produced when the anionic reductant was added to reaction mixtures containing  $\text{FeCl}_3 \cdot 6\text{H}_2\text{O}$ . The resulting yields and product distributions were better than when AA was used, but not as high as with the normal system based on **3**. When ascorbate was used with **3**, however, no lavender color was produced and yields were lower than usual.

Attempts were also made to determine the affect on the reaction of the concentration of  $\text{O}_2$ , the amount of reductant present, the solvent and the temperature. In these experiments, the lack of reproducibility was particularly disturbing; occasionally no reaction would occur. Nonetheless, several factors were apparent. Under pure  $\text{O}_2$ , the lavender solid quickly faded to a pale green color and the amount of oxidation products formed was significantly reduced. As would be expected, the presence of more reductant led to the formation of more products. Increasing the amount of reductant 10-fold, however, did not increase the product formation 10 fold. Only a ~2 fold increase was observed, but the same reaction time was used in both cases and it is possible that the system with more reductant would have achieved a higher yield given a greater length of time. Reactions run with acetone as solvent consistently gave higher yields than reactions run simultaneously with acetonitrile as solvent. Furthermore, acetone systems showed almost twice the product specificity, giving cyclohexanol to cyclohexanone ratios of

nearly 40/1. The affect of temperature was the most difficult to interpret. Some of the inconsistency may have resulted from the lower concentration of air in the solvent at higher temperature, a factor which was not considered at the time. The best yields for the system in either acetonitrile or acetone were achieved when the reaction mixture was heated to near reflux. At room temperature, in acetonitrile, oxidative yields of ~150% with product ratios of ~25/1 were achieved, under reflux a yield of 585% was observed with a ratio of 32/1. For acetone, yields of ~450% with a ~35/1 product distribution could be achieved at room temperature and nearly 950% with a 40/1 ratio was observed at higher temperatures. All these values are for 100 fold excess reductant and reaction times of 40-75 hrs.

In order to allow for more control over the system, the procedure described in Protocol 4 was developed. The purple precipitate formed in solutions of **3** on addition of AA under N<sub>2</sub>. No oxidation products were observed in the solution until the flask was exposed to dry, compressed air, when, within 15 min, significant amounts of oxidation products accumulated. While some variability in reaction rates still occurred, in general, for systems containing 2.5 X 10<sup>-5</sup> mol **3** and ~5 X 10<sup>-4</sup> mol AA, ~3.8 mol cyclohexanol per mol **3** formed in 48 hr. Only 0.1 mol cyclohexanone was produced in the same time period.<sup>34</sup> The yield on the reductant was ~20%. In Figure 2A, a graph of product formation versus time for this reaction is displayed. After 48 hr the rate of reaction approaches zero, presumably as a result of complete consumption of the supply of reductant. Direct oxidation of AA by O<sub>2</sub> is catalyzed by iron salts<sup>35</sup> and this reaction is probably occurring in competition with productive oxidation. If another 20 equivalents of AA was added to the reaction mixture after 48 hr, however, the rate increased to produce another 70-75% of the yield in the next 48 hr with only slight loss of product specificity (Figure 2A).

---

<sup>34</sup> Neither cyclohexanol or cyclohexanone appeared to react appreciably under the reaction conditions even at much higher concentrations than produced in these experiments. Cyclohexanol may be oxidized at a very low rate to cyclohexanone, but this reaction is probably not the source of cyclohexanone formed in the oxidation reactions.

<sup>35</sup> Martell, A.E.; *Adv. Chem. Ser.* **1982**, *200*, 153-178.

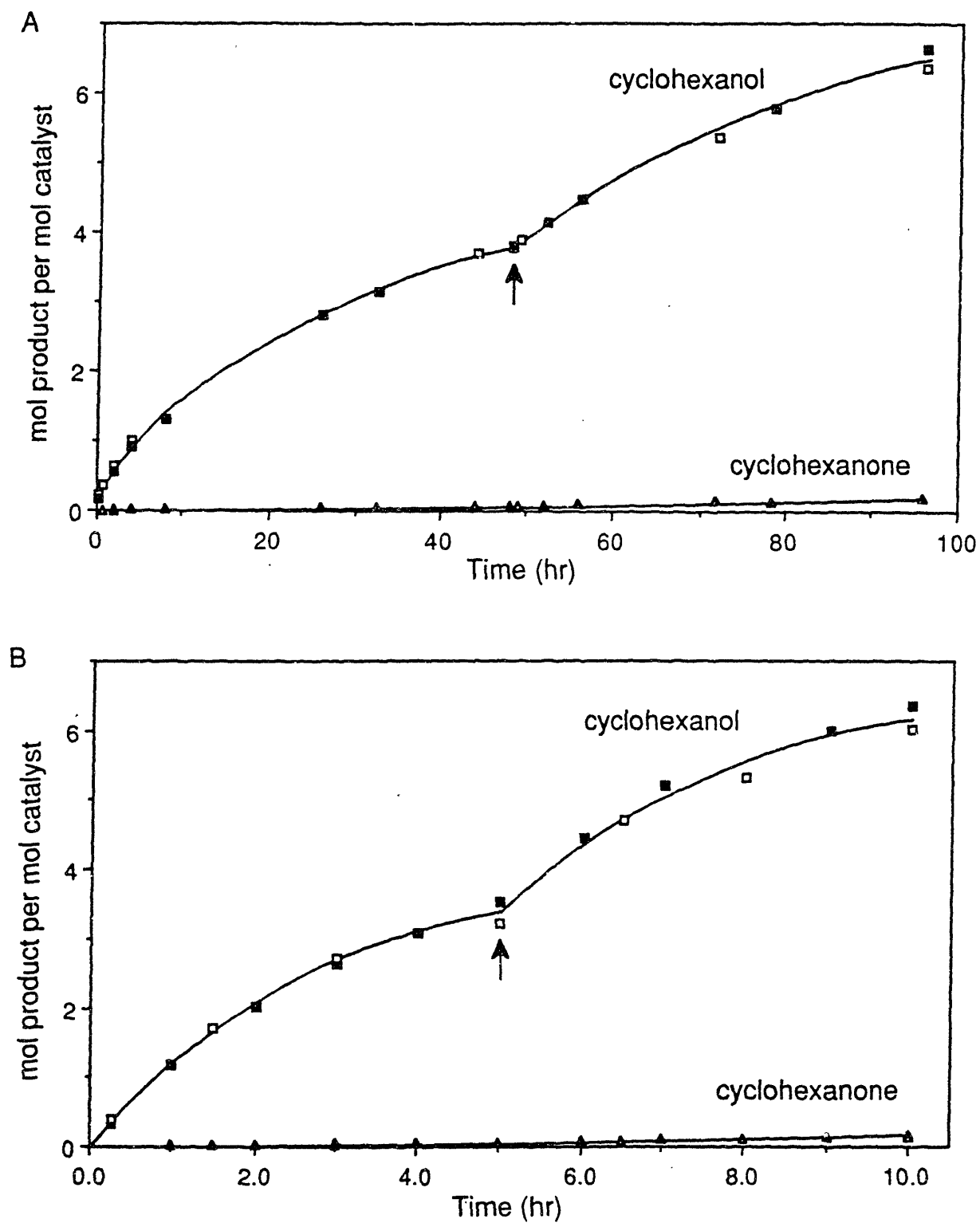
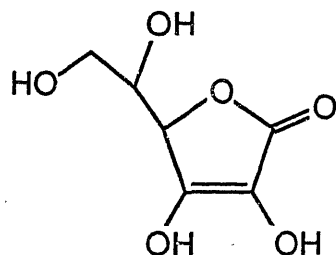
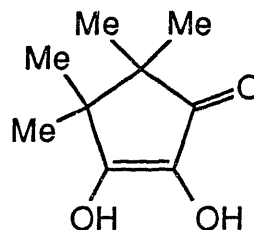


Figure 2. Rate of formation of cyclohexanol and cyclohexanone for 3 in the presence of A) AA and B) TMRA. Open and closed symbols denote duplicate runs. The arrow marks the addition of a second 20 equivalents of reductant

When TMRA became available in sufficient quantities, this analog of AA was also tested for reactivity in the system. TMRA provides the advantage of greater solubility in



Ascorbic Acid



Tetramethyl Reductic Acid

organic solvents but the disadvantage of more complicated oxidation chemistry.<sup>36</sup> Its primary two electron product is the triketone, analogous to AA, but ring opened products can form upon further oxidation. When TMRA was added to reaction mixtures containing **3**, a purple colored solution developed. This solution was capable of the same type of chemistry as the heterogeneous mixture described above. As can be seen in Figure 2B, however, its rate of reaction is much more rapid than that of systems containing **3** and AA. In 4-5 hours, the TMRA system can produce around ~3.5 mol of cyclohexanol with only 1/50th that amount of cyclohexanone. Again, the addition of more reductant leads to the formation of more products, about 75% of the yield of the first addition. On one occasion, a third 20 equivalents of TMRA was added to a reaction mixture. The final yield was 9.6 mol cyclohexanol and 0.35 mol cyclohexanone (~16% yield on the reductant).

**Controls.** Since **3** can be viewed as a simple iron chloride,  $(\text{Et}_4\text{N})[\text{FeCl}_4]$ ,  $\text{FeCl}_3(\text{anhydrous})$  and  $\text{FeCl}_2(\text{anhydrous})$  were tested for activity under the same conditions. The activity of **3** versus that of  $(\text{Et}_4\text{N})[\text{FeCl}_4]$  and  $\text{FeCl}_2(\text{anhydrous})$  for the production of cyclohexanol is shown in Figure 3. When AA is the reductant, **3** is about 4 times as active as either of the mononuclear catalysts. With TMRA, it is 10 to 12 times as active. When AA is added to solutions containing  $(\text{Et}_4\text{N})[\text{FeCl}_4]$  under  $\text{N}_2$  the solution appears to pale slightly.

<sup>36</sup> Inbar, S.; Ehret, A.; Norland, K. *Abstracts of Papers*, National Meeting of the Society of Photographic Sciences, Minneapolis, MN, 1987.

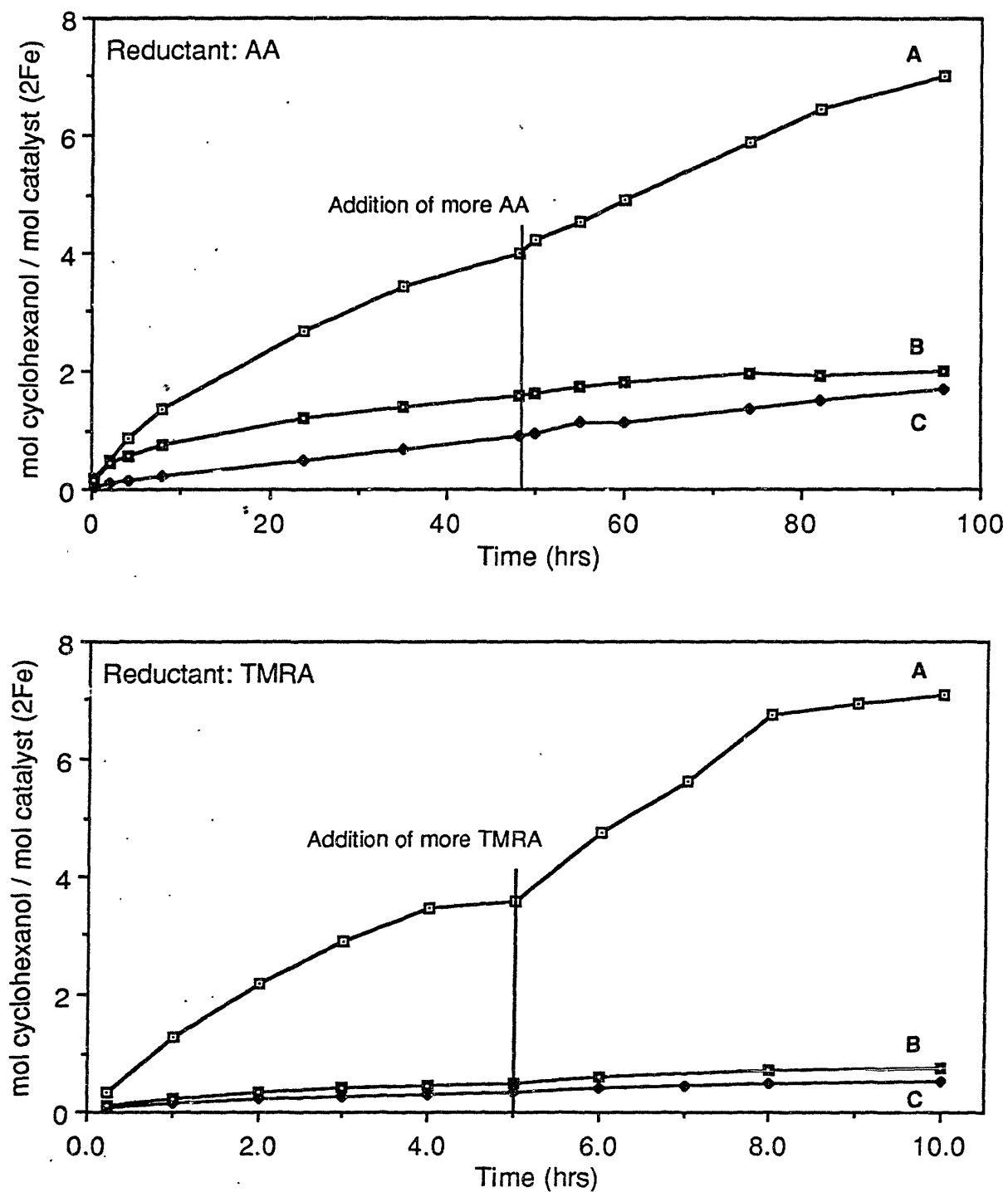


Figure 3. Rate of formation of cyclohexanol for 3 (A) versus  $\text{FeCl}_2(\text{anhydrous})$  (B) and  $(\text{Et}_4\text{N})[\text{FeCl}_4]$  (C). The upper graph represents the results with AA as the reductant and the lower graph the results with TMRA as the reductant.

Upon exposure to air, however, a small amount of purple precipitate forms. This catalyst demonstrates similar specificity to **3**, but with much lower turnover. It would appear as though a small amount of the same active species were forming in these solutions as forms from **3**. With TMRA no lavender color is ever apparent in solution and the yields are much lower.

Reactions with  $\text{FeCl}_3$ (anhydrous) and  $\text{FeCl}_2$ (anhydrous) are characterized by a very different type of reactivity. The yellow color of solutions of  $\text{FeCl}_3$  fade perceptively on addition of AA and remain yellow throughout the reaction. The excess reductant which usually remains as a solid in other reaction mixtures, slowly disappears over the course of reactions with  $\text{FeCl}_3$ . While this catalyst does show some activity toward oxidation of cyclohexane, these products do not represent the major peaks in GC traces from these solutions. Even before reactions with this catalyst are exposed to air, considerable reactivity occurs in the solution. Although all of the products have not been identified, the major one would appear to be isopropanol from the reduction of acetone. The presence of ferric chloride would appear to activate AA for the reduction of acetone. When AA is replaced with TMRA the same reactivity was observed.

When the ferrous salt is employed as a catalyst, no activity is seen under  $\text{N}_2$ . The salt is only very slightly soluble in the acetone/ cyclohexane mixture and no reaction appears to occur on the addition of AA. When air is introduced into the mixture, however, products quickly build up in the solution (Figure 3). The iron salt forms a fine purple suspension which fades to pale green after several hours. At first, cyclohexane oxidation products are the major ones with about 4 times as much alcohol as ketone forming. A number of other small peaks are also apparent in the trace. After about 20 hr, however, the type of activity observed in the ferric chloride reactions predominates. The peak corresponding to isopropanol becomes the largest in the trace and the rate of formation of cyclohexane oxidation products becomes very low. The addition of a second batch of reductant has little effect on this rate (Figure 3). The addition of TMRA to mixtures with  $\text{FeCl}_2$  under  $\text{N}_2$  causes the iron compound to dissolve and

form a yellow solution. When this solution is exposed to air, it turns very dark blue, but is considerable less reactive than the mixture with AA.

One of the remarkable features of the systems based on **3** and AA or TMRA is their specificity for cyclohexane oxidation, and this feature is clearly lost when FeCl<sub>2</sub> replaces **3**. In Figure 4, GC traces developed from reaction mixtures containing **3** or FeCl<sub>2</sub> with AA or TMRA are shown. The trace from the **3**/AA system show only one major peak, that corresponding to cyclohexanol, in addition to the standard peak. Small peaks corresponding to cyclohexanone and two other unidentified products are the only other signals of significant intensity apparent in the trace. When TMRA is the solvent, cyclohexanol is still the major product but several new sharp peaks and a large broad signal also appear in the trace. The large broad signal arises from dehydrotetramethyl reductic acid, as determined by GC-MS, and the other new peaks have been tentatively identified as other TMRA oxidation products.<sup>37</sup>

The traces from the FeCl<sub>2</sub> systems are not nearly as clean. The traces were developed near the end of the oxidation experiment and isopropanol has become the major product in the system with AA. The lower specificity for alcohol over ketone is also apparent from the trace. The major peak in the trace from the reaction mixture containing TMRA appears to be one of the oxidation products of TMRA. The lower activity of the mononuclear compound with this reductant versus AA is also clear from a comparison of these traces. A comparison of the traces from the systems containing **3** to those from systems containing FeCl<sub>2</sub> support the conclusion that the nature of the catalytic activity in these two systems is distinctly different.

Other simple metal chlorides were also tested for activity in the presence of AA and TMRA. In general, none of the metals demonstrated significant activity toward the oxidation of cyclohexane. Reactions in the presence of AA were allowed to proceed for 24 hr and their yields should be compared to ~2.5 mol cyclohexanol per mol **3** (>250% yield) produced under similar conditions. With TMRA, reactions were followed for 5 hr during which time ~3.5 mol

---

<sup>37</sup> When solid TMRA which had decomposed in air over time was dissolved in acetone, a GC trace of the resulting solution exhibited these sharp peaks.

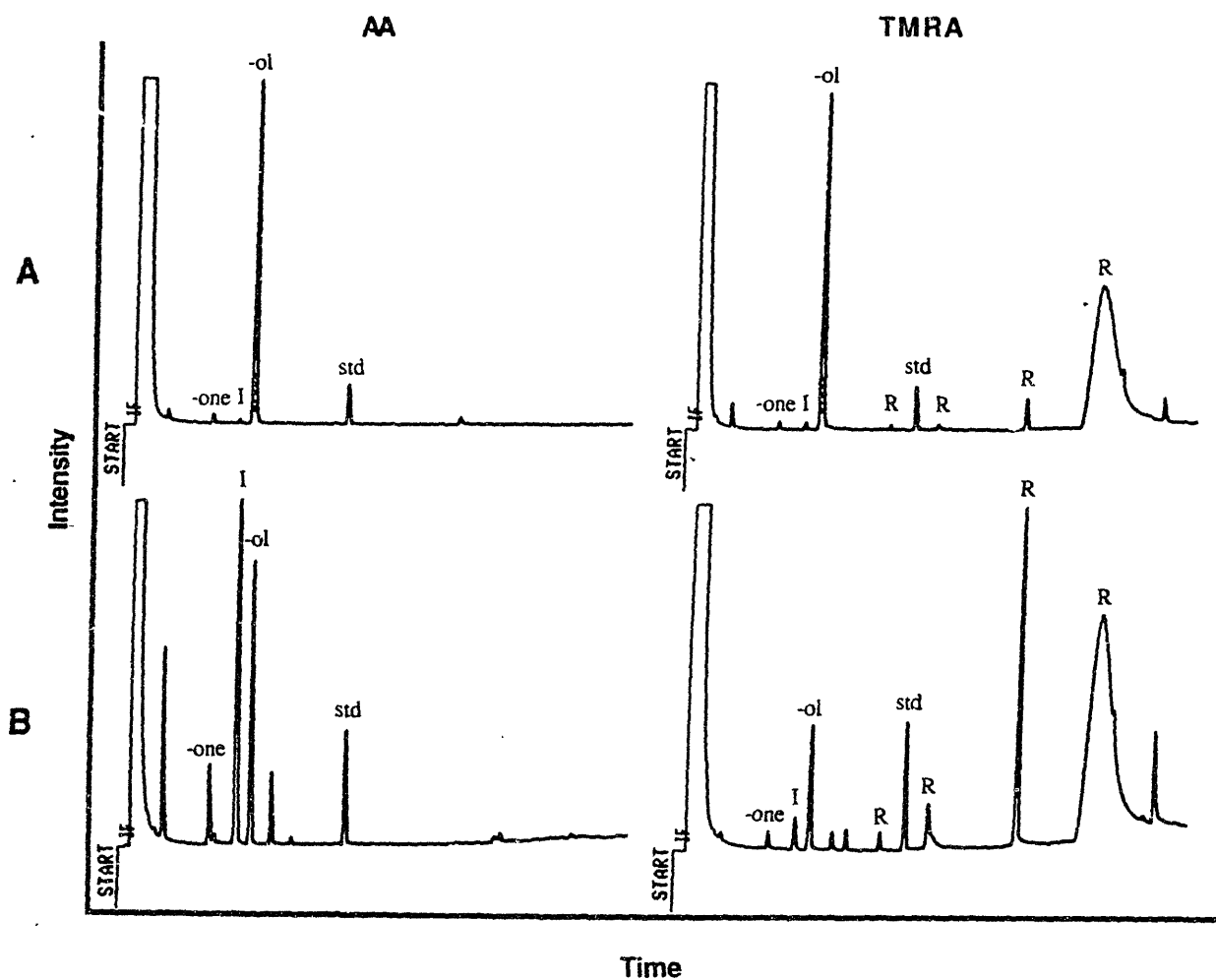


Figure 4. GC traces recorded of samples from cyclohexane oxidation reaction mixtures containing A) 3 or B)  $\text{FeCl}_2$ (anhydrous) in acetone. The samples were collected near the end of the experiments, after the second addition of reductant. The peaks are labelled as follows: -ol, cyclohexanol; -one, cyclohexanone; std, standard (methylbenzoate); R, peaks from oxidized reductant; I, isopropanol. (A trace amount of isopropanol is present in the acetone as an impurity.)



cyclohexanol was produced per mol 3 (>350% yield). When AA was the reductant, nickelous chloride appeared completely unreactive. Similarly, cobaltous chloride produced less than 1% yield of cyclohexanol. Stannous and manganous chloride demonstrated some reactivity in the system but in both cases a number of peaks appeared in the GC traces and no more than 0.20 mol total cyclohexane oxidation products per mol metal ion were formed in 24 hr. Since dehydroTMRA is soluble, the results from reactions with TMRA also showed whether or not the metal ion catalyzed the oxidation of the reductant. With nickel, very little TMRA oxidation occurred and, at best, a trace amount of cyclohexane oxidation products were detected. Likewise, with cobalt, essentially no oxidation of TMRA was observed and less than 2% oxidation of cyclohexane. Stannous chloride demonstrated similar activity with TMRA as with AA, < 0.10 mol products per mol Sn(II), but did not appear to catalyze the oxidation of TMRA. Manganous ion appeared to catalyze the oxidation of TMRA, though not to the extent observed for iron and copper. Several products were detected by GC, but less than 10% oxidation of cyclohexane occurred. Addition of base to the system changed the ratio of TMRA oxidation products and may have enhanced the activity of the metal ion slightly. Not surprisingly, TMRA was rapidly oxidized in the systems containing copper ions. Attack on acetone was observed, but only a trace of cyclohexanol was formed. The addition of base changed the ratio of products from acetone attack, but did not affect the oxidation of cyclohexanol appreciably. Thus, the reactivity observed with AA or TMRA appears to be specific for iron. Even copper, which is known to catalyze the oxidation of AA even more efficiently than iron<sup>34</sup>, showed essentially no activity in this system.

**Factors affecting reactivity of system.** Attempts have been made to identify factors which affect the reactivity of the system. In one such experiment,  $[\text{Fe}_2\text{OCl}_6]^{2-}$  was synthesized with the  $(\text{Bz}_3\text{PhP})^+$  cation instead of  $(\text{Et}_4\text{N})^+$ . This change in catalyst had no effect on product distribution and caused an increase in activity. Agitation of the reaction mixture was observed to affect the rate of reaction, but no systematic study of this factor was carried out. In the case of the AA system, agitation is required to keep the solids suspended in

the solution. Even the homogeneous system, however, is likely to be affected by the rate of agitation since this rate will control the introduction of air into the solution.

The solvent effect mentioned earlier was checked under the new protocol and a reaction run in acetonitrile was observed to have greater initial rates but to reach a plateau much earlier than a reaction run simultaneously in acetone (Figure 5). This variance may result from several factors, not the least of which may be the miscibility of cyclohexane and acetone. Also, ascorbic acid is more soluble in acetone than in acetonitrile so that more active species may form in this solution. When AA is added to **3** in acetone, the mixture develops a much darker purple color, and more purple solid appears to form, than from the same mixture in acetonitrile. The rate of oxidation of AA may vary from solvent to solvent as well, so that the reductant may be more quickly exhausted in acetonitrile. Early experiments suggested that the solvent difference held for TMRA as well, which would suggest that the solubility of AA is not an important factor. No careful study has been carried out with this reductant, however.

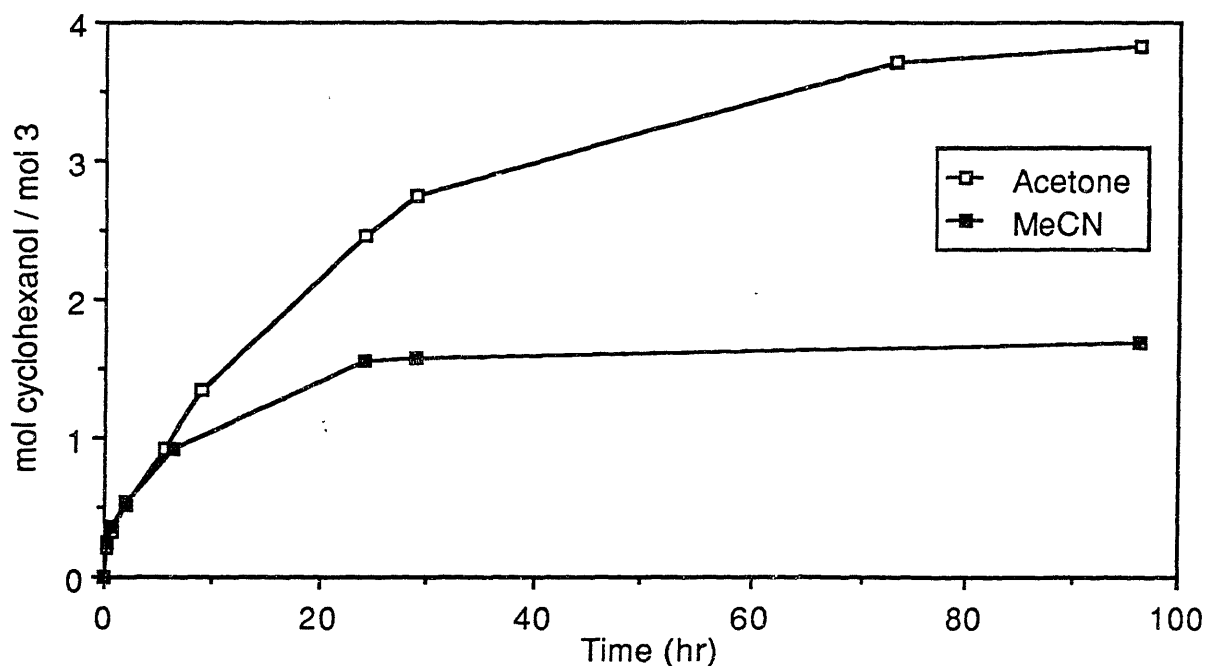


Figure 5. Effect of solvent on cyclohexanol formation catalyzed by **3** in the presence of AA.

The reactivity of the system was discovered accidentally to be inhibited by impurities in the substrate. When "general" instead of "analytical" grade cyclohexane was unintentionally used as substrate, significantly lower activity was observed. No extraneous products were detected by GC;<sup>38</sup> less oxidation simply occurred. One factor in this inhibition may have been the lowering of the actual concentration of substrate present in the system. In separate a experiment, a system with 1.0 ml ( $9.2 \times 10^{-3}$  mol) cyclohexane and 14 ml acetone was compared to one with 5.0 ml ( $4.6 \times 10^{-2}$  mol) substrate and 10 ml acetone (usual conditions), and the former produced only half as much cyclohexane as the latter in 24 hr. In this experiment, though, the change in the overall polarity of the system was not taken into account. It is also possible that some of the impurities in the lower grade cyclohexane were actual inhibitors of the catalytic species.

As expected, the concentration of the catalyst present in the system had an effect on the rate of the reaction, but surprisingly had little effect on the yield. Also surprising was that the concentration of catalyst was inversely proportional to rate of reaction. Only a non-rigorous study of this effect was carried out. Systems with 3 and AA or TMRA were run with the normal concentration of catalyst, half the concentration of catalyst and one-tenth the concentration of catalyst. The amount of reductant was also reduced proportionally so that 20 mols per mol 3 were present in each mixture. The amount of cyclohexane, however, was not varied. Therefore, the results may reflect the changes in catalyst to substrate ratio as well as overall concentration of catalyst. Representative results from these experiments are shown in Table III. The entries for early time periods show that the more dilute solutions have accumulated more cyclohexanol per mol catalyst. The overall yield of the reactions remains about 3.5-4.0 mol cyclohexanol per mol catalyst regardless of the concentration and the length of time necessary to reach this value. Thus, the yield on reductant remains essentially the same. If the major pathway for non-productive reductant oxidation is by an independent

---

<sup>38</sup> Oxidation products of lower boiling compounds might have eluted with the solvent under the thermal program employed and may not have been detected for this reason.

Table III

TIME VERSUS CYCLOHEXANOL PRODUCED AT VARIOUS CATALYST CONCENTRATIONS

t (hr)	(Et <sub>4</sub> N) <sub>2</sub> [Fe <sub>2</sub> OCl <sub>6</sub> ] / AA			(Et <sub>4</sub> N) <sub>2</sub> [Fe <sub>2</sub> OCl <sub>6</sub> ] / tmRA			
	1.7mM	0.83mM	0.17mM	t (hr)	1.7mM	0.83mM	0.17mM
0.5	0.28	0.34	0.80	0.5	0.62	1.1	2.9
6.0	1.0	1.0	2.0	2.0	1.9	3.0	3.3
24.0	1.9	2.3	3.5	4.0	2.8	3.9	3.3
48.0	2.9	3.8	3.9	8.0	3.4	4.1	--
-ol/-one:	40/1	42/1	22/1		58/1	44/1	30/1

Values for cyclohexanol given as mol product / mol catalyst

Reactions were carried out as described in Protocol 4.

reaction then it would seem peculiar that this reaction should show the same concentration dependence as the alkane oxidation reaction. If consumption of the reductant is a result of competition with the substrate for the highly oxidizing intermediate, however, such a dependence would be predicted. As the rate of the reaction increases the specificity decreases, as can be clearly seen in the results from the TMRA experiments (Table III). The effect of concentration on the reactivity of systems containing  $(\text{Et}_4\text{N})[\text{FeCl}_4]$  was examined in a similar matter and the same results were observed. As the concentration decreased, the rate increased, but the total catalytic yield remained much lower than observed for systems with **3**.

The addition of stoichiometric amounts of base was found to enhance greatly the activity of the mononuclear complex  $(\text{Et}_4\text{N})[\text{FeCl}_4]$  with either reductant while having a far less dramatic effect on that of **3**. This same general conclusion was supported by four separate experiments, although the results of each were significantly different. In the first experiment, a stoichiometric amount of recently distilled lutidine (1 mole per mole Fe) was added to solutions of **3** and  $(\text{Et}_4\text{N})[\text{FeCl}_4]$ . No apparent change resulted from the addition to the solution of **3** and the lavender precipitate developed as usual upon addition of AA. The  $(\text{Et}_4\text{N})[\text{FeCl}_4]$  solution also did not appear to change on addition of the base, but when the mixture was shaken after the addition of AA, it darkened slightly and a lavender hue was apparent on the surface of the AA. Upon exposure to air, more lavender precipitate appeared to form. Both reaction mixtures gave very similar product formation profiles (Figure 6A). The initial rate of reaction was much more rapid than normal and levelled off more rapidly at higher yield than usual. When this experiment was repeated with a slight modification several days later, different results were achieved. For the second experiment, the lutidine was passed over a short column of activated alumina in an effort to remove any water from the base. The dried base was then diluted with freshly prepared acetone and added to solutions of **3** and  $(\text{Et}_4\text{N})[\text{FeCl}_4]$  as before. While under  $\text{N}_2$ , the same color changes were observed. The reactions this time, however, while still essentially identical to each other, proceeded at a rate lower than usual (Figure 6B). Some months later, the same type of experiment was carried out

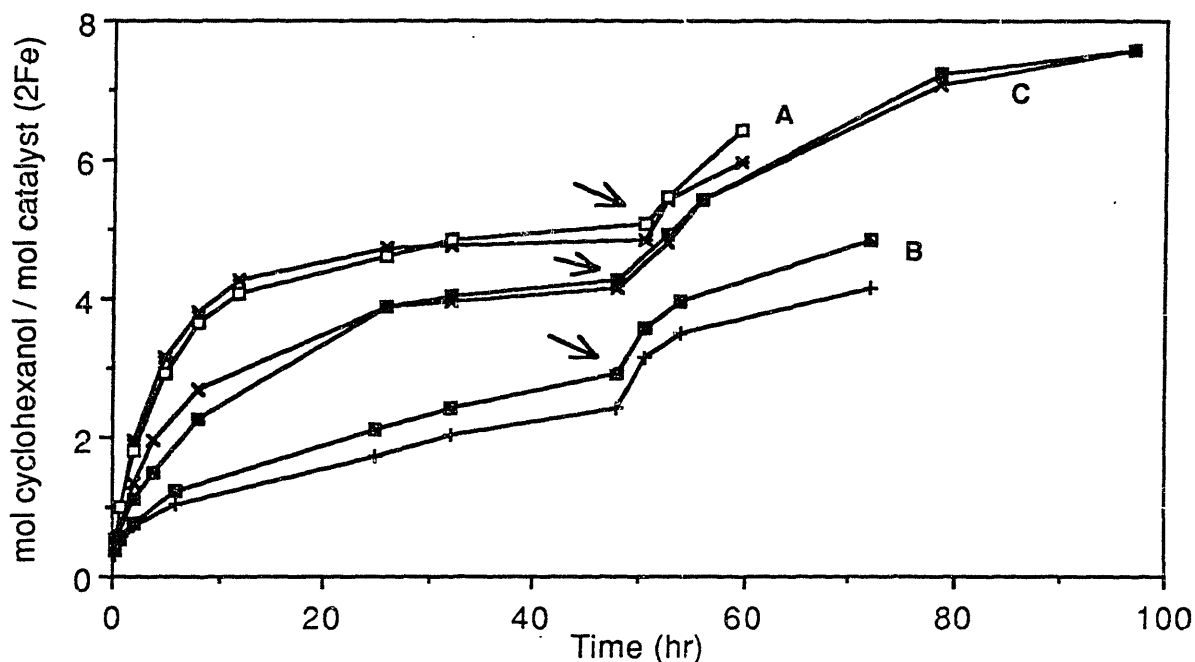


Figure 6. The effect of base on cyclohexanol formation catalyzed by **3** and  $(\text{Et}_4\text{N})[\text{FeCl}_4]$  in the presence of AA. A) Results of first experiment with lutidine. B) Results of second experiment with lutidine (dry lutidine). C) Results from experiment with  $\text{Et}_3\text{N}$ . Square symbols: **3**. Hash marks:  $(\text{Et}_4\text{N})[\text{FeCl}_4]$ . Arrows indicate addition of a second 20 equivalents of reductant.

with  $\text{Et}_3\text{N}$  both with AA and TMRA as reductants. Only half the amount of base used previously was added to the reactions for these experiments (1 mole per 2 mole Fe). With AA, the  $(\text{Et}_4\text{N})[\text{FeCl}_4]$  system developed purple solids while under  $\text{N}_2$ , and with TMRA a purple solution was formed. The intensity of the solution appeared less than that of the normal system with **3** run simultaneously. The results from the AA systems were nearly superimposable (Figures 6C and 7) and the rate and yields were slightly elevated but not to the extent seen in the first lutidine experiment. The effect on each catalyst can be compared in Figure 7. With TMRA as the reductant, the  $(\text{Et}_4\text{N})[\text{FeCl}_4]$  system produced slightly less than the simultaneous run with **3** and no base, and the addition of base to **3** raised the rate and yield slightly. The results of the TMRA experiment are shown in Figure 8.

These results suggest that the higher activity of the dinuclear complex may simply result from the presence of the bridging oxygen as an endogenous base. It is difficult, however, to

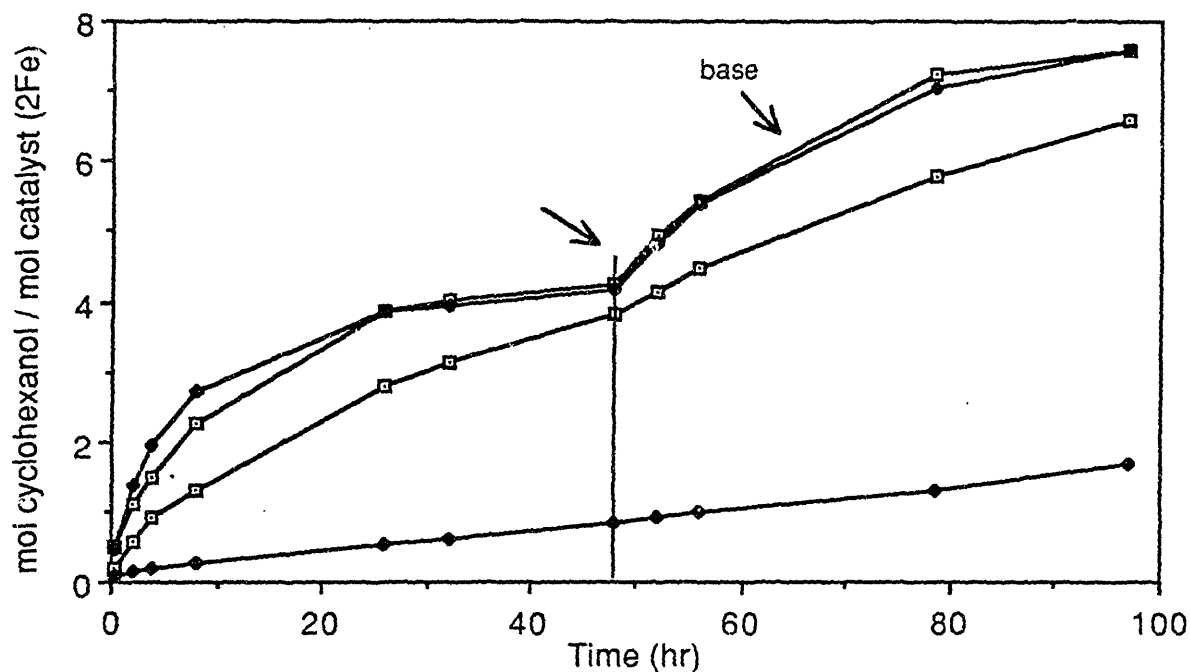


Figure 7. Effect of  $\text{Et}_3\text{N}$  on cyclohexanol formation catalyzed by **3** and  $(\text{Et}_4\text{N})[\text{FeCl}_4]$  in the presence of AA. Upper curves represent reaction mixtures containing base. Lower curves show activity under usual conditions. Open symbols: **3**. Closed symbols:  $(\text{Et}_4\text{N})[\text{FeCl}_4]$ . Arrow marks addition of a second 20 equivalents of reductant.

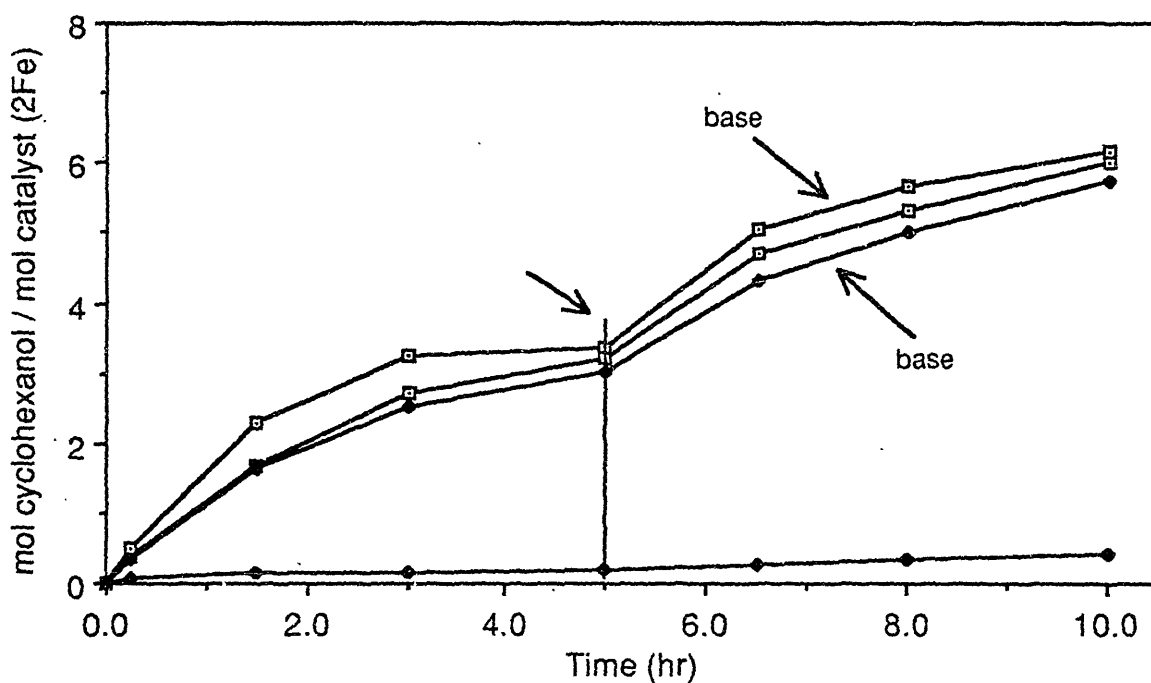


Figure 8. Effect of  $\text{Et}_3\text{N}$  on cyclohexanol formation catalyzed by **3** and  $(\text{Et}_4\text{N})[\text{FeCl}_4]$  in the presence of TMRA. Curves from reactions containing base are marked. Open symbols: **3**. Closed symbols:  $(\text{Et}_4\text{N})[\text{FeCl}_4]$ . Arrow marks addition of a second 20 equivalents of reductant.

rule out entirely the possibility that the presence of base favors the formation of dinuclear species. The dramatic change in the rate of the reaction when the base was predried could signify that the presence of water is also important. The combination of water and base in the reaction mixture before the addition of reductant would favor the formation of oxo-bridged species, but whether or not it is this equilibrium which is important to the oxidation chemistry will have to be determined in further experiments.

**Probing the nature of the oxidant and mechanism.** In order to gain insight into the type of active oxidant which might be involved in the oxidation by this system, reactivity toward an alkene substrate was examined. Production of epoxides from alkenes is generally considered to be an indication of oxo transfer as opposed to free radical autoxidation chemistry.<sup>10b</sup> Therefore, a series of reactions was run with cyclohexene as the substrate. The reactions were run twice in acetone and once in acetonitrile. For **3** and (Et<sub>4</sub>N)[FeCl<sub>4</sub>] the results were essentially the same in either solvent. The major product from the oxidation catalyzed by **3** in the presence of AA was the allylic alcohol, 2-cyclohexen-1-ol, but the epoxide, cyclohexene oxide, was the secondary product (Figure 9). Furthermore, a significant amount of the epoxide had formed by the earliest time point and more continued to form throughout the reaction. The ratio of cyclohexenol/ cyclohexene oxide/ cyclohexenone changed little throughout a 24 hr reaction time. Once the reductant is consumed, however, autoxidation will occur and this influence can be seen in the slightly greater relative amounts of allylic products versus epoxide at 24 hr compared to 10 hr.<sup>39</sup> Another interesting aspect of the product ratio is the large amount of allylic alcohol versus allylic ketone formed. In the autoxidation catalyzed by **3**, the ketone was the major product (Figure 10). The autoxidation also displayed a typical free radical product formation profile with an induction period followed by a period of accelerating

---

<sup>39</sup> The stability of the three products to the conditions of the reaction was tested. Both cyclohexenol and cyclohexene oxide were decomposed to undetermined products. Less than 5% decomposition occurred over a 24 hr time period at concentrations similar to those achieved in the oxidation reactions.



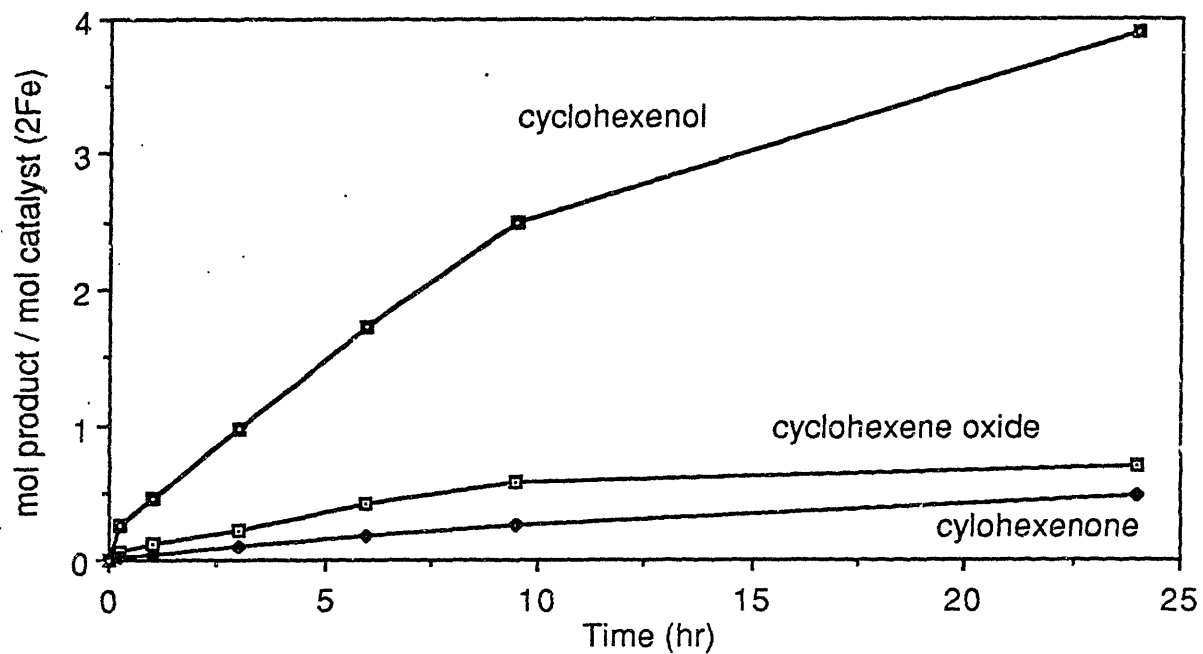


Figure 9. Oxidation of cyclohexene by air catalyzed by 3 in the presence of AA in acetone.

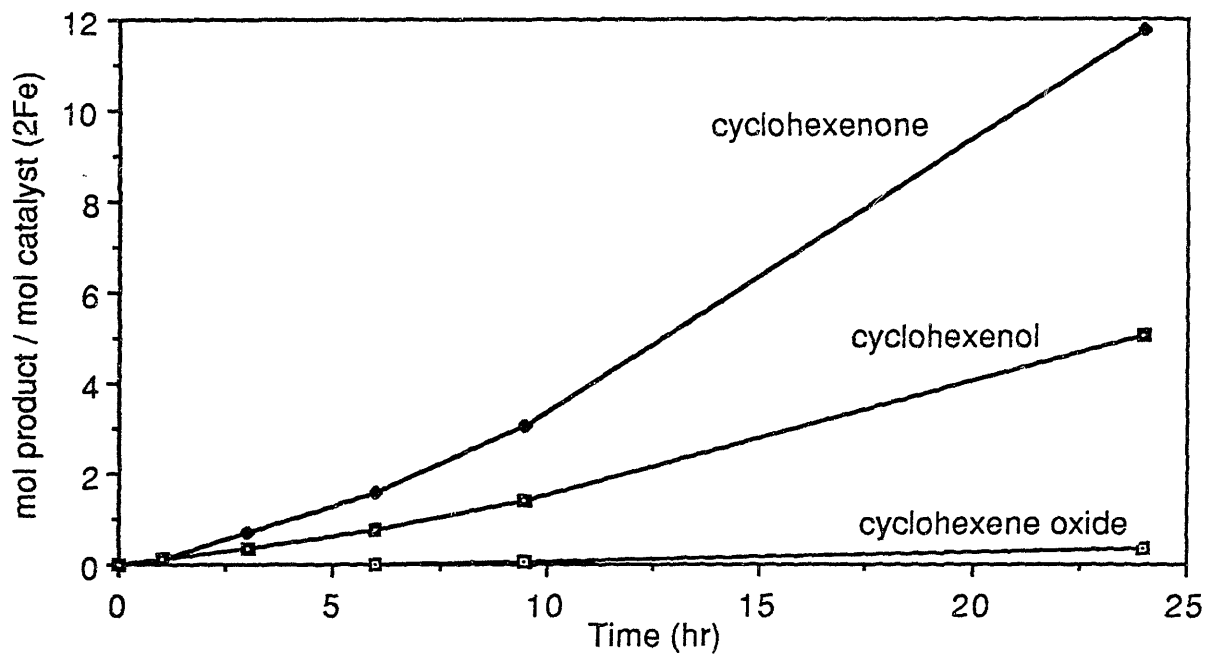


Figure 10. Autoxidation of cyclohexene catalyzed by 3 in acetone.

rates (Figure 10). This behavior was clearly different from the profile of the oxidation which occurred in the presence of AA (Figure 9). Like the profiles for the alkane oxidation, the rate of formation starts off high and decreases as the reductant is consumed. Nearly identical chemistry but with only 1/2 to 1/3 the yield was observed for catalysis with  $(Et_4N)[FeCl_4]$  and AA (Figure 11).

When  $FeCl_2$ (anhydrous) was the catalyst, different behavior was observed. Overall, extremely low amounts of oxidation products were formed with acetone as the solvent (Figure 12). At the earliest time point, a significant quantity of epoxide was detected in the mixture, but less and then no epoxide was detected after that point. The major product to be detected by GC was not a simple oxidation product of cyclohexene, and isopropanol from attack on acetone was the second most prevalent product after 5 hr. Curiously, not even autoxidation was catalyzed by  $FeCl_2$  in acetone. Only trace amounts of allylic products formed. When acetonitrile was used as solvent only autoxidation was observed. In the presence of AA, a greater proportion of cyclohexenol to cyclohexenone was formed, 1.56/1 compared to 0.78/1, but only small amounts of epoxide formed in either mixture (0.02 or less relative to cyclohexenone). The reactions in both solvents exhibited an induction period of more than 4 hr before a significant amount of products accumulated. The behavior of the  $FeCl_2$  catalyzed oxidation of cyclohexene further emphasizes the difference between the activity of this compound and **3** in the presence of AA and  $O_2$ .

In another attempt to probe the nature of the mechanism of the reaction, 3 sets of reactions were run in the presence of a radical trap, 2,6 di-*tert*-butyl-4-methylphenol (BHT). In each case BHT was added to one of two identically prepared systems. When 20-fold excess of BHT versus the catalyst was added to a system containing **3** and AA, an inhibition of about 30% of the initial rate was observed, but after 24 hr, the amount of products present was very similar to that formed in the system without BHT. A similar set of experiments with  $FeCl_2$  using 30-fold excess BHT, showed initially no effect on the reaction rate, but the overall yield was reduced. Oddly, there was no effect on the product distribution. The products assumed to

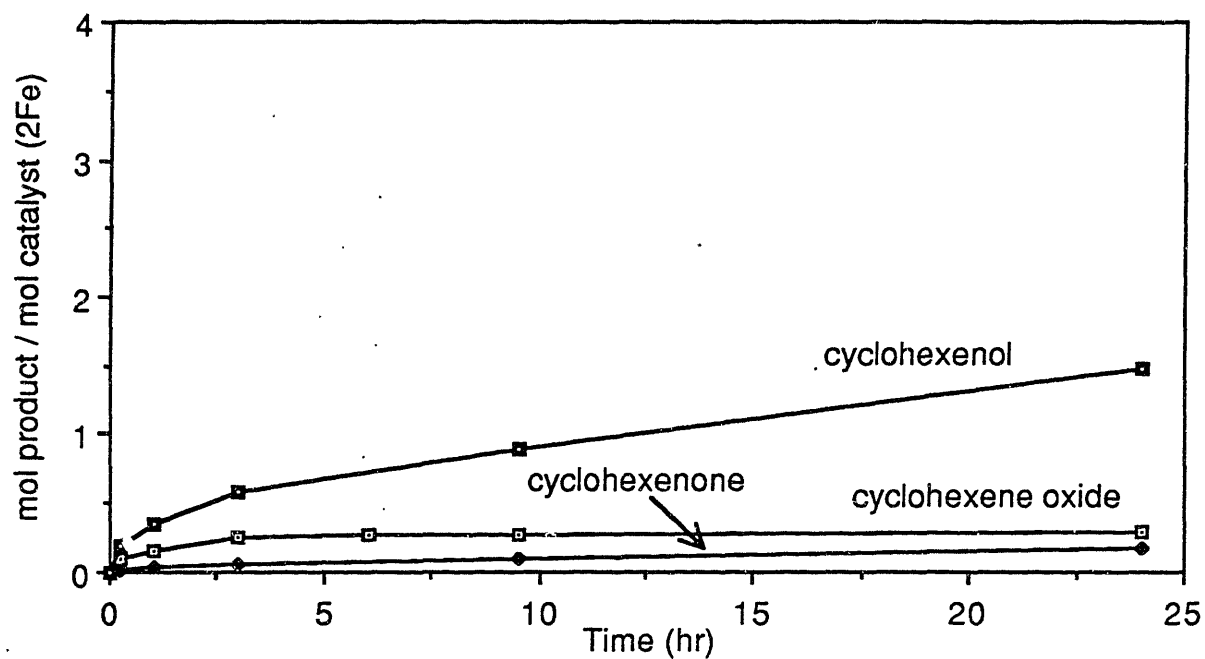


Figure 11 Oxidation of cyclohexene by air catalyzed by  $(\text{Et}_4\text{N})[\text{FeCl}_4]$  in the presence of AA in acetone. The same scale has been used as in Figure 9.

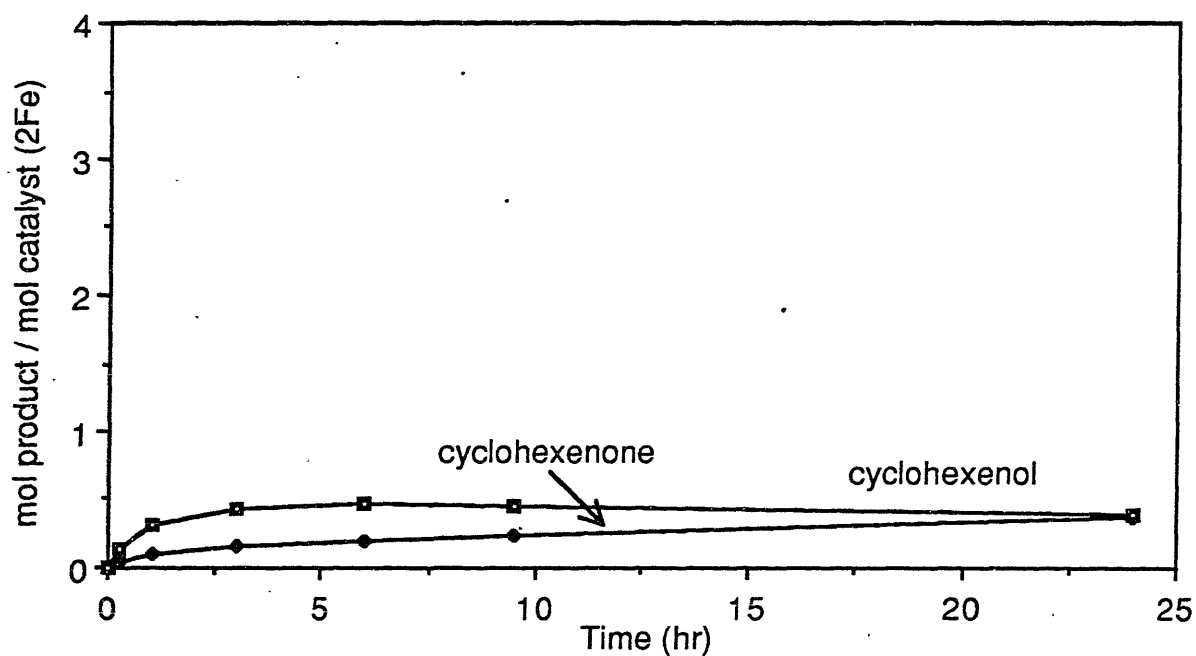


Figure 12 Oxidation of cyclohexene by air catalyzed by  $\text{FeCl}_2(\text{anhydrous})$  in the presence of AA in acetone. The same scale has been used as in Figure 9.

result from attack on acetone were present in the usual concentrations. The same procedure was repeated for **3** and FeCl<sub>2</sub> two other times using 200-fold excess BHT, once with AA and once with TMRA. The results were inconclusive. In all cases the yield of product was inhibited. Usually, the most dramatic difference was seen in the first aliquot analyzed, reflecting the initial rate of the reaction. With AA, **3** was inhibited to about 60% of the reaction without BHT and FeCl<sub>2</sub> to about 45%. Less effect was seen with TMRA; **3** produced about 75% of the control in the first 15 min and FeCl<sub>2</sub> about 85%. In these experiments, while the radical trap was present in excess of the catalyst and the reductant, it was always at concentrations significantly lower than the substrate. With this fact in mind, the inhibition observed may suggest a radical component to the mechanism. The fact that a 10-fold increase in radical trap did not alter the extent of inhibition, however, might suggest that the addition of BHT may have a secondary effect such as that resulting from a solute in the reaction mixture. Further studies with more controls will have to be performed before the significance of these results can be interpreted.

A preliminary measurement of a deuterium isotope effect was also carried out. Reactions were run with 2 ml perdeuteriocyclohexane and 2 ml cyclohexane present. The cyclohexanol produced from each substrate could be detected by GC and the two products were nearly completely separated on the FFAP column. The integrals for the two peaks were used to estimate the amount of each substrate that had reacted in a given amount of time. For AA, some variation in the ratio of deuterated and undeuterated products was seen during the course of the reaction. During the first 5 hr, while the rate of reaction is decreasing, the  $k_H/k_D$  increased from ~2.0 to 3.0. From 5.0 hr to 27 hr, while the rate is nearly constant, the  $k_H/k_D$  remained constant at  $3.0 \pm 0.1$ . With TMRA, a  $k_H/k_D$  of  $2.5 \pm 0.1$  was observed throughout the reaction. While this is a significant  $k_H/k_D$  ratio, in the same range as those measured by Barton<sup>25</sup> and Tabushi<sup>7</sup> for their systems and not far from the range of 4-5 found for MMO,<sup>2</sup> it is substantially lower than values of 12-16 measured for porphyrin systems with PhIO.<sup>5</sup> The

breaking of the C-H bond would appear to be important in the rate determining step(s) of the mechanism, although a pure hydrogen extraction step is not necessarily indicated.

In general, several conclusions can be drawn about the nature of the active oxidant and the type of mechanism involved in oxidations catalyzed by **3** in the presence of AA or TMRA. While epoxide was not the major product formed in the oxidation of cyclohexene, a significant amount was produced and the ratio of products was very different from that of the free radical autoxidation catalyzed by **3**. The rate of product formation was also unlike that of autoxidation, showing the same type of curve produced by the oxidation of cyclohexane. These results suggest that the system does not simply activate oxygen to form the allylic peroxide, which is the first product detected in autoxidation by metalloporphyrins,<sup>6b</sup> or, by analogy, the alkyl peroxide. Furthermore, since the alkane oxidation proceeds smoothly in acetone, hydroxyl radical intermediates (Fenton chemistry) are ruled out.<sup>40</sup> Also, aqueous hydrogen peroxide was added to **3** in acetone and in acetonitrile with cyclohexane and the type of reactivity produced was very different from that observed with the catalytic system. The high selectivity for cyclohexanol was not reproduced and many other products in addition to cyclohexanol and cyclohexanone were detected. Although the product formation profiles manifested by the oxidation reactions would be unusual for a pure free radical mechanism, the involvement of a free radical at some step in the mechanism cannot be ruled out.

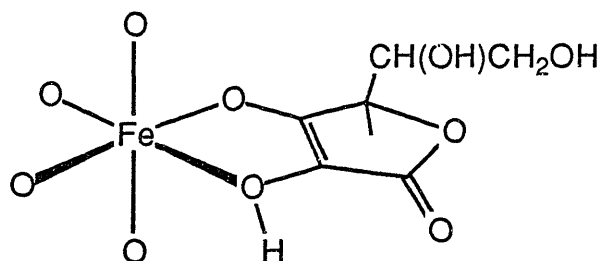
**Preliminary attempts at characterization of the purple species.** The purple colored species which forms on the addition of AA or TMRA to **3** has been assumed to be a iron-AA or iron-TMRA complex. There is precedence in the literature for highly colored iron-AA species. At acidic pH in water, solutions of AA and iron are usually colorless. At higher pH, however, deeply colored complexes have been stabilized.<sup>41</sup> Among the first to study the

---

<sup>40</sup> (a) Walling, C.; *Acc. Chem. Res.* 1975, 8, 125-131. (b) Walling, C.; El-Taliawi, G.M.; *J. Am. Chem. Soc.* 1973, 95, 844-847.

<sup>41</sup> (a) Laurence, G.S.; Ellis, K.J. *J. Chem. Soc., Dalton Trans.* 1972, 1667-1670. (b) Kurbatova, G.T.; Kriss, E.E.; Grigor'eva, A.S.; *Russian J. Inorg. Chem.* 1981, 26, 982-984. (c) Martinez, P.; Uribe, D. *Z. Naturforsch.* 1982, 37b, 1446-1449. (d) Martinez, P.; Zuluaga, J.; Uribe, D. *Inorg. Chim. Acta* 1987, 136, 11-16.

formation of a colored iron-AA complex were Lawrence and Ellis.<sup>40a</sup> Using stopped flow techniques they observed a colored intermediate characterized by a  $\lambda_{\text{max}}$  at 560 nm in the reduction of ferric ion by AA. They concluded that the colored species was a 1:1 Fe(III): ascorbate complex which was quickly reduced after forming. Several years later, Kurbatova *et al.* studied the same system but concluded that the colored species was a mixed-valent, polynuclear, hydroxo-bridged species of indeterminate composition.<sup>40b</sup> Martinez and Uribe were able to isolate a deep blue solid from a solution of ferric ion and AA by the addition of sodium propionate.<sup>40c</sup> They characterized it as mononuclear from the Mössbauer spectrum and determined the composition to be  $(\text{AscH})_2\text{Fe}^{\text{III}}\text{OH}$  from elemental analysis. In addition, they suggest a bidentate mode of binding for the ascorbate as shown below. Clarke *et al.* have



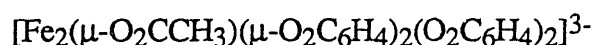
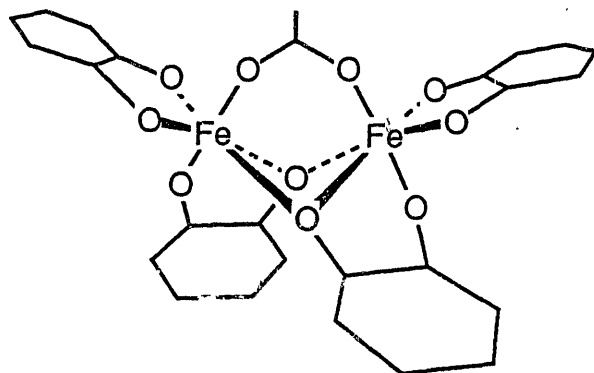
Proposed ascorbate binding mode in  $[(\text{AscH})_2\text{Fe}^{\text{III}}\text{OH}]$

recently studied the reaction of AA and TMRA with ruthenium and synthesized 1:1 complexes with monodentate binding proposed.<sup>42</sup> The color of the complex depends upon the pH at which it was synthesized. Blue, green and purple complexes are described with  $\lambda_{\text{max}}$  at  $\sim 680$  nm for the blue and green complexes and  $\sim 550$  nm for the purple. All the complexes in the literature have molar extinction coefficients for the visible band on the order of magnitude of  $500 \text{ M}^{-1}\text{cm}^{-1}$ .

One other complex of interest in relation to the colored species formed in the oxidation reactions is  $[\text{Fe}_2(\mu\text{-O}_2\text{CCH}_3)(\mu\text{-O}_2\text{C}_6\text{H}_4)_2(\text{O}_2\text{C}_6\text{H}_4)_2]^{3-}$  which was originally synthesized by

<sup>42</sup> Bryan, D.M.; Pell, S.D.; Kumar, R.; Clarke, M.J.; Rodriguez, V.; Sherban, M.; Charkoudian, J. *J. Am. Chem. Soc.* **1988**, *110*, 1498-1506.

Anderson *et al.*<sup>43</sup> This complex is a dinuclear catecholate complex with bridging catecholates as shown below. A bridging mode of this type might also be possible for ascorbate. The



dinuclear catecholate complex exhibits visible band which exhibits pronounced solvent dependence. The  $\lambda_{\text{max}}$  in MeOH is observed at 560 nm,<sup>42</sup> in CH<sub>3</sub>CN at ~540 nm and in aqueous acetone at ~525 nm. In MeOH, the molar extinction coefficient per iron is ~2700 M<sup>-1</sup>cm<sup>-1</sup>.<sup>42</sup>

When 20-fold excess TMRA is allowed to react with **3** in acetone, the resulting solution exhibits a visible band at  $\lambda_{\text{max}} = 525$  nm with a molar extinction coefficient of ~520 M<sup>-1</sup>cm<sup>-1</sup>, assuming all the iron has reacted to form the colored complex (Figure 13). This band shifts to lower energy in acetonitrile,  $\lambda_{\text{max}} = \sim 550$  nm. The shape and solvent dependence of this band are very similar to those of the dinuclear compound (Figure 13), but the extinction coefficient is similar to that of the mononuclear species. The deep blue color that results from the introduction of air into solutions containing FeCl<sub>2</sub> and TMRA has a different  $\lambda_{\text{max}}$ , 565 nm. The shape of the band suggests that a second absorption at lower energy is contributing to the intensity in this region (Figure 13).

Since the visible spectra of the purple complex did not help to determine its nuclearity, several other experiments were performed to attempt to address this issue. The possibility that

<sup>43</sup> Anderson, B.F.; Webb, J.; Buckingham, D.A.; Robertson, G.B. *J. Inorg. Biochem.* 1982, 16, 21-32.

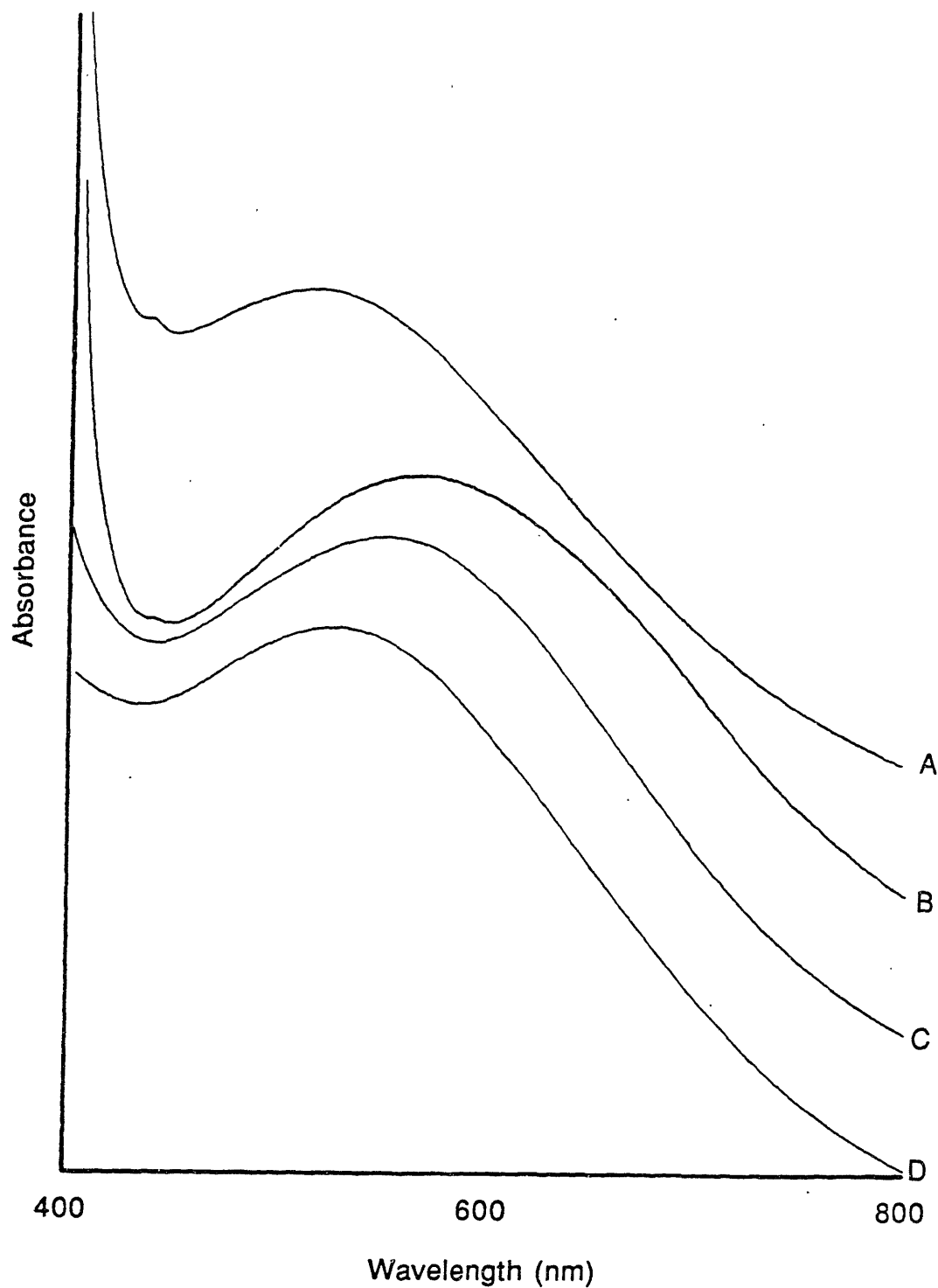


Figure 13. Visible spectra of intensely colored iron-reductive acid complexes. A) Spectrum of the purple complex generated by adding 20 equivalents of TMRA to **3** in acetone. B) Spectrum of acetone solution containing 20:1 mixture of TMRA and  $\text{FeCl}_2$  after having been exposed to air for 10 min. C) Spectrum of  $[(\text{AscH})_2\text{FeOH}]$  in water. D) Spectrum of  $(\text{BzPh}_3\text{P})_3[\text{Fe}_2(\mu\text{-O}_2\text{CCH}_3)(\mu\text{-O}_2\text{C}_6\text{H}_4)_2(\text{O}_2\text{C}_6\text{H}_4)_2]$  in aqueous acetone.



the dinuclear complex, **3**, might be decomposing to mononuclear species before the addition of reductant was raised. The stability of the complex in CH<sub>3</sub>CN was studied by UV-visible spectroscopy. The dinuclear complex exhibits characteristic bands between 200 and 400 nm.<sup>44</sup> At the concentrations used in the oxidation experiments, essentially no decomposition was observed in over 24 hr. At more dilute concentrations, or if water was added to the system, decomposition occurred much more rapidly. Since acetone is opaque in the region of the electronic spectrum necessary to study this complex, the stability of **3** in this solvent was determined by solution magnetic measurements. On standing in acetone, solutions of **3** deposit an orange precipitate and it was thought that this behavior might be indicative of decomposition to mononuclear species. The magnetic moment of a solution of **3** in deuterated acetone or deuterated acetonitrile, as measured by the Evans method,<sup>45</sup> did not change appreciably in 48 hrs. During this time, orange precipitate had collected in the bottom of the tube containing the sample in acetone, but the presence of this solid had little effect on the magnetic moment of the complex in solution. This result suggests that the precipitate may be a higher order iron-oxo oligomer which forms without breaking the dinuclear units.

The addition of 10 equivalents of TMRA to solutions of **3** in acetone did have a dramatic effect on the magnetic moment in solution. Approximating the concentration of the paramagnetic species in solution based on the concentration of dinuclear complex added, a value of ~6.0  $\mu$ B per iron was calculated. The value calculated for the dinuclear complex alone in acetone was 1.8  $\mu$ B per iron.<sup>46</sup> The change in  $\Delta v$  for solutions 17.5 mM in **3** was over 10-fold, from ~55 Hz for the dinuclear iron compound to ~569 Hz for the purple solution. The value of 6.0  $\mu$ B would fit well for a simple high spin mononuclear ferric species and certainly suggests that all antiferromagnetic coupling between iron atoms has been lost. Protonation of the oxo bridge could have caused such a change in magnetic moment. Also, the large magnetic

---

<sup>44</sup> Armstrong, W.H.; Lippard, S.J. *Inorg. Chem.* **1985**, *24*, 981-982.

<sup>45</sup> (a) Evans, D.F.; *J. Chem. Soc.* **1958**, 2003-2005. (b) Live, D.H.; Chan, S.I. *Anal. Chem.* **1970**, *42*, 791-792.

<sup>46</sup> No diamagnetic correction was attempted for either of these values.

moment, might result from an iron stabilized TMRA-radical species formed by a one electron oxidation of the reductant.

On two separate occasions, attempts were made to study the purple solution generated by the addition of TMRA to solutions of **3** by NMR spectroscopy. On the first occasion, the sample of TMRA used was not as pure as those used in the later experiment. The purple solution was generated in CD<sub>3</sub>CN by the addition of 10-fold excess of TMRA to a 4.5 mmol solution of **3**. A <sup>1</sup>H NMR spectrum of this solution revealed strong, broad resonances at 2.3, 2.8, and 4.1 ppm and a series of more than 20 small resonances appearing between 3 and 18 ppm. The peaks at 2.3 and 4.1 ppm probably arise from the (Et<sub>4</sub>N)<sup>+</sup> ion in the solution. The peak at 2.8 could be the methyl resonance of the excess TMRA shifted by bulk paramagnetism from its normal position ~1.0 ppm. The series of small peaks remains baffling and may be a reflection of the impurity of the reductant. Underlying some of these small peaks was a broad resonance centered at ~8.0 ppm which might be assigned as a methyl resonance from bound TMRA but such an assignment would need to be confirmed by recording another spectrum.

More interesting was the <sup>13</sup>C spectrum which, in addition to resonances from the cation and excess reductant, showed a very broad resonance at ~185 ppm and two inverted signals which could have resulted from "folding" of resonances in the 500 -800 ppm region. In an effort to confirm the presence of these bands and obtain a better spectrum of them, a purple solution was generated by adding 10-fold excess of analytically pure TMRA to a solution of **3** in CD<sub>3</sub>COCD<sub>3</sub>. An extremely broad window was used in collecting a <sup>13</sup>C NMR spectrum. Unfortunately, except for a roll in the baseline around 180 ppm which could be assigned as an extremely broad resonance, no sign of the shifted resonances previously observed were apparent in this spectrum. The sample was exposed to air briefly, and another spectrum collected, but no change had occurred. Oddly a series of small sharp resonances which were dismissed as arising from oxidized TMRA in the first sample were also present in the second sample. Each of these peaks appeared to correspond to one of the TMRA resonances. In the paramagnetic acetone solution, the TMRA resonances are observed at 21.4, 42.5, 126.0 and

202.0 ppm. The series of small sharp resonances occur at 18.6, 49.1, 83.0, 210.4 ppm. Possibly, judging from the high magnetic moment measured for the solution, any paramagnetically shifted resonances are too broad to be observed. On the other hand, it is possible that the sharp resonances arise from bound reductant. Their intensities appeared to be  $\sim 1/10$ th those of the corresponding free TMRA resonances, which could support the proposal that they arise from a 1:1 complex of **3** and TMRA. Either way, these experiments did not appreciably advance the characterization of the purple complex present in the oxidation systems.

### Summary and Conclusions

In attempts to develop a functional model for methane monooxygenase, an interesting system for the catalytic hydroxylation of alkanes by dioxygen has been discovered. This system, based on the dinuclear compound, **3**, and AA or TMRA exhibits remarkably clean reactivity with cyclohexane producing 40 to 50 times as much cyclohexanol as cyclohexanone and only trace amounts of other products. The rate of reaction in the presence of AA is extremely slow, with initial rates around 0.8 mol cyclohexanol/ mol **3**/ hr which drop off very quickly so that the rate after 5 hr is only  $\sim 0.10$  mol cyclohexanol/ mol **3**/ hr and continues to decrease. With TMRA the rate is considerably greater, but still only  $\sim 1.2$  mol cyclohexanol/ mol **3**/ hr for the first 2 hr and decreases after that time. For either system the yield on the reductant is  $\sim 20\%$ . Cyclohexene is converted to mostly 2-cyclohexen-1-ol with cyclohexene epoxide as the secondary product and 2-cyclohexen-1-one as the minor product when catalyzed by **3** in the presence of AA. The rate of reaction is not much accelerated over the rate seen for cyclohexane oxidation; at best, it is a factor of 2 greater.

These characteristics are different from most of the porphyrin systems reported in the literature.<sup>7,14-17,19-24</sup> The majority of these systems efficiently epoxidize olefins but are 5 to 10 times less reactive toward alkanes. Also, none of the systems with the possible exception of that recently published by Shilov<sup>22</sup> exhibit the specificity for alcohol over ketone production

manifested by our system. The early mononuclear iron systems also lack product specificity with ratios of alcohol to ketone of, at best, 7 or 8 to 1.<sup>10-12</sup> The system described by Mimoun demonstrates very similar activity to that described herein.<sup>13</sup> The turnover and yield on reductant are similar, as is the specificity reported for cyclohexanol production. The system produces mostly 2-cyclohexen-1-ol from cyclohexene although it does not yield any epoxide product. In the Mimoun system, however, simple ferrous and ferric chloride are provided as the iron catalyst and those salts do not show the same activity as **3** in our system. In fact, FeCl<sub>2</sub> and FeCl<sub>3</sub> exhibit different activity from each other in the presence of AA or TMRA in acetone. Furthermore, manganous chloride, cupric chloride and nickelous chloride are all active catalysts to some extent in the Mimoun system while none of these metal ions is active in our system. While the active oxidant may be similar in both systems, that which forms in the **3**/ reductic acid/ O<sub>2</sub> system is clearly dependent on iron which does not appear to be the case for the Mimoun system.

The nature of the catalytic species in the **3**/ reductic acid/ O<sub>2</sub> system remains unknown. It may be the purple complex formed on the addition of AA or TMRA to **3**. A darkly colored species has been detected in almost every system which has shown significant activity. The addition of base to systems containing (Et<sub>4</sub>N)[FeCl<sub>4</sub>] led to the formation of a purple complex but in apparently lower yield than in systems with **3**. Nonetheless, the (Et<sub>4</sub>N)[FeCl<sub>4</sub>]/ base systems gave equivalent yields of oxidation, which seems unusual if the purple complex is the active catalyst. All of the known darkly colored iron-AA complexes have been characterized as Fe(III) complexes. If the purple species is a ferric complex, then AA and TMRA must not reduce **3** completely, which could have interesting implications as far as the mechanism of activity is concerned.

It is also unclear at this point whether the active species is mononuclear or dinuclear. There are several appealing aspects to the proposal of a dinuclear catalyst. The reduction of each oxygen atom requires two electrons which could be readily provided by a dinuclear system. Furthermore, the roll proposed for an acyl group in activation of the O-O bond<sup>17,18</sup>

would be unnecessary in a diiron system. Side on coordination of the dioxygen unit bridging two irons could readily stabilize a peroxide unit and assist in the cleavage of the O-O bond.<sup>47</sup> A mechanism for the oxidation of alkanes by dioxygen based on a dinuclear oxo-bridged iron catalyst has been proposed (Figure 14). Nonetheless, it is clear that the addition of base to the mononuclear system renders it as active as the dinuclear system which may mean that the catalyst is mononuclear, but, as stated previously, is not definitive evidence. Other oxo-bridged species did not show significant activity toward the oxidation of cyclohexane by air.

Even if the catalyst is mononuclear, the chemistry of the system described herein is interesting and intriguing. One would not expect  $\text{FeCl}_3$  and  $(\text{Et}_4\text{N})[\text{FeCl}_4]$  to exhibit such radically different behavior. Both are essentially simple ferric chlorides. The first, however, readily attacks acetone under dinitrogen and shows only moderate and essentially promiscuous behavior when exposed to dioxygen, whereas the latter is active only toward the oxidation of cyclohexane. The chemistry supported by  $\text{FeCl}_3$  is identical to that in systems with  $\text{CuCl}_2$  suggesting it is not iron specific, but no other metal tested demonstrated the clean and selective oxidation supported by  $(\text{Et}_4\text{N})[\text{FeCl}_4]$  and **3**. Sawyer *et al.* have recently reported a similar difference in activity between  $\text{FeCl}_3$  and  $[\text{FeCl}_4]^-$ .<sup>48</sup> While they observe the activation of  $\text{H}_2\text{O}_2$  for monooxygenation of substrates in non-aqueous solvents in the presence of  $\text{FeCl}_3$ , the activity is much reduced for  $[\text{FeCl}_4]^-$ . They attribute the difference to the loss of Lewis acidity for the iron in the presence of excess chloride. Whether it is this type of effect or the presence of a counter ion to stabilize an ionic intermediate which is important in the reductive acid/ $\text{O}_2$  systems cannot be determined at this time, but this difference in activity is undoubtedly a significant clue to the mechanism of reactivity in these systems.

Initial studies to develop systems based on the known hemerythrin model compounds, **1** and **2**, were not very fruitful. Catalytic activity for **2** in the presence of reductive acids was

---

<sup>47</sup> A dinuclear species with a proposed bridging peroxide group has appeared in the literature. The complex is reported to catalyze the epoxidation of alkenes by hydrogen peroxide. Murch, B.P.; Bradley, F.C.; Que, L. *J. Am. Chem. Soc.* **1986**, *108*, 5027-5028.

<sup>48</sup> Sawyer, D.T.; Spencer, L.; Sugimoto, H. *Israel J. Chem.* **1987/88**, *28*, 3-12.

discovered but was assumed to result from the same active intermediate formed from the reductants and 3. The product specificity in the reactions with 2, however, were not as good as those achieved with 3 which suggests that the systems may produce different active species and that the role of 2 as a catalyst may be worthy of more study. In systems with 2, the dinuclear core was not likely to have been destroyed since the orange color characteristic of 2 was regenerated with time. On the other hand, the 3/ reductic acid/ O<sub>2</sub> system may not contain an active dinuclear species. The chemistry carried out by this system, however, is novel and interesting and may be relevant to that in MMO or other biological oxygenases.

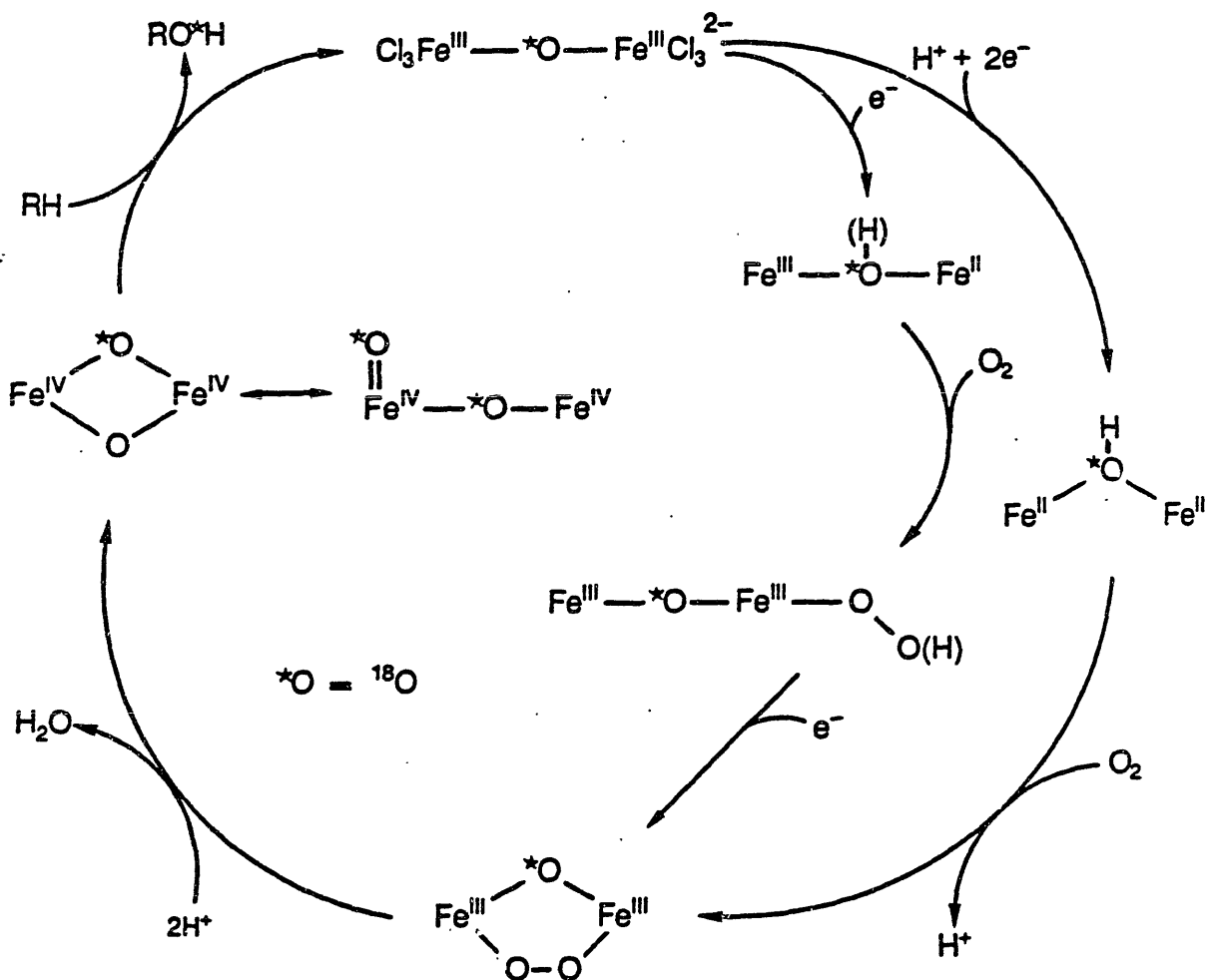


Figure 14. Proposed mechanism for the oxidation of alkanes by dioxygen based on an oxo-bridged dinuclear iron catalyst.

## APPENDIX I

Vibrational Analysis of  $[\text{Fe}_2\text{O}(\text{O}_2\text{P}(\text{OC}_6\text{H}_5)_2)_2(\text{HBpz}_3)_2]$

Vibrational spectroscopy is a very important tool in bioinorganic chemistry.<sup>1</sup>

Resonance Raman techniques often allow for the identification of metal ligand vibrations arising from a biologically important metal center. The strong symmetric stretching frequency of the M-O-M unit has been a particularly useful feature by which to identify diiron centers in proteins.<sup>2</sup> Since the position of the stretch and its shift upon <sup>18</sup>O substitution are characteristic of the Fe-O-Fe bond angle, structural information can be obtained from the spectra as well.<sup>3</sup> Furthermore, excitation profiles of resonance enhanced bands can be used to identify charge transfer bands in the optical spectra of the proteins.<sup>1</sup>

As a result, vibrational spectroscopy is also a good method for evaluating model compounds for biologically important metal centers. Not surprisingly, the hemerythrin model compounds, [Fe<sub>2</sub>O(O<sub>2</sub>CCH<sub>3</sub>)<sub>2</sub>(HBpz<sub>3</sub>)<sub>2</sub>], **1**,<sup>4</sup> and [Fe<sub>2</sub>O(O<sub>2</sub>CCH<sub>3</sub>)<sub>2</sub>(TACN)<sub>2</sub>]<sup>2+</sup>, **2**,<sup>5</sup> exhibit Fe-O-Fe stretching frequencies in the same region of the spectrum as hemerythrin and its derivatives. The positions of the bands in the model compounds, however, are at higher energy than those in hemerythrin (Hr) or another diiron protein, ribonucleotide reductase (RR).<sup>6</sup> This difference is considered to be a result of the smaller bridge angle in the model compounds as compared to those proposed for the proteins.

The bridge exchange chemistry of **1** has allowed for the synthesis of an analog of **1** with a larger bridge angle. Diphenylphosphate, as well as other carboxylates, was found to

<sup>1</sup> (a) Carey, P.R. *Biochemical Applications of Raman and Resonance Raman Spectroscopies*; Academic: New York, 1982. (b) Parker, F.S. *Applications of Infrared, Raman, and Resonance Raman Spectroscopy in Biochemistry*; Plenum; New York, 1983. (c) Spiro, T.G., ed., *Biological Applications of Raman Spectroscopy*; Vol 1 and 2, Wiley, New York, 1987.

<sup>2</sup> Sanders-Loehr, J. *ACS Symp. Ser.* **1988**, in press.

<sup>3</sup> Wing, R.M.; Callahan, K.P. *Inorg. Chem.* **1969**, *8*, 871-874.

<sup>4</sup> (a) Armstrong, W.H.; Lippard, S.J. *J. Am. Chem. Soc.* **1983**, *105*, 4837-4838. (b) Armstrong, W.H.; Spool, A.; Papaefthymiou, G.C.; Frankel, R.B.; Lippard, S.J. *J. Am. Chem. Soc.* **1984**, *106*, 3653-3667.

<sup>5</sup> (a) Wieghardt, K.; Pohl, K.; Gebert, W. *Angew. Chem., Int. Ed. Engl.* **1983**, *22*, 727. (b) Spool, A.; Williams, I.D.; Lippard, S.J. *Inorg. Chem.* **1985**, *24*, 2156-2162.

<sup>6</sup> Sjöberg, B.-M.; Sanders-Loehr, J.; Loehr, T.M. *Biochemistry* **1987**, *26*, 4242-4247.



exchange readily into the bridging positions in **1**.<sup>7</sup> A crystal structure of the resulting compound,  $[\text{Fe}_2\text{O}(\text{O}_2\text{P}(\text{O}_2\text{C}_6\text{H}_5)_2)_2(\text{HBpz}_3)_2]$ , **3**, revealed that its structure was nearly identical to that of **1** with the exception of the Fe-O-Fe angle. The larger "bite size" of the phosphate caused this angle to expand to  $134.7^\circ$  as compared to  $123.6^\circ$  in **1**. The Fe-O bond lengths also increased slightly to accommodate the larger bridge angle. This Fe-O-Fe angle is much closer to those proposed for the proteins.<sup>6</sup> Therefore, a vibrational analysis of **3** was undertaken. The results of this analysis taken together with those of similar analyses of **1** and **2** form an interesting series which reflects the dependence of the Fe-O-Fe stretching frequencies and Fe-O force constants on the bridge angle. Excitation profiles in the visible region of the three complexes were also compared, but no firm conclusions could be drawn from the data.

## Experimental Section

A Spex 1401 double monochromator instrument equipped with a cooled RCA 31034 photomultiplier tube with photon counting electronics was used to record the Raman spectra. The spectrometer was interfaced with a North Star computer for ease of collection, manipulation, storage, and plotting of data. The spectra were plotted on a 4662 Tektronix Interactive Digital Plotter. A tunable argon laser (Coherent Radiation Model 52 and Spectra Physics Model 164) was used to produce all excitation wavelengths. Both  $90^\circ$  and back-scattering geometries were employed. When a back-scattering geometry was employed, the samples were sealed in 5 mm NMR tubes and spun. The power incident at the sample was 40-50 mW and the slits were set at 200/250/200. Since the samples could not be spun when a  $90^\circ$  configuration was employed, lower powers and wider slit setting were sometimes required.

---

<sup>7</sup> Armstrong, W.H.; Lippard, S.J. *J. Am. Chem. Soc.* **1985**, *107*, 3730-3731.

For the excitation profile, a 90° geometry was used. The sample was sealed in a small capillary and held stationary in the beam. Because of the opacity of the sample, it was necessary to pass the beam through the sample close to edge of the capillary rather through the middle. The power incident at the sample was 10 mW for the 465.8 nm and 476.5 nm lines and 20 mW for all other lines. The slits were set at 300/400/300 and the spectra collected at ambient temperature. The solvent line at 704 cm<sup>-1</sup> was used as an internal reference. The relative intensities of the peaks at different excitation wavelengths were calculated versus the peak using peak height as a measure of intensity.<sup>4b</sup> Since the peaks being compared were within 500 cm<sup>-1</sup> of each other in the spectrum, no corrections were made for the dependence of the intensity on wavenumber shift and detector sensitivity.<sup>8</sup> No corrections were made for sample absorption. The signal-to-noise ratio of each spectrum was minimized by scanning the window 3 to 5 times and averaging the scans. To ensure against variations in heat, spurious light, or mechanical manipulations causing an erroneously high or low value at a given wavelength, several spectra were recorded at each wavelength and the calculated intensity ratios averaged.

Initially, a sample of [Fe<sub>2</sub>O(O<sub>2</sub>P(OC<sub>6</sub>H<sub>5</sub>)<sub>2</sub>)<sub>2</sub>(HBpz<sub>3</sub>)], **3**, was prepared by saturating 0.5 ml of CH<sub>2</sub>Cl<sub>2</sub> with the compound and sealing it under vacuum in a 5 mm NMR tube. A back-scattering geometry was used to collect the spectrum. The identical spectrum was obtained when a 90° geometry was employed but the signal-to-noise was much better and interference from glass scattering was eliminated. The compound appeared to be stable in the beam as determined by <sup>1</sup>H NMR and visible spectroscopy. Substitution of <sup>18</sup>O into the bridging position was accomplished as previously reported.<sup>4b</sup>

An IBM System 9000 computer interfaced to an IBM IR/32 Spectrometer was used to record the FTIR spectra. The spectra were plotted on a line printer. Pellets made from 100 mg of KBr and 2 to 3 mg of **3** or its <sup>18</sup>O substituted derivative were used to generate the spectra.

---

<sup>8</sup> Strommen, D.P.; Nakamoto, K. *Laboratory Raman Spectroscopy*; Wiley: New York, 1984.

The peaks were computer chosen from absorbance spectra. Several difference spectra were generated and the difference peaks chosen by hand from the display screen.

## Results and Discussion

In order to determine the symmetric and asymmetric stretching frequencies associated with the Fe-O-Fe unit, the vibrational spectra of **3** and its  $^{18}\text{O}$  substituted derivative were obtained. From the Raman spectra (Figure 1), the position of the symmetric stretch,  $\nu_s(\text{Fe-O-Fe})$ , was determined to be  $478\text{ cm}^{-1}$  in the  $^{16}\text{O}$  compound and  $464\text{ cm}^{-1}$  in the  $^{18}\text{O}$  compound. The only other feature observed to shift upon isotopic substitution was a small, broad band that appeared at  $950\text{ cm}^{-1}$  in the  $^{16}\text{O}$  spectrum and shifted under a band at  $927\text{ cm}^{-1}$  in the  $^{18}\text{O}$  spectrum. This band is assigned as the first overtone of the symmetric stretch. In order to uncover the position of the asymmetric stretches in the FTIR spectra, a difference spectrum had to be generated. While comparison of the  $^{16}\text{O}$  and  $^{18}\text{O}$  spectra revealed changes in the intensities of the strong ligand bands which occur in the region around  $750\text{ cm}^{-1}$  (Figure 2), the actual position of the  $\nu_{as}$  bands could only be determined from a difference spectrum. This approach clearly revealed bands at  $767\text{ cm}^{-1}$  and  $725\text{ cm}^{-1}$  in the  $^{16}\text{O}$  and  $^{18}\text{O}$  spectra, respectively (Figure 3). Careful inspection of the difference spectrum revealed that the feature at lowest energy has a  $^{16}\text{O}$  peak at  $475\text{ cm}^{-1}$  and an  $^{18}\text{O}$  peak at  $463\text{ cm}^{-1}$  which correspond closely to the  $\nu_s(\text{Fe-O-Fe})$  values from the Raman spectra. Assigning this feature to the symmetric stretch is not unreasonable since, from symmetry arguments, both the symmetric and asymmetric stretches should be allowed in both the Raman and infrared spectrum, although with different intensities. In fact, slight differences between the Raman spectra of the  $^{16}\text{O}$  and  $^{18}\text{O}$  complexes in the region of  $750\text{ cm}^{-1}$  could be detected upon close examination, but the presence of a solvent band at  $742\text{ cm}^{-1}$  made it impossible to locate the asymmetric stretching band.

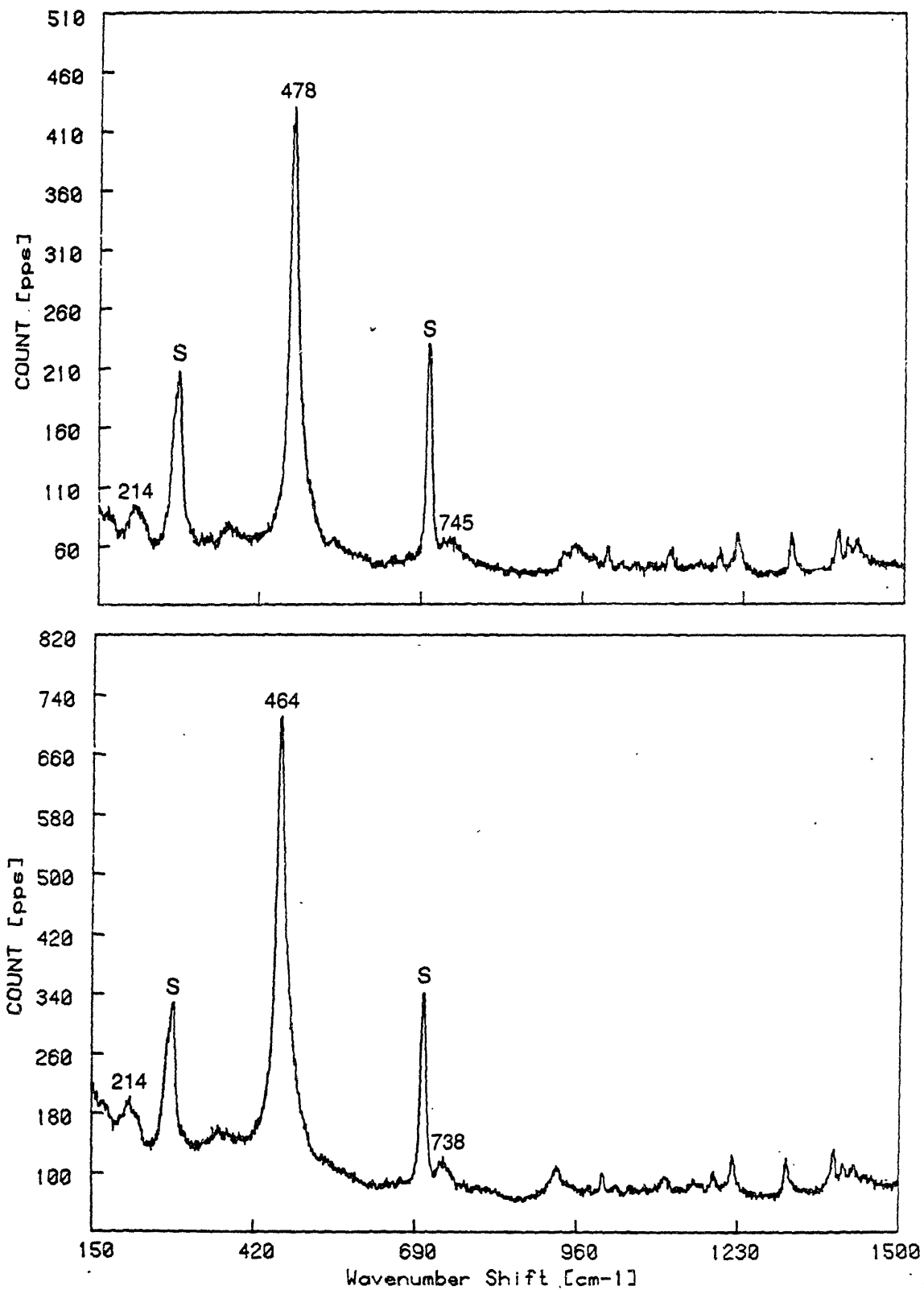


Figure 1. Raman spectra of 3 (top) and its <sup>18</sup>O substituted derivative (bottom) in CH<sub>2</sub>Cl<sub>2</sub> with 457.9 nm excitation. The major solvents peaks are labelled with S.

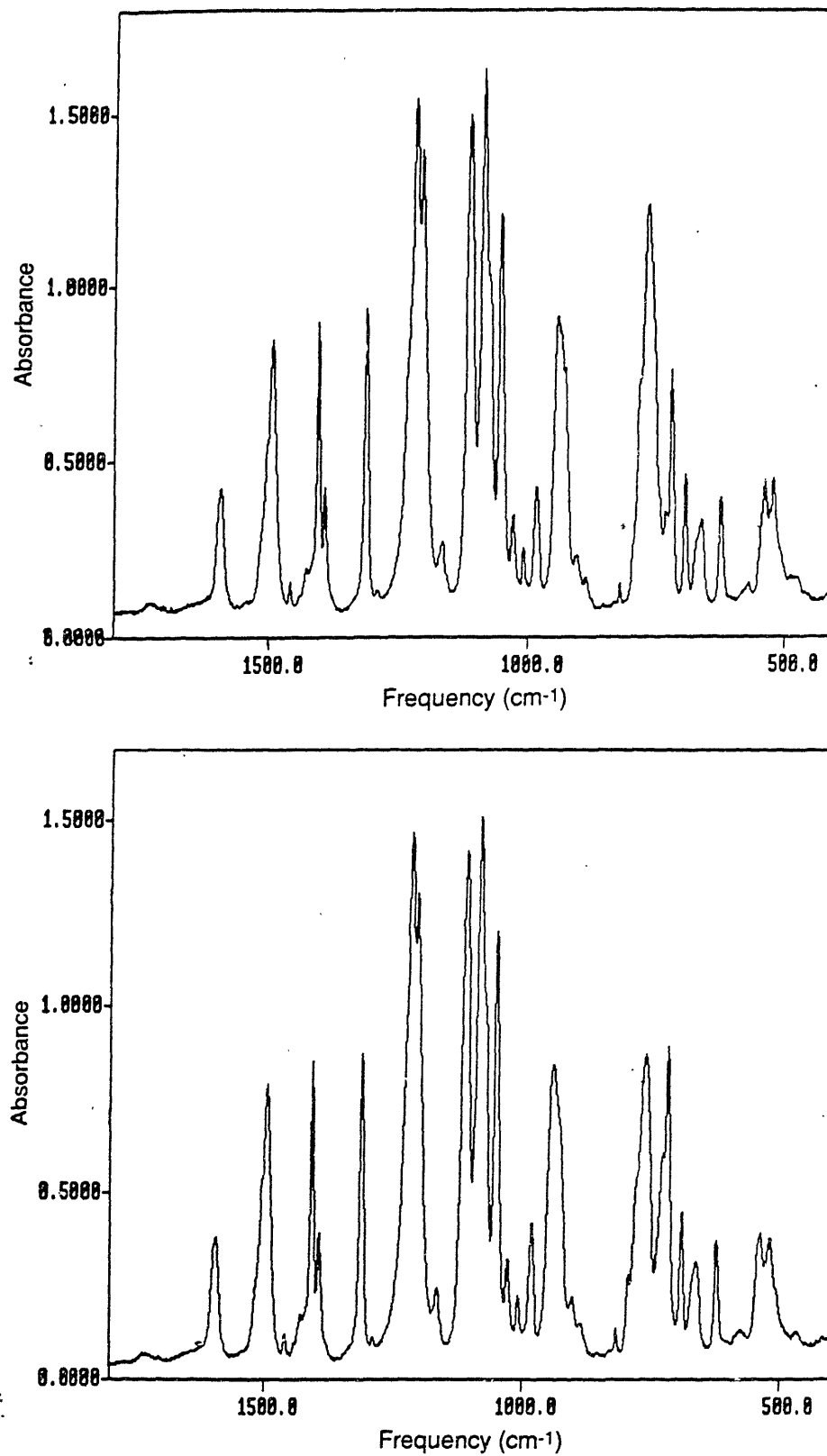


Figure 2. FTIR spectra of **3** (top) and its <sup>18</sup>O substituted derivative (bottom). Note differences in intensity of bands around 750 cm<sup>-1</sup>.

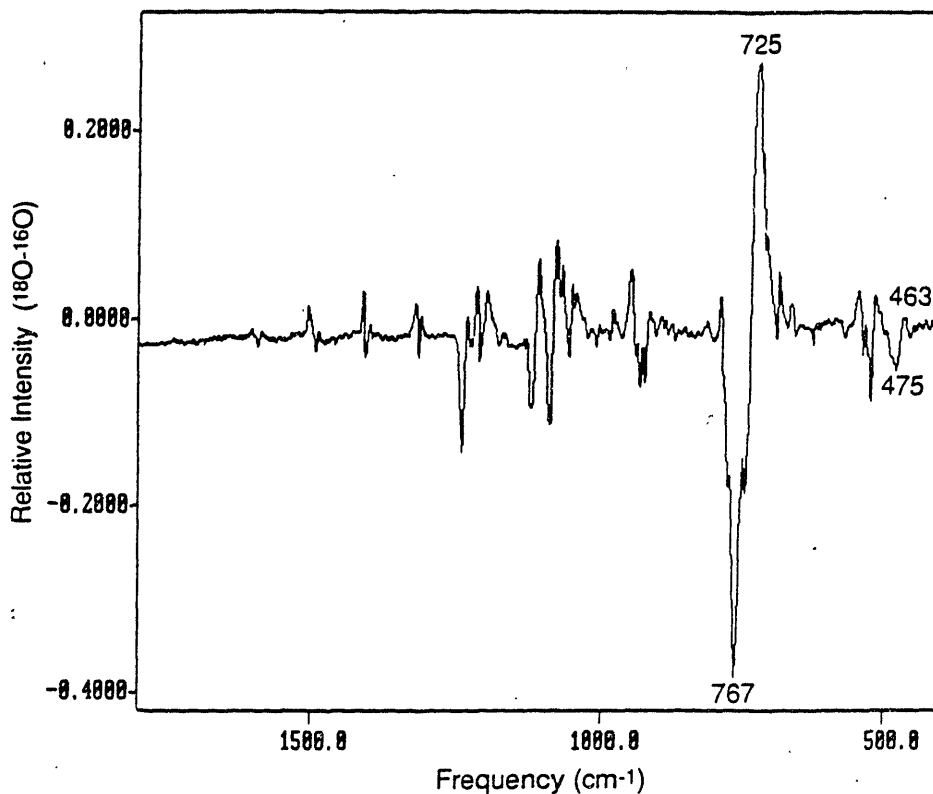


Figure 3. FTIR difference spectrum generated by subtracting the upper ( $^{16}\text{O}$ ) spectrum from the lower ( $^{18}\text{O}$ ) spectrum shown in Figure 2.

All of the peaks in the Raman spectrum of **3** are compiled and assigned in Table I. The shoulder on the low energy side of the  $286\text{ cm}^{-1}$  solvent band is a peak which appears at  $278\text{ cm}^{-1}$  when the solvent is acetonitrile. A peak occurs at approximately the same frequency in the spectra of **1**,<sup>4b</sup> **2**,<sup>5b</sup> and  $[\text{Fe}_2\text{O}(\text{O}_2\text{CCH}_3)_2(\text{Me}_3\text{TACN})_2](\text{PF}_6)_2$ .<sup>9</sup> This band had been previously assigned to an Fe-N(ligand) stretching mode by analogy to the  $292\text{ cm}^{-1}$  band in the spectrum of azidomethemerythrin which had been assigned as a Fe-N(histidine) stretch. The latter band has now been reassigned as the Fe-O-Fe deformation mode because it was seen to shift when  $^{18}\text{O}$  was substituted into the bridging position.<sup>10</sup> No such shift was apparent in compounds **1**, **2**, or **3**. Also, these bands produce excitation profiles which are distinctly different from those produced by the  $\nu_s(\text{Fe-O-Fe})$  bands. The variations in resonance

<sup>9</sup> Roth, M.E.; Hartman, J.; Lippard, S.J., unpublished results.

<sup>10</sup> Shiemke, A.K.; Loehr, T.M.; Sanders-Loehr, J. *J. Am. Chem. Soc.* **1984**, *106*, 4951-4956.

Table I

## ASSIGNMENT OF OBSERVED RAMAN BANDS FOR 3

Band (cm <sup>-1</sup> )		Probable Source
<sup>16</sup> O	<sup>18</sup> O	
214	214	Fe-N(ligand), Fe-O(phosphate) <sup>a</sup>
282(sh)	280(sh)	(occurs at 278 in CH <sub>3</sub> CN) Fe-N(ligand)
370	--	Fe-O(phosphate) <sup>a</sup>
478	464	$\nu_s$ (Fe-O-Fe)
745	738	solvent band with contributions from $\nu_{as}$ (Fe-O-Fe)
929	927	(HBpz <sub>3</sub> ) <sup>-</sup> <sup>b</sup>
950(br)	927 <sup>c</sup> (br)	2 $\nu_s$
1006	1005	phenyl ring stretch
1108	1108	(HBpz <sub>3</sub> ) <sup>-</sup>
1193	1189	(HBpz <sub>3</sub> ) <sup>-</sup>
1220	1220	(HBpz <sub>3</sub> ) <sup>-</sup>
1311	1311	(HBpz <sub>3</sub> ) <sup>-</sup>
1390	1390	(HBpz <sub>3</sub> ) <sup>-</sup>
1406	1406	(HBpz <sub>3</sub> ) <sup>-</sup>

<sup>a</sup> These bands are assigned by analogy to similar bands in 1 (See reference 12).

<sup>b</sup> Ligand bands were assigned based on the spectrum of [Fe(HBpz<sub>3</sub>)<sub>2</sub>]ClO<sub>4</sub> described in reference 4b.

<sup>c</sup> A broad band appears under the small sharp peak at 927.

Table II

COMPARISON OF VIBRATIONAL DATA FOR 1, 2 AND 3<sup>a</sup>

Complex	Fe-O-Fe angle (°)	$\nu_s$ (cm <sup>-1</sup> )	$\nu_{as}$ (cm <sup>-1</sup> )	$k_d$ (mdyn/Å)	$k_{dl}$ (mdyn/Å)
2	118.7	540 (523) <sup>b</sup>	749 (716)	3.21	0.21
1	123.6	528 (511)	751 (721)	3.24	0.35
3	134.7	478 (464)	767 (725)	3.24	0.46

<sup>a</sup> Data for 1 and 2 from references 4b and 5b, respectively

<sup>b</sup> The values in parentheses are for <sup>18</sup>O substituted complexes.

intensities are especially pronounced in the TACN and Me<sub>3</sub>TACN complexes.<sup>9,11</sup> Furthermore, the assignment of the band ~275 cm<sup>-1</sup> in **1** as arising from a Fe-N(ligand) stretch has been confirmed by a normal mode analysis carried out by a separate group of researchers.<sup>12</sup> This group also contends that the original assignment of the 292 cm<sup>-1</sup> peak in the Hr spectrum as a Fe-N stretch is the correct assignment.

Peaks in the 190 to 220 cm<sup>-1</sup> region have also been assigned to the  $\mu$ -oxo deformation mode.<sup>13</sup> The peak at 214 cm<sup>-1</sup> in the spectrum of **2**, however, does not show any shift upon isotopic substitution which contradicts such an assignment. Furthermore, the normal mode analysis of **1** suggested that the deformation mode in this type of complex would be strongly coupled to other vibrations.<sup>12</sup> The vibration with greatest percentage of deformation character was assigned to 104 cm<sup>-1</sup>, lower than the frequencies examined in this study. Based on the analysis of **1**, the band at 214 cm<sup>-1</sup> in the spectrum of **3** most likely arises from another Fe-N(ligand) stretching mode.

The stretch and stretch-stretch (interactive) force constants,  $k_d$  and  $k_{dd}$ , for the Fe-O-Fe moiety in **3** were calculated from simplified secular equations derived from a normal mode analysis based on local C<sub>2v</sub> symmetry.<sup>3</sup> The constants calculated for the natural isotope of **2** are  $k_d = 3.24$  mdyn/Å and  $k_{dd} = 0.46$  mdyn/Å. These constants predict values of 464 cm<sup>-1</sup> and 728 cm<sup>-1</sup> for the stretching modes of the <sup>18</sup>O substituted complex. The observed values of 464 cm<sup>-1</sup> and 725 cm<sup>-1</sup> match the calculated values well and suggest that the approximations necessary to simplify the calculations are appropriate for this system.

The values obtained from these calculations allow for an interesting comparison among compounds **1**, **2**, and **3**. The pertinent data for comparing these compounds appear in Table II. Clearly, the positions of the symmetric and asymmetric stretching modes shift to lower and

---

<sup>11</sup> Spool, A. Ph.D. Thesis, Columbia University, 1984.

<sup>12</sup> Czernuszewicz, R.S.; Sheats, J.E.; Spiro, T.G. *Inorg. Chem.* **1987**, *26*, 2063-2067.

<sup>13</sup> Sheats, J.E.; Czernuszewicz, R.S.; Dismukes, G. C.; Rheingold, A. L.; Vasili, P.; Stubbe, J.; Armstrong, W.H.; Beer, R.H.; Lippard, S.J. *J. Am. Chem. Soc.* **1987**, *109*, 1435-1444.



higher energy, respectively, as the Fe-O-Fe bond angle is increased, as predicted. Compounds **1** and **3** are particularly useful in this comparison since the symmetry and ligand environment around the iron remain essentially unchanged; only the  $\mu$ -oxo angle is altered. Perhaps, then, it should not be surprising that the Fe-O force constant for these two compounds are calculated to be identical within rounding approximations. The slightly longer Fe-O bond length in **2** does not seem to have affected the value of  $k_d$ . The change in force constant responsible for the energy shift of the bands is the interactive constant, which changes from 0.35 mdyn/Å in **1** to 0.46 mdyn/Å in **3**. The constants calculated for **2** extend the series. The Fe-O force constant is a bit smaller for this compound but probably well within the error range for these calculations. Also, **2** is not an analog of **1** and **3**; the symmetry and ligand environment around the metal centers are different than in **1** or **3**. Nonetheless, it is clear that the  $k_{dd}$  is most responsible for the shifts in the positions of the stretching bands. The increase in  $k_{dd}$  with increasing Fe-O-Fe angle can be explained by an increase in the orbital overlap between metal centered orbitals of  $d_{xz}$ ,  $d_{yz}$  orientation and the p-type orbitals on the bridging oxygen atom.

The force constants calculated for another complex,  $[\text{Fe}_2\text{OCl}_6]^{2-}$ , emphasize the importance of the above series. The Fe-O bond length for this compound is 1.755 Å and the Fe-O-Fe angle is 155.6°. <sup>14</sup> The Fe-O bond length is slightly smaller than those in **1**, **2**, or **3**, but the Fe-O-Fe angle is considerably larger. The  $\nu_s$  and  $\nu_{as}$  of this compound have been reported at 458 cm<sup>-1</sup> and 870 cm<sup>-1</sup> shifting to 440 cm<sup>-1</sup> and 826 cm<sup>-1</sup> upon <sup>18</sup>O substitution. <sup>15</sup> Here again, the symmetric stretch has moved to lower, and the asymmetric to higher, energy but this compound cannot really be considered part of the same series as **1**, **2**, and **3**. Although the Fe-O force constant is reported as 3.24 mdyn/Å, <sup>15</sup> the simplified equations referred to above yield a different value. Completing the calculations with the <sup>16</sup>O values gives  $k_d = 4.24$  mdyn/Å and  $k_{dd} = 1.00$  mdyn/Å. The vibrational frequencies for the <sup>18</sup>O substituted

<sup>14</sup> Drew, M.G.B.; McKee, V.; Nelson, S.M. *J. Chem. Soc., Dalton Trans.* **1978**, 80-90.

<sup>15</sup> Solbrig, R.M.; Duff, L.L.; Shriber, D.F.; Klotz, I.M. *J. Inorg. Biochem.* **1982**, *17*, 69-74

compound calculated using these constants are  $450\text{ cm}^{-1}$  and  $828\text{ cm}^{-1}$ . The match for the asymmetric stretch is good but that for the symmetric stretch relatively poor. An examination of the spectrum<sup>15</sup> reveals part of the problem. The symmetric stretch shifts on top of another band centered around  $425\text{ cm}^{-1}$  in the  $^{16}\text{O}$  spectrum. The presence of this band underlying the oxo stretch in the  $^{18}\text{O}$  spectrum may have caused the band to appear at a lower frequency.<sup>16</sup> The large values calculated for  $k_d$  and  $k_{dd}$  do not seem unreasonable considering the structure of this anion. The symmetry around each iron is tetrahedral with no ligand trans to the bridging oxygen to weaken the Fe-O interaction. The oxo bridge is the only linkage holding the dinuclear complex together. If the Fe-O bonds were not strong, the compound would not form. Thus, while it is true that  $[\text{Fe}_2\text{OCl}_6]^{2-}$  has a larger angle and interactive constant than **1**, **2**, or **3**, clearly other factors are involved in determining its vibrational features.

The influence of other factors must also be considered when comparing the stretching frequencies of **3** to those of the proteins. While the bridging angle matches well with those proposed for the proteins,  $134.7^\circ$  in **3** with  $135^\circ$  and  $138^\circ$  in Hr and RR, respectively, the  $\nu_s$  (Fe-O-Fe) in **3** occurs at lower energy than in either protein. The  $\nu_s$  (Fe-O-Fe) has been assigned at  $486\text{ cm}^{-1}$  in oxy-Hr and  $492\text{ cm}^{-1}$  in hydroxymet-Hr.<sup>6</sup> In RR, the band is found at  $493\text{ cm}^{-1}$ .<sup>6</sup> As the angle in the model compounds changed from  $123.6^\circ$  to  $134.7^\circ$ , the position of the  $\nu_s$  (Fe-O-Fe) changed from being higher in energy to being lower in energy than the proteins. The variance of 10 to  $20\text{ cm}^{-1}$  between **3** and the proteins is probably a result of greater distortions from octahedral coordination around the iron atoms in the proteins, or the influence of hydrogen bonding to the oxo-bridge. Interestingly, no enhanced Fe-O(H)-Fe stretch could be detected for the hydroxo-bridged analog of **1**.<sup>17</sup>

Unfortunately, very little can be said about the excitation profile of the symmetric Fe-O-Fe stretch of **3** (Figure 4). It bears little resemblance to the profiles of the analogous stretch

---

<sup>16</sup> The band at  $422\text{ cm}^{-1}$  is identified as a pyridinium ring stretch from the cation but it appears with the same relative intensity in the spectrum of the tetraethylammonium salt as well.

<sup>17</sup> Roth, M.E.; Lippard, S.J. unpublished results.

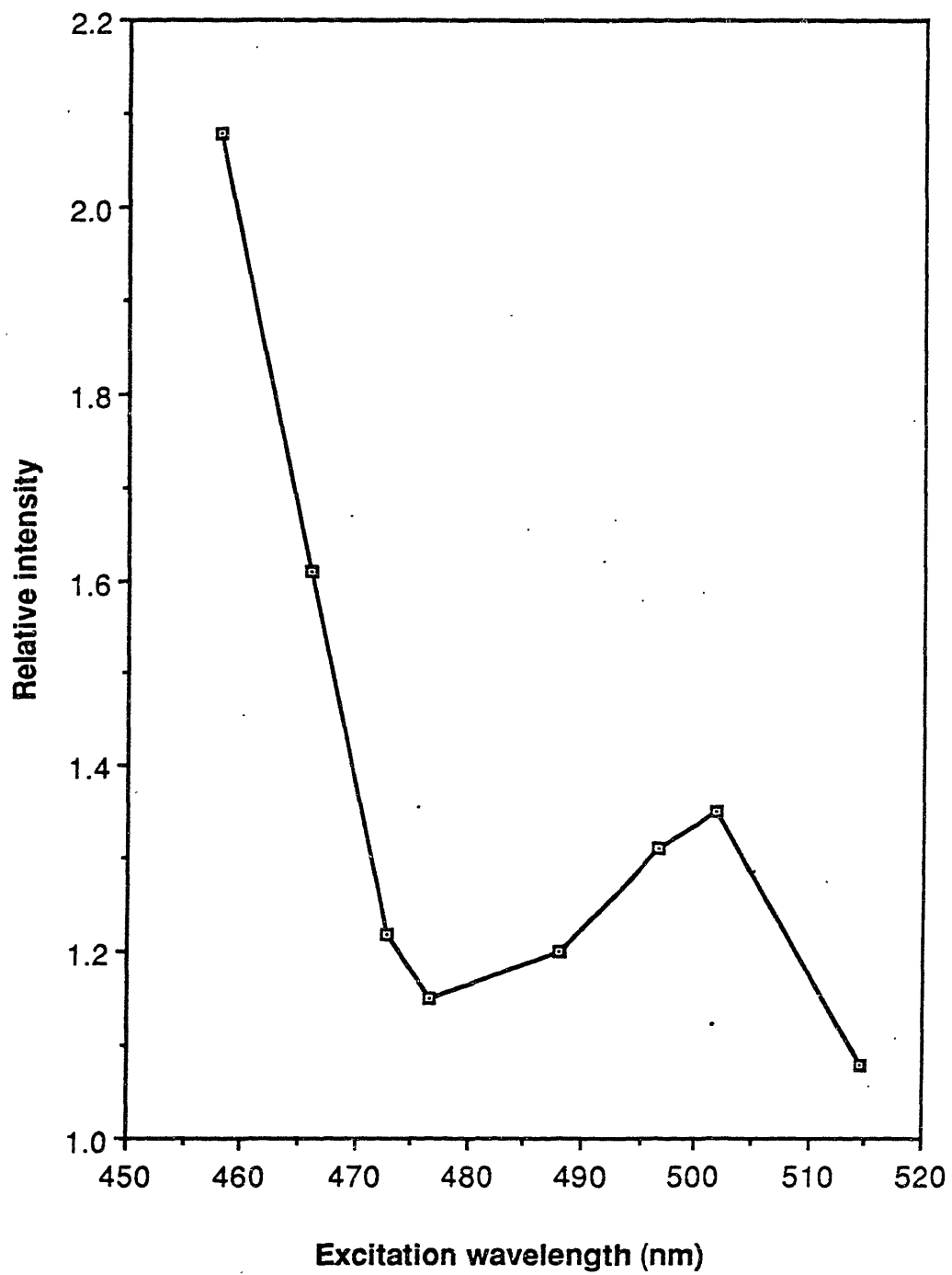


Figure 4. Excitation profile of the  $\nu_s$  (Fe-O-Fe) of 3 generated using available wavelengths from an Ar laser.

in **1** and **2**. Both of the acetate complexes show only weak resonance enhancement in the visible region with their profiles showing maximum enhancement at 514.5 nm. The profile of **3** shows resonance enhancement of approximately the same magnitude occurring at ~450 nm. The actual peak was not located owing to the limitations of the argon laser. A small maximum at ~500 nm is also apparent in the profile. The visible spectrum of **3**, however, is also considerably different from that of **1** or **2**. While the spectra of the latter two compounds have several distinct features in the 450 to 550 nm range, the spectrum of **3** has a small shoulder at 478 nm and no other feature below 550 nm. The band appearing at 625 nm in the spectrum of **3** is similar to the one at 695 nm in the spectrum of **1**. In fact the whole visible spectrum of **3** could be described as that of **1** shifted to higher energy, causing many of the features like those in **1** to become buried in the intense ligand absorptions in the 250 nm to 400 nm region (Figure 5). If this is a reasonable assessment of the spectrum of **3**, then it follows that the band responsible for the resonance enhancement of **1** at 514.5 nm has shifted to higher energy and is responsible for the enhancement at 454 nm in the excitation profile of **3**. Either of two factors could be responsible for the shift to higher energy: the change in ligand field strength which results from substituting diphenylphosphate for acetate or the change in the degree to which the metal centers are magnetically coupled.<sup>7</sup> Molecular orbital calculations will be necessary for further analysis of the visible spectra or excitation profiles of these complexes.

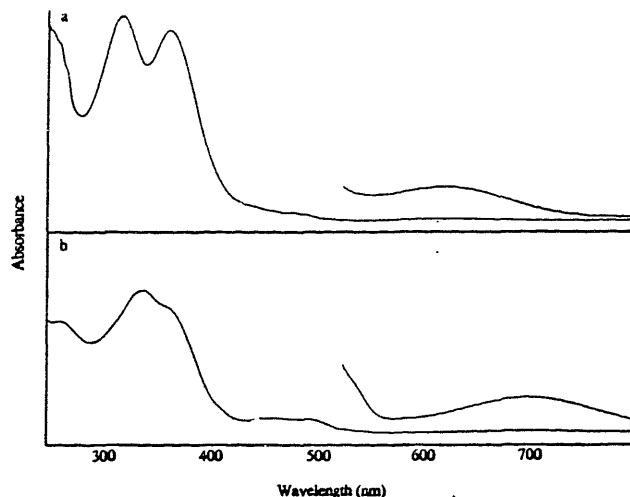


Figure 5. UV-visible spectra of (a) **3** and (b) **1** from 250 to 800 nm in  $\text{CH}_2\text{Cl}_2$ .

APPENDIX II  
Programs for Collection and Plotting of Sequential Spectra  
for use with a Perkin-Elmer Series 3600 Data Station  
and PECUV Software

In order to allow for the collection of sequential UV-visible data to follow time dependent spectral changes, two programs were written to be used in the OBEY command of the PECUV software available for a Perkin-Elmer Series 3600 data station and Lamda 7 Spectrophotometer. The first program collects spectra and stores them in sequentially labelled files. The limits of the spectra, the frequency of data points, and the number of spectra to be collected are all entered within the program. At the present time, however, spectra cannot be plotted during data collection. Also, the time variable must be entered external to the program through the EDIT mode; and, unfortunately, the time delay begins after the spectrum is stored so that, for accurate kinetic work, the actual time between collection of each spectrum must be measured by hand. The second program will automatically plot spectra with file ID labels that end in consecutive numbers. Any spectrum may be bypassed at the command of the operator. The chart, however, must be reset by hand between each spectrum.<sup>1</sup>

To use the programs, they must be copied onto the disk on which data are to be stored. The program to collect the data is named KIN01 and can be initiated within PECUV by entering the name after depressing the OBEY key. The program is set to pause 300 seconds which will leave just over 5 min between scans. To change this value, the data station must be in the PETOS utilities mode and a disk containing the EDIT task must be in one of the disk drives. When "EDIT MFD1: KIN01.OY" is typed in response to the PETOS prompt, the EDIT routine will be entered and the desired program retrieved. To change the delay time, type "68 <return>". The following line will appear on the screen "68.00 DO PAUSE 300". The time in seconds can be changed by typing "c/300/N/ <return>" where N is the desired length of

---

<sup>1</sup> It is possible to make the chart automatically reset after each spectrum which would allow for plotting during collection and eliminate error from incorrectly aligning the paper while resetting it during the plotting program. To make the chart reset, another variable must be assigned by the operator and the variable entered after the CHART command as a separate step in the program. That the CHART command could be used in this manner was not known at the time the programs were written.

time in seconds. The edited line should appear on the screen as line 68, if the change has been successful. Once the change has been accomplished the file must be saved using the SAVE command. If SAVE is entered, the file will be saved without changing the file name. To change the file name, the following sequence must be entered: "SAVE MFD1: FILID.OY"<sup>2</sup> where FILID is the file name and does not exceed 5 alphanumeric figures. The EDIT routine may be exited by typing STOP after which PECUV may be entered and the file run through the OBEY command. To run the plotting program, "PLOT1" should be entered after activating the OBEY command.

---

<sup>2</sup> The "OY" signifies that the program is an OBEY command program.

## KIN01.OY

```
DO SCLEAR
DO UCLEAR
&BREAK L20
*
*           KINETICS PROGRAM           WRITTEN BY MARY E. ROTH, AUG. 1986.
*
*           THIS PROGRAM IS SET UP TO COLLECT A KINETICS RUN.
*
*
*THE TIME DELAY BETWEEN SCANS IS APPROXIMATELY 5 MINUTES.
*
*ALL OTHER VARIABLES FOR THE RUN WILL BE CHOSEN BY YOU.
*
*EACH SPECTRUM WILL BE SAVED SEPARATELY UNDER ID 'S INCREASING BY 1)
*E.G. KN001, KN002, KN003, ETC.
*
*AT THIS TIME, THE SPECTRA CANNOT BE PLOTTED DURING THE COLLECTION
*OF THE DATA. THE STORED SPECTRA MAY BE PLOTTED AUTOMATICALLY
*USING THE PLOT1 "OBEY" PROGRAM.
*
*ALL RESPONSES MUST BE ENTERED BY PRESSING "RETURN".
*
*TO BEGIN PLEASE TYPE 0
*TO EXIT PROGRAM PRESS "BREAK" AND "RETURN".
&ENTER A1
DO SCLEAR
*TO CHOOSE SCAN RANGE, FIRST ENTER LONGER WAVELENGTH.
&ENTER A2
*%A2
*NOW ENTER THE END OF THE SCAN RANGE (SHORTER WAVELENGTH).
&ENTER A3
*%A3
*YOU MUST ALSO CHOOSE HOW OFTEN YOU WISH A DATA POINT COLLECTED.
*THIS VALUE MUST BE BETWEEN 1 AND 0.2 NM.
&ENTER A4
*%A4
*ENTER FILE NAME [FILID] USING TWO LETTERS FOLLOWED BY THREE NUMBERS.
*THE LAST TWO NUMBERS MUST BE 01, E.G. MR001 OR MR201 OR KN401, ETC.
&ENTER A6
*%A6
*ENTER THE NUMBER OF CYCLES DESIRED.
* **NOTE** MAXIMUM NUMBER OF FILES AVAILABLE ON DISK IS 85.
&ENTER A5
*%A5
*THIS IS YOUR LAST CHANCE TO MAKE SURE EVERYTHING IS READY.
*PRESS "RETURN" TO CONTINUE OR "BREAK" AND "RETURN" TO EXIT PROGRAM.
```



```
DO DISPLAY OFF
DO PAUSE
DO SCLEAR
.CALC U1=%A1
.CALC U2=%A2
.CALC U3=%A3
.CALC U4=%A4
.CALC U5=%A5
SET WAIT OFF
DO DISPLAY ON
&L1 SCAN X %U2 %U3 %U4
&ERROR L15
DO SCLEAR
DO DISPLAY OFF
SAVE X %A6
&ERROR L16
&INCR A6
.CALC U1=U1+1
.CALC U7=U5-U1
&IF U7 L5 L10 L5
&L5 DO DISPLAY ON
DO PAUSE 300
&GOTO L1
&L10 DO DISPLAY ON
*END OF RUN
&GOTO L25
*AN ERROR HAS BEEN DETECTED IN THE SCAN COMMAND.
*PLEASE CHECK THAT YOU HAVE ENTERED ALL VARIABLES CORRECTLY.
&GOTO L20
&L16 DO DISPLAY ON
*AN ERROR HAS BEEN DETECTED IN THE SAVE COMMAND.
*THE FILID YOU ENTERED MAY ALREADY EXIST, OR THE DISK MAY BE FULL.
&L20 *YOU HAVE EXITED THE PROGRAM AND MUST PRESS OBEY TO BEGIN AGAIN.
&L25 DO DISPLAY OFF
SET WAIT ON
DO DISPLAY ON
      END OF FILE
```

## PLOT1.OY

```

DO SCLEAR
DO UCLEAR
&BREAK L20
*      MULTIPLE PLOT PROGRAM          WRITTEN BY MARY E. ROTH, AUG. 1986
*
*   THE PURPOSE OF THIS PROGRAM IS TO PLOT AUTOMATICALLY ON THE
*   SCREEN AND ON PAPER SEQUENTIAL SPECTRA FROM A KINETICS RUN.
*
*
*THE FILIDS OF ALL THE SPECTRA TO BE PLOTTED MUST BE IN A
*SERIES WITH THE LAST NUMBER INCREASING BY 1.
*E.G. KN201 KN202, KN203 AND KN204 MAY BE PLOTTED, BUT
*KN201, KN203 AND KN205 MAY NOT BE PLOTTED AUTOMATICALLY WITHOUT
*BEING RENAMED.
*
*IN ORDER TO PLOT THE SPECTRA ON PAPER, THE CHART MUST ALREADY BE ON.
*BECAUSE THE DATA STATION IS STUPID, YOU WILL HAVE TO LINE UP THE
*CHART MANUALLY BEFORE EACH PLOT. WHEN THE INSTRUMENT IS READY
*TO PLOT, IT WILL PROMPT YOU WITH "READY?" THIS IS YOUR CHANCE TO
*ALIGN THE CHART. WHEN YOU ARE READY, RESPOND WITH "Y" OR "RETURN".
*IF YOU DO NOT WISH TO PLOT A PARTICULAR SPECTRUM, YOU MAY BYPASS IT
*BY PRESSING "N". THE PROGRAM WILL CONTINUE ON, CALLING UP THE NEXT
*SPECTRUM IN THE SEQUENCE.
*
*PRESS "RETURN" WHEN YOU ARE READY TO CONTINUE.
DO DISPLAY OFF
DO PAUSE
DO SCLEAR
DO DISPLAY ON
*IF YOU WISH A HARD COPY OF THE SPECTRA, ENTER "1", IF NOT, "0".
&ENTER A9
*%A9
*
*
*TO INITIATE THE PROGRAM, PLEASE PRESS 0.
*TO EXIT THE PROGRAM PRESS "BREAK" AND "RETURN".
&ENTER A1
DO SCLEAR
*ENTER THE FILID OF THE FIRST SPECTRUM IN THE SERIES.
&ENTER A2
*%A2
*
*ENTER THE TOTAL NUMBER OF SPECTRA YOU WISH TO PLOT.
&ENTER A3
*%A3
*

```

```

*ENTER THE ABSORBANCE SCALE DESIRED, STARTING WITH THE LOWER LIMIT.
*E.G. 0.0,1.0
&ENTER A4,A5
*%A4,%A5
*
*ENTER THE REGION YOU DESIRE TO PLOT, START WITH THE LONGER WAVELENGTH.
*E.G. 800,350
* **NOTE** THE LONGER WAVELENGTH MUST BE ENTERED FIRST!
&ENTER A6,A7
*%A6,%A7
*
*PLEASE CHECK YOUR ENTRIES AND MAKE SURE EVERYTHING IS CORRECT.
*PRESS "RETURN" TO CONTINUE OR "BREAK" AND "RETURN" TO EXIT PROGRAM.
DO DISPLAY OFF
DO PAUSE
DO SCLEAR
CALC U1=%A1
CALC U3=%A3
CALC U4=%A4
CALC U5=%A5
CALC U6=%A6
CALC U7=%A7
CALC U9=%A9
SET SCALE A %U4 %U5
&ERROR L12
&L5 RETRUE X %A2
&ERROR L15
DO DISPLAY ON
VIEW X %U6 %U7
&ERROR L16
DO DISPLAY OFF
DO SCLEAR
&IF U9 L6 L7 L6
&L5 DO DISPLAY ON
PLOT X %U6 %U7 A
DO SCLEAR
DO DISPLAY OFF
&L7 CALC U1=U1+1
CALC U8=U3-U1
&INCR A2
&IF U8 L5 L10 L5
&L10 DO DISPLAY ON
*ALL THE SPECTRA ARE NOW PLOTTED.
&GOTO L25
&L12 DO DISPLAY ON
*YOU HAVE ENTERED THE ABSORBANCE SCALE PARAMETERS INCORRECTLY.

```

```
&GOTO L20
&L15 DO DISPLAY ON
*AN ERROR HAS BEEN DETECTED IN THE RETRIEVE COMMAND.
*SOMETHING MUST BE WRONG WITH THE FILID YOU ENTERED.
&GOTO L20
&L16 *YOU HAVE ENTERED THE WAVELENGTH PARAMETERS INCORRECTLY.
&L20 *YOU HAVE EXITED THE PROGRAM AND MUST PRESS "OBEY" TO START AGAIN.
&L25 *
      END OF FILE
```

## ACKNOWLEDGEMENTS

As is appropriate, I will start by acknowledging and thanking Steve Lippard for being my Advisor for the past five years. He told me the most important result of my graduate career was that I should have become educated and that, I feel assured, I have. The members of the Lippard group, past and present, have played an overwhelming role in the education I gained during my stay at MIT. From them I learned more science than I could have imagined possible five years ago and much about many other things besides chemistry. I owe a special thanks to the post-docs and senior graduates students in my subgroup who lent me a hand (read: led me by the hand) during my first years: Bill Armstrong, Dani Gibson, Phil Stremple, Bill Davis, Sergiu Gorun and Alan Spool. The Lippard group has always been a colorful one with a distinct international flavor and to everyone who added to that aura, I say thanks. Thanks to Wes Sundquist, also, for seeing it through with me-- all five years, I'm glad you could be here when I finished.

To the Lippard group I also owe thanks for introducing me to some very dear friends without whom I know I would not have seen this sweet end. To Patty Bianconi, for sharing it all, from start to finish; to Stuart Bristow for being exactly who he is; to Sue Bruhn (The title is all yours, now.) for helping with the finishing touches-- of my stay, my outfits, my hair, my thesis..., many, many thanks. Thanks, too, to Lynn Rardin for all computer assistance rendered and for carrying on the Kenyon legacy.

Outside the group, I would like to thank Marion Curley without whose excellent assistance I doubt that many of us would get our degrees, or at least not without paying large sums of money in fines. Thanks also to Bob in the Purchasing Office for always being friendly, courteous, and extremely helpful; and to Jeanne Owens and Debbie Western (formerly) of the Chemistry Department Spectrometry Laboratories for their friendliness, patience and assistance.

Outside of MIT, I would like to acknowledge the members of the chemistry department at Kenyon College, particularly Dr. Gordon Johnson, for always believing in me and having faith in my abilities. I wish to thank my parents, Alice and John Roth, for showing the same quality; also, for their love and for having taught me the importance of seeing things through. Finally, last, but certainly not least, my deep appreciation to Andy who represents at least one thing I gained during my stay at MIT that I will keep with me for the rest of my life.